THE UNIVERSITY OF CHICAGO

EXPLORING YORKIE'S FUNCTION AT THE CELL CORTEX

A DISSERTATION SUBMITTED TO

THE FACULTY OF THE DIVISION OF THE BIOLOGICAL SCIENCES

AND THE PRITZKER SCHOOL OF MEDICINE

IN CANDIDACY FOR THE DEGREE OF

DOCTOR OF PHILOSOPHY

COMMITTEE ON DEVELOPMENT, REGENERATION AND STEM CELL BIOLOGY

BY

JIAJIE XU

CHICAGO, ILLINOIS

DECEMBER 2018

TABLE OF CONTENTS

LIST OF FIGURES..... v

LIST OF TABLES.....viii

ACKNOWLEDGEMENTS.....ix

STATEMENT OF CONTRIBUTIONS..... x

ABSTRACT.....xi

CHAPTER 1: Introduction……1

1.1 Overview……...……...…….1

1.2 The Hippo signaling pathway……...……1

1.3 Major upstream regulators of the Hippo pathway in *Drosophila* …….....6

1.4 Regulation of the Hippo pathway by mechanical force…….…….….12

1.5 Functional interactions between apical basal polarity proteins and the Hippo pathway….16

1.6 Concluding remarks and dissertation outline……...21

CHAPTER 2: Yorkie functions at the cell cortex to promote myosin activation in a non-transcriptional manner……23

2.1 Introduction…..……..…….……...…….23

2.2 Results……...……..25

2.3 Discussion……...……63

2.4 Methods…….....68

CHAPTER 3: Functional interactions of Yorkie and apical polarity proteins at the cell cortex

3.1 Introduction…..……..…….……...…….79

3.2 Results……...……..80

3.3 Discussion……...…..104

3.4 Methods…….....108

CHAPTER 4: Discussion: conclusions and future directions……....111

APPENDIX A: Live imaging of Hippo pathway components in *Drosophila* imaginal discs…….....126

APPENDIX B: Investigating the mechanism of Yorkie's cortical recruitment……..…....138

APPENDIX C: Investigating the subcellular localization of Strn-Mlck…..…….....144

APPENDIX D: Myr-Yki and Yki do not affect Strn-Mlck kinase activity in an *in vitro* kinase assay……151

REFERENCES……..……164

LIST OF FIGURES

Figure 1.1 The Hippo signaling pathway and its major regulators in Drosophila…..…….4

Figure 1.2 Tension promotes uniform growth ……..15

Figure 1.3 Apical-basal polarity in epithelial cells ……...18

Figure 2.1 Yki localizes to the apical junctional region (AJR) in addition to the nucleus……....26

Figure 2.2 Myristoylation signal sequence targets Yki to the cell cortex……..29

Figure 2.3 Cortical Yki promotes activation of myosin……30

Figure 2.4 Cortical Yki promotes activation of myosin independently of Yki transcriptional activity……...…….33

Figure 2.5 Yki promotes activation of myosin in normal development……..…..35

Figure 2.6 Yki promotes activation of myosin in *wts* mutant clones…….37

Figure 2.7 Cortical Yki promotes growth……..…40

Figure 2.8 Cortical Yki promotes growth via the Hippo pathway…….....41

Figure 2.9 Cortical Yki promotes growth via endogenous Yki…….43

Figure 2.10 Cortical Yki recruits Sd to the cell cortex……..44

Figure 2.11 Cortical Yki does not recruit Wts to the apical junctional region (AJR) to cause its inactivation…….45

Figure 2.12 Screening for kinase that mediates Yki's myosin activation function……47

Figure 2.13 Yki promotes myosin activation through Strn-Mlck……..50

Figure 2.14 Yki is able to recruit Strn-Mlck to the cell cortex……..52

Figure 2.15 Strn-Mlck negatively regulates Hippo pathway in normal development……...54

Figure 2.16 The N-terminal region of Yki is necessary and sufficient for myosin activation…..55

Figure 2.17 Identification of the critical amino acids for myosin activation function of Yki…..58

Figure 2.18 The *yki*^{AcidA} mutation does not affect the transcriptional function of Yki…….59

Figure 2.19 The myosin-activation function of Yki is required for proper growth…….62

Figure 3.1 Yki is able to recruit Hippo pathway components to the AJR independent of its transcriptional function…….81

Figure 3.2 Membrane-localized Yki is able to recruit Hippo pathway members to the cell membrane……..83

Figure 3.3 Yki is not required for assembly of Hippo signaling complex at the AJR……..84

Figure 3.4 Yki promotes Wts phosphorylation…….86

Figure 3.5 Membrane-localized Yki is able to recruit apical polarity proteins to the AJR……..88

Figure 3.6 Yki is not required for localizing apical polarity protein to the AJR……..89

Figure 3.7 Apical polarity gene knockdown enhances the overgrowth phenotype of Yki expression……..…91

Figure 3.8 Depleting Baz does not affect Adherens Junctions or other apical polarity proteins..92

Figure 3.9 Depleting Baz causes overgrowth in the presence of one extra copy of yki……...94

Figure 3.10 Depleting Baz causes increased expression of Hippo pathway reporter *bantam-GFP*, but not *ex-lacZ* or *Diap1-lacZ*……..….95

Figure 3.11 Depleting Baz results in increased JNK dependent apoptosis, concealing an overgrowth phenotype ……..96

Figure 3.12 Mer and Baz does not affect localization or abundance of each other……..…98

Figure 3.13 Depleting aPKC resulted in cell-autonomous and non-cell-autonomous up-regulation of Hippo pathway reporters……...……99

Figure 3.14 Depleting aPKC resulted in activation of JNK signaling and apoptosis……..100

Figure 3.15 aPKC RNAi induced non-cell-autonomous growth depends on JNK signaling…..102

Figure 3.16 Synergism between yki expression and aPKC knockdown does not require JNK signaling ……..103

Figure 4.1 CAAX tagged Yki^{1-34} but not full length Yki activates myosin…….……115

Figure 4.2 Ectopic expression of Strn-Mlck caused increase in myosin activation but not growth…….…….118

Figure 4.3 Strn-Mlck regulates growth through both kinase dependent and kinase independent mechanisms……..120

Figure A.1 Setup for live-imaging of Hippo pathway components on an inverted microscope…….……..132

Figure A.2 Examples of Hippo pathway components imaged in live tissues…….…….133

Figure A.3 Mechanical force promotes nuclear and cortical Yki localization……....136

Figure B.1 Ex is sufficient but not required for cortical localization of Yki……..…….139

Figure B.2 Hippo pathway components are not required for cortical localization of Yki…..….140

Figure B.3 Depleting Adherens Junctions components disrupts cortical localization of Yki….141

Figure C.1 Adding GFP tag at the endogenous locus of Strn-Mlck with CRISPR…….……146

Figure C.2 Strn-Mlck-GFP expression in larval tissue……...….148

Figure D.1 Strn-Mlck phosphorylates Sqh *in vitro*……..…153

Figure D.2 Co-transfection of Myr-Yki or Yki does not affect Strn-Mlck mediated Sqh phosphorylation……..…..154

LIST OF TABLES

Table 2.1 Mean Dorsal/Ventral (D/V) pSqh Fluorescence Intensity Ratio…….……..39

Table 2.2 Effect of different Yki mutations on pSqh increase…….....…….57

Table 2.3 Key resource used in Chapter 2…….68

Table 3.1 Key resource used in Chapter 3…….…..108

Table B.1 Key resource used in Appendix B…….……..142

ACKNOWLEDGEMENTS

I would first like to thank my advisor, Rick Fehon, for his guidance throughout all six years of graduate school. I have learned so much from Rick on how to be a successful scientist. Rick is always there to talk about results and he has the amazing ability to find the silver lining in seemingly useless data. There are so many times when I walked into his office in dismay with some negative results and walked out with exciting new ideas. In addition to teaching me how to do great science, Rick has helped me tremendously to improve my writing and oral presentations so that I can present my science to others more effectively.

I would like to thank Fehon lab members: Pam, Ting, Kritin, Danielle, Cynthia, Hitoshi, Will, Sherzod and Stephan; Ashley, Yi-wen, and members of the Horne-Badovinac lab and Rebay lab for their support and encouragement, as well as their thoughtful input into my research. Special thanks to Will for his friendship. I thank my thesis committee members, Sally, Ed, and Robert for their valuable guidance and advice. I also thank Michael Glotzer and Chip Ferguson for their suggestions on my research and my manuscript. I thank King-Lau Chow at HKUST for introducing me to the fascinating field of developmental biology. I also thank 2014 MBL Embryology Course directors, lecturers, and students for an unforgettable summer of science and fun.

I thank my program chair Ilaria Rebay, Kristine Gaston, Pilar Frankowicz, Debra Brown and other DRSB and MGCB administrative staff for providing excellent logistic support. I thank the Children's Tumor Foundation for two years of financial support.

Lastly, I would like to thank my parents. They have made so much sacrifice to support my graduate study in a country thousands of miles away. I thank them for their unconditional love and support.

STATEMENT OF CONTRIBUTIONS

The majority of the work described in this dissertation is my own, however some of the work was initiated and/or performed by others. For the work described in Chapter 2, Dr. Pamela Vanderzalm generated the UAS-Myr-Yki and UAS-Myr-Yki$^{\Delta NH}$ transgenes, and performed initial characterization of UAS-Myr-Yki phenotypes. Dr. Michael Ludwig generated the Yki-YFP transgene. Dr. Ting Su performed live imaging of Yki-YFP in *wts* null clones. Sherzod Tokamov helped with mapping the region of Yki responsible for myosin activation and initiated the GrabFP experiments. For the work described in Chapter 3, Dr. Vanderzalm initiated the project to examine potential non-transcriptional functions of Yki in organizing the Hippo signaling complex and promoting accumulation of apical polarity proteins. Specifically Dr. Vanderzalm performed the majority of the experiments showing that Hippo pathway components and apical polarity proteins are recruited upon ectopic expression of various Yki transgenes. For the exploratory work on Strn-Mlck's ability to phosphorylate Squash described in Chapter 4, Yupu Wang developed the *in vitro* kinase assay and generated the two Stretchin-Mlck kinase dead mutants. All of the other experiments presented in this dissertation and analyses were performed by me under the guidance and supervision of Dr. Richard Fehon.

ABSTRACT

The Hippo signaling pathway is an evolutionarily conserved mechanism that controls organ size in animals. Pathway output is mediated by Yorkie, a transcriptional co-activator that positively regulates transcription of genes that promote tissue growth. In addition, Yorkie and its mammalian ortholog YAP have been observed to localize to the cell cortex and there is growing evidence that they may have cytoplasmic functions that are independent of their nuclear functions as transcriptional coactivators.

In this dissertation I explore potential functions of Yorkie at the cell cortex. I first identify a novel function of Yorkie to promote activation of myosin through a myosin regulatory light chain kinase, Stretchin-Mlck. This Yorkie function is not dependent on its transcriptional activity and is required for larval and adult tissues to achieve appropriate size. Recent studies have shown that cytoskeletal tension can activate both Yorkie and YAP, resulting in increased nuclear localization and tissue growth. Therefore, I propose that cortical Yorkie functions in a feed-forward 'amplifier' loop that promotes myosin activation, and thereby greater Yorkie activity, in response to tension.

Many of the Hippo pathway components and regulators concentrate at the cell cortex where apical polarity proteins reside. In this dissertation I find a possible role for Yorkie in organizing Hippo pathway components at the cell cortex. I also further analyze the functional interactions between the Hippo pathway and apical polarity proteins and identify two apical polarity proteins Bazooka and atypical protein kinase C as potential positive regulators of the Hippo pathway.

Together, the findings described in this dissertation provide new insights into the regulation of the Hippo pathway and point to new directions for future studies.

CHAPTER 1

Introduction

1.1 Overview

One of the fundamental questions in developmental biology is how animal organs grow to appropriate sizes. The discovery of the Hippo signaling pathway and its crucial role in growth regulation has begun to suggest answers to the question of organ size control. In this introductory chapter, I will provide a review of the Hippo signaling pathway and its major regulators in *Drosophila* to provide a background for my dissertation.

1.2 The Hippo signaling pathway

Core components of the Hippo signaling pathway and their discoveries

Genetic mosaic screens for an over-proliferation phenotype in *Drosophila* identified the first component of the Hippo pathway, *warts* (*wts*), which encodes a Nuclear Dbf-2 Related (NDR) family kinase (Justice et al. 1995; T. Xu et al. 1995). *salvador* (*sav*), *hippo* (*hpo*), and *mob as tumor suppressor* (*mats*) were subsequently identified as components of the Hippo pathway using similar genetic mosaic screens. *hpo* encodes a Sterile20-like kinase that phosphorylates and activates Wts (Wu et al. 2003; Harvey, Pfleger, and Hariharan 2003; Udan et al. 2003; Pantalacci, Tapon, and Léopold 2003). *sav* encodes a WW-repeat protein that physically interacts with and activates Hpo (Tapon et al. 2002; Kango-Singh 2002). *mats* encode a mob superfamily protein that physically interacts with Wts to promote its activity (Lai et al. 2005; X. Wei, Shimizu, and Lai 2007). A yeast two-hybrid screen identified the oncoprotein and transcriptional co-activator Yorkie (Yki) as the substrate of Wts and the effector of the Hippo pathway (J. Huang et al. 2005). Combing yeast two-hybrid screens and analysis of the enhancer sequence of a Hippo pathway

target gene, the TEAD/TEF family transcription factor Scalloped (Sd) was identified as the nuclear partner of Yki that mediates the transcriptional output of the Hippo pathway (Lei Zhang et al. 2008; Wu et al. 2008). The pathway components upstream of Yki are referred to as the Hippo pathway and Yki is referred to as the effector of the pathway in this dissertation.

According to current models, when the Hippo pathway is active, Hpo phosphorylates and activates Wts, which in turn phosphorylates Yki. Phosphorylated Yki is sequestered in the cytoplasm by interacting with a cytoplasmic protein 14-3-3 (Figure 1.1A left panel)(Wu et al. 2003; J. Huang et al. 2005; Oh and Irvine 2008; Dong et al. 2007; Oh, Reddy, and Irvine 2009). When the Hippo pathway is inactive, unphosphorylated Yki goes to the nucleus and binds to Sd to promote transcription of genes that promote growth (Figure 1.1A right panel)(Wu et al. 2008; Lei Zhang et al. 2008).

The Hippo pathway is an ancient signaling pathway that is conserved from the unicellular lineage amoeboid holozoan *Capsaspora owczarzaki* to mammals (Sebe-Pedrs et al. 2012). Due to its relevance to human health, the Hippo pathway is well studied in mammalian model systems in addition to *Drosophila*. The mammalian orthologs of Hpo, Sav, Wts, Mats, Yki, and Sd are Mammalian sterile 20-like 1/2 (MST1/2), Salvador (SAV1), Large tumor suppressor homolog 1/2 (LATS1/2), MOB kinase activator 1A/B (MOB1A/B), Yes-associated protein (YAP)/transcriptional co-activator with PDZ binding motif (TAZ), and TEAD1-4, respectively (Figure 1.1A) (F. X. Yu, Zhao, and Guan 2015).

Transcriptional regulation of Hippo pathway targets through Yki

The Hippo pathway regulates growth through transcriptional regulation of its target genes that promote growth. These target genes include the apoptosis inhibitor *Death-associated inhibitor*

of apoptosis 1 (*Diap1*), the cell cycle regulator *Cyclin E* (CycE) (Wu et al. 2003), and the growth promoting microRNA *bantam* (Nolo et al. 2006; Thompson and Cohen 2006). The Hippo pathway effector Yki itself lacks a DNA binding domain so it cooperates with transcription factors to promote target gene expression. Sd is the first and best characterized transcription factor that interacts with Yki in the nucleus to mediate transcriptional output of the Hippo pathway. Recently, Tondu-domain-containing growth inhibitor (Tgi) has been found to compete with Yki for Sd binding, resulting in inhibition of Hippo target gene transcription (Guo et al. 2013; Koontz et al. 2013). When Sd is bound by Tgi, it serves as a transcriptional repressor to inhibit Yki target gene expression. Upon inactivation of the Hippo pathway, Yki translocates into the nucleus to displace Tgi from Sd, leading to target gene transcription (Koontz et al. 2013). Interestingly, the Yki target *bantam* can repress expression of Tgi, thus forming a positive feedback loop to amplify Yki activity (Shen et al. 2015).

In addition to Sd, other transcription factors have been found to interact with Yki. Those transcription factors include Mothers against Dpp (Mad) and a Homothrax (Hth) -Teashirt (Tsh) complex (Alarcón et al. 2009; Peng, Slattery, and Mann 2009; Oh and Irvine 2011). Both Yki-Mad and Yki-Hth-Tsh activate transcription of *bantam*. Mad is the effector of the Decapentaplegic (Dpp) signaling pathway, and its interaction with Yki indicates cross-talk between the Hippo and Dpp pathways in growth regulation. *hth* and *tsh* are expressed in the progenitor domain of the eye imaginal discs and together with Yki they promote cell proliferation (Peng, Slattery, and Mann 2009). These findings suggest that Yki use different transcription factors depending on the cellular context.

Figure 1.1

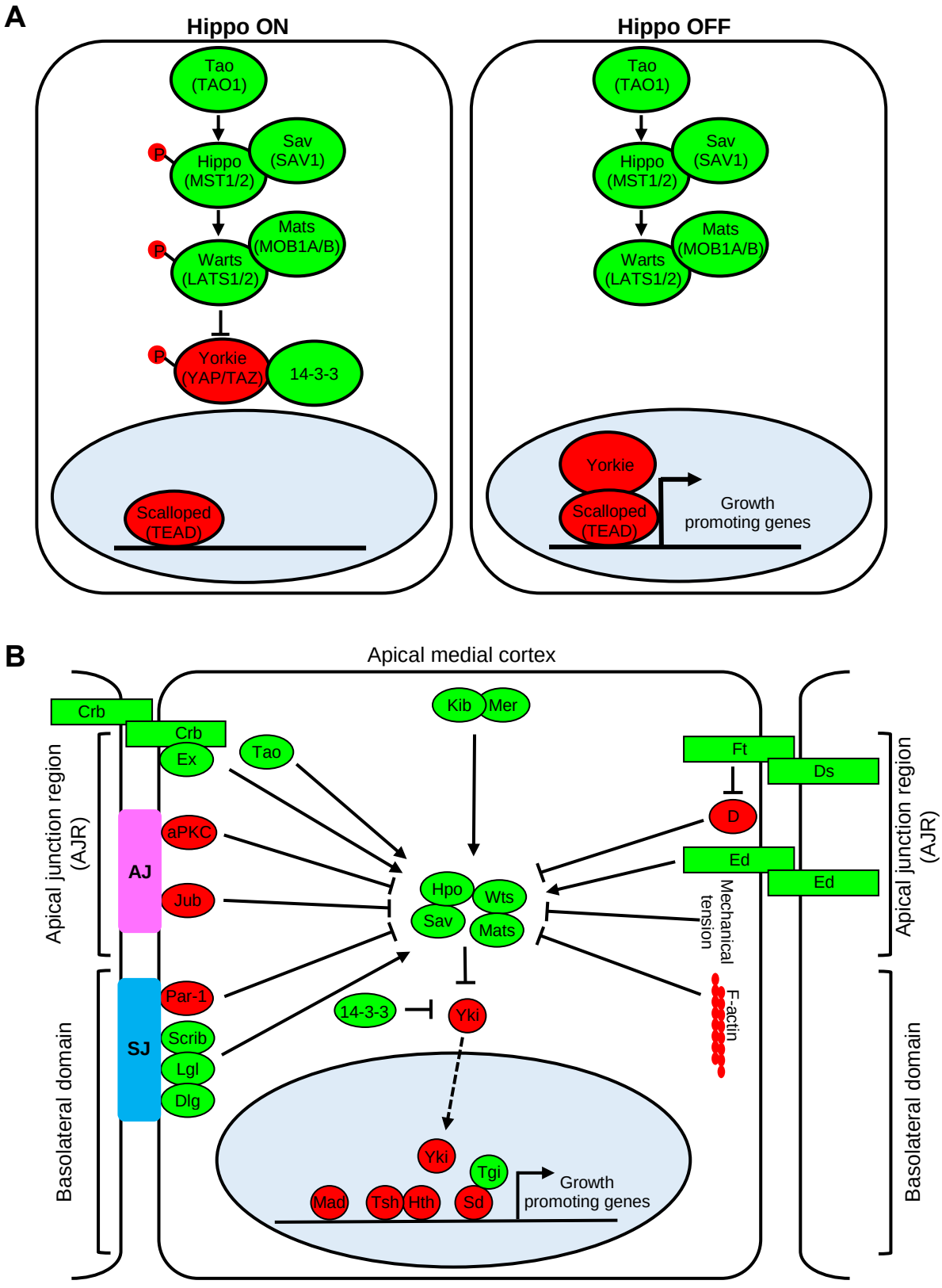
A
Hippo ON
Tao (TAO1)
Sav (SAV1)
Hippo (MST1/2)
Mats (MOB1A/B)
Warts (LATS1/2)
Yorkie (YAP/TAZ)
14-3-3
Scalloped (TEAD)
Hippo OFF
Tao (TAO1)
Sav (SAV1)
Hippo (MST1/2)
Mats (MOB1A/B)
Warts (LATS1/2)
Yorkie
Scalloped (TEAD)
Growth promoting genes
B
Apical medial cortex
Crb
Crb
Ex
Tao
Kib
Mer
Ft
Ds
D
Ed
Ed
aPKC
Jub
AJ
Hpo
Wts
Sav
Mats
Mechanical tension
F-actin
Par-1
Scrib
Lgl
Dlg
SJ
14-3-3
Yki
Yki
Tgi
Mad
Tsh
Hth
Sd
Growth promoting genes
Apical junction region (AJR)
Basolateral domain
Apical junction region (AJR)
Basolateral domain

Figure 1.1 continued
The Hippo signaling pathway and its major regulators in *Drosophila*
According to current models, when the Hippo pathway is on, Hippo (Hpo) phosphorylates and activates Warts (Wts), which in turn phosphorylates Yorkie (Yki). Phosphorylated Yki issequestered in the cytoplasm by interacting with a cytoplasmic protein 14-3-3. Scaffolding proteins Salvador (Sav) and Mob as tumor suppressor (Mats) promote Hpo and Wts activity respectively (**A left panel**). When the Hippo pathway is off, unphosphorylated Yki goes to the nucleus and binds to Scalloped (Sd) to promote transcription of genes that promote growth (**A right panel**). Mammalian homologs of pathway components are shown in parenthesis.
Growth-promoting proteins are depicted in red and growth repressors in green.

Hippo pathway is regulated by various factors including the following (**B**): aPKC, atypical protein kinase C; Crb, Crumbs; D, Dachs; Dlg, Discs large; Ds, Dachsous; Ed, Echinoid; Ex, Expanded; Ft, Fat; Hth, Homothorax; Jub, Ajuba LIM protein; Lgl, Lethal giant larvae; Mad, Mothers against decapentaplegic (Dpp); Mer, Merlin; Scrib, Scribble; Sd, Scalloped; Tgi, Tondu domain-containing growth inhibitor; Tsh, Teashirt; Zyx, Zyxin.
Growth-promoting proteins are depicted in red and growth repressors in green. See detailed description of these proteins in text.
AJ, adherens junction; SJ, septate junction. (Adapted from Irvine and Harvey 2015)

How Yki and its transcription factor partners activate target gene transcription is still not fully understood. Recent studies show that Yki interacts with several chromatin-modifying proteins including GAGA factor (GAF), the Brahma complex, the Mediator complex and a subunit of the Trithorax-related histone H3 lysine 4 methyltransferase complex, Nuclear receptor coactivator 6 (Ncoa6) (Jin et al. 2013; Oh et al. 2013; Qing et al. 2014). Together these studies suggest that Yki regulates transcription via multiple mechanisms including recruitment of general transcription factors, modification of chromatin structure and epigenetic markers.

Unlike other major signaling pathways such as Dpp, Wingless, and Notch pathways, no ligand-receptor pair for the Hippo pathway has been identified so far. Instead, a complex input network regulates the Hippo pathway and the list of Hippo pathway regulators keeps growing (Figure 1.1B). In the following three sections, I will discuss the major regulators of the Hippo pathway in *Drosophila*.

1.3 Major upstream regulators of the Hippo pathway in *Drosophila*

Expanded, Merlin, and Kibra

The first identified upstream regulators of the Hippo pathway are two FERM (Four-point-one, Ezrin, Radixin, Moesin) domain proteins, Expanded (Ex) and Merlin (Mer) (Hamaratoglu et al. 2006). Ex and Mer physically interact with each other (McCartney et al. 2000). Loss-of-function mutations in either gene causes overgrowth and simultaneous deletion of both genes results in even greater overgrowth (McCartney et al. 2000; Hamaratoglu et al. 2006; Maitra et al. 2006). Loss of either gene causes upregulation of Hippo pathway target genes and both genetically interact with Hippo pathway components (Hamaratoglu et al. 2006). Later genetic screens identified a WW and C2 domain protein Kibra (Kib) to function upstream of the Hippo pathway

kinase cascade (Baumgartner et al. 2010; Genevet et al. 2010; J. Yu et al. 2010). *kib* mutations cause overgrowth and up-regulation of Hippo pathway targets. Kib protein physically associates with both Mer and Ex and the three of them can co-localize at the apical junctional region, suggesting that these three proteins can function together to regulate the Hippo pathway (Baumgartner et al. 2010; Genevet et al. 2010; J. Yu et al. 2010; Formstecher et al. 2005). Interestingly, genetic analysis reveals Ex, Mer, and Kib can each function independently of the others (Hamaratoglu et al. 2006; Baumgartner et al. 2010; J. Yu et al. 2010).

The mechanisms by which Ex, Mer, and Kib activate the Hippo pathway are still not well understood. FERM domain proteins serve as linkers between membrane proteins and the cortical cytoskeleton (Bretscher, Edwards, and Fehon 2002), suggesting the cell cortex may be an important hub for integrating upstream inputs of the Hippo pathway. Recent studies have found that Ex, Mer, and Kib positively regulate the Hippo pathway by recruiting pathway components to specific cortical domains to promote their activation. Mer has been shown to recruit Wts to the plasma membrane to promote its activation (Yin et al. 2013). Ex can function as a scaffold that recruits Wts to the apical junctional region where it interacts with and can be activated by Hpo (S. Sun, Reddy, and Irvine 2015). Our lab has found that Mer and Kib can activate Hippo signaling in parallel to Ex at a spatially distinct cellular domain, the apical cortex (Su et al. 2017). Taken together, Ex, Mer, and Kibra may activate Hippo pathway at distinct sub-cellular locations, possibly mediating different inputs of the Hippo pathway. An alternative mechanism has been proposed for Ex to regulate the Hippo pathway in addition to acting through the kinase cascade. Ex physically interacts with Yki and can potentially sequester Yki at the apical junctional region to prevent it from entering the nucleus, thereby inhibit its activation (Badouel et al. 2009).

In addition to acting as upstream regulators of the Hippo pathway, Ex, Mer, and Kib are transcriptional targets of the pathway (Hamaratoglu et al. 2006; Genevet et al. 2010). This suggests the existence of a negative feedback loop in which Yki activation turns on expression of positive regulators of the Hippo pathway (Boggiano and Fehon 2012; Irvine and Harvey 2015).

Tao and Par-1

Two kinases directly regulate the activity of Hpo through phosphorylation. The Sterile-20 like kinase Tao phosphorylates the activation loop of Hpo to promote its activity (Boggiano, Vanderzalm, and Fehon 2011; Poon et al. 2011). In contrast, the polarity kinase Par-1 promotes Hpo phosphorylation at a different site to restrict its activity. In addition, Par-1 inhibits interaction between Hpo and Sav to promote Sav dephosphorylation and destabilization, further down-regulating Hippo pathway activity (H.-L. Huang et al. 2013). Recently, Schip1, a *Drosophila* homolog of the mammalian Schwannomin interacting protein 1 (SCHIP1) was found to recruit Tao to the cell membrane to promote Hpo membrane localization and activation (Chung, Augustine, and Choi 2016). Interestingly, both Tao and Par-1 have been shown to regulate microtubules in *Drosophila*, raising the possibility that the microtubule cytoskeleton may be involved in Hippo pathway regulation (Doerflinger 2003; Liu et al. 2010; Boggiano, Vanderzalm, and Fehon 2011).

In addition to Par-1, several other apical basal polarity proteins are involved in Hippo pathway regulation and will be discussed in detail in Section 1.5.

The Fat signaling pathway

The first identified transmembrane protein that regulates the Hippo pathway is the protocadherin Fat (Silva et al. 2006; Cho et al. 2006; Bennett and Harvey 2006; Willecke et al. 2006). Another protocadherin, Dachsous (Ds), serves as a ligand for Fat (Matakatsu and Blair 2004). In addition, the Fat signaling pathway has a well characterized role in regulating planar cell polarity in epithelial tissue (Reddy and Irvine 2008), though planar cell polarity itself does not appear to regulate the Hippo pathway. Loss of Fat leads to overgrowth and up-regulation of Hippo pathway target genes *CycE* and *Diap1*, as has been shown for multiple Hippo pathway components. In addition, *fat* genetically interacts with Hippo pathway components (Silva et al. 2006; Cho et al. 2006; Bennett and Harvey 2006; Willecke et al. 2006). Three mechanisms have been proposed through which Fat signaling positively regulates the Hippo pathway. Firstly, Fat signaling is required for proper localization of the Hippo pathway upstream regulator Ex to the apical junctional region (Bennett and Harvey 2006; Cho et al. 2006; Silva et al. 2006; Willecke et al. 2006). Secondly, Fat signaling promotes Wts protein abundance by inhibiting Wts degradation mediated by the atypical myosin Dachs (Cho et al. 2006; Rauskolb et al. 2011; Bosch et al. 2014; Rodrigues-Campos and Thompson 2014). Thirdly, Fat acts via atypical myosin Dachs to prevent Wts from transitioning to an active conformation thereby inhibit its activity (Vrabioiu and Struhl 2015).

Recently, Fat-Ds signaling has been found to be bidirectional with Fat and Ds acting as receptor and ligand for each other in both PCP regulation and Hippo pathway regulation (G. Pan et al. 2013; Degoutin et al. 2013). The WD40 repeat protein Riquiqui (Riq) and the DYRK-family kinase Minibrain (Mnb) were found to function downstream of Ds to promote Yki activity through phosphorylation-dependent inhibition of Wts (Degoutin et al. 2013). Therefore, Fat signaling can

both inhibit Yki activity through a Fat-Dachs axis and promote Yki activity through a Ds-Mnb axis. How these two opposing effects are coordinated in normal development is not clear.

Actin cytoskeleton

Hippo pathway upstream regulators introduced so far all concentrate at cell junctions and the cell cortex, raising an interesting possibility that the actin cytoskeleton beneath the plasma membrane may be important for Hippo pathway regulation. Indeed, F-actin has been identified as a negative regulator of the Hippo pathway. Ectopic accumulation of F-actin caused by loss of Capping proteins, or ectopic expression of an activated version of the *Drosophila* formin Diaphanous resulted in increased Yki activity and strong overgrowth (Fernández et al. 2011; Sansores-Garcia et al. 2011). Interestingly, mutations in Hippo pathway genes *ex, Mer, hpo, sav, wts,* and *mats* all cause increased F-actin accumulation. Therefore, the Hippo pathway and F-actin might mutually suppress each other. This could help sustain Hippo pathway activity in normal conditions as activation of the Hippo pathway will suppress its negative regulator F-actin.

How F-actin regulates the Hippo pathway remains poorly understood. F-actin may affect the Hippo pathway by regulating the sub-cellular localization of pathway components. For instance, the Hpo orthologs MST1/2 colocalize with F-actin and are activated upon F-actin depolymerization in cultured mammalian cells (Densham et al. 2009). Another possibility is that F-actin might sense and transduce mechanical forces to regulate the Hippo pathway as mechanical force has recently been identified as an important regulator of the pathway (See Section 1.4 for details).

Cell–Cell adhesion and junctional proteins

In addition to the actin cytoskeleton, cell-cell adhesion and junctional proteins such as Ajuba LIM protein (Jub), Zyxin, and Echinoid regulate the Hippo pathway in *Drosophila*. Jub is localized at the apical junctional region and stabilizes preassembled cadherin complexes (Nola et al. 2011). Depleting Jub results in down-regulation of Hippo pathway target genes *Diap1* and *cycE* and tissue undergrowth, resembling the Yki depletion phenotypes. In addition, *jub* genetically interacts with the Hippo pathway (Das Thakur et al. 2010). A recent study suggests Jub inhibits Hippo pathway activity by sequestering and inhibiting Wts at the adherens junctions (AJs) (Rauskolb et al. 2014).

Another LIM domain protein Zyxin (Zyx) has been identified as a negative Hippo pathway regulator (Rauskolb et al. 2011; Gaspar et al. 2015). Loss of Zyx leads to reduced Yorkie activity and undergrowth. One study found that Zyx localizes to the apical junctional region where it cooperates with Dachs to promote Wts degradation, thereby inhibiting Hippo pathway activity (Rauskolb et al. 2011). This study places Zyxin in the Fat signaling branch of Hippo pathway regulation. Another study found Zyx interacts with the actin-binding protein Enabled (Ena) to promote Yki activity and tissue growth (Gaspar et al. 2015). Since Ena promotes F-actin polymerization, this study places Zyx in the F-actin branch of Hippo pathway regulation. Zyxin has been implicated in mechano-transduction at cell adhesive structures (Hirata, Tatsumi, and Sokabe 2008), hinting at the possibility that mechanical cues can regulate the Hippo pathway (See Section 1.4 for details).

Echinoid (Ed) is an immunoglobulin domain-containing transmembrane protein and a component of AJ's that cooperates with E-Cadherin in cell adhesion (S.-Y. Wei et al. 2005). Loss of Ed activates Yki, leading to increased Hippo pathway target gene expression and tissue

overgrowth. Mechanistically, Ed positively regulates the Hippo pathway by physically interacting with and stabilizing Sav at AJ's (Yue, Tian, and Jiang 2012).

In mammalian cells, several additional cell-cell adhesion and junctional proteins have also been identified as regulators of the Hippo pathway. These include The tight junctions proteins CRB1-3, Angiomotin family proteins AMOT, AMOTL1, and AMOTL2, Zonula occludens (ZO)1 and ZO2, and AJ components α-catenin and E-cadherin (F.-X. Yu and Guan 2013). These results highlight the importance of the apical junctional region as the hub for Hippo pathway regulation.

1.4 Regulation of the Hippo pathway by mechanical force

An exciting development in the Hippo field in recent years is the identification of mechanical force as a pathway regulator. Initial evidence that mechanical forces modulate the Hippo pathway comes from studies in mammalian cultured cells. A pioneering study found that mammalian YAP/TAZ activity is regulated by extracellular matrix (ECM) stiffness: cells grown on stiff fibronectin-coated acrylamide hydrogels exhibit nuclear YAP/TAZ localization and increased target gene transcription, whereas cells grown on soft hydrogels exhibit cytoplasmic YAP/TAZ localization and reduced target gene transcription. In addition, such regulation is dependent on tension of the actomyosin cytoskeleton, but is independent of the MST/LATS kinase cascade (Dupont et al. 2011). Another study found that YAP/TAZ is activated in cells exposed to mechanical stresses, such as stretching, location at edges, or stiffness of the ECM. (Aragona et al. 2013). This study also shows LATS activity is not required for mechanical force mediated YAP/TAZ activation. Together these two studies suggest the presence of an unidentified YAP/TAZ-antagonist that acts in parallel with the Hippo kinase cascade. Alternatively, a recent study suggests mechanical force can activate YAP by physically flattening the nucleus, which

stretches nuclear pores and thereby reduces their mechanical resistance to molecular transport, leading to increased YAP nuclear import (Elosegui-Artola et al. 2017). On the other hand, LATS dependent tension activation of YAP has also been reported recently. This study shows tension promotes LIMD1-mediated recruitment of LATS to the cell-cell junctions to inhibit its activity (Ibar et al. 2018). How these different mechanisms are used during tissue growth *in vivo* remains to be investigated.

Studies in *Drosophila* confirm mechanical force as a Hippo pathway regulator. In wing imaginal discs, a Rho kinase-mediated increase in myosin activation leads to Yki activation. Mechanistically, increased tension is believed to induce a conformational change in α-catenin. This leads to recruitment of the Wts inhibitor Jub to the AJs, which in turn sequesters Wts to inhibit its function (Rauskolb et al. 2014).

Further evidence that tension regulates the Hippo pathway in *Drosophila* comes from two studies on the cytoskeletal protein Spectrin. Spectrin forms hexagonal networks at the cell cortex in all animal cells and has been reported to have mechanosensory properties (Deng et al. 2015; Fletcher et al. 2015). Mechanistically, Spectrin seems to function in parallel to the Jub-Wts pathway (Deng et al. 2015; Fletcher et al. 2015). Depleting Spectrin results in Yki activation due to increased tension mediated by activation of the actomyosin network (Deng et al. 2015; Fletcher et al. 2015). These studies suggest Spectrin can relay mechanical cues to the Hippo pathway.

How cytoskeletal tension regulates normal development of organs is still not clear. In *Drosophila* imaginal discs, there are usually high levels of growth promoting morphogens in the center, which would predict higher proliferation in the center of the tissue. However, what has been observed is uniform growth throughout the tissue. This means morphogen level alone is not sufficient to fully explain tissue growth (Hariharan 2015). In a recent review, Hariharan

synthesized recent discoveries and summarized a model in which tension may promote uniform tissue growth during *Drosophila* imaginal discs development (Figure 1.2) (Hariharan 2015). As the center part of the tissue grows, it stretches the periphery. The resulting tension could activate Yki to promote growth. Thus, Yki activation at the periphery could compensate for non-uniform morphogen levels across tissues and promote uniform tissue growth (Aegerter-Wilmsen et al. 2007; Aegerter-Wilmsen et al. 2012; Hariharan 2015).

Several recent studies have provided support for the hypothesis that tension promotes uniform growth. Measurements of recoil velocity following laser ablation of actomyosin cables along cell-cell junctions has been used as a readout for cytoskeletal tension. Using this method, two studies found cells at the periphery of the disc are under higher tension than cells at the center (Legoff, Rouault, and Lecuit 2013; Mao et al. 2013). Additionally, junctional tension observed in wing imaginal discs decreases as the tissue grows, reaching the lowest at the late third instar larval stage. Interestingly, this correlates with low proliferation in the disc (Rauskolb et al. 2014). Another study showed that artificially increased growth in clones of wing imaginal discs reduces cytoskeletal tension, which in turn decreases the activation of Yki (Y. Pan et al. 2016). This study suggests a mechanical feedback in which increased Yki activation and cell proliferation reduces tension and deactivates Yki. Such feedback could contribute to evenly distributed growth (Y. Pan et al. 2016).

Figure 1.2

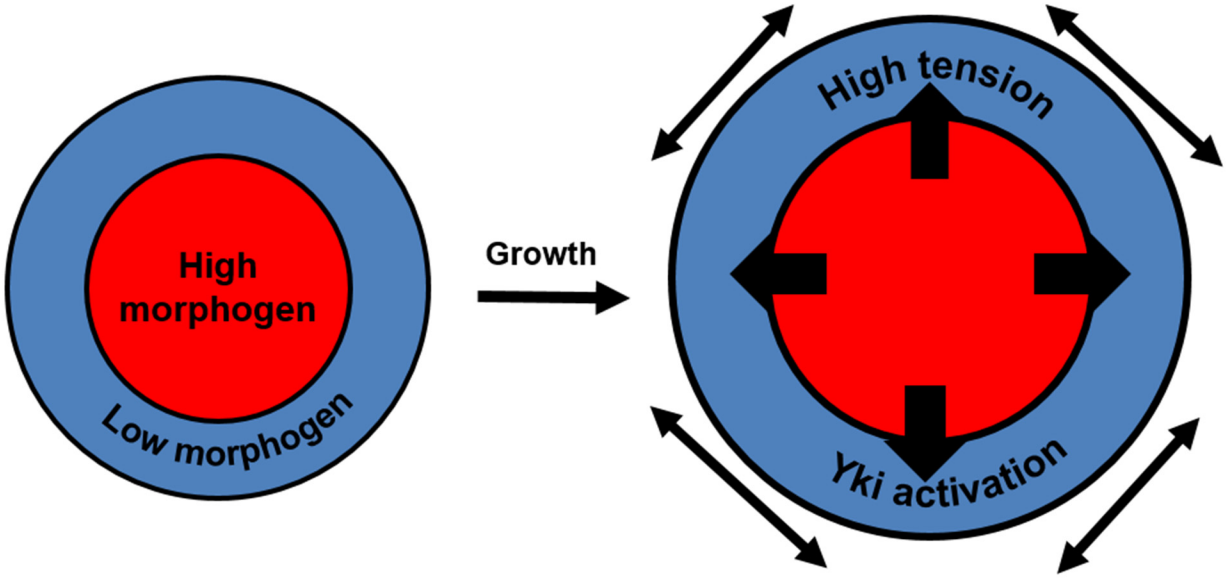

Tension promotes uniform growth
In *Drosophila* imaginal discs, there are usually high levels of growth promoting morphogens in the center. As the center part of the tissue grows, it stretches the periphery, causing higher tension, which could activate Yki to promote growth. Yki activation at the periphery could compensate the lower morphogen level results in uniform tissue growth.
(Adapted from Hariharan 2015)

1.5 Functional interactions between polarity proteins and the Hippo pathway

Polarity proteins establish and maintain apical-basal polarity in epithelial cells

Epithelial cells are highly polarized in that their cell membrane is partitioned into discrete domains to carry out distinct functions. The apical domain contacts the external environment or a lumen, the lateral domain connects neighboring cells to form an epithelial sheet, and the basal domain anchors the epithelial sheet to the basement membrane (Laprise and Tepass 2011; Campanale, Sun, and Montell 2017). Epithelial cells are connected primarily through two sets of cell-cell junctions. In *Drosophila*, they are the adherens junction (AJ) located at the apical end of the lateral domain and the septate junction (SJ) located just basal to the AJs (Figure 1.3). AJs provide cohesion between neighboring cells whereas SJs limit paracellular diffusion to support the barrier function and the selective permeability of epithelia (Banerjee, Sousa, and Bhat 2006; Laprise and Tepass 2011).

AJs divide the cortical region into apical and basolateral domains. Two distinct sets of polarity proteins localize to these domains to establish and maintain their identity through complex interactions (St Johnston and Ahringer 2010; Nance and Zallen 2011; Laprise and Tepass 2011; Campanale, Sun, and Montell 2017). Apical polarity proteins localize to the apical domain and are usually divided into two functional groups: the Par complex and the Crumbs (Crb) complex. The Par complex consists of atypical protein kinase C (aPKC), its regulatory subunit Par6, the Rho-GTPase Cdc42, and the scaffolding protein Bazooka (Baz; *Drosophila* homolog of the *C. elegans* and mammalian Par3). The Crb complex consists of the transmembrane protein Crb, Stardust (Sdt; *Drosophila* homolog of mammalian PALS1), and the scaffolding protein Patj. Basolateral polarity proteins localize to the basolateral domain and include the Lethal giant larvae (Lgl)/Discs large (Dlg)/Scribble (Scrib) group, the Yurt (Yrt)/ Coracle (Cora)/Na+,K+-

ATPase/Neurexin IV (Nrx-IV) group and the kinase Par1(Laprise and Tepass 2011; Tepass 2012). Positive feedback within the apical polarity proteins and basolateral polarity proteins and cross-inhibition between the two sets of proteins establish and maintain apical-basal polarity of epithelial cells (Figure 1.3).

Basolateral polarity proteins Scrib, Dlg, and Lgl regulate the Hippo pathway

The basolateral polarity protein genes *lgl, dlg,* and *scrib* were originally identified as "neoplastic" tumor-suppressors as loss of any of these genes in the entire animal results in multilayered and invasive tumors in *Drosophila* imaginal discs (Bilder 2004). Later studies have connected the overgrowth phenotype to over-activation of Yki, suggesting the three basolateral polarity proteins are positive regulators of the Hippo pathway (Enomoto and Igaki 2011; Richardson and Portela 2017).

The regulation of Hippo signaling by Lgl may be context dependent. Disrupting Lgl in both eye and wing imaginal discs causes Yki activation. In the eye imaginal discs where clonal Lgl loss does not disrupt cell polarity or activate Jun kinase signaling (JNK signaling pathway, a MAPK signaling pathway regulated by diverse cellular stresses including disruption of cell polarity (Bogoyevitch et al. 2010)) , Hpo is mislocalized, suggesting Lgl promotes proper localization of Hpo (Grzeschik et al. 2010). By contrast, in the wing imaginal discs, depleting Lgl with RNAi disrupted cell polarity and caused activation of JNK signaling. JNK signaling in turn activates Yki (G. Sun and Irvine 2011). Furthermore, one report suggests JNK activates the Wts inhibitor Jub through phosphorylation (G. Sun and Irvine 2013), providing a mechanistic link between basolateral polarity, JNK signaling and Yki activity.

Figure 1.3

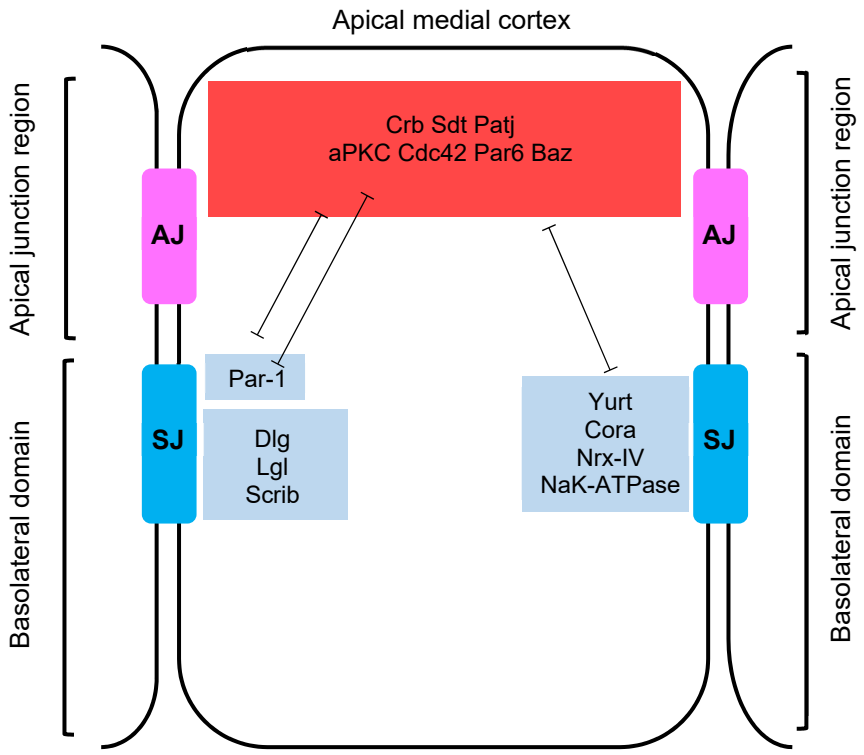

Apical-basal polarity in epithelial cells
Apical-basal polarity in epithelial cells are established and maintained by polarity proteins. Apical polarity proteins are usually divided into two functional groups: the Par complex and the Crumbs (Crb) complex. The Par complex consists of atypical protein kinase C (aPKC), Par6, Cdc42, and Bazooka (Baz). The Crb complex consists of Crb, Stardust(Sdt), Patj. Basolateral include the Lethal giant larvae (Lgl)/Discs large (Dlg)/Scribble (Scrib) group, the Yurt (Yrt)/ Coracle (Cora)/Na+,K+-ATPase/Neurexin IV (Nrx-IV) group and the kinase Par1. Positive feedback within the apical polarity proteins and basolateral polarity proteins and negative-feedback loops between the two sets of proteins establish and maintain apical-basal polarity of epithelial cells.

AJ, adherens junction; SJ, septate junction. (Adapted from Laprise and Tepass 2011)

The regulation of the Hippo pathway by Scrib is even more complicated. Unlike *lgl* mutant clones that mildly overgrow, *scrib* mutant clones are eliminated by the neighboring cells through cell competition (Grzeschik et al. 2010 Chen et al. 2012). Depleting Scrib using RNAi causes down-regulation of Hippo pathway target gene *Diap1* (Grzeschik et al. 2010). These results suggest that Yki is inactivated in *scrib* mutant clones, seemingly inconsistent with Scrib's role as a positive regulator of the Hippo pathway. Interestingly, blocking JNK signaling in *scrib* clones leads to Yki activation and reverts the clone loss phenotype to a severe overgrowth phenotype, suggesting JNK signaling actively represses Yki activity in *scrib* clones. This effect presumably outweighs the release of Yki suppression by Scrib (Chen et al. 2012). How JNK signaling represses Yki in this scenario is unknown, though one study suggests JNK can inhibit Yki activity through Wts (Enomoto et al. 2015).

Apical polarity proteins Crb and aPKC regulate the Hippo pathway

Apical polarity proteins reside in the apical cell cortex where many Hippo pathway components concentrate. Not surprisingly, they have been found to regulate the Hippo pathway. Crb was the first apical polarity protein found to be involved in Hippo pathway regulation. Both ectopic expression and loss of Crb result in Yki activation, up-regulation of Hippo pathway target genes, and overgrowth (Chen et al. 2010; Ling et al. 2010; Robinson et al. 2010; Grzeschik et al. 2010). On one hand, Crb physically interacts with Ex and recruits Ex to the apical junctional region to promote Hippo pathway activity (Chen et al. 2010; Ling et al. 2010; Robinson et al. 2010; Grzeschik et al. 2010). On the other hand, Crb also promotes ubiquitin-mediated degradation of Ex through E3 ubiquitin ligase F-box protein Slimb/β-TrCP (Slmb) (Ribeiro et al. 2014).

Therefore, Crb allows for precise tuning of Hippo pathway activity through its dual regulation of Ex.

aPKC is also implicated in Hippo pathway regulation. Expression of a dominant-negative aPKC transgene suppresses Hippo pathway inactivation in *lgl* clones (Grzeschik et al. 2010). Ectopic expression of a membrane tethered aPKC with a CAAX prenylation motif ($aPKC^{CAAX}$) causes mis-localization of Hpo, activation of Yki, and up-regulation of Hippo pathway target genes, recapitulating the *lgl* mutant phenotype (Grzeschik et al. 2010; G. Sun and Irvine 2011). These results suggest aPKC may negatively regulate the Hippo pathway through Lgl inhibition. Up to now there is no published loss-of-function analysis on aPKC to further test this hypothesis.

Regulation of apical polarity proteins by the Hippo pathway

The functional interactions between polarity proteins and Hippo signaling are not unidirectional. In the original studies on *wts*, hypertrophy of the apical domain was observed by electron microscopy in *wts* clones (T. Xu et al. 1995; Justice et al. 1995). Two recent studies found that inactivation of multiple Hippo pathway components as well as ectopic expression of Yki result in increased abundance of apical polarity proteins Crb, aPKC and Patj at the AJR (Genevet et al., 2009; Hamaratoglu et al., 2009). The hypertrophy of the apical domain and increased abundance of apical polarity proteins are dependent on Crb as removing Crb suppresses these phenotypes (Genevet et al. 2009; Hamaratoglu et al. 2009). Surprisingly, *crb* transcription is not affected upon ectopic Yki expression, suggesting *crb* is not a Hippo pathway target gene. Likewise, *aPKC* is not a clear Hippo pathway target gene (Genevet et al. 2009). These results suggest at least two non-mutually exclusive explanations. First, there may be a transcriptional target of Yki that is required to promote apical hypertrophy together with Crb. Second, the increased abundance of apical

polarity proteins may be caused by a post-translational mechanism. One possible cellular mechanism for apical hypertrophy in Hippo mutant clones is through regulation of endocytosis. In fact, the Yki targets *ex* and *Mer* have been found to affect endocytosis (Maitra et al. 2006). Alternatively, Yki may have a previously unidentified non-transcriptional function to directly influence stability of apical polarity proteins.

The mutual regulation of apical polarity proteins and the Hippo pathway raises the possibility of feedback regulation between them (Tepass 2012). This feedback could work in a scenario in which a minor defect in apical basal polarity is counteracted by enhanced Yki-dependent enrichment of apical polarity proteins. This could be important during morphogenetic changes and wound-healing, in which the apical basal polarity machinery undergoes rapid remodeling and therefore may be temporarily compromised (Tepass 2012).

1.6 Concluding remarks and dissertation outline

The regulation of the Hippo pathway has evolved into a complex network over the past two decades, with new players added at an unprecedented pace. Additional regulators are likely to be discovered to add even more complexity into this regulatory network. However, within this ever more puzzling network, there are two recurring themes. The first theme is that most Hippo pathway regulation seems to happen at the cell cortex. Both the core components of the pathway and most of its regulators are localized at this region. Mis-localization of the core components leads to pathway inactivation whereas recruitment of the core components to the cortex promotes pathway activation. This region also integrates inputs from mechanical cues and biochemical signals to regulate pathway activity. Future studies on how different modes of regulation are

coordinated and integrated at the cortex would provide a better understanding of the logic of Hippo pathway regulation.

The second major theme in Hippo signaling is feedback regulation. Multiple positive and negative feedback loops have been proposed to regulate Hippo pathway output. How these feedback loops are coordinated during normal development is another key area of future studies.

In this dissertation, I will focus on two mechanims of Hippo pathway regulation, namely cytoskeletal tension and apical polarity proteins. In Chapter 2, I will describe a novel function of Yki at the cortex to promote tension, the molecular mechanism of this function, and its physiological relevance in normal growth. In Chapter 3, I will describe further analysis of the functional interactions between apical polarity proteins and the Hippo pathway. Together, these studies elucidate new modes of Hippo pathway regulation and hopefully will help us gain more insights into organ size regulation in development.

CHAPTER 2

Yorkie functions at the cell cortex to promote myosin activation in a Non-transcriptional manner

2.1 Introduction

The Hippo signaling pathway is an important regulator of growth that controls cell proliferation, apoptosis and differentiation (Irvine and Harvey, 2015; Yu et al., 2015). The core components of the Hippo pathway consist of upstream regulators, a kinase cascade including Tao, Hippo (Hpo) and Warts (Wts), and a downstream effector, Yorkie (Yki). Despite intensive studies since its discovery more than a decade ago, the molecular mechanisms through which the Hippo pathway is regulated *in vivo* are yet to be fully understood.

Studies so far identify Yki as a transcriptional co-activator that functions in the nucleus to promote target gene expression. Current models propose that when the Hippo pathway is active Yki is phosphorylated and retained in the cytoplasm, while in the absence of pathway activity Yki remains unphosphorylated and accumulates in the nucleus. Thus, the activation state of the Hippo pathway regulates Yki's subcellular localization and activity. This cytoplasmic versus nuclear localization of Yki has been the focus of past studies on Yki regulation, with an underlying assumption that cytoplasmic Yki is sequestered from the nucleus and therefore is transcriptionally inactive.

In epithelial cells, the Apical Junctional Region (AJR) is an important hub for regulation of Hippo pathway activity (Boggiano and Fehon, 2012; Meng et al., 2016; Sun and Irvine, 2016; Su et al., 2017). The AJR is a cortical region that extends from the lateral edge of the apical cortex through the adherens junctions (AJs). The upstream regulators of the Hippo pathway as well as the core kinases have been shown to localize to the AJR where they organize into signaling complexes

(Boggiano and Fehon, 2012; Sun et al., 2015; Chung et al., 2016). The AJR also contains actomyosin networks that both generate and respond to cytoskeletal tension. Importantly, in both vertebrates and *Drosophila* cytoskeletal tension has been implicated as a negative regulator of the Hippo pathway. Increased cytoskeletal tension promotes Yki or YAP/TAZ (vertebrate orthologues of *Drosophila yki*) nuclear localization and transcriptional activity (Dupont et al., 2011; Aragona et al., 2013; Rauskolb et al., 2014).

In this study, we demonstrate a novel function of Yki at the cell cortex separate from its well characterized role as a transcriptional co-activator. We show that endogenously expressed Yki accumulates at the AJR, particularly under conditions where upstream pathway activity is reduced. Remarkably, experimentally tethering Yki to the cell cortex results in strong activation of cortical myosin in a manner that is independent of Yki's transcriptional functions. Structure/function analysis indicates that the N-terminal domain of Yki is responsible for this function, and mutation of this domain using CRISPR/Cas9 genome editing results in tissue undergrowth. Furthermore, we show that Yki promotes myosin activation via the upstream regulatory kinase Stretchin-Mlck. We propose a model in which Yki at the cell cortex promotes myosin activation, which in turn activates Yki by suppressing the Hippo pathway, thereby forming a positive feedback loop. Such positive feedback may serve to amplify the effects of tension on Yki's growth promoting activity independently of, and antagonistically to, the transcriptionally-based negative feedback previously proposed.

This chapter was published in Developmental Cell (Xu et al. 2018).

2.2 Results

Yki localizes to the apical junctional region (AJR) in addition to the nucleus

We recently described a YFP-tagged Yki transgene, expressed under its normal promoter, whose subcellular distribution responds to pathway activity (Su et al., 2017). To better characterize Yki subcellular localization at different states of pathway activity, we generated *wts* mutant clones and used confocal imaging to examine Yki-YFP localization in live wing imaginal tissues. While wild-type cells displayed a primarily diffuse cytoplasmic distribution of Yki-YFP, in *wts* clones we observed strong nuclear Yki-YFP localization (Figure 2.1B-B'), as previously reported (Oh and Irvine, 2008; Su et al., 2017). We also found strong enrichment of Yki-YFP at the AJR in *wts* mutant cells (Figure 2.1C-C'), as previously reported (Oh et al., 2009). Furthermore, careful observation of apical sections through wild-type cells revealed less distinct but still clear junctional accumulation in normal tissues as well (Figure 2.1D). We noted that while readily apparent in live tissues, this junctionally-localized Yki was much less obvious after fixation (data not shown), which likely explains why it has not been reported previously.

One possible interpretation of these results is that when Hippo pathway activity is decreased, Yki not only accumulates in the nucleus, but also is recruited to the AJR. To further test this idea, we inactivated the Hippo pathway in an alternative fashion by inducing increased cytoskeletal tension. Recent studies in Drosophila have shown that cytoskeletal tension generated by activation of myosin represses pathway activity, resulting in increased Yki target gene expression (Rauskolb et al., 2014). We found that ectopic expression of activated *Drosophila* non-muscle myosin II regulatory light chain Spaghetti Squash (Sqh^{DD}), which constitutively activates myosin contractility (Mitonaka et al., 2007), resulted in a modest increase in nuclear Yki (Figure 2.1E) and also resulted in marked Yki accumulation at the AJR (Figure 2.1F). This result again

Figure 2.1

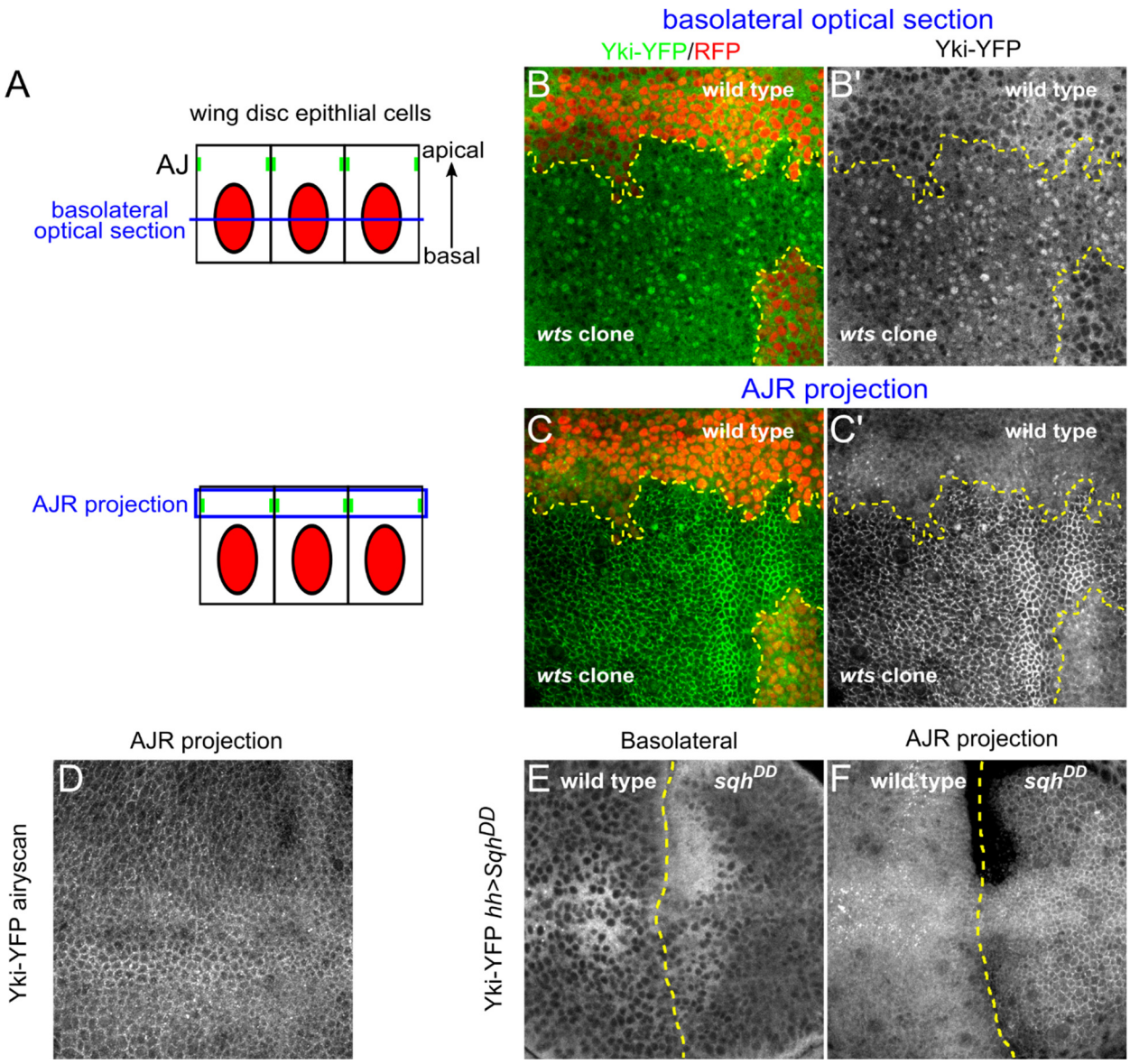
A
wing disc epithlial cells
AJ
apical
basal
basolateral
optical section
AJR projection
basolateral optical section
Yki-YFP/RFP
Yki-YFP
B
wild type
wts clone
B'
wild type
wts clone
AJR projection
C
wild type
wts clone
C'
wild type
wts clone
AJR projection
D
Yki-YFP airyscan
Basolateral
AJR projection
Yki-YFP hh>SqhDD
E
wild type
sqhDD
F
wild type
sqhDD

Figure 2.1 continued
Yki localizes to the apical junctional region (AJR) in addition to the nucleus

(A) Illustrations showing cross-sectional views of the imaginal epithelium and the approximate positions of basolateral and AJR images shown in this study. As indicated in blue, basolateral images are single sections while AJR views are maximal projections of a small number of apical sections to compensate for curvature of the epithelium.
(B-C') The effect of Hippo pathway inactivation on Yki subcellular localization. In basal sections of live tissues containing wts null mitotic clones (clone marked by the absence of RFP and a yellow dashed line), Yki-YFP is primarily cytoplasmic in normal imaginal tissue, but is strongly nuclear in *wts* mutant cells (B-B'). Apically, Yki-YFP is slightly enriched at the apical cortex in normal tissues, but strongly recruited to the AJR in wts null clones (C-C').
(D) Yki localizes to the AJR in normal tissues. A super-resolution image (using the Zeiss Airyscan that improves resolution and signal-to-noise) of a live wing disc carrying two copies of endogenously expressed Yki-YFP in a yki^{B5} null background. A maximum projection of apical optical sections shows cortical localization of Yki-YFP apically.
(E-F) The effect of increasing cytoskeletal tension on Yki subcellular localization. Decreasing Hippo pathway activity by increasing cytoskeletal tension in cells that express a constitutively active form of the myosin regulatory light chain, SqhDD, caused increased nuclear and AJR localization of Yki-YFP. The boundary of SqhDD expression, under the control of *hh>Gal4*, is marked with a dashed yellow line.

indicates that Yki can accumulate both in the nucleus and at the AJR, and further that increased cytoskeletal tension results in greater cortical Yki accumulation.

Cortical Yki promotes activation of myosin independently of Yki transcriptional activity

We next asked if cortical Yki could have a previously unrecognized cellular function in developing tissues. As an initial test, we generated a form of Yki that is constitutively targeted to the cell cortex by fusing the myristoylation signal sequence from *Drosophila* Src kinase to the N-terminus of Yki (Myr-Yki, Figure 2.2A). Myr-Yki expressed in the wing epithelium appeared tightly membrane associated and enriched in the apical domain of cells, as has previously been observed for other Myr-tagged proteins (Neisch et al., 2013; Figure 2.2B-C'').

Observation of the wing imaginal disc revealed that expression of Myr-Yki using the *apterous-Gal4* (*ap-Gal4*) driver caused an indentation or furrowing of the epithelium just inside the boundary of expression, while expression of wild-type Yki did not (Figure 2.3A-B). We previously observed a similar epithelial indentation phenotype from mild Rho1 activation in the wing epithelium, which we inferred was caused by increased myosin-based contractility (Neisch et al., 2013). To test if this was the case in cells expressing Myr-Yki, we used a phospho-specific antibody against Sqh (pSqh), as an assay for myosin activity (Zhang and Ward, 2011). Remarkably, we observed a dramatic increase of pSqh staining that was specific to Myr-Yki expressing cells (Figure 2.3E-E'). We also examined myosin levels because myosin is known to accumulate at the cell cortex in response to cytoskeleton tension (Fernandez-Gonzalez et al., 2009; Rauskolb et al., 2014; Kim et al., 2015; Pan et al., 2016). Sqh levels at the cortex assayed either by Sqh antibody staining or using the sqh:mCherry reporter (Martin et al., 2009) increased in cells expressing Myr-Yki. (Figure 2.3G-J). Together these results indicate that cortically targeted Yki

Figure 2.2

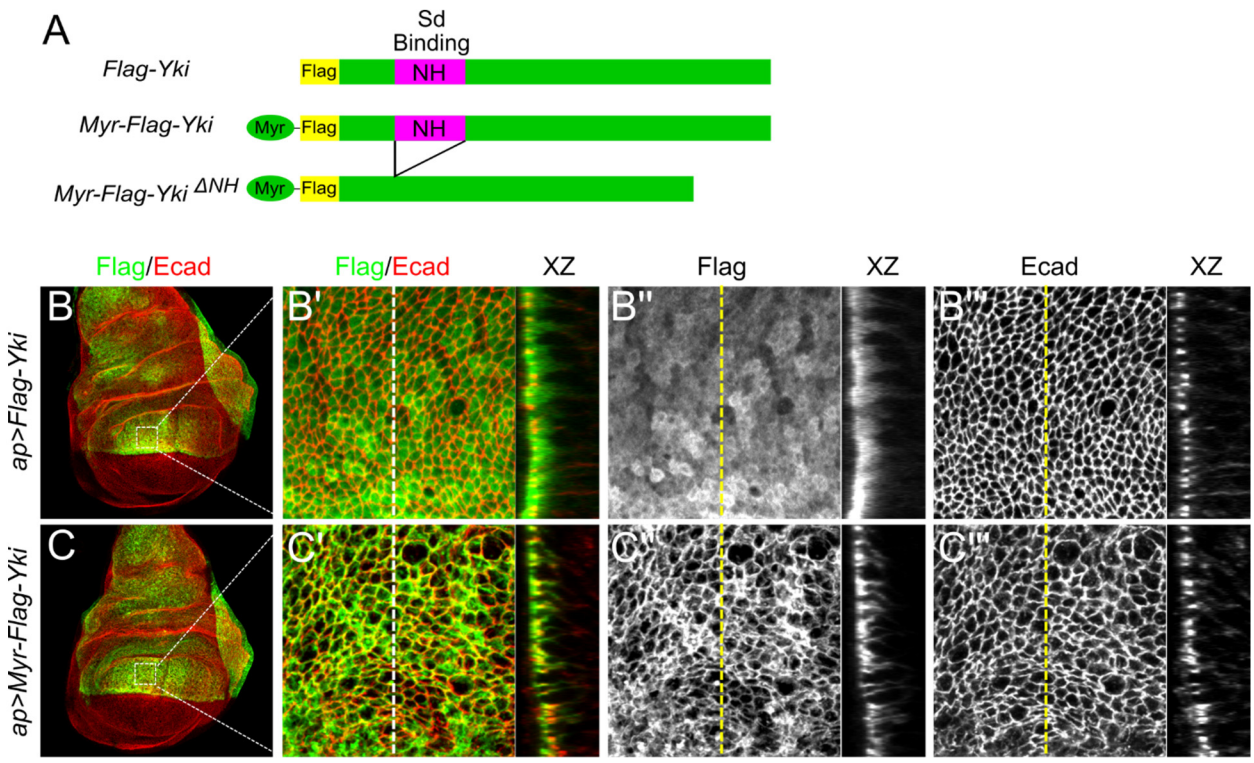

Myristoylation signal sequence targets Yki to the cell cortex

(A) Cartoons showing UAS transgenes used in B-C. To provide a membrane tether, an N-terminal myristoylation signal sequence was added to Yki (Myr-Yki) or YkiΔNH (Myr-YkiΔNH). The NH domain binds Scalloped (Sd).

(B-C) Myr-yki expressed in the wing epithelium is tightly membrane-associated and enriched at the AJR.

Flag-tagged wild-type Yki and Myr-Yki were ectopically expressed in the dorsal compartment of wing discs and stained with anti-Flag and anti-Ecad. Ecad staining was used to mark AJs. Boxes in B, C) indicate area of wing disc shown in (B' -B''' and C-C'''). Wild-type Yki appeared mostly cytoplasmic whereas Myr-Yki is enriched cortically. XZ planes show cross-section views as marked by the dashed lines.

Figure 2.3

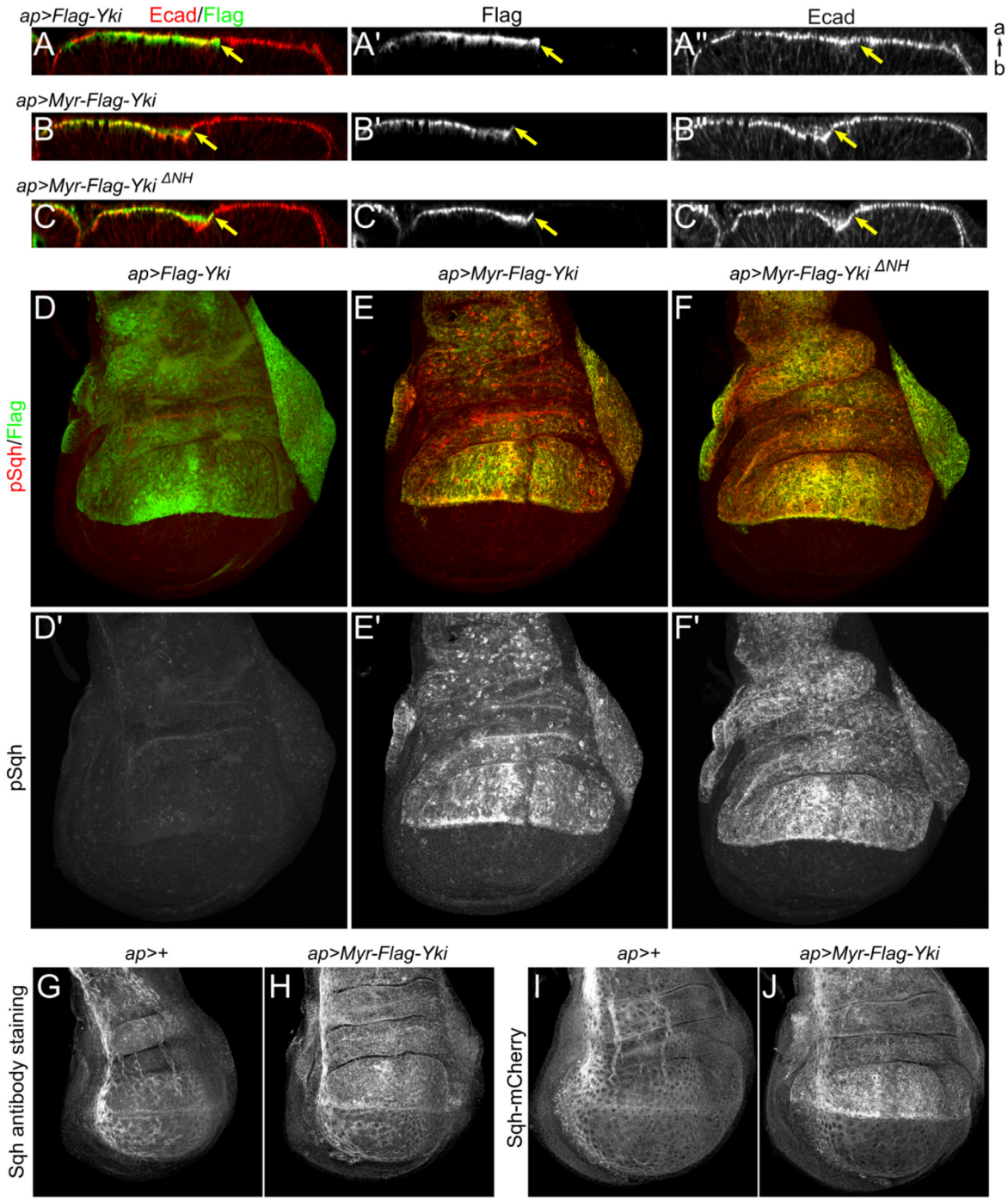
ap>Flag-Yki
Ecad/Flag
Flag
Ecad
A
A'
A''
a
b
ap>Myr-Flag-Yki
B
B'
B''
ap>Myr-Flag-Yki ΔNH
C
C'
C''
ap>Flag-Yki
ap>Myr-Flag-Yki
ap>Myr-Flag-Yki ΔNH
pSqh/Flag
D
E
F
pSqh
D'
E'
F'
ap>+
ap>Myr-Flag-Yki
ap>+
ap>Myr-Flag-Yki
Sqh antibody staining
G
H
Sqh-mCherry
I
J

Figure 2.3 continued
Cortical Yki promotes activation of myosin

(A-C") Ectopic expression of membrane-associated Yki induces indentation of the epithelium. apterous-Gal4 (ap-Gal4) was used to drive expression of transgenes in the dorsal compartment of wing discs. Optical cross-sections of the epithelium show that expression of Myr-Yki or Myr-YkiΔNH, but not wild-type Yki, induces indentation of wing disc epithelium at the expression boundary (marked by yellow arrows). Ecad staining marks adherens junctions. a, apical; b, basal.
(D-F') Ectopic expression of membrane-associated Yki induces increased myosin activation. Anti-phospho-Sqh (pSqh), which specifically recognizes activated myosin regulatory light chain, was used to assay myosin activation. Expression of Myr-Yki or Myr-YkiΔNH, but not wild-type Yki, induces a dramatic increase in pSqh staining, indicating increased myosin activation. Images are maximal projections of apical optical sections.
(G-J) Membrane-associated Yki promotes cortical accumulation of myosin.
Anti-Sqh staining and a sqh:mCherry reporter were used to assay Sqh levels in cells expressing Myr-Yki. Myr-Yki caused a noticeable increase in anti-Sqh staining and Sqh-mCherry fluorescence, indicating increased myosin accumulation at the cell cortex.

strongly induces myosin activation, and suggest that Yki, whose activity is regulated by actomyosin contractility, might in turn feedback on the actomyosin activation state in the disc epithelium.

Previous studies have shown that YAP positively regulates myosin activity by transcriptionally upregulating genes that activate the myosin regulatory light chain or inhibit myosin light chain phosphatases (Porazinski et al., 2015; Lin et al., 2017). However, in our experiments, Myr-Yki, which was targeted to the plasma membrane, should have been transcriptionally inactive. Consistent with the idea that Myr-Yki functions at the cell cortex rather than in the nucleus to promote myosin activation, ectopic expression of wild-type Yki caused neither indentation of the imaginal epithelium nor increased pSqh staining (Figure 2.3A, D-D').

An alternative possibility is that while Myr-Yki itself is sequestered at the cell cortex, it has a dominant-negative effect on the upstream Hippo pathway machinery. As a result, endogenously expressed Yki could promote greater expression of pathway targets that activate myosin. Therefore, we next tested if the Myr-Yki induced myosin activation depends on endogenous Yki. We examined myosin activation in *yki* null clones that expressed either wild-type Yki or Myr-Yki using mosaic analysis with a repressible cell marker (MARCM; Figure 2.4A-B'). Expression of wild-type Yki did not cause upregulation of pSqh (Figure 2.4A-A'). Conversely, in *yki* null clones that expressed Myr-Yki, pSqh staining was still dramatically increased (Figure 2.4B-B'). These results indicate Myr-Yki induced myosin activation does not depend on increased expression of target genes driven by endogenous Yki.

Finally, to further rule out the possibility that Yki-mediated transcription plays a role, we tested the effect of removal of Scalloped (Sd), the main DNA-binding partner of Yki that is necessary for its transcriptional output (Wu et al., 2008). We generated *sd* null clones that

Figure 2.4

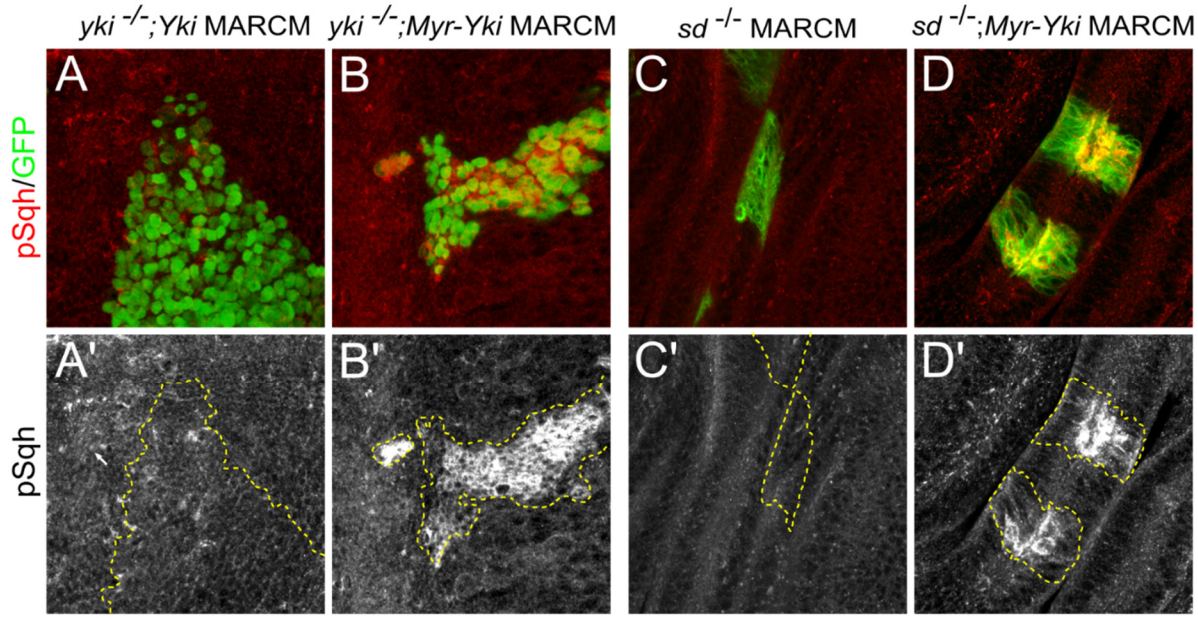

Cortical Yki promotes activation of myosin independently of Yki transcriptional activity
(A-B') Myosin activation caused by membrane-associated Yki is not dependent on endogenous Yki. Either wild-type Yki or Myr-Yki is expressed in yki null (ykiB5) mitotic clones (marked by GFP expression) using the MARCM technique. pSqh staining increases dramatically in Myr-Yki expressing cells but not in wild-type Yki expressing cells, suggesting that myosin activation is not downstream of Yki transcriptional activity.
(C-D') Myosin activation caused by membrane-associated Yki is not dependent on Sd. When expressed in sd null (sd47M) mitotic clones (marked with GFP) using the MARCM technique, Myr-Yki induces increased pSqh, indicating that Yki/Sd-mediated transcription is not required for myosin activation.
See also Figure S1.

simultaneously expressed Myr-Yki and found that pSqh was again dramatically increased (Figure 2.4D-D'). In addition, we generated a *Myr-yki*$^{\Delta NH}$ transgene that lacked the NH domain that mediates the binding between Yki and Sd (Wu et al., 2008). Expression of Myr-Yki$^{\Delta NH}$ also caused activation of myosin and indentation of the imaginal epithelium (Figure 2.3C-C'', F-F'). Together these results support the model that Yki has a non-transcriptional function at the cell cortex to promote myosin activation.

Yki promotes myosin activation under physiological conditions and in response to Hippo pathway inactivation

While myristoylated Yki is a useful tool for examining the role of Yki at the cell cortex, using ectopic expression of an artificially membrane-attached form of Yki could produce artifactual results. To test if endogenous Yki promotes myosin activation under normal physiological conditions, we depleted Yki with RNAi and assayed myosin activation using pSqh staining. Because Yki is required for tissue growth and strong knockdown causes severe tissue loss, we used a temperature sensitive allele of Gal80 (Gal80^{ts}; McGuire et al., 2003) and shifted to restrictive temperature two days prior to dissection to reduce Yki expression without causing significant cell death. Consistent with our hypothesis, we found that depleting Yki resulted in reduced myosin activation (Figure 2.5A-D). Together with the observations that endogenously expressed Yki-YFP localizes to the cortex (Figure 2.1D) and ectopically expressed wild-type Yki did not appreciably affect pSqh levels (Figure 2.3D-D'), this experiment suggests that Yki normally functions at the cortex to promote myosin activity.

If the model that cortical Yki activates myosin is correct, then our observation that endogenous Yki strongly accumulates at the AJR in *wts* mutant cells (Figure 2.1C) predicts that

Figure 2.5

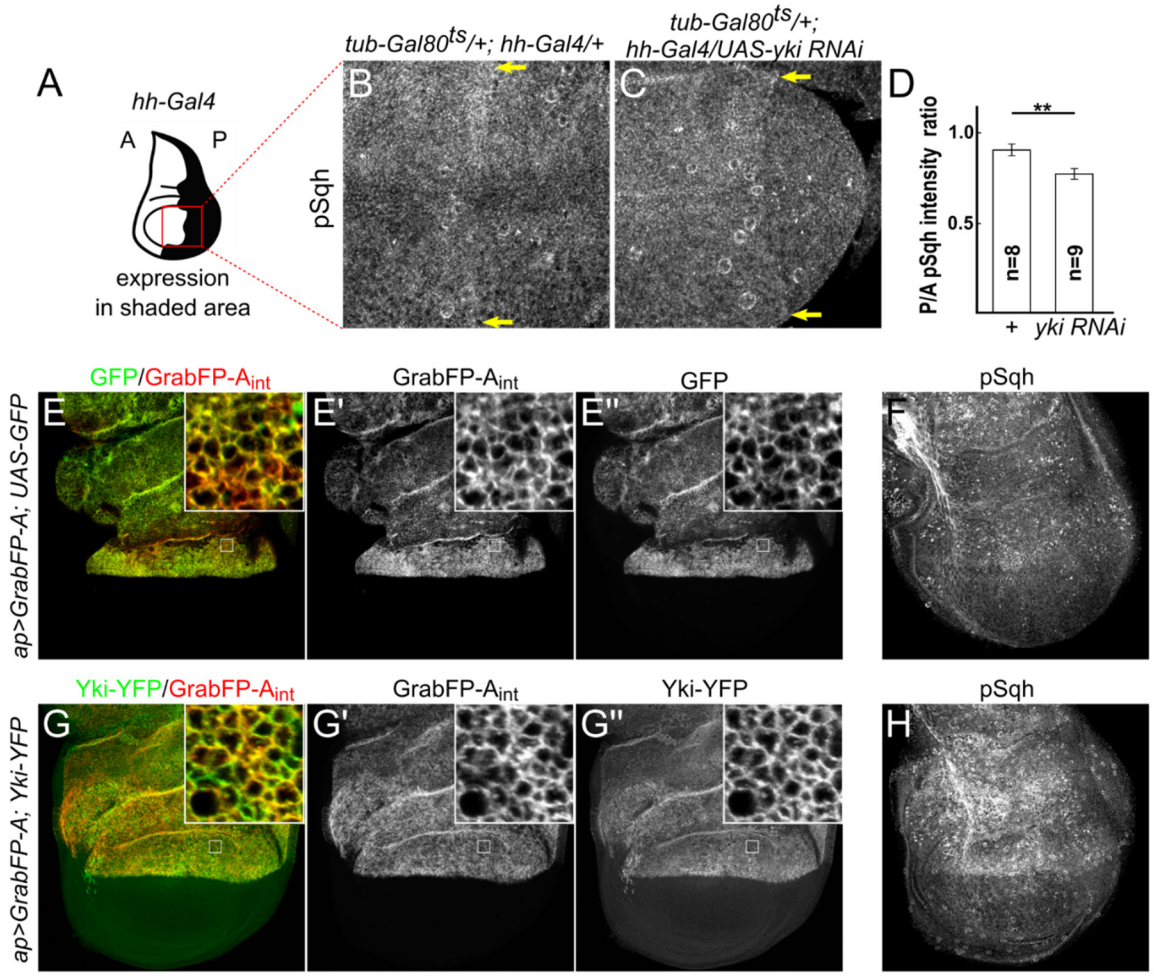

Yki promotes activation of myosin in normal development

(A) Cartoon showing expression domain of *hh-Gal4* in the wing disc. Red box indicates the approximate area of the wing shown in (B) and (C). A, anterior; P, posterior.

(B and C) Depletion of Yki results in decreased Sqh activation. Expression of a *yki RNAi* transgene for 2 days prior to dissection results in decreased pSqh staining, indicating Yki normally promotes Sqh activation. Images are maximal projections of apical optical sections. Yellow arrows indicate the hh-Gal4 expression boundary.

(D) Quantification of the ratio of pSqh staining fluorescence intensity between posterior (P) and anterior (A) compartments. There is a significant reduction of pSqh ratio in *yki RNAi* wing discs. Data are represented as mean ± SEM. Asterisks represent statistical significance of the difference between selected groups (**$p < 0.01$, one-way ANOVA and Tukey's honest significant difference (HSD) test, n = number of wing discs).

(E-H) Endogenously expressed Yki-YFP anchored at the cortex promotes myosin activation. GrabFP-Aint was used to target GFP (E-E'') or Yki-YFP (G-G'') to the AJR. Targeted Yki-YFP (H), but not GFP (F), caused increased pSqh staining.

these cells should also display increased myosin activation. Indeed, we found that loss of *wts* caused increased pSqh staining (Figure 2.6A-A'). We also examined myosin levels using Sqh:GFP and Zip:GFP (Zip=Zipper, *Drosophila* non-muscle myosin II heavy chain) reporters and found increased myosin levels at the cortex in *wts* clones (Figure 2.6C-D'). Furthermore, depletion of Yki in *wts* clones prevented an increase in pSqh staining (Figure 2.6B-B'), suggesting that endogenously expressed Yki can promote myosin activation in the wing epithelium.

While these results indicate that endogenous Yki promotes myosin activation in the imaginal epithelium, they do not distinguish between a transcriptional vs. non-transcriptional role in promoting myosin activation. Indeed, as noted earlier mammalian YAP, a Yki orthologue, is known to drive transcription of genes that promote myosin activation. To address this question further, we first asked if the increased pSqh staining observed in *wts* mutant cells is Sd-dependent by expressing a *sd*-RNAi transgene in *wts* mutant clones by MARCM. We performed these experiments in the eye imaginal disc where Sd is not required for cell viability (Koontz et al., 2013). Compared to *wts* control clones, these clones were irregular in shape, generally small (Figure 2.6F-F') and lethal in the wing (not shown), indicating that Sd was effectively depleted. In these clones, we observed increased pSqh staining relative to surrounding cells, consistent with the idea that Yki can promote myosin activation independent of its transcriptional activity. However, we note that pSqh staining in this experiment appeared somewhat weaker than in *wts* mutant control clones, suggesting the possibility that Yki has both non-transcriptional and transcriptional effects on myosin activity. Regardless, the combined observations that Yki is required for pSqh activation in wts clones and that pSqh activation was retained in the absence of Sd indicate that endogenous Yki can activate myosin in a transcriptionally-independent manner.

Figure 2.6

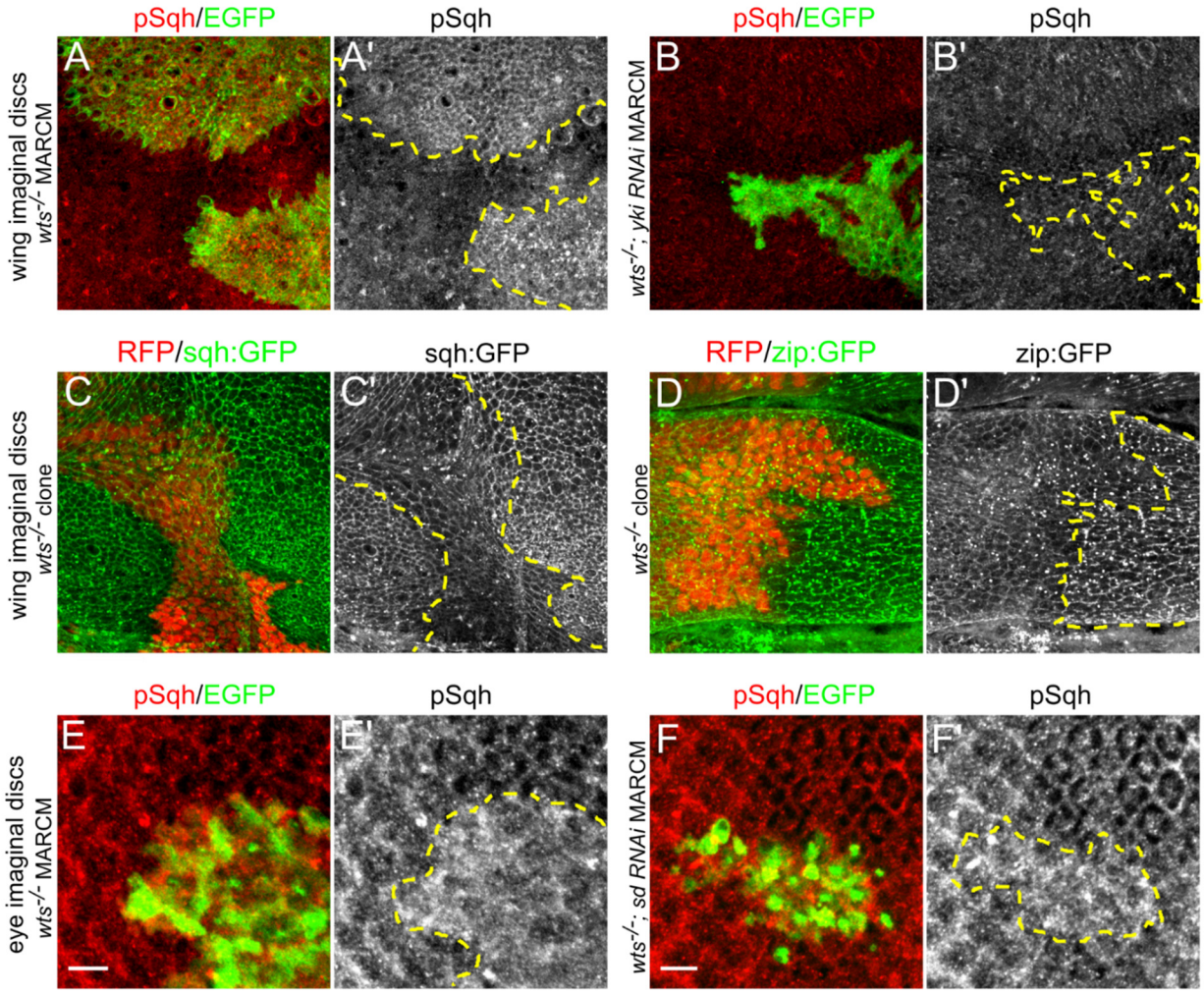

Yki promotes activation of myosin in *wts* mutant clones

(A-B') Yki promotes myosin activation in response to Hippo pathway inactivation. pSqh staining was increased in *wts* null (wts^{X1}) mitotic clones in wing discs (A-A'; clone marked with GFP and yellow dashed lines), suggesting Yki promotes myosin activation upon Hippo pathway inactivation. This increased pSqh staining is suppressed when Yki is depleted in *wts* null clones (B-B'; clone marked with GFP and yellow dashed lines), suggesting endogenous Yki can promote myosin activation.

(C-D') Sqh:GFP and Zip:GFP reporters were used to assay myosin levels in wts clones. Lack of RFP and yellow dashed lines mark wts^{X1} clones. Loss of *wts* caused increased Sqh:GFP (C') and Zip:GFP (D' levels, consistent with increased myosin activation.

(E-F') Yki promotes myosin activation independent of its transcriptional function. pSqh staining was increased in wts^{X1} null mitotic clones in eye discs (E-E'; clone marked with GFP and yellow dashed lines). This increased pSqh staining is maintained when Sd is depleted in *wts* null clones (F-F'; clone marked with GFP and yellow dashed lines), suggesting Yki promotes myosin activation independent of its transcriptional function.

As a further test of Yki's ability to activate myosin at the cortex, we made use of the GrabFP system to recruit Yki-YFP to the junctional cortex by expressing the GrabFP-A_{int} trap, which uses the Bazooka minimal localization domain tethered to an anti-GFP nanobody (Harmansa et al., 2017). Expression of this transgene strongly recruited endogenously-expressed Yki-YFP to the cortex and promoted increased pSqh staining (Figure 2.5G-H). Although qualitatively quite similar, the degree of Sqh activation was less than that observed from Myr-Yki (Table 2.1), consistent with the much lower levels of Yki-YFP expressed from its endogenous promoter in this experiment compared to Myr-Yki expressed under the Gal4/UAS system.

Cortical Yki promotes growth via the Hippo pathway

Previous studies found that increased activation of myosin results in overgrowth due to inactivation of the Hippo pathway (Rauskolb et al., 2014; Deng et al., 2015). We therefore asked if myosin activation induced by Myr-Yki has a similar effect. Consistent with this idea, both Myr-Yki and Myr-Yki$^{\Delta NH}$ caused overgrowth when expressed in the wing, similar to expression of wild-type Yki (Figure 2.7A-D, I). To test if Myr-Yki induced overgrowth is myosin-dependent, we genetically reduced myosin activity by removing one dose of *sqh* or *zip* and found that this partially suppressed the Myr-Yki overgrowth phenotype in the adult wing (Figure 2.7E-I). In contrast, heterozygosity for either *sqh* or *zip* had no effect on the overgrowth induced by ectopic expression of wild-type, untethered Yki (Figure 2.7I). Additionally, expression of Myr-Yki and Myr-Yki$^{\Delta NH}$ caused increased expression of the Hippo pathway reporter *expanded-lacZ* (*ex-lacZ*) (Figure 2.8B-C), consistent with greater Yki activity.

The model that cortical Yki promotes growth by repressing Hippo pathway activity predicts that the observed overgrowth should be dependent on endogenous Yki. To test this, first

Table 2.1

Mean Dorsal/Ventral (D/V) pSqh Fluorescence Intensity Ratio

Genotype	Mean D/V pSqh ratio	SEM	Sample size	p
apGal4>+	1.10	0.02	9	NA
apGal4>Myr-Yki (Random insertion)	2.82	0.09	10	<0.0001
apGal4>Myr-Yki (86Fb integration)	3.84	0.23	10	<0.0001
apGal4>Myr-Yki^{AcidA} (86Fb integration)	1.32	0.03	10	0.0001
apGal4>Myr-Yki$^{1-34}$-GFP (86Fb integration)	1.65	0.02	10	<0.0001
apGal4>Yki (Random insertion)	1.22	0.02	10	0.005
*apGal4>GrabFP-A$_{int}$, UAS-GF*P	1.16	0.02	11	NA
apGal4>GrabFP-A$_{int}$, Yki-YFP	1.38	0.03	10	<0.0001

Sqh activation quantified as the ratio of pSqh fluorescence intensity between D/V compartments. p value is calculated using One-Way ANOVA and Games-Howell post-hoc test. Different Yki transgenes were compared with control. GrabFP-A_{int}, Yki-YFP was compared with GrabFP-A_{int}, UAS-GFP. SEM: Standard Error of Mean.

Figure 2.7

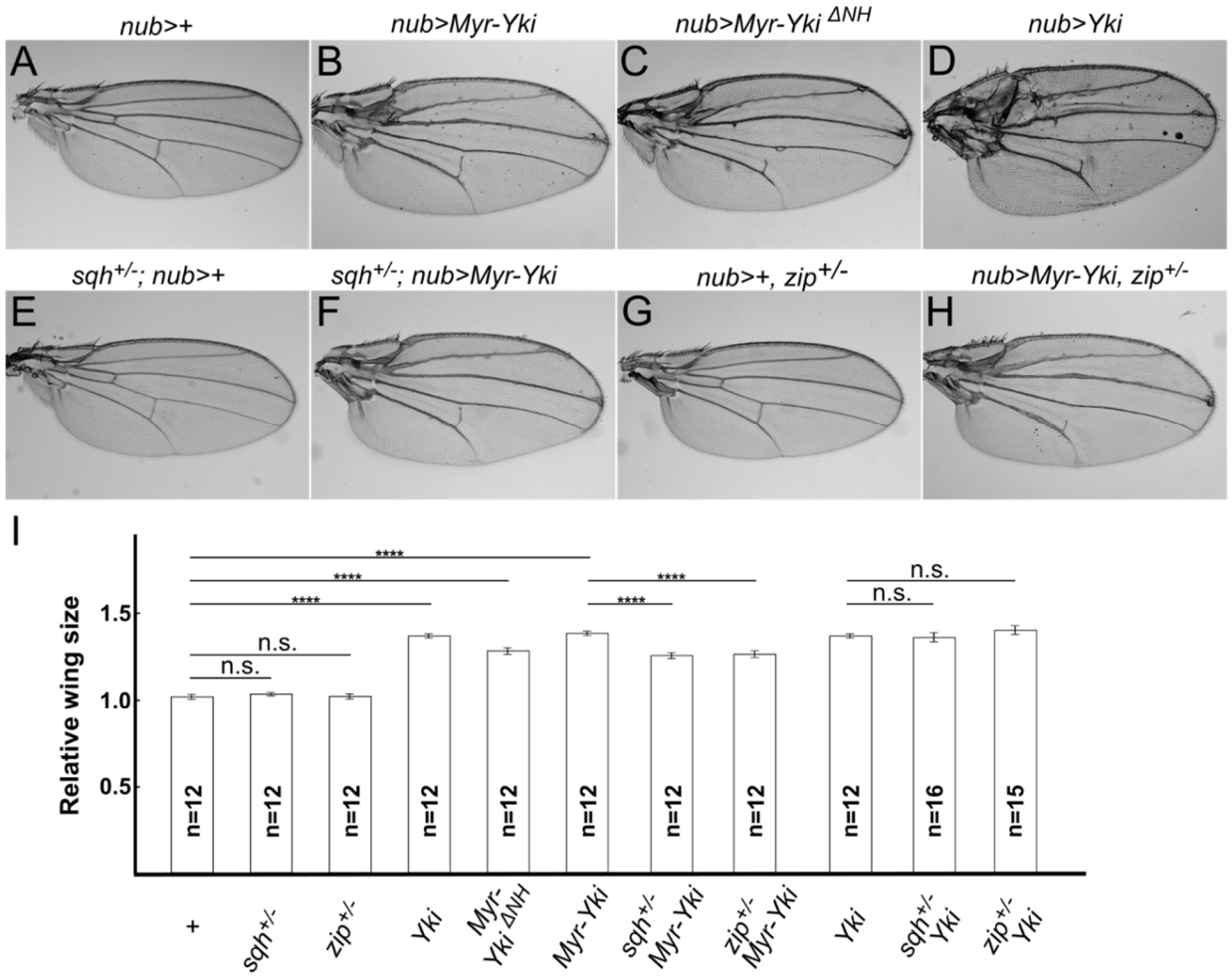

Cortical Yki promotes growth

(A–D) Expression of both wild-type and membrane-tethered Yki in the wing causes overgrowth. *nub-Gal4* was used to drive expression of the indicated Yki transgenes in the wing blade. Representative images of female adult wings (cultured at 18°C) of indicated genotypes are shown. Myr-Yki, Myr-YkiΔNH, and wildtype Yki all caused overgrowth.

(E–H) Myr-Yki-mediated overgrowth depends on myosin activity. Removing one dose of the regulatory light chain *sqh* (*sqh*^{AX3}) or the non-muscle myosin *zip* (*zip*^{1}) did not affect wing size on its own and partially suppressed the Myr-Yki overgrowth phenotype.

(I) Quantification of wing sizes for the indicated genotypes. Heterozygosity for sqh or zip suppressed the overgrowth induced by cortical, Myr-tagged Yki but not wild-type Yki. Data are represented as mean ± SEM. Asterisks represent statistical significance of the difference between selected groups (****$p < 0.0001$; n.s., not significant [$p > 0.05$], one-way ANOVA and Tukey's HSD test, n = number of wings).

Figure 2.8

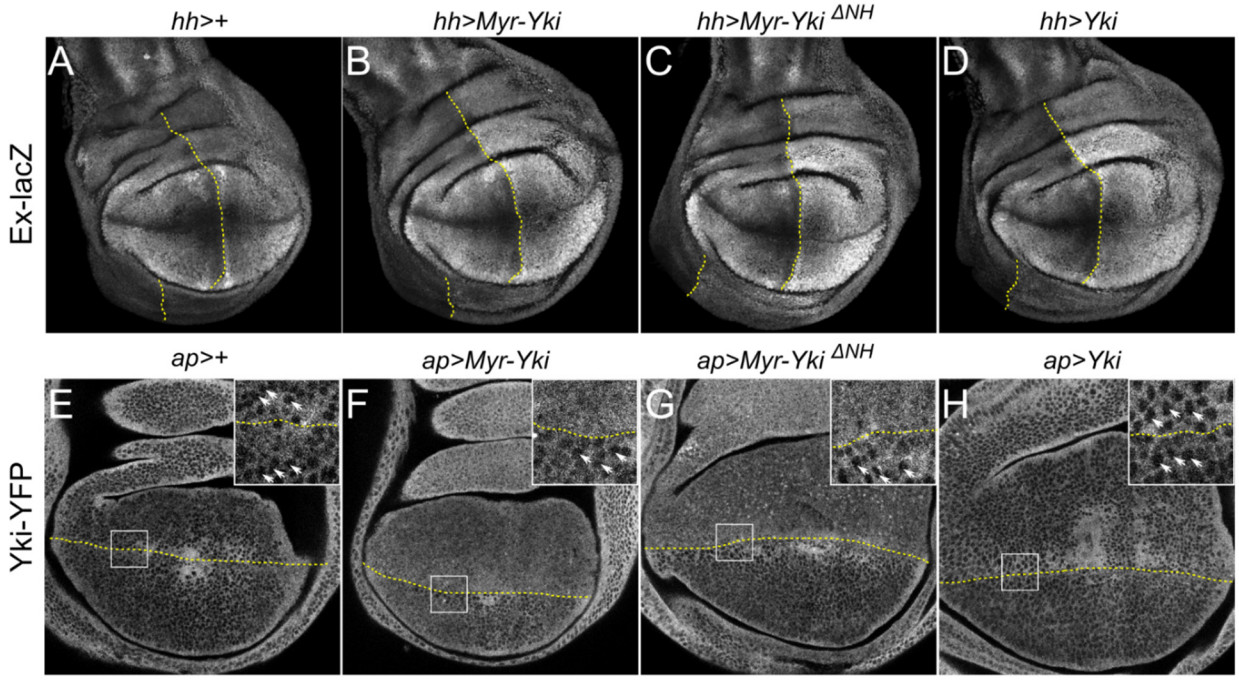

Cortical Yki promotes growth via the Hippo pathway

(A-D) Ectopic expression of Yki transgenes in wing discs causes upregulation of the Hippo pathway reporter ex-lacZ. *hh-Gal4* was used to drive expression of Yki transgenes in the posterior compartment of wing discs. The boundary of expression is marked with a dotted yellow line.
(E–H) Ectopic expression of membrane-associated Yki in wing discs causes increased nuclear localization of Yki-YFP. At the position of these optical sections, the nuclei are seen as dark circles surrounded by diffuse, cytoplasmically localized Yki-YFP in normal tissue (below the dotted yellow lines). *ap-Gal4* was used to drive expression of Yki transgenes in the dorsal compartment (above the dotted lines) of wing discs. Myr-Yki and Myr-YkiΔNH, but not wild-type Yki, caused increased nuclear localization of Yki-YFP. Boxes denote regions shown in high-magnification insets; white arrows indicate nuclei.

we examined the effect of Myr-Yki expression on nuclear localization of endogenously-expressed Yki-YFP. Both Myr-Yki and Myr-Yki$^{\Delta NH}$ caused increased nuclear accumulation of Yki-YFP relative to wild-type cells (Figure 2.8E-G). Interestingly, ectopic expression of wild-type Yki, which caused similar overgrowth to Myr-Yki expression (Figure 2.7A-D) actually resulted in slightly decreased nuclear localization of endogenously-expressed Yki-YFP (Figure 2.8H). This is expected if the ectopically expressed untethered Yki competes with endogenously-expressed Yki-YFP for nuclear entry or retention. Furthermore, we generated MARCM clones that expressed Myr-Yki, Myr-Yki$^{\Delta NH}$, or wild-type Yki in the background of a *yki* null allele. Only wild-type Yki was able to rescue undergrowth of *yki* null clones (Figure 2.9). Together our results indicate that ectopically expressed cortical Yki promotes growth by activating myosin and inactivating the Hippo pathway, thereby allowing endogenous Yki to enter the nucleus and promote growth.

Because Yki physically interacts with Sd and Wts, we considered the possibility that Myr-Yki might alter pathway activity by sequestering an interacting component at the cell cortex. To address this, we first stained wing imaginal discs with anti-Sd and found that while *Myr-Yki* expression caused dramatic cortical Sd accumulation, *Myr-Yki$^{\Delta NH}$* did not (Figure 2.10A-C'''). The observation that both the Myr-Yki and Myr-Yki$^{\Delta NH}$ transgenes caused myosin activation and overgrowth indicates that recruitment of Sd to the cell cortex is not required. Next, we asked if the effect of Myr-Yki on pathway output and growth might be attributable to the ability of Yki to bind Wts, which could sequester Wts cortically so that it cannot participate in Hippo pathway signaling. We detected no increased cortical accumulation of endogenously expressed Wts-YFP in response to Myr-Yki expression (Figure 2.11A-B'), though we did notice a slight alteration in the appearance of Wts that we speculate might be related to increased cortical contractility induced by Myr-Yki. To further test if Myr-Yki interferes with Wts function, we compared the effect of

Figure 2.9

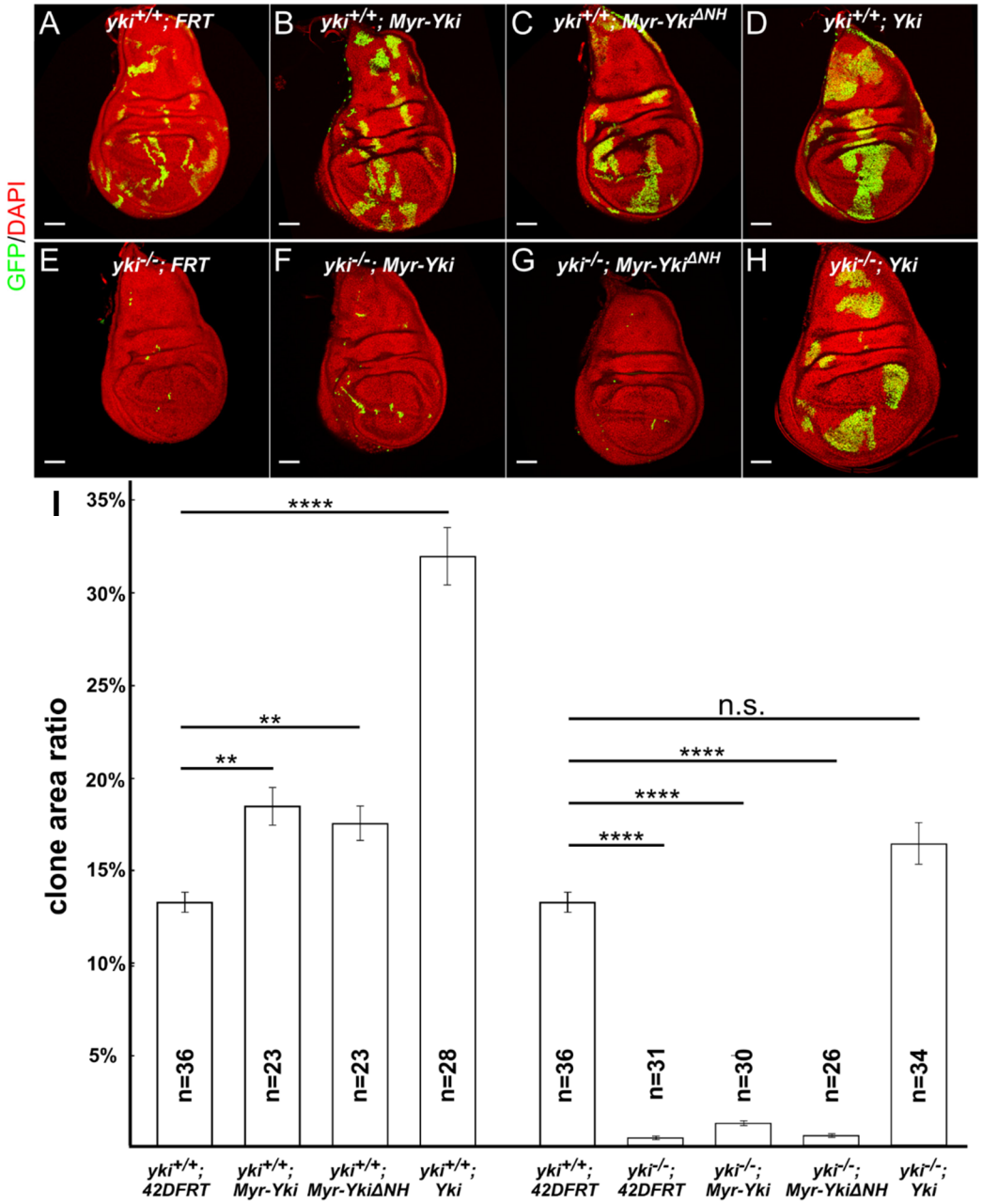

Cortical Yki promotes growth via the Hippo pathway

(A-H) MARCM clones expressing *Myr-Yki, Myr-YkiΔNH, or* wild-type *Yki* in the background of wild-type *yki* (A-D) or *yki* null (*yki*^{B5}) (E-H) were generated. All three transgenes caused overgrowth in the background of wild-type *yki. yki* null clones undergrew as expected. Wild-type *Yki* rescued the undergrowth of *yki* null clones. *Myr-Yki* and *Myr-YkiΔNH* did not rescue.
(I) Quantification of growth of mosaic clones of the indicated genotypes. Clone area ratio was obtained by dividing area of all GFP marked clones by the area of the entire disc. Data are represented as mean ± SEM. Asterisks represent statistical significance of the difference between selected groups (**** $p < 0.0001$, *** $p < 0.001$, ** $p<0.01$, n.s. [not significant, $p>0.05$], One-way ANOVA and Games-Howell test, n = number of wing discs).

Figure 2.10

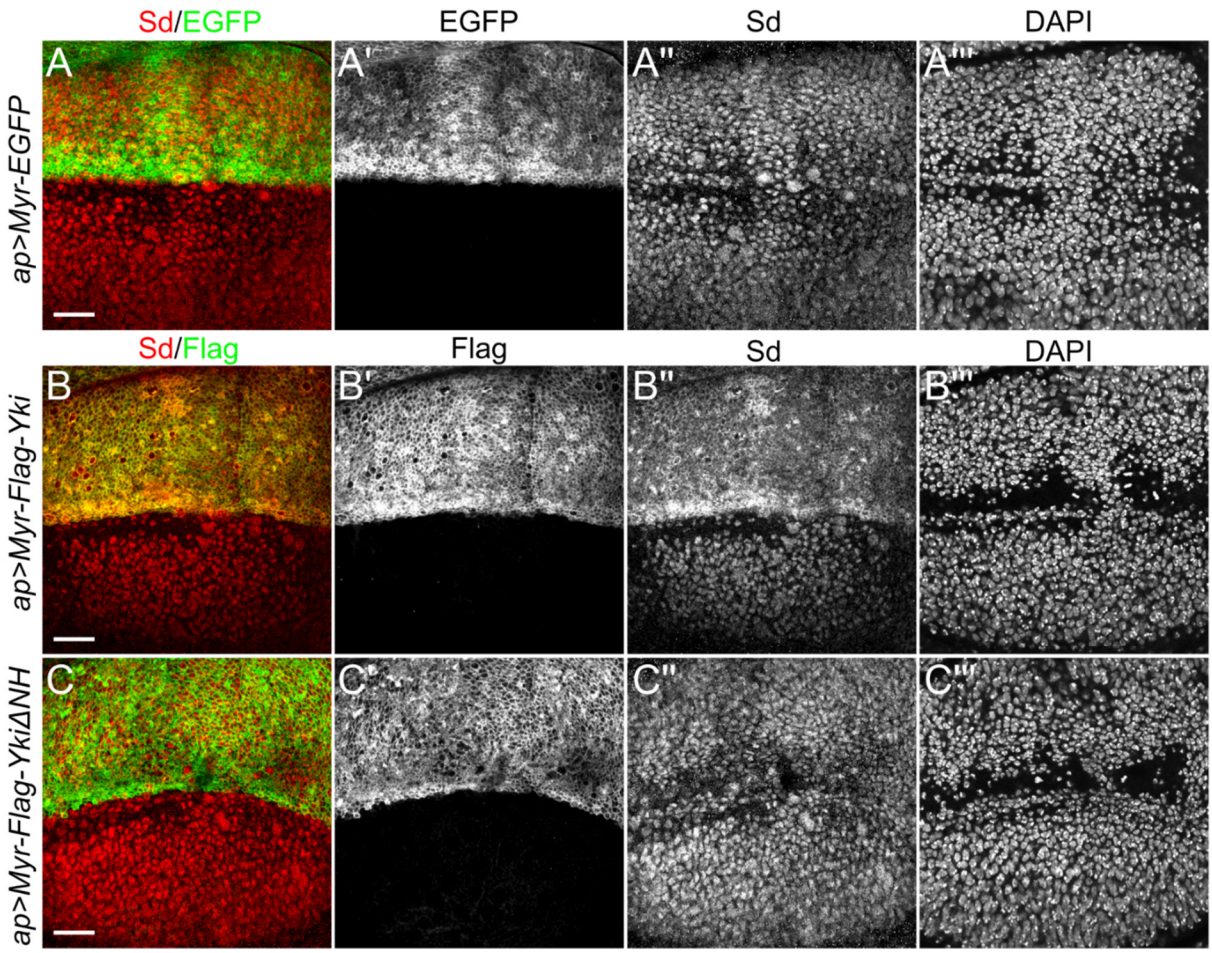

Cortical Yki recruits Sd to the cell cortex

(A-C''') *Myr-EGFP* (control) and Flag-tagged *Myr-Yki* and *Myr-YkiΔNH* were ectopically expressed in the dorsal compartment of wing imaginal discs. Anti-flag staining was used to visualize Myr-Yki and Myr-YkiΔNH localization. DAPI was used to show nuclei. Anti-Sd staining showed nuclear localization in cells expressing *Myr-EGFP* (A'') and *Myr-YkiΔNH* (C''). In contrast, in cells expressing *Myr-Yki,* Sd co-localized with Myr-Yki at the cell cortex (B'').

Figure 2.11

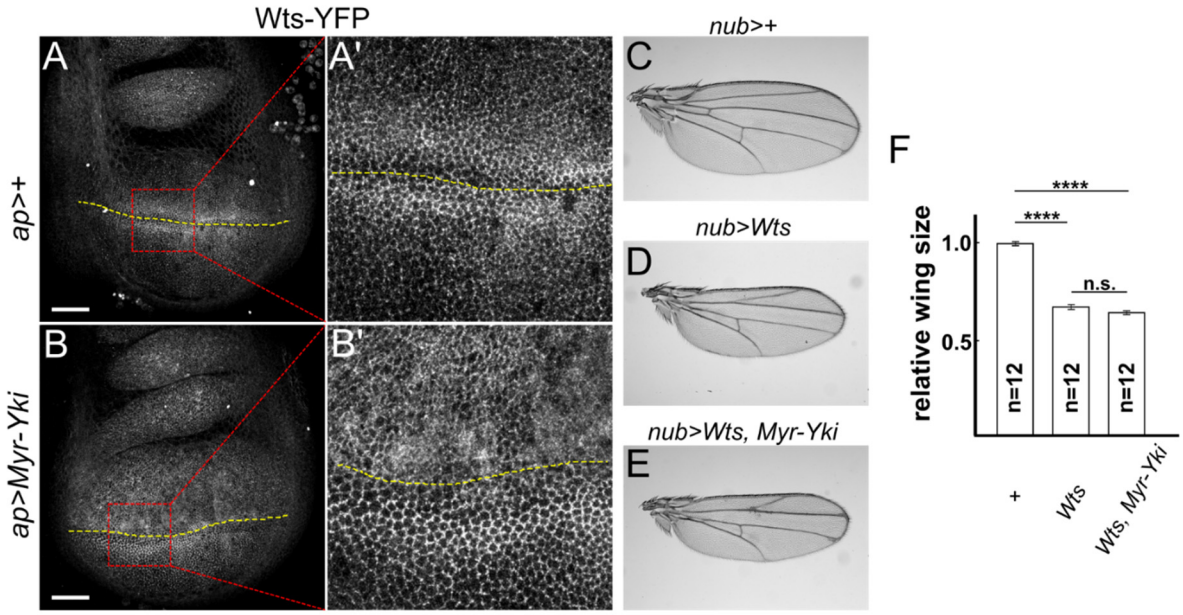

Cortical Yki does not recruit Wts to the apical junctional region (AJR) to cause its inactivation

(A-B') Myr-Yki does not sequester Wts at the AJR. Endogenously expressed Wts-YFP was examined with (B-B') or without Myr-Yki (A-A') expression. Myr-Yki expression did not cause increased cortical accumulation of Wts-YFP (B-B'). Red boxes denote regions shown in higher magnification insets (A',B'). The boundary of expression is marked with a dotted yellow line.
(C-F) Myr-Yki does not suppress Wts induced undergrowth. Representative images of female adult wings of indicated genotypes are shown (cultured at 18 °C). Ectopic expression of Wts in the wing caused strong undergrowth (D) compared with control (C). Myr-Yki expression did not suppress Wts induced undergrowth (E). (F) Quantification of wing sizes for the indicated genotypes. Data are represented as mean ± SEM. Asterisks represent statistical significance of the difference between selected groups (**** $p<0.0001$; n.s.: not significant [$p > 0.05$], One-way ANOVA and Tukey's HSD test, n = number of wings).

ectopic Wts expression alone to co-expression with Myr-Yki and found that co-expression of Myr-Yki failed to suppress Wts induced undergrowth of the wing (Figure 2.11C-F). Together these results argue against the hypothesis that Myr-Yki promotes growth by sequestering or otherwise inactivating Wts.

Yki activates Sqh via the Sqh kinase Stretchin-Mlck (Strn-Mlck)

To better understand the mechanism by which cortical Yki regulates myosin activity, we next screened known or predicted *Drosophila* myosin light chain kinases to determine if they were necessary for Yki-induced Sqh activation. Specifically, we simultaneously expressed Myr-Yki and one of at least two independent RNAi transgenes each for *Rho kinase* (*Rok*), *Death-associated protein kinase related* (*Drak*), *bent* (*bt*), *spaghetti-squash activator* (*sqa*), *genghis khan* (*gek*), *Stretchin-Mlck* (*Strn-Mlck*), *sticky* (*sti*), or *AMP-activated protein kinase α subunit* (*AMPKα*) in the wing epithelium (Maroto et al., 1992; Dong et al., 2002; D'Avino et al., 2004; Neubueser and Hipfner, 2010; Nie et al., 2014). RNAi lines for only two genes, *AMPKα and Strn-Mlck*, had any detectable effect on pSqh levels (Figure 2.12). One out of six tested *AMPKα* RNAi lines (TRiP.JF01951) displayed weak suppression (Figure 2.12U). Because this suppression was much weaker than that caused by *Strn-Mlck* RNAi and two validated *AMPKα* RNAi lines, VDRC1827 (Choi, Kim, and Chung 2011) and VCRC1060200 (Stenesen et al., 2013), did not suppress pSqh staining, we focused on Strn-Mlck and did not further pursue AMPKα.

Two non-overlapping Strn-Mlck RNAi lines, TRiP.JF02278 (Strn-Mlck RNAi 1) and TRiP.JF021 (Strn-Mlck RNAi 2), suppressed the increased pSqh staining caused by Myr-Yki expression (Figure 2.12N-O). Strn-Mlck is a member of the Titin/Myosin Light Chain Kinase family (Champagne et al., 2000). Adding expression of a *Dicer-2* (*Dcr-2*) transgene to increase

Figure 2.12

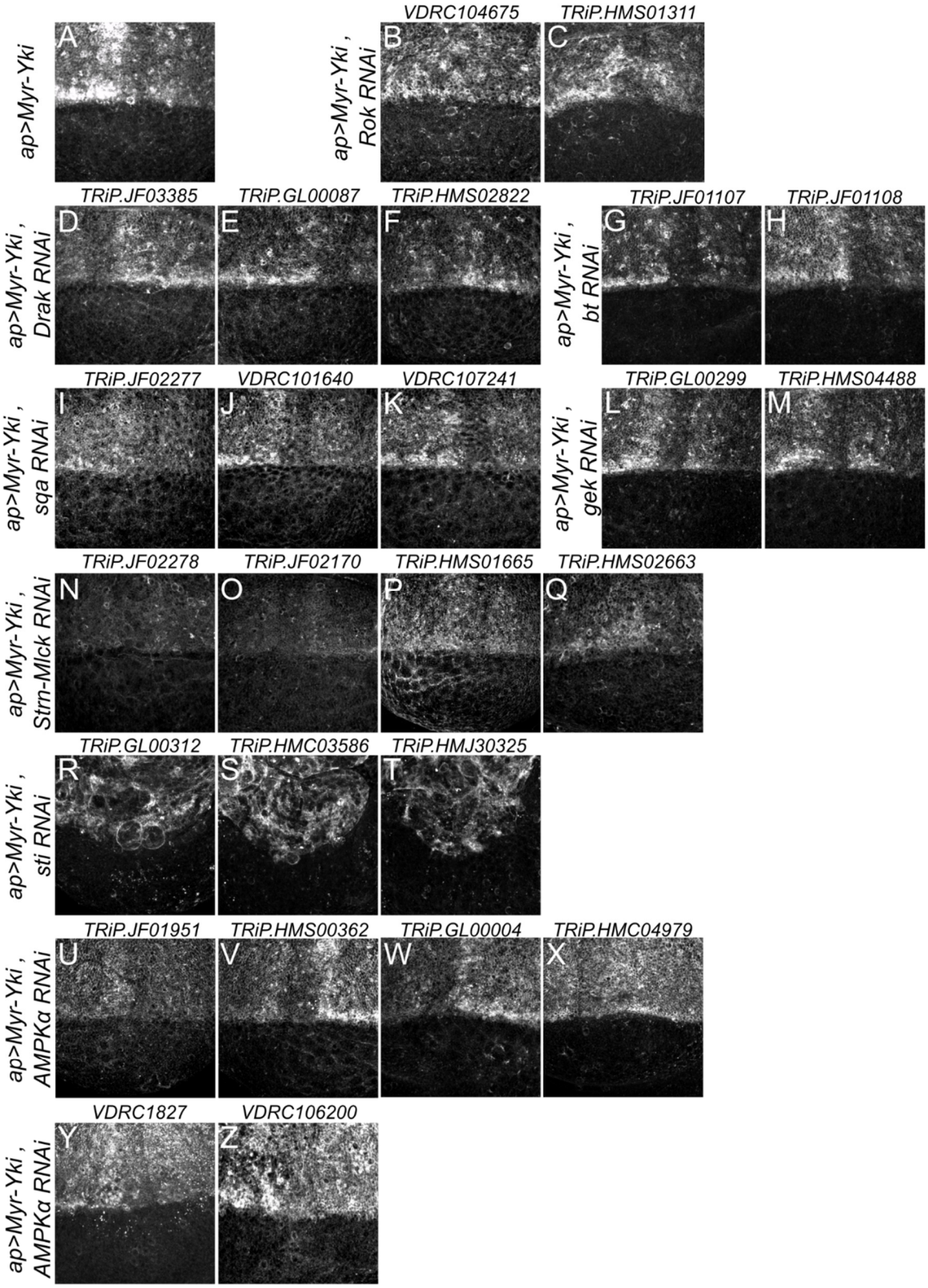
ap>Myr-Yki
A
ap>Myr-Yki , Rok RNAi
VDRC104675
TRiP.HMS01311
B
C
ap>Myr-Yki , Drak RNAi
TRiP.JF03385
TRiP.GL00087
TRiP.HMS02822
D
E
F
ap>Myr-Yki , bt RNAi
TRiP.JF01107
TRiP.JF01108
G
H
ap>Myr-Yki , sqa RNAi
TRiP.JF02277
VDRC101640
VDRC107241
I
J
K
ap>Myr-Yki , gek RNAi
TRiP.GL00299
TRiP.HMS04488
L
M
ap>Myr-Yki , Stm-Mlck RNAi
TRiP.JF02278
TRiP.JF02170
TRiP.HMS01665
TRiP.HMS02663
N
O
P
Q
ap>Myr-Yki , sti RNAi
TRiP.GL00312
TRiP.HMC03586
TRiP.HMJ30325
R
S
T
ap>Myr-Yki , AMPKα RNAi
TRiP.JF01951
TRiP.HMS00362
TRiP.GL00004
TRiP.HMC04979
U
V
W
X
ap>Myr-Yki , AMPKα RNAi
VDRC1827
VDRC106200
Y
Z

Figure 2.12 continued
Screening for kinase that mediates Yki's myosin activation function

(A-C) Yki does not activate myosin via Rok. Two independent RNAi transgenes for Rok were used to deplete Rok in cells expressing *Myr-Yki* and stained with pSqh antibody to assay myosin activation. Neither RNAi suppressed the *Myr-Yki*-induced pSqh increase, suggesting that cortical Yki does not act through Rok to activate myosin.
(D-Z) Screening for Sqh kinases that mediate the myosin activation function of cortical Yki. To screen known or predicted *Drosophila* myosin light chain kinases to determine if they are necessary for Yki-induced Sqh activation, at least two independent RNAi transgenes for the following kinases were co-expressed in wing imaginal discs with *Myr-Yki: Death-associated protein kinase related* (*Drak*), *bent* (*bt*), *spaghetti-squash activator* (*sqa*), *genghis khan* (*gek*), *Stretchin-Mlck* (*Strn-Mlck*), *sticky* (*sti*), or *AMP-activated protein kinase α subunit* (*AMPKα*). TRiP or Vienna Drosophila Resource Center (VDRC stocks) identifiers are indicated. Two Strn-Mlck RNAi lines (TRiP.JF02278, TRiP.JF021) strongly suppressed the increased pSqh staining caused by Myr-Yki expression. One AMPKα RNAi line (TRiP.JF01951) displayed weak suppression.

Strn-Mlck RNAi efficiency strongly increased this effect (Figure 2.13E-F). No null *Strn-Mlck* alleles have been described, but the two RNAi lines described above recognize distinct domains and display indistinguishable phenotypes, suggesting they are specific for *Strn-Mlck*. We also found that Strn-Mlck RNAi 1 strongly repressed expression of a UAS-Strn-Mlck transgene (Figure 2.13A-B).

We next tested whether depleting Strn-Mlck also suppressed other Myr-Yki phenotypes. Strn-Mlck depletion strongly suppressed the increased nuclear Yki-YFP accumulation (Figure 2.13G-H), increased expression of *ex-lacZ* (Figure 2.13P-Q), and overgrowth of adult wings (Figure 2.13K-L, O) caused by Myr-Yki expression. Indeed, depletion of Strn-Mlck appeared epistatic to Myr-Yki with regard to overall wing growth. In contrast, Strn-Mlck depletion only weakly suppressed the overgrowth caused by expression of wild-type Yki (Figure 2.13M-O). Altogether our results suggest that Strn-Mlck functions downstream of cortical Yki to activate Sqh but is not required for nuclear Yki to promote growth.

We confirmed that depletion of Strn-Mlck did not affect Myr-Yki localization (Figure 2.13C-D), though we did note that the level of Myr-Yki expression was lower when Strn-Mlck was depleted. We do not understand the basis of this observation, though it does not appear to be due to transgene competition (data not shown) and we note that different Myr-Yki transgenes that express at different levels still promote overgrowth (data not shown) and Sqh activation to high levels (Table 2.1).

To understand how Yki and Strn-Mlck cooperate to promote myosin activity, we next looked at the effect of Myr-Yki expression on localization of transgenically-expressed, tagged Strn-Mlck (isoform B; FlyBase) in the wing imaginal epithelium. When expressed alone, Strn-Mlck was localized to a sub-cortical band that is distinct from the junctional marker Ecad (Figure

Figure 2.13

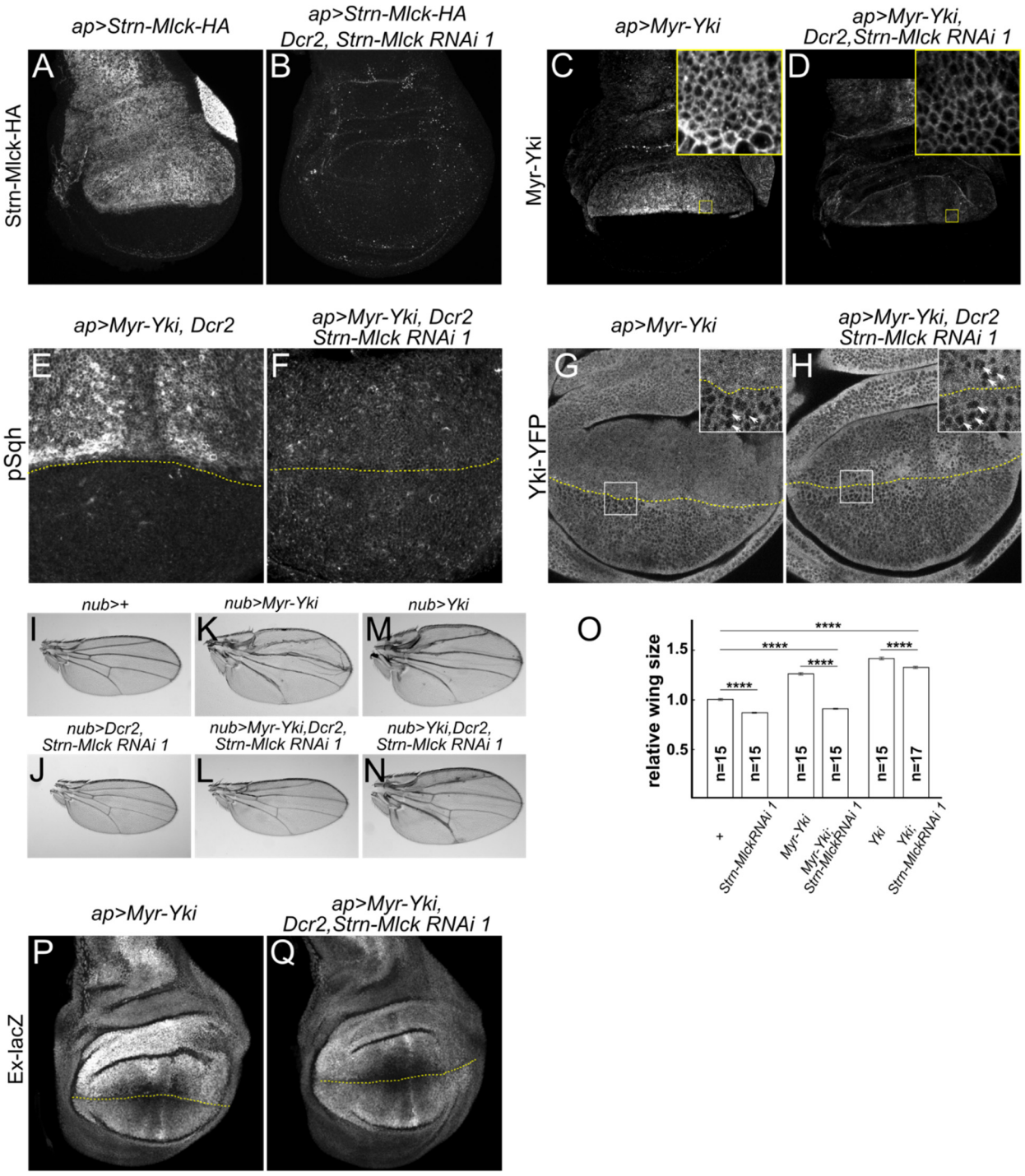
ap>Strn-Mlck-HA
ap>Strn-Mlck-HA Dcr2, Strn-Mlck RNAi 1
Strn-Mlck-HA
A
B
ap>Myr-Yki
ap>Myr-Yki, Dcr2,Strn-Mlck RNAi 1
Myr-Yki
C
D
ap>Myr-Yki, Dcr2
ap>Myr-Yki, Dcr2 Strn-Mlck RNAi 1
pSqh
E
F
ap>Myr-Yki
ap>Myr-Yki, Dcr2 Strn-Mlck RNAi 1
Yki-YFP
G
H
nub>+
nub>Myr-Yki
nub>Yki
I
K
M
nub>Dcr2, Strn-Mlck RNAi 1
nub>Myr-Yki,Dcr2, Strn-Mlck RNAi 1
nub>Yki,Dcr2, Strn-Mlck RNAi 1
J
L
N
O
relative wing size
1.5
1.0
0.5
****
n=15
n=15
n=15
n=15
n=15
n=17
+
Strn-MlckRNAi 1
Myr-Yki
Myr-Yki; Strn-MlckRNAi 1
Yki
Yki; Strn-MlckRNAi 1
ap>Myr-Yki
ap>Myr-Yki, Dcr2,Strn-Mlck RNAi 1
Ex-lacZ
P
Q

Figure 2.13 continued
Yki promotes myosin activation through Strn-Mlck

(A-B) *Strn-Mlck RNAi 1* strongly knocked down expression of a UAS-Strn-Mlck-HA transgene, suggesting this RNAi transgene effectively depletes endogenous Strn-Mlck.
(C-D) *Strn-Mlck RNAi 1* does not affect subcellular localization of Myr-Yki. Yellow boxes denote regions shown in high magnification insets. Note the fluorescence intensity was lower in Strn-Mlck RNAi cells, indicating lower protein level. Samples were stained together and acquired with the same parameters.
(E-F) Strn-Mlck depletion by RNAi strongly suppresses Myr-Yki-mediated myosin activation. UAS-Dcr2 was used to enhance efficiency of the RNAi transgenes. The expression boundary is marked by dashed yellow lines.
(G-H) Strn-Mlck depletion suppresses Myr-Yki-induced nuclear Yki-YFP localization. The expression boundary is marked by dashed yellow lines. Boxes denote regions shown in high-magnification insets; white arrows indicate nuclei.
(I–O) Strn-Mlck depletion completely suppresses Myr-Yki-mediated overgrowth. Representative images of adult male wings of the indicated genotypes are shown (I–N) together with quantification of the results (O). Expression of *Strn-Mlck RNAi 1*, either alone or in the background of Myr-Yki, caused undergrowth of the wing. In contrast, Strn-Mlck depletion did not completely suppress the overgrowth caused by expression of wild-type Yki. Data in (O) are represented as mean ± SEM. Asterisks represent statistical significance of the difference between selected groups (****$p < 0.0001$, one-way ANOVA and Tukey's HSD test, n = number of wings).
(P-Q) *Strn-Mlck RNAi* suppresses Myr-Yki-induced up-regulation of *ex-lacZ*, a reporter for Hippo pathway activity. The dotted yellow line indicates the boundary of transgene expression (expression is above the line).

Figure 2.14

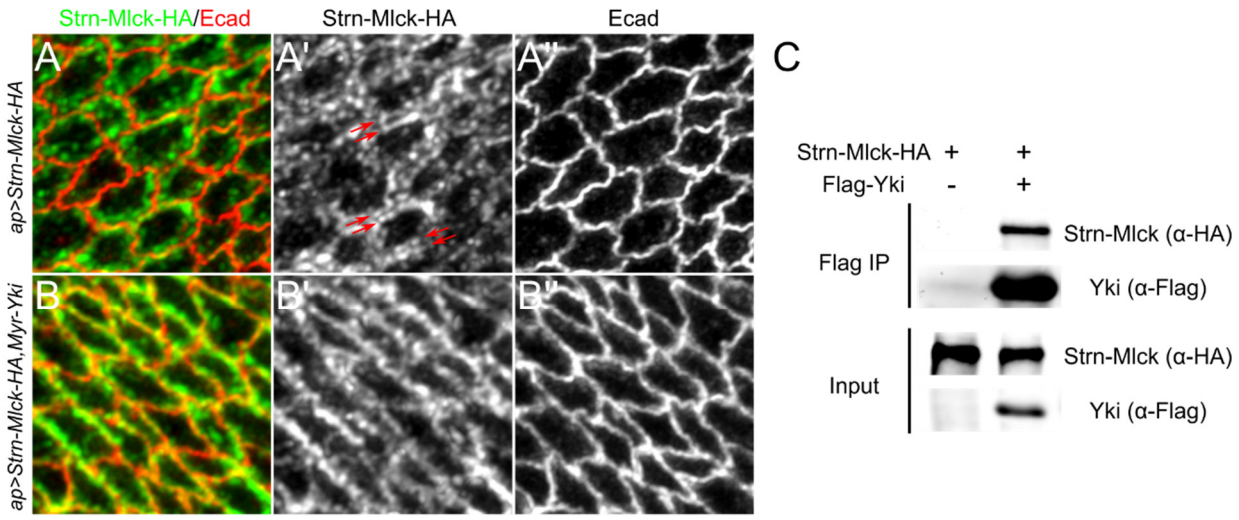

Yki is able to recruit Strn-Mlck to the cell cortex

(A-B'') Myr-Yki recruits Strn-Mlck to the junctional region. Transgenically expressed, Strn-Mlck was localized to a sub-cortical band that is distinct from the junctional marker Ecad (L–L00, indicated with red arrows). Co-expression of Myr-Yki resulted in greater junctional localization of Strn-Mlck. Strn-Mlck was tagged with hemagglutinin (HA) and detected with HA antibody staining.

(C) Strn-Mlck and Yki form a complex in S2 cells. HA-tagged Strn-Mlck and Flag-tagged Yki were co-expressed in S2 cells. Lysates were immunoprecipitated with anti-Flag and immunoblotted. Strn-Mlck co-immunoprecipitated with Yki, suggesting they can form a complex. IP, immunoprecipitation.

2.14A-A''), a localization that is strikingly similar to Sqh (called the apical cytocortex in Tsoumpekos et al., 2018). In contrast, co-expression of Myr-Yki and Strn-Mlck appeared to recruit Strn-Mlck to the junctional region (Figure 2.14B-B''), suggesting that Yki and Strn-Mlck can form a complex. To address this possibility, we co-expressed these proteins in S2 cultured cells and found that they readily co-IP from cell lysates (Figure 2.14C). Together these experiments suggest that Yki and Strn-Mlck form a complex and that in tissues cortical Yki may recruit Strn-Mlck, thereby promoting Sqh activation.

Since Strn-Mlck depletion alone caused undergrowth, we asked if Strn-Mlck regulates growth via the Hippo pathway during normal development. We found that strong depletion of Strn-Mlck caused reduced expression of the Hippo pathway reporters *Diap1-lacZ* and *fj-lacZ* in wing imaginal discs (Figure 2.15A-E). Similar results have been found for other known negative regulators of the Hippo pathway (Das Thakur et al., 2010; Rauskolb et al., 2011), suggesting Strn-Mlck is a negative regulator of the Hippo pathway during normal development.

The N-terminal region of Yki is necessary and sufficient for myosin activation

We next mapped the region within Yki that is responsible for activating myosin. We first tested if we could recapitulate the pSqh increase phenotype in *Drosophila* S2 cells. Expression of Myr-Yki caused a dramatic increase in pSqh staining. (Figure 2.16C). To map the region of Yki responsible for this increase, we generated truncated Yki fragments with a myristoylation signal sequence, expressed them individually in S2 cells, and found that an N-terminal fragment encoding the first 34 amino acids was both necessary and sufficient to activate myosin (Figure 2.16A-F).

Figure 2.15

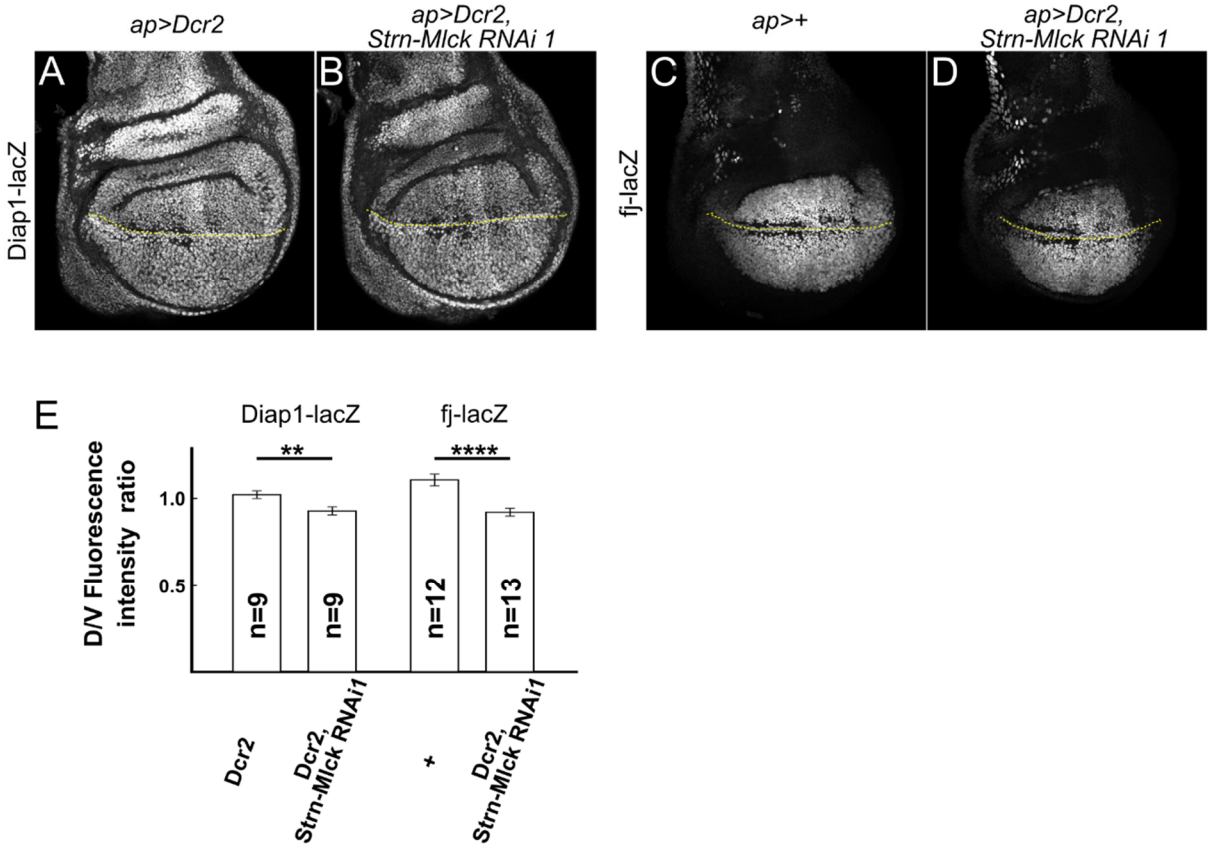

Strn-Mlck negatively regulates the Hippo pathway in normal development
Strn-Mlck RNAi caused reduced expression of *Diap1-lacZ* (A-B) and *fj-lacZ* (C-D), two Hippo pathway reporters, indicating that Strn-Mlck negatively regulates the Hippo pathway.
Quantification of the dorsal-ventral (D/V) ratio of Diap1-lacZ and fj-lacZ staining intensity is displayed in (E). Dotted yellow lines indicate the boundary of transgene expression. Data are represented as mean ± SEM. Asterisks represent statistical significance of the difference between selected groups (** $p<0.01$, **** $p<0.0001$. One-way ANOVA and Tukey's HSD test, n = number of wing discs).

Figure 2.16

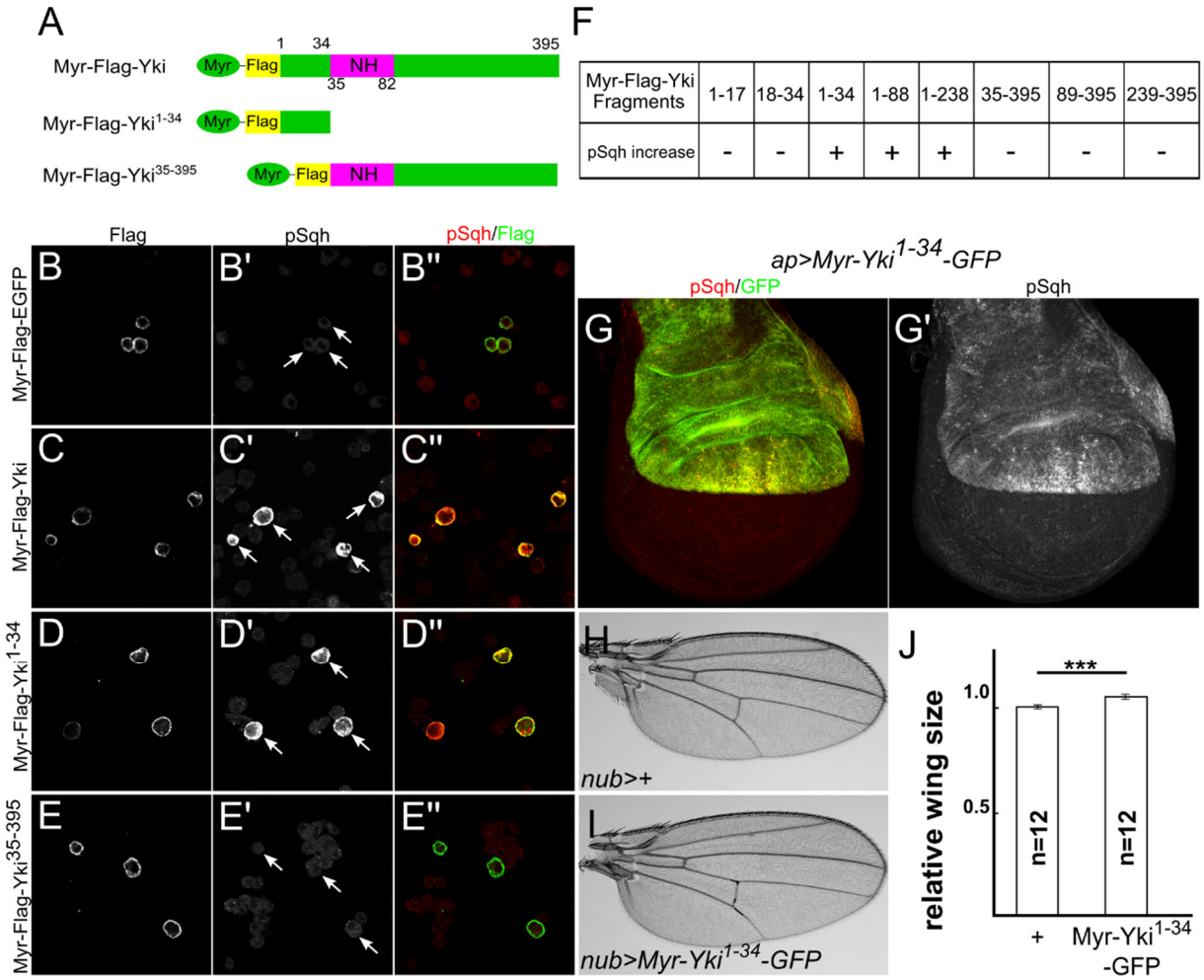

The N-terminal region of Yki is necessary and sufficient for myosin activation

(A) Cartoons showing Myr-Yki fragments used in (C-E").

(B-F) Mapping of the myosin activation region using S2 cells transfected with the indicated constructs and stained for Flag and pSqh. Myr-Yki and Myr-Yki$^{1-34}$ cause increased pSqh staining, while Myr-Yki$^{35-395}$ and Myr-EGFP do not. White arrows indicate transfected cells. In (F), the full panel of tested deletion constructs is displayed. Fragments 1-34, 1-88, 1-238 each induce Sqh activation whereas their complementary C-terminal fragments 35-395, 89-395, 239-395 do not. Further subdivision of the 1-34 region (fragments 1-17 and 18-34) disrupted the ability to activate Sqh.

(G-G') Expression of *UAS-Myr-Yki$^{1-34}$-GFP* in the dorsal compartment of the wing is sufficient to induce myosin activation.

(H-J) Expression of *UAS-Myr-Yki$^{1-34}$-GFP* causes overgrowth of the wing. Representative images of adult female wings of the indicated genotypes are shown (H-I), together with quantification of the results (J). Data are represented as mean ± SEM. Asterisks represent statistical significance of the difference between selected groups (*** $p<0.001$, One-way ANOVA, n = number of wings).

To test if this N-terminal fragment is sufficient to activate myosin *in vivo*, we generated *UAS-Myr-yki$^{1-34}$-GFP* transgenic animals. When expressed in the wing imaginal disc, Myr-Yki$^{1-34}$-GFP activated myosin (Figure 2.16G-G') and caused overgrowth of adult wings (Figure 2.16H-J). These effects were similar to, but weaker than, the phenotypes observed for full-length Myr-Yki (Figures. 2.3E-E', 2.7A-B, Table 2.1), possibly because other regions of Yki also contribute to myosin activation.

Uncoupling the transcriptional and myosin-activating functions of Yki

The data presented so far suggest that Yki has a non-transcriptional function at the cell cortex to promote myosin activation through its N-terminal domain. To understand the developmental significance of this function, we sought to disable it without affecting Yki's transcriptional functions. An initial attempt—deleting aa1-34 from the *yki* locus via CRISPR/Cas9—resulted in strong reduction of Yki expression (data not shown). As an alternative approach, we generated a series of smaller deletions and point mutations in the aa1-34 region and tested their ability to activate Sqh when expressed in S2 cells (Table 2.2). These studies led us to focus on a short stretch of acidic residues in the first 34 amino acids of Yki protein sequence (Figure 2.17A). Mutation of these residues to Alanine blocked Sqh activation in S2 cells (Figure 2.17B-C'') and wing imaginal discs (Figure 2.17D-E'). Using CRISPR/Cas9, we then generated the *yki^{AcidA}* allele at the *yki* locus. This mutation does not affect Yki expression (Figure 2.18A-B'). To ask if this allele visibly affects Yki's transcriptional activity, we examined expression levels of the Hippo pathway reporter *Diap1-lacZ* as well as the Hippo pathway transcriptional target *expanded* (*ex*) and found they were not detectably affected in *yki$^{AcidA/AcidA}$* clones (Figure 2.18C-D'). Additionally, to test the *yki^{AcidA}* allele under conditions where it should be maximally

Table 2.2

Effect of different Yki mutations on pSqh increase

Mutation	First 34 amino acids sequence	pSqh increase
Original	MLTTMSASSNTNSLIEKEIDDEDMLSPIKSNNLV…	YES
Del2-11	M_____NSLIEKEIDDEDMLSPIKSNNLV…	NO
Del12-23	MLTTMSASSNT_____MLSPIKSNNLV…	NO
Del24-34	MLTTMSASSNTNSLIEKEIDDED_____…	YES
Del2-6	M_____ASSNTNSLIEKEIDDEDMLSPIKSNNLV…	YES
Del7-11	MLTTMS_____NSLIEKEIDDEDMLSPIKSNNLV…	NO
Del12-17	MLTTMSASSNT_____ EIDDEDMLSPIKSNNLV…	NO
Del18-23	MLTTMSASSNTNSLIEK_____ MLSPIKSNNLV…	NO
8-13A	MLTTMSAAAAAAALIEKEIDDEDMLSPIKSNNLV…	NO
S8A	MLTTMSAASNTNSLIEKEIDDEDMLSPIKSNNLV…	NO
S9A	MLTTMSASANTNSLIEKEIDDEDMLSPIKSNNLV…	NO
N10A	MLTTMSASSATNSLIEKEIDDEDMLSPIKSNNLV…	NO
T11A	MLTTMSASSNANSLIEKEIDDEDMLSPIKSNNLV…	NO
N12A	MLTTMSASSNTASLIEKEIDDEDMLSPIKSNNLV…	YES
S13A	MLTTMSASSNTNALIEKEIDDEDMLSPIKSNNLV…	NO
AcidA	MLTTMSASSNTNSLIAKAIAAAAMLSPIKSNNLV…	NO

Various mutated forms of Yki are tagged with myristoylation signal sequence at their N termini and transfected in *Drosophila* S2 cells to test their effect on pSqh increase.

Figure 2.17

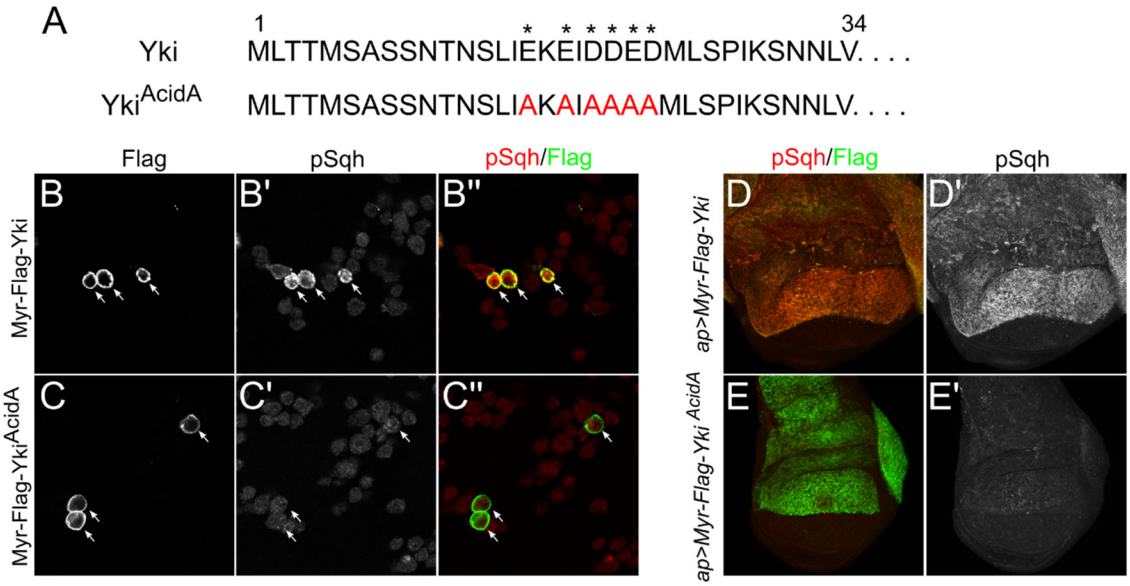

Identification of the critical amino acids for myosin activation function of Yki

(A) Sequences of the first 34 amino acids of wild-type Yki and the Yki^{AcidA} allele. Asterisks indicate acidic amino acids.

(B–E') Mutation of acidic residues at the N terminus of Yki blocks its ability to activate myosin. S2 cells expressing membrane-associated wild-type Myr-Yki (B–B') and Myr-YkiAcidA (C–C'). Myr-Yki^{AcidA} fails to activate Sqh. White arrows indicate transfected cells. Wing imaginal discs expressing Myr-Yki^{AcidA} also fail to activate Sqh (D–E'). The two transgenes were integrated at the same landing site to ensure comparable expression levels.

Figure 2.18

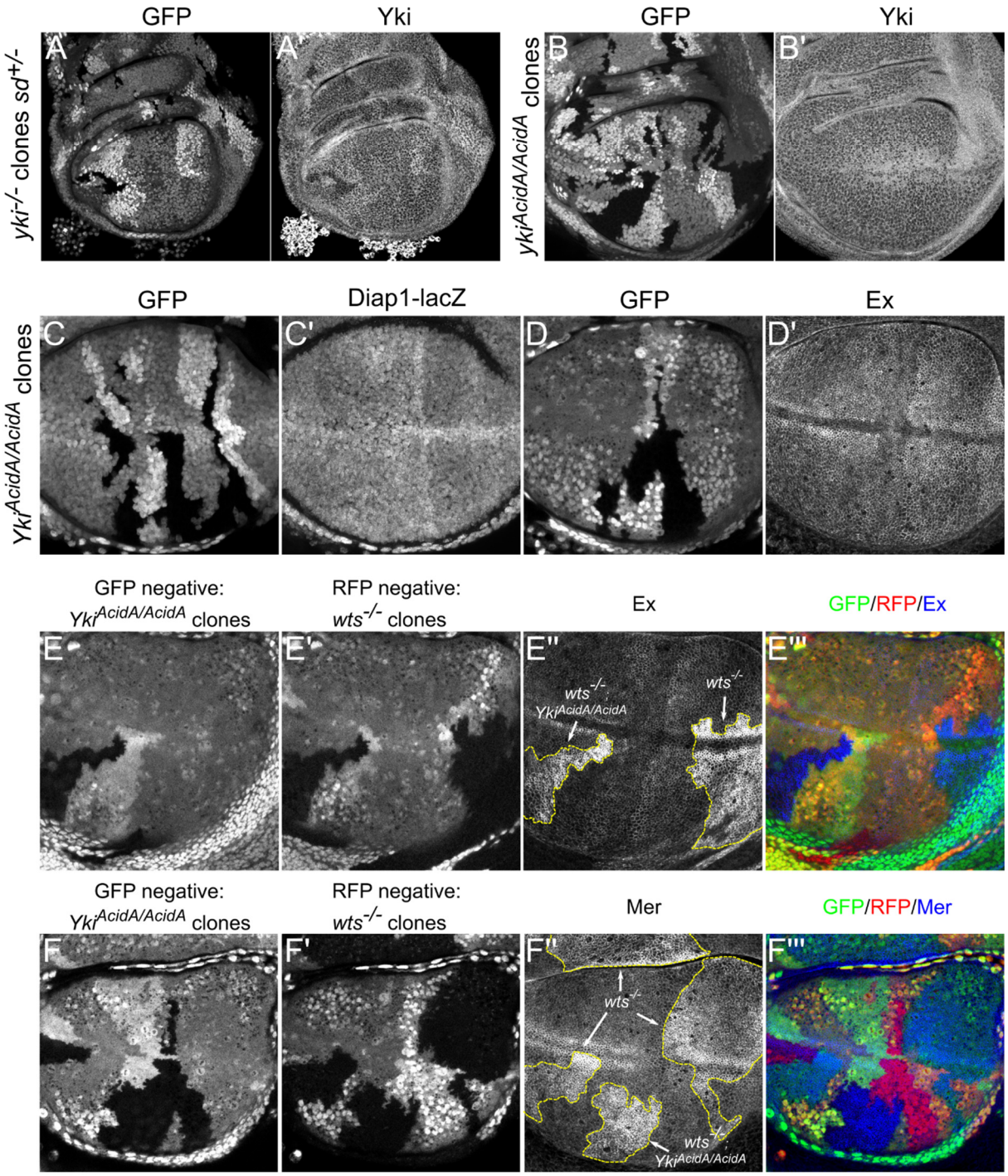
GFP
Yki
yki-/- clones sd+/-
A
A'
GFP
Yki
ykiAcidA/AcidA clones
B
B'
GFP
Diap1-lacZ
YkiAcidA/AcidA clones
C
C'
GFP
Ex
D
D'
GFP negative:
YkiAcidA/AcidA clones
RFP negative:
wts-/- clones
Ex
GFP/RFP/Ex
E
E'
E''
wts-/-; YkiAcidA/AcidA
wts-/-
E'''
GFP negative:
YkiAcidA/AcidA clones
RFP negative:
wts-/- clones
Mer
GFP/RFP/Mer
F
F'
F''
wts-/-
wts-/-; YkiAcidA/AcidA
F'''

Figure 2.18 continued
The *yki*^{AcidA} mutation does not affect the transcriptional function of Yki

(A-B') The *yki*^{AcidA} mutation does not affect *yki* expression level. *yki* null (*yki*^{B5}) clones were generated in a *sd* heterozygous background (*sd*$^{47M/+}$) because cells lacking Yki survive better when dosage of *sd*, which on its own represses target gene expression (Koontz et al., 2013), is decreased. Despite some background staining, anti-Yki staining is clearly reduced in *yki* null clones. Also note that Yki staining is noticeably increased in sister clones in which there are two copies of wild-type *yki*. In contrast, anti-Yki staining was not affected in *yki*$^{AcidA/AcidA}$ clones or sister clones relative to surrounding *yki*$^{AcidA/+}$ cells, indicating that Yki expression level is not affected by the mutation.
(C-D') The *yki*^{AcidA} mutation does not affect *yki* target gene expression under normal physiological conditions. Expression of the *Diap1-lacZ* transcriptional reporter and anti-Ex staining are not altered in *yki*$^{AcidA/AcidA}$ clones, suggesting the *yki*^{AcidA} mutation does not detectably reduce *yki* target gene expression.
(E-F''') The *yki*^{AcidA} mutation is able to fully activate *yki* target gene expression in response to Hippo pathway inactivation. To test if the *yki*^{AcidA} mutation affects Yki transcriptional function under conditions where it should be maximally transcriptionally active, expression of the Yki targets Mer and Ex was compared between *wts*$^{-/-}$ (*wts*$^{X1/X1}$) clones and *wts*$^{-/-}$*; yki*$^{AcidA/AcidA}$ double clones. In both types of clones, expression of Mer and Ex are dramatically increased in a similar fashion, suggesting that *yki*^{AcidA} mutation does not affect Yki's transcriptional activity. Dashed yellow lines mark clone boundaries.

transcriptionally active, we examined the expression of Yki targets in clones that were simultaneously mutant for *yki*^{AcidA} and *wts*. In these cells, Yki transcriptional activity should be uncoupled from any upstream pathway activity, as well as the tension mediated feedback we propose, because tension-mediated pathway regulation is thought to be carried out via sequestration of Wts (Rauskolb et al., 2014). Comparison of *wts*$^{-/-}$ (;*yki*$^{+/AcidA}$) clones to *wts*$^{-/-}$; *yki*$^{AcidA/AcidA}$ double mutant clones showed that staining of Ex and Merlin (Mer), another Yki target, increased similarly in both genotypes (Figure 2.18E-F'''). Taken together these results suggest that the *yki*^{AcidA} mutation affects Yki's myosin activation function but not its transcriptional function.

We then analyzed the growth phenotypes of *yki*^{AcidA} animals. *yki*^{AcidA} homozygous adults were viable but smaller than heterozygotes, as were their imaginal discs and wings (Figure 2.19A-E, G, H). Animals transheterozygous for *yki*^{AcidA} over *yki*^{B5}, a null allele, were pupal lethal and displayed even smaller wing imaginal discs (Figure 2.19D-F, H). Interestingly, these wing imaginal discs not only were smaller, but also appeared more bilaterally symmetrical along anterior-posterior axis than normal wing discs (Figure 2.19F). Together these results suggest that Yki's function in promoting myosin activation is important for organ size control and perhaps organ morphogenesis. However, further studies will be required to fully understand how this domain and its ability to promote myosin activation function in tissue growth and morphogenesis.

Figure 2.19

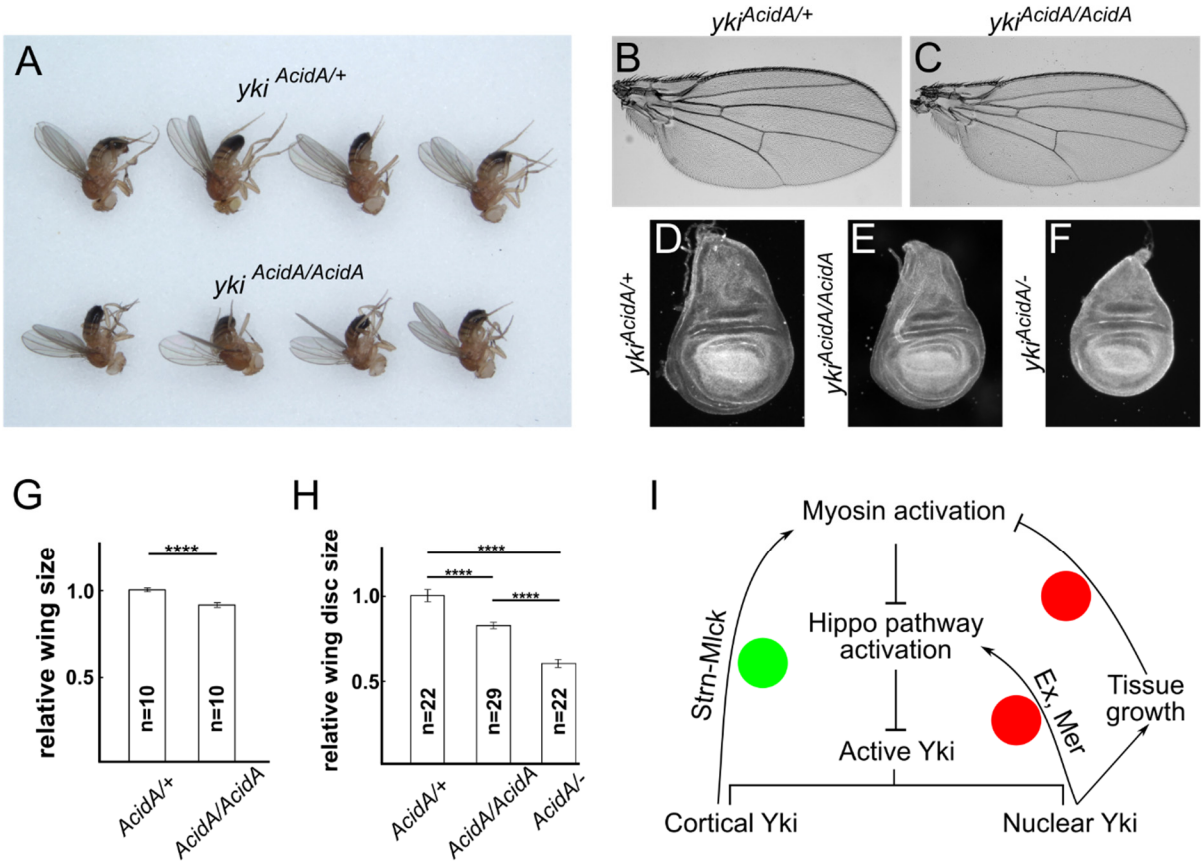

The myosin-activation function of Yki is required for proper growth

(A-H) *yki*^{AcidA} mutation caused unundergrowth. Homozygous *yki*^{AcidA} adults are smaller than controls (A). Representative images show that adult female wings from animals homozygous for the *yki*^{AcidA} allele are undergrown (B-C). Larval wing imaginal discs are similarly undergrown (D-F), with *yki*^{AcidA}/*yki*^{B5} (*yki*$^{AcidA/-}$) animals displaying the strongest phenotype (the latter genotype does not survive to adults). Quantification of adult wing and larval wing disc sizes of the indicated genotypes confirms these differences (G-H). Data are represented as mean ± SEM. Asterisks represent statistical significance of the difference between selected groups (**** $p<0.0001$, One-way ANOVA and Tukey's HSD test, n = number of wings [G] / wing discs [H]).

(I) Model of feedback regulation of the Hippo pathway. Two negative feedback mechanisms have been proposed in the regulation of the Hippo pathway (red circles). One is mediated through transcriptional upregulation of upstream components, including Mer and Ex, and the other is a consequence of morphogen-driven growth at the center of tissues and the resulting compression of those cells. We propose a positive feedback mechanism (green circle) in which cortical Yki at the AJR promotes myosin activation and increased tension via Strn-Mlck, which in turn further activates Yki by suppressing the Hippo pathway. See the Discussion for more details.

2.3 Discussion

Collectively, our results reveal a previously unrecognized role for Yki at the cell cortex where it promotes myosin activation through the myosin regulatory light chain kinase Strn-Mlck. Two aspects of these findings are unexpected. First, Yki has traditionally been viewed as a transcriptional co-activator that functions in the nucleus to promote target gene expression. The results presented here indicate Yki also acts via a non-transcriptional mechanism to control non-muscle myosin II contractility. While surprising, several previous studies have suggested that Yki and its vertebrate orthologues YAP and TAZ, might have additional, non-nuclear functions. For example, cytoplasmic YAP has been shown to inhibit TGF-β/Smad signaling (Varelas et al., 2010a) and evidence suggests that TAZ and Yki can act in the cytoplasm to inhibit Wnt/β-catenin signaling (Varelas et al., 2010b). Interestingly, although YAP has been shown to localize to the cell-cell junctions in primary human keratinocytes (Schlegelmilch et al., 2011), and cortical localization of Yki in *Drosophila* has been reported in the eye (Badouel et al., 2009) and wing imaginal discs (Zhang et al., 2009), these observations have been interpreted as inhibition of Yki/YAP nuclear function by sequestration in the cytoplasm. The results presented here indicate that Yki also has an active role at the cell cortex, to promote myosin activity, and that this function is important for growth regulation.

A second unexpected aspect of our findings is that they suggest that Yki functions in a positive feedback loop that promotes myosin activation, and thereby greater Yki activity, in response to tension. We have shown that cortical Yki promotes myosin activation via the Sqh kinase Strn-Mlck, and that this increased myosin activity in turn can activate Yki, presumably by repressing the Hippo pathway. Further, our observations indicate that Hippo pathway downregulation and Yki activation caused by loss of *wts* result in 1) increased cortical

accumulation of Yki and 2) increased myosin activation. Taken together, our results suggest the existence of a non-transcriptional, positive feedback loop between Yki and myosin activation (Figure 2.19I). This positive feedback loop could potentially serve to amplify the effect of tension on Yki activity and therefore tissue growth.

A recent model suggests that Yki's ability to sense tension and promote growth might be particularly important at the periphery of tissues, where morphogen levels, and therefore morphogen-driven proliferation, should be lower (Aegerter-Wilmsen et al., 2007, 2012; Hariharan, 2015). According to one version of this model, morphogen-driven growth at the center of tissues exerts tension at the periphery, which in turn might cause tension-mediated activation of Yki function. In agreement with this idea, recent empirical measurements in the wing imaginal disc indicate higher tension at the periphery of wing blade (Mao et al., 2013). The positive feedback mechanism described here could be particularly important for promoting growth at the periphery of developing tissues.

To further test the positive feedback model of Yki function in normal development, we identified a short stretch of amino acids in the N-terminus of Yki that is both necessary and sufficient for its ability to promote myosin activation. We mutated this sequence to generate the yki^{AcidA} allele that lacks myosin activation activity but at the same time retains normal transcriptional function. Strikingly, yki^{AcidA} homozygous animals display overall undergrowth, and smaller wing imaginal discs in particular, indicating that this region of Yki is important for its growth promoting function.

In addition, $yki^{AcidA/-}$ wing imaginal discs show morphological defects: they lost asymmetry along anterior-posterior axis outside of the pouch region (Figure 2.19F). We do not know yet

whether these defects are due to loss of the proposed feedback mechanism, but studies are currently underway to examine this question.

How is this positive feedback mechanism down-regulated to prevent overgrowth? Two sources of negative feedback have been proposed in Hippo pathway regulation in *Drosophila* (Figure 2.19I, red circles). First, when Yki is activated, it drives expression of positive upstream regulators of the Hippo pathway including Ex and Mer. These proteins will in turn activate the Hippo pathway to suppress Yki activity (Boggiano and Fehon, 2012). Second, Yki activation causes growth, which can reduce tension at the center of tissues, leading to de-repression of the Hippo pathway and Yki inactivation (Moberg et al., 2005; Pan et al., 2016). These sources of negative feedback require target gene transcription (and growth) and therefore would be expected to act more slowly than the positive feedback we propose.

Another important question is how does Yki localize to the cell cortex to promote myosin activation? One possible mechanism is that Yki is recruited via a previously described interaction with Ex, which strongly localizes to the AJR (Badouel et al., 2009; Su et al., 2017). Additionally, Yki has been shown to interact with several other pathway components, including Kibra (Kib), Hpo, Wts, Ajuba (Jub) and 14-3-3 (Genevet and Tapon, 2011). Our preliminary experiments have not clearly implicated any of these proteins in localizing Yki to the cortex (data not shown), though it is possible either that partial depletion by RNAi is not sufficient to see an effect, or a multiprotein complex is responsible. Other factors could also recruit Yki to the AJR, and further experiments will be required to resolve this question.

Our results indicate that Strn-Mlck is an integral part of the cortical Yki-myosin positive feedback loop. The *Strn-Mlck* locus is proposed to generate three distinct sets of protein isoforms, with the largest isoform encoding a huge Titin-like 926 kDa protein (Champagne et al., 2000).

Previous functional studies of Strn-Mlck have focused on its function in indirect flight muscles (Patel and Saide, 2005; Schönbauer et al., 2011) or actomyosin flow after wounding (Antunes et al. 2013). However, Strn-Mlck's function in regulating myosin activity has not been thoroughly examined, nor has its expression in non-muscle tissues. Interestingly, although previous studies have shown that Rok driven cytoskeletal tension can regulate Yki activity, our results indicate that Yki acts through Strn-Mlck, but not Rok, to promote myosin activation. Thus, our data suggest that while all forms of cytoskeletal tension likely affect Hippo pathway activity, Yki itself regulates tension specifically via Strn-Mlck. Interestingly, Strn-Mlck has two flexible PEVK domains whose conformation changes when stretched (Champagne et al., 2000; Linke, 2000). Thus the functional interaction between Yki and Strn-Mlck could represent yet another means by which physical tension regulates pathway output in growing tissues.

Similar to Yki in *Drosophila*, vertebrate YAP also can promote myosin activation. However, the underlying mechanisms appear to be different. Our results uncover a role for Yki at the cell cortex to promote myosin activity whereas studies in mouse and in Medaka found that YAP does so by increasing transcription of genes encoding proteins that activate the myosin regulatory light chain (Porazinski et al., 2015; Lin et al., 2017). In addition, The N-terminal myosin activation domain of *Drosophila* Yki does not display clear sequence homology with vertebrate YAP. This could mean *Drosophila* has a distinctive, non-transcriptional mechanism to generate Yki-myosin positive feedback. Even though the specific mechanism through which Yki promotes myosin activation does not appear to be conserved in vertebrates, positive feedback between cytoskeletal tension and the activity of Yki or YAP seems to be a well-conserved but still poorly understood feature of the Hippo pathway. While it is clear that the non-transcriptional positive feedback we propose for Yki would be temporally distinct from the transcriptionally-based

negative feedback mechanism, it is not as clear how YAP's positive and negative feedback effects would be distinctly interpreted in developing tissues. Further studies in both *Drosophila* and vertebrate systems will be required to understand how these competing inputs are integrated into the process of tissue growth during development.

2.4 Methods

Table 2.3 Key resource used in Chapter 2

REAGENT or RESOURCE	SOURCE	IDENTIFIER
Antibodies		
Guinea pig anti-Ex	Maitra et al., 2006	N/A
Guinea pig anti-Sqh1P	Zhang and Ward, 2011	N/A
Mouse anti Sqh	Zhang and Ward, 2011	N/A
Mouse anti-Flag	Sigma	Cat#F1804
Rat anti-Ecad	Developmental Studies Hybridoma Bank	Cat#AB_528120
Guinea pig anti-Sd	Guss et al., 2013	N/A
Rabbit anti-Yki	Oh and Irvine, 2008	N/A
Rabbit anti-HA	Santa Cruz	Cat#sc-805
Mouse anti-Flag agarose beads	Sigma	Cat#A2220
Chemicals, Peptides, and Recombinant Proteins		
Normal goat serum	Jackson ImmunoResearch	Cat# 005000001
16% formaldehyde	Electron Microscopy Sciences (EMS)	Cat#15710
S2 medium	Sigma	Cat# S9895
10% Fetal Bovine Serum	Thermo Fisher Scientific	Cat#16000044
Didodecyldimethylammonium bromide	Sigma	Cat# 359025
Methyl salicylate	Thermo Fisher Scientific	Cat#119368
Experimental Models: Organisms/Strains		
D. melanogaster: UAS-sqh^{DD}	Mitonaka et al., 2007	N/A
D. melanogaster: UAS-Flag-Yki	This study	N/A

Table 2.3 continued.

D. melanogaster: UAS-Myr-Flag-Yki (Random insertion)	This study	N/A
D. melanogaster: UAS-Myr-Flag-Yki (Site specific integration)	This study	N/A
D. melanogaster: UAS-Myr-Flag-Yki$^{\Delta NH}$	This study	N/A
D. melanogaster: UAS-Myr-Flag-Yki$^{1-34}$-GFP(Site specific integration)	This study	N/A
D. melanogaster: UAS-Myr-Flag-Yki^{AcidA} (Site specific integration)	This study	N/A
D. melanogaster: UAS-yki RNAi	Vienna Drosophila RNAi Center	40497
D. melanogaster: UAS-yki RNAi	Vienna Drosophila RNAi Center	104523
D. melanogaster: UAS-sd RNAi	Vienna Drosophila RNAi Center	101497
D. melanogaster: UAS-Dcr2	Bloomington Drosophila Stock Center	24650
D. melanogaster: UAS-Dcr2	Bloomington Drosophila Stock Center	24651
D. melanogaster: UAS-Strn-Mlck RNAi	Bloomington Drosophila Stock Center	JF02278
D. melanogaster: UAS-Strn-Mlck RNAi	Bloomington Drosophila Stock Center	JF02170
D. melanogaster: UAS-Strn-Mlck RNAi	Bloomington Drosophila Stock Center	HMS01665
D. melanogaster: UAS-Strn-Mlck RNAi	Bloomington Drosophila Stock Center	HMS02663
D. melanogaster: UAS-Rok RNAi	Vienna Drosophila RNAi Center	104675
D. melanogaster: UAS-Rok RNAi	Bloomington Drosophila Stock Center	HMS01311
D. melanogaster: UAS-Drak RNAi	Bloomington Drosophila Stock Center	JF03385

Table 2.3 continued.

D. melanogaster: UAS-Drak RNAi	Bloomington Drosophila Stock Center	GL00087
D. melanogaster: UAS-Drak RNAi	Bloomington Drosophila Stock Center	HMS02822
D. melanogaster: UAS-sqa RNAi	Bloomington Drosophila Stock Center	JF02277
D. melanogaster: UAS-sqa RNAi	Vienna Drosophila RNAi Center	101640
D. melanogaster: UAS-sqa RNAi	Vienna Drosophila RNAi Center	107241
D. melanogaster: UAS-bt RNAi	Bloomington Drosophila Stock Center	JF01107
D. melanogaster: UAS-bt RNAi	Bloomington Drosophila Stock Center	JF01108
D. melanogaster: UAS-gek RNAi	Bloomington Drosophila Stock Center	GL00299
D. melanogaster: UAS-gek RNAi	Bloomington Drosophila Stock Center	HMS04488
D. melanogaster: UAS-sti RNAi	Bloomington Drosophila Stock Center	GL00312
D. melanogaster: UAS-sti RNAi	Bloomington Drosophila Stock Center	HMC03586
D. melanogaster: UAS-sti RNAi	Bloomington Drosophila Stock Center	HMJ30325
D. melanogaster: UAS-AMPKα RNAi	Bloomington Drosophila Stock Center	JF01951
D. melanogaster: UAS-AMPKα RNAi	Bloomington Drosophila Stock Center	HMS00362
D. melanogaster: UAS-AMPKα RNAi	Bloomington Drosophila Stock Center	GL00004
D. melanogaster: UAS-AMPKα RNAi	Bloomington Drosophila Stock Center	HMC04979
D. melanogaster: UAS-AMPKα RNAi	Vienna Drosophila RNAi Center	1827

Table 2.3 continued.

D. melanogaster: UAS-AMPKα RNAi	Vienna Drosophila RNAi Center	106200
D. melanogaster: 82BFRT wts^{X1}	Xu et al., 1995	N/A
D. melanogaster:42DFRT yki^{B5}	Huang et al., 2005	N/A
D. melanogaster:19AFRT sd^{47M}	Wu et al., 2008	N/A
D. melanogaster: sqh^{AX3}/FM	Jordan and Karess, 1997	N/A
D. melanogaster: Diap1-lacZ	Hay et al., 1995	N/A
D. melanogaster: ex-lacZ	Hamaratoglu et al., 2006	N/A
D. melanogaster: fj-lacZ	Bloomington Drosophila Stock Center	6370
D. melanogaster: sqh:mCherry	Martin et al., 2009	N/A
D. melanogaster: sqh:GFP	Vienna Drosophila RNAi Center	318484
D. melanogaster: zip:GFP	Rauskolb et al., 2014	N/A
D. melanogaster: zip^{1}/Cyo	Young et al., 1993	N/A
D. melanogaster: w^{1118}; yki^{B5} {yki-YFP} VK37	This study	N/A
D. melanogaster: nub-Gal4	Bloomington Drosophila stock center	38418
D. melanogaster: hh-Gal4	Tetsuya Tabata	N/A
D. melanogaster: *ap-Gal4*	Bloomington Drosophila stock center	3041
D. melanogaster: w^{1118}; {Wts-YFP} VK37	This study	N/A
D. melanogaster: y M{vas-int.Dm}ZH-2A w; M{3xP3-RFP.attP}ZH-86Fb	Bloomington Drosophila stock center	24749
D. melanogaster: UAS-Strn-Mlck-HA	This study	N/A
D. melanogaster: Kr[If-1]/CyO; UAS-GrabFP-A$_{Int}$/TM6	Bloomington Drosophila stock center	68178
D. melanogaster: y w vas-Cas9	Bloomington Drosophila stock center	52669

Table 2.3 continued.

Oligonucleotides		
Yki 5' Homology arm forward 5AGCACCTGCgatcTACTGAAAGTAG AGGTGATTAGTTGTTAACGAG3	Integrated DNA Technologies	N/A
Yki 5' Homology arm reverse 5TTTCTAGGGTTAACATATAAAAGG CACTTATTGTATACAAACGAAAAC3	Integrated DNA Technologies	N/A
Yki 3' Homology arm forward including AcidA substitution 5TTCTAGGGTTAACGACGATGTCAG CCAGCAGCAATACAAACAGCCTGA TCGccAAGGccATCGcCGcCGccGcCA TGCTTTCGCCGATtAAGTCgAACAAC CTG3	Integrated DNA Technologies	N/A
Yki 3' Homology arm reverse 5CGACGGCTCTTCCTTGTAGTATGA CTGCAAGTAGAGAGAACAC3	Integrated DNA Technologies	N/A
Guide RNA sequence 5ACCAGGTTGTTGGACTTGAT3	Integrated DNA Technologies	N/A
Recombinant DNA		
pU6-BbsI-chiRNA	Addgene	Cat#45946
pAWH	Drosophila Genomics Resource Center	1096
pUAST-Myr	Neisch et al., 2013	N/A
pUASTattB	Bischof et al., 2007	N/A
Strn-Mlck EST	Drosophila Genomics Resource Center	RH61010
pAWH-Strn-Mlck (Strn-Mlck-HA)	This study	N/A

Table 2.3 continued.

pHD-ScarlessDsRed	Drosophila Genomics Resource Center	1364
Software and Algorithms		
Image J	NIH	https://imagej.nih.gov/ij/
R 3.5.0	The R Foundation	https://www.r-project.org/

Drosophila **husbandry**

Drosophila melanogaster was cultured using standard techniques at 25°C (unless otherwise noted). Both male and female animals were used (unless otherwise noted). All crosses were performed at 25°C unless otherwise noted. For clone induction, heat shocks were performed 60-84 hr after egg laying using the following program: 38°C for 1hr, 25°C for 1hr, 38°C for 1h, 25°C for 1hr in an EchoTherm IN35 incubator (Torrey Pines Scientific).

Drosophila **Genetics**

Drosophila stocks used in this study are listed in Key Resources table.

To generate mutant clones or MARCM clones, the following genotypes were used:

yki$^{-/-}$*; Yki* MARCM clones:

hsFLP, tub-Gal4, UAS-GFP; 42DFRT yki^{B5}*/42DFRT tub-Gal80; UAS-Flag-Yki/+*

yki$^{-/-}$*; Myr-Yki* MARCM clones:

hsFLP, tub-Gal4, UAS-GFP; 42DFRT yki^{B5}*/42DFRT tub-Gal80; UAS-Myr-Flag-Yki/+*

yki$^{-/-}$*; Myr-Yki*$^{\Delta NH}$ MARCM clones:

hsFLP, tub-Gal4, UAS-GFP; 42DFRT yki^{B5}*/42DFRT tub-Gal80; UAS-Myr-Flag-Yki*$^{\Delta NH}$*/+*

sd$^{-/-}$ MARCM clones:

hsFLP, tub-Gal80, 19AFRT/sd^{47M}*, 19AFRT; tub-Gal4, UAS-GFP/+*

sd$^{-/-}$*; Myr-Yki* MARCM clones:

hsFLP, tub-Gal80, 19AFRT/sd^{47M}*, 19AFRT; tub-Gal4, UAS-GFP/UAS-Myr-Flag-Yki*

wts$^{-/-}$ clones with *Yki-YFP :*

hsFLP; ykiB5, Yki-YFP/ykiB5, Yki-YFP; 82BFRT wts^{X1}*/82BFRT Ubi-RFP*

wts$^{-/-}$; *yki RNAi* clones:

hsFLP; UAS-yki RNAi/+; 82BFRT wts^{X1}*/82BFRT Ubi-RFP*

wts$^{-/-}$; *sd RNAi* clones:

hsFLP; UAS-sd RNAi/+; 82BFRT wts^{X1}*/82BFRT Ubi-RFP*

wts$^{-/-}$ clones with *sqh:GFP*:

hsFLP; 82BFRT wts^{X1}*, sqh:GFP/82BFRT Ubi-RFP*

wts$^{-/-}$ clones with *zip:GFP*:

hsFLP; zip:GFP/+; 82BFRT wts^{X1}*/82BFRT Ubi-RFP*

The *yki*^{AcidA} allele was generated using the Scarless CRISPR/Cas9 genome engineering technique (http://flycrispr.molbio.wisc.edu/scarless). A 1.5kb left homology arm containing the 5' UTR and first 3bp of exon1 of *yki* and a 1.0kb right homology arm containing 1kb of *yki* sequence from the 4th bp of exon1 were cloned by homologous recombination (Gibson et al., 2009) into pHD-ScarlessDsRed (Drosophila Genomics Resource Center) as the donor template. Two silent

mutations were introduced at the 84th and 90th bp of exon1 (ATCAAGTCC was mutated to ATtAAGTCg) to destroy the guide recognition site in the donor template. This plasmid was co-injected with a pU6- Bbs1-chiRNA based plasmid expressing the guideRNA (5'-ACCAGGTTGTTGGACTTGAT-3') into *vas-Cas9* embryos. G0 flies were crossed to w^{1118} and individual DsRed positive F1s were selected to establish stocks. The DsRed marker cassette was then removed through a single cross to a source of the PBac transposase (*w^{1118}; CyO, P{Tub-PBac\T}2/wg^{Sp-1}*; BL8285). The *yki^{AcidA}* allele was verified by sequencing.

All crosses were performed at 25°C unless otherwise noted. For clone induction, heat shocks were performed 60-84 hr after egg laying using the following program: 38°C for 1hr, 25°C for 1hr, 38°C for 1h, 25°C for 1hr in an EchoTherm IN35 incubator (Torrey Pines Scientific).

Expression Constructs and transgenic line generation

UAS-Myr-Flag-Yki was generated by cloning the Yki cDNA (based on transcript isoform F, NCBI RefSeqID NM_001043103) into a Gateway pTFW (*Drosophila* Genomics Resource Center) that had been modified to include a *Drosophila* Src kinase myristoylation consensus sequence at the N-terminus of any gene cloned in-frame (pUAST-Myr) (Neisch et al., 2013). UAS-Myr-Flag-Yki$^{\Delta NH}$ was generated by using site-directed mutagenesis primers designed to create an in-frame deletion of 47 amino acids from the coding sequence of Yki (deleting aa 35-82 based on transcript isoform F). UAS-Myr-Flag-Yki$^{1-17}$, UAS-Myr-Flag-Yki$^{18-34}$, UAS-Myr-Flag-Yki$^{1-34}$, UAS-Myr-Flag-Yki$^{35-395}$, UAS-Myr-Flag-Yki$^{1-88}$, UAS-Myr-Flag-Yki$^{89-395}$, UAS-Myr-Flag-Yki$^{1-238}$, UAS-Myr-Flag-Yki$^{239-395}$ were generated by cloning corresponding Yki fragments into pTFW-Myr construct.

Strn-Mlck-HA construct was generated by cloning Strn-Mlck isoform B CDS from BDGP ESTs collection clone RH61010 (*Drosophila* Genomics Resource Center) into a Gateway pAWH (*Drosophila* Genomics Resource Center) vector.

P-element transformation was used to generate transgenic animals carrying either *UAS-Myr-Yki* or *UAS-Myr-Yki$^{\Delta NH}$* (Duke University Model Systems Genomics). Multiple lines were isolated and tested for each. Lines on the third chromosome were selected for further experimentation.

Site specific integration of *UAS-Myr-Yki$^{1-34}$-GFP*, *UAS-Myr-Yki^{AcidA}, UAS-Myr-Yki* were performed by cloning respective Yki constructs into a modified pUASTattB (Bischof et al. 2007) vector that adds a myristoylation consensus sequence and a 3X Flag at the N terminus, followed by injection into *y M{vas-int.Dm}ZH-2A w; M{3xP3-RFP.attP}ZH-86Fb* embryos.

Site specific integration of *UAS-Strn-Mlck-HA* was performed by cloning Strn-Mlck isoform B with C terminal HA tag into pUASTattB vector and injected into *y M{vas-int.Dm}ZH-2A w; M{3xP3-RFP.attP}ZH-86Fb* embryos.

Immunostaining and live imaging of wing imaginal discs

Wandering third instar wing discs were dissected in Schneider's *Drosophila* Medium (Sigma) supplemented with 10% Fetal Bovine Serum (Thermo Fisher Scientific) and fixed in 2% paraformaldehyde/PBS solution for 20 min. The following primary antibodies were used: guinea pig anti-Sqh1P (1:300), mouse anti Sqh (1:1000) mouse anti-Flag (1:25000), rat anti-Ecad (1:2000), mouse anti-β-galactosidase (1:500), guinea pig anti-Sd (1:1000), rabbit anti-Yki (1:1000), guinea pig anti-Ex (1:5000). All secondary antibodies (Jackson ImmunoResearch Laboratories) were used at 1:500 or 1:1000. Immunostaining samples were imaged using either a

Zeiss LSM 510, LSM800, or LSM 880 scanning confocal microscope and the images were manipulated with *Image J.*

Live imaging was done as previously described (Su et al., 2017). Wing imaginal discs were placed under coverslip supported by polystyrene beads with a nominal diameter of 53µm (Bangs Laboratories).

Immunostaining and imaging of S2 cells

3.5×10^6 S2 cells were transfected with 250ng Ubi-Gal4 and 250ng of the indicated UAS constructs using DDAB (dimethyldioctadecyl-ammonium bromide, Sigma) (Han, 1996) at 250 µg/ml in six well plates. Cells were fixed 2-3 days after transfection in 2% paraformaldehyde/PBS solution for 10 min and stained and imaged as described above for imaginal tissues.

Co-Immunoprecipitation

3.5×10^6 S2 cells were transfected with 250ng Ubi-Gal4, 250ng of pAWH-Strn-Mlck (Strn-Mlck-HA under the actin5C promoter), and 250ng of pUASt constructs or 250ng Ubi-Gal4, 250ng of Strn-Mlck-HA, and 250ng of UAS-Flag-Yki constructs using DDAB (dimethyldioctadecyl-ammonium bromide, Sigma) (Han, 1996) at 250 µg/ml in six well plates. IPs were performed 2-3 days after transfection. Cells were harvested and lysed in buffer containing 25 mM Hepes, 150 mM NaCl, 1 mM EDTA, 0.5 mM EGTA, 0.9 M glycerol, 0.1% Triton X-100, 0.05% deoxycholic acid, 0.5 mM DTT, and Complete protease inhibitor cocktail (Roche). Flag IPs were performed using anti-Flag M2 agarose beads (Sigma-Aldrich). IP reactions were performed at 4°C overnight. For immunoblotting, 8% SDS-PAGE gels were used and transferred onto nitrocellulose. Antibodies were used at the following concentrations: mouse anti-Flag M2 at 1:50,000 (Sigma-

Aldrich), rabbit anti-HA at 1:5,000 (Rockland). Fluorescently labeled IRdye800 (Rockland) and Alexa Fluor 680 (Invitrogen) secondary antibodies were used at a concentration of 1:5,000. Images of the blots were obtained using Odyssey CLx with ImageStudio software (LI-COR Biosciences).

Quantification and statistical analysis

Image J was used to quantify mean fluorescence intensity in selected regions of the wing imaginal discs. To quantify adult wing sizes, wings were mounted in methyl salicylate and photographed with the same settings on a Zeiss Axioplan 2ie microscope using a Canon camera (EOS rebel T2i). Subsequent measurements of wing size and statistical analyses were processed using Image J and R, respectively.

All statistical comparisons between means were performed by One-way ANOVA with Tukey's HSD test in R with the exception of Fig.S3 and Supplement Table 1, in which One-way ANOVA and Games-Howell test was used. Statistical significance of results between compared groups was indicated as follows: **** ($p \leq 0.0001$), *** ($p \leq 0.001$), ** ($p \leq 0.01$), n.s. (not significant, $p > 0.05$).

CHAPTER 3

Functional interactions of Yorkie and apical polarity proteins at the cell cortex

3.1 Introduction

Apical basal polarity has recently been found to interact with the Hippo signaling pathway to regulate tissue growth in epithelial cells. Apical basal polarity is established and maintained by polarity proteins through complex molecular interactions at the cell cortex (St Johnston and Ahringer 2010; Nance and Zallen 2011; Laprise and Tepass 2011; Campanale, Sun, and Montell 2017; also see Chapter 1). The net result of these interactions is that proteins that promote apical identity (apical polarity proteins) accumulate at the junction and apical domains, while the basolateral polarity proteins accumulate in the basolateral domain.

Recent studies suggest that the apical and junctional cell cortex is an important site of Hippo pathway regulation in *Drosophila* and mammalian epithelia (Genevet and Tapon, 2011, Boggiano and Fehon, 2012; Meng et al., 2016; Sun and Irvine, 2016; Su et al., 2017). The Hippo pathway upstream regulators Crumbs, (Crb), Merlin (Mer), Kibra (Kib) and Expanded (Ex), as well as the core kinase components Hippo (Hpo) and Warts (Wts) are all enriched at the apical cell cortex (McCartney et al., 2000; Cho et al., 2006; Grzeschik et al., 2010). Interestingly, these pathway components are organized into different signaling complexes in distinct cortical regions. For example, Crb and Ex recruit Hpo and Wts to the junctional cortex whereas Mer and Kib recruit Hpo and Wts to the apical medial cortex (S. Sun and Irvine 2016; Su et al. 2017). Recruitment of the core components to the cortex promotes pathway activation whereas mis-localization of the core components leads to pathway inactivation (Boggiano and Fehon 2012; Irvine and Harvey 2015). In the previous chapter, I showed that Yki has a non-transcriptional function at the apical

cell cortex. In this chapter, I will further explore Yki's potential non-transcriptional function at the apical cell cortex.

Accumulating evidence suggests there are reciprocal regulations between the apical polarity proteins and the Hippo pathway. Apical polarity proteins Crumbs (Crb) and atypical Protein Kinase C (aPKC) have been implicated in regulating the Hippo pathway. Conversely, inactivation of multiple Hippo pathway components as well as ectopic expression of Yki result in increased abundance of apical polarity proteins at the apical cell cortex (Genevet et al., 2009; Hamaratoglu et al., 2009). In this chapter, I will investigate potential regulation of the Hippo pathway by two apical polarity proteins Bazooka (Baz, the Drosophila orthologue of Par-3) and aPKC.

3.2 Results

Membrane-localized Yki is able to recruit Hippo pathway members to the cell cortex

The upstream regulators of the Hippo pathway as well as the core kinases have been shown to localize to the apical cell cortex where they organize into signaling complexes (Boggiano and Fehon, 2012; Sun et al., 2015; Chung et al., 2016). In Chapter 2 we showed that Yki localizes to the apical junctional region (AJR) under normal conditions. Previously our lab found ectopically expressed wild type Yki resulted in increased abundance of Hippo pathway components at the AJR (data not shown). To test if this effect is due to transcriptional function of Yki, we utilized $Yki^{\Delta NH}$ and Myr-Yki, two versions of transcriptionally inactive Yki described in Chapter 2. Myr-Yki is forced to the cell membrane through myristoylation whereas $Yki^{\Delta NH}$ lacks the NH domain that mediates the binding between Yki and its nuclear partner Sd. We ectopically expressed $Yki^{\Delta NH}$ and Myr-Yki to see if transcriptionally inactive Yki has a similar effect. Indeed, both caused

Figure 3.1

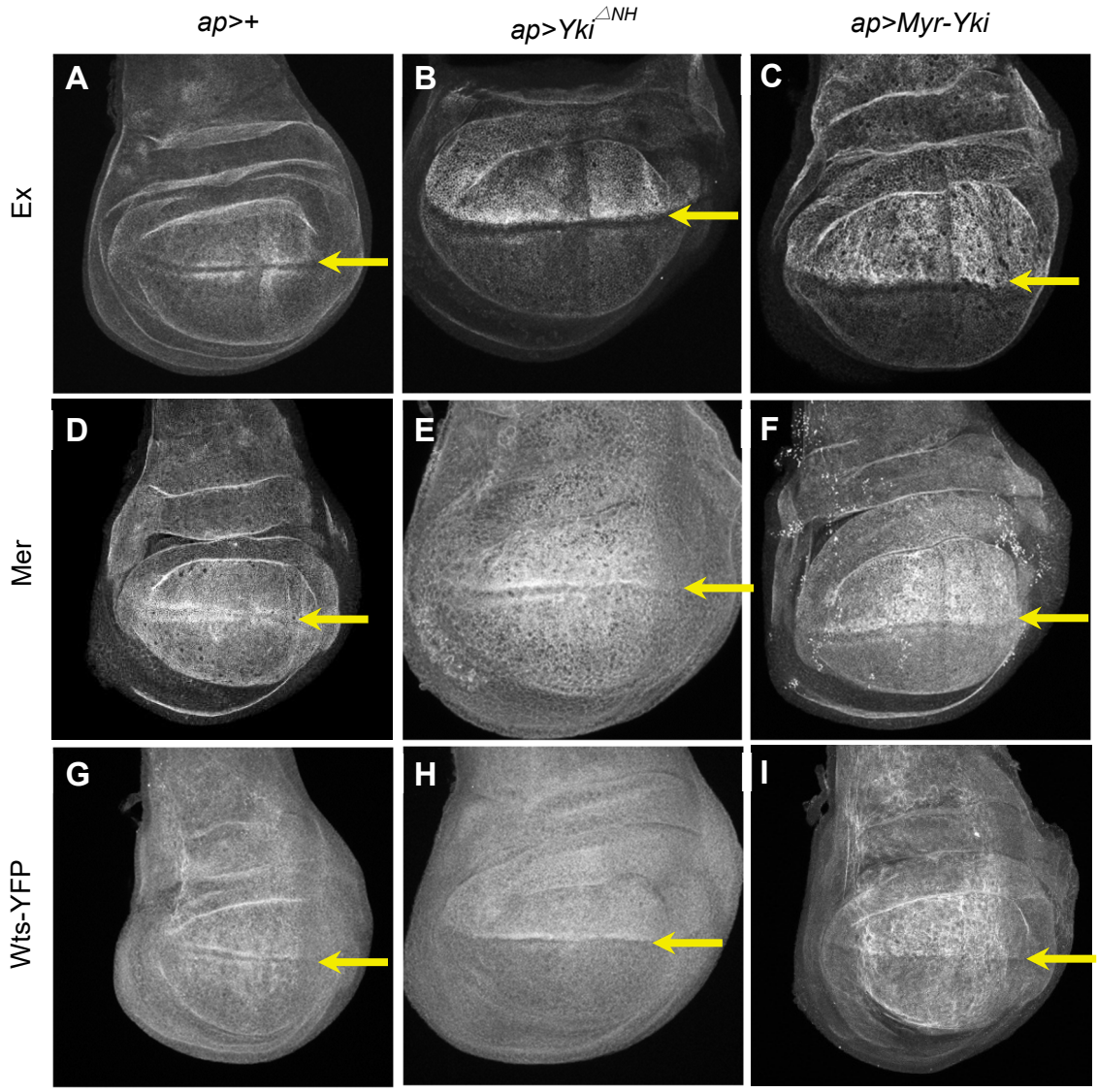

In Collaboration with P. Vanderzalm

Yki is able to recruit Hippo pathway components to the AJR independent of its transcriptional function

Ectopic expression of Yki$^{\Delta NH}$ (**B, E, H**) and Myr-Yki (**C, F, I**) with *ap-Gal4* driver resulted in increased accumulation of Ex, Mer, and Wts-YFP at the apical junctional region.

Yellow arrows indicate expression boundary. Cells above the yellow arrows express corresponding transgenes.

increased Ex, Mer, and Wts accumulation at the AJR (Figure 3.1A-I). This result led us to speculate that cortical Yki may be involved in organizing signaling complexes at the AJR.

It is interesting to note that in this experiment we used an antibody against GFP to detect Wts-YFP. In contrast, when we used live imaging in Chapter 2 to directly detect Wts-YFP we did not observe increased Wts-YFP accumulation in response to Myr-Yki expression (Figure 2.11B-B'). A possible explanation for this apparent difference is that Myr-Yki expression does not alter Wts-YFP levels but rather allows Wts-YFP to be more stably fixed and thereby is more resistant to solubilization during antibody staining.

To test our hypothesis that cortical Yki may also be involved in organizing the signaling complexes, we asked if cortical Yki is able to recruit other Hippo pathway components in S2 cells. We again utilized the Myr-Yki construct to force Yki to the cell cortex. When expressed in S2 cells, Myr-Yki was sufficient to recruit the co-expressed Hippo pathway components Ex, Mer, Hpo, and Wts, to the cell membrane (Figure 3.2A-D).

Together the results in wing imaginal discs and S2 cells suggest Yki can organize Hippo pathway components at the AJR. To test if Yki normally does this, we asked whether removing Yki genetically would cause loss of upstream Hippo pathway components from the AJR. *yki* null clones in the wing imaginal discs occur at very low frequency and are usually very small because Yki is required for cell proliferation. Previously, we found that using a *sd* heterozygous background can increase the viability of *yki* clones. In the absence of Yki, Sd functions as a transcriptional repressor to inhibit Yki target genes (Koontz et al. 2013). Presumably genetically removing half of Sd in *sd* heterozygotes can reduce the suppression of Yki target genes thereby improving viability of *yki* clones. We found that Ex and Mer are still properly localized at the AJR

Figure 3.2

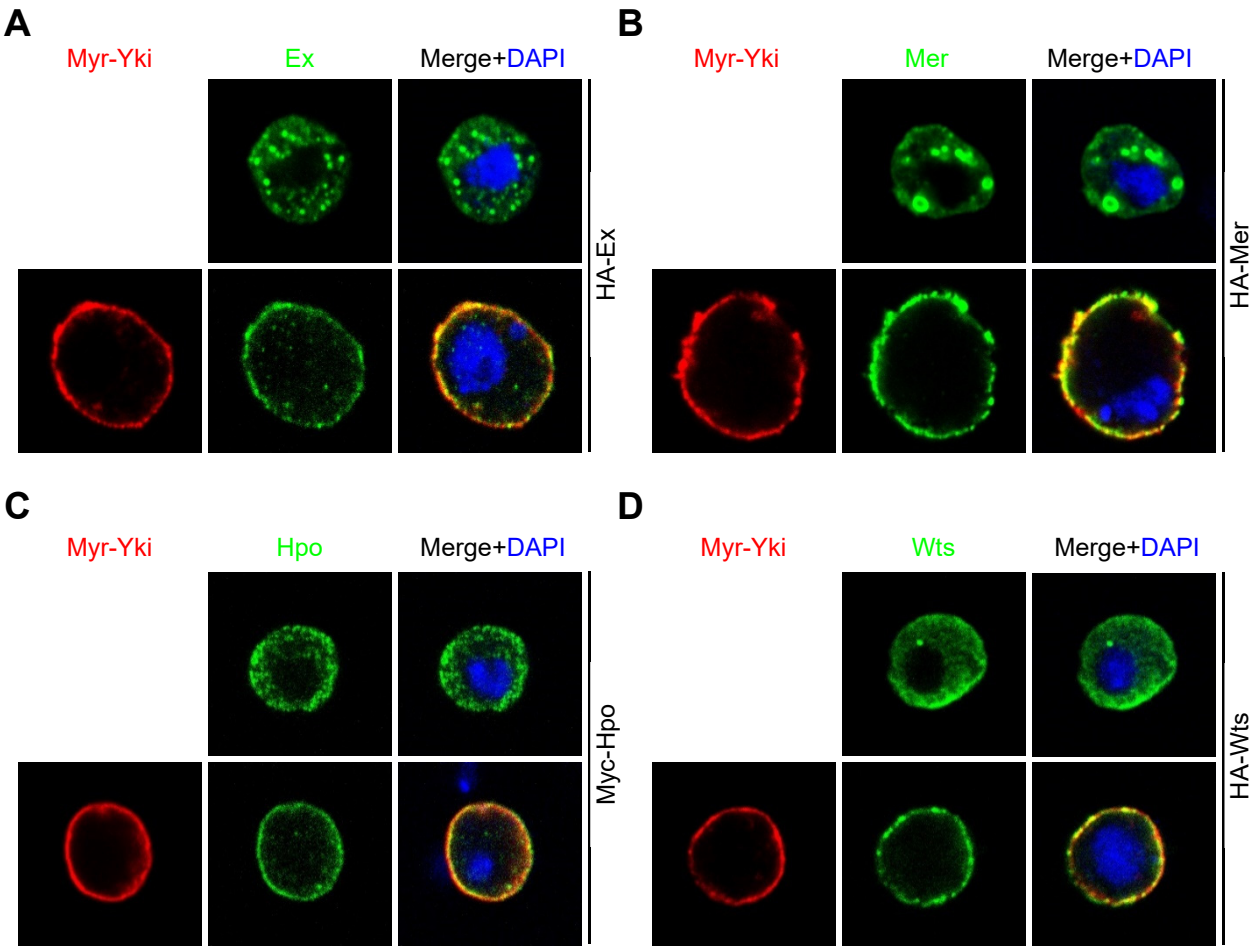

Membrane-localized Yki is able to recruit Hippo pathway members to the cell membrane
In each panel, the first rows show S2 cells transfected with Hippo pathway components alone. All the Hippo pathway components were mostly cytoplasmic. The second rows show S2 cells co-transfected with Myr-Yki. Co-transfection of Myr-Yki with Hippo pathway components Ex (**A**), Mer (**B**), Hpo (**C**), and Wts (**D**) resulted in membrane localization of these components.

Myr-Yki staining is shown in red, Hippo pathway components stainings are shown in green, DAPI is shown in blue.

Figure 3.3

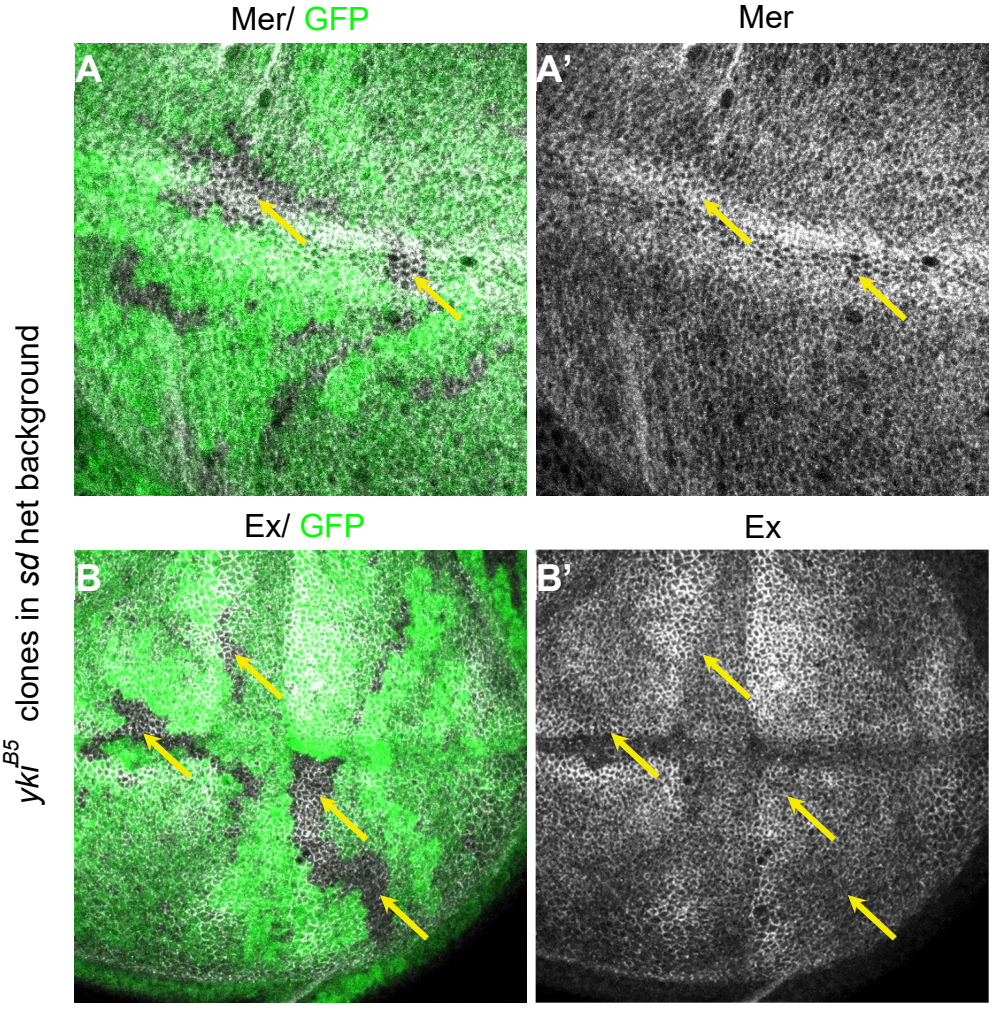

Yki is not required for assembly of Hippo signaling complex at the AJR

yki^{B5} mitotic clones were generated in *sd*$^{+/-}$ background to enhance clone viability. Localization and abundance of Hippo pathway regulators Mer (**A**) and Ex (**B**) were not affected in *yki*^{B5} clones, suggesting Yki is not required for assembly of Hippo signaling complex at the AJR.

Yellow arrows indicate *yki*^{B5} clones.

but we did not examine other pathway components. Together our data suggest Yki is not required to recruit upstream components to the cell cortex, but does not rule out the possibility that Yki recruits more downstream components or facilitates formation of active signaling complexes.

Yki promotes Wts activation

Negative feedback is a common feature built into signaling pathways. In the Hippo pathway, the Yki transcriptional targets Mer and Ex are also positive regulators of the Hippo pathway. Activation of Yki will lead to up-regulation of *Mer* and *ex* expression, which in turn is thought to cause activation of the Hippo pathway and inhibit Yki (Hamaratoglu et al. 2006). However, this has not been demonstrated directly in tissue. We tested this model by expressing various Yki transgenes in wing imaginal discs and examining Hippo pathway activity. We utilized an antibody specific for the phosphorylated, active form of Wts as a readout of upstream pathway activity (J. Yu et al. 2010; Boggiano, Vanderzalm, and Fehon 2011; Yin et al. 2013). Expression of wild type Yki and transcriptionally activated Yki with its Wts phosphorylation site mutated into Alanine (YkiSA) both caused activation of Wts, consistent with the negative feedback model (Figure 3.4).

Our observation that Yki can recruit other pathway members to the cell cortex raises an alternative possible mechanism for negative feedback - that Yki may facilitate assembly of Hippo signaling complexes and thereby promote pathway activity at the AJR independently of its transcriptional function. To test this idea, we asked how transcriptionally inactivated $Yki^{\Delta NH}$, $Yki^{\Delta NH}SA$ and Myr-Yki affect Wts activation. Ectopic expression of $Yki^{\Delta NH}$, $Yki^{\Delta NH}SA$ did not cause strong Wts activation. However, Myr-Yki caused robust Wts activation similar to that of wild-type Yki (Figure 3.4), suggesting that cortical Yki can assemble upstream components into

Figure 3.4

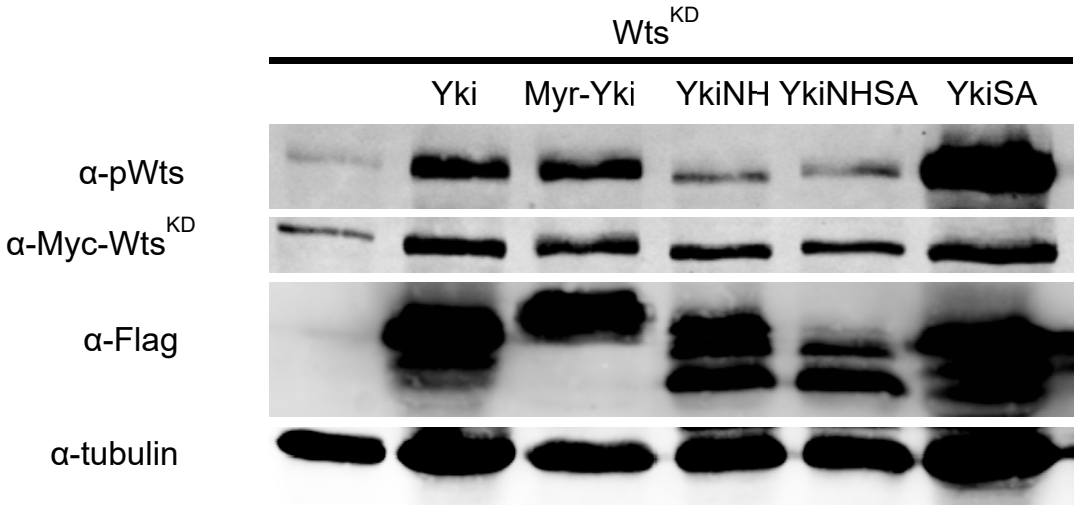

Yki promotes Wts phosphorylation
Phosphorylation of a Myc tagged kinase dead version of Wts were analyzed in lysates isolated from wing imaginal discs expressing corresponding transgenes with *ap-Gal4* driver. Expression of wild type Yki and transcriptionally activated YkiSA, and membrane targetd Myr-Yki caused dramatic increase of Wts phosphorylation whereas expression of transcriptionally inactive Yki$^{\Delta NH}$ and Yki$^{\Delta NH}$SA did not strongly affect Wts activation.

an active complex. Together, these results could indicate that Yki regulates the phosphorylation of Wts through both transcriptional activity and non-transcriptional activity: expression of Yki or YkiSA primarily acts through transcriptional activity to activate Wts whereas Myr-Yki primarily acts through non-transcriptional activity. However, as demonstrated in Chapter 2, Myr-Yki induced Wts activation could be caused indirectly by transcriptional activation of endogenous Yki. Additional work is needed to distinguish these hypotheses.

Membrane-localized Yki is able to recruit apical polarity proteins to the cell cortex

Apical polarity proteins reside in the apical cell cortex and have been found to regulate Hippo pathway activity. On the other hand, activation of Yki, either by mutations in Hippo pathway components or ectopic expression of Yki, results in increased abundance of apical polarity proteins Crb, aPKC and Patj at the AJR (Genevet et al., 2009; Hamaratoglu et al., 2009). Intriguingly, neither *crb* nor *aPKC* is transcriptionally regulated by Yki (Genevet et al. 2009), suggesting the increase of these proteins is not caused by Yki transcriptional function. To test if the increase of apical polarity proteins is dependent on Yki transcriptional function, we ectopically expressed transcriptionally inactive $Yki^{\Delta NH}$ and Myr-Yki to see if they could also affect the abundance of apical polarity proteins at the cell cortex. Indeed, both $Yki^{\Delta NH}$ and Myr-Yki caused increased accumulation of apical polarity proteins Crb, Baz, and aPKC at the cell cortex (Figure 3.5A-I). In contrast, the basolateral polarity protein Discs large (Dlg) was not affected (Figure 3.5J-L), suggesting the effect is specific to apical polarity proteins. To test if Yki is required for their localization at the apical cell cortex, we asked whether removing Yki genetically would cause loss of these proteins from the AJR. We generated *yki* mutant clones in a *sd* heterozygous

Figure 3.5

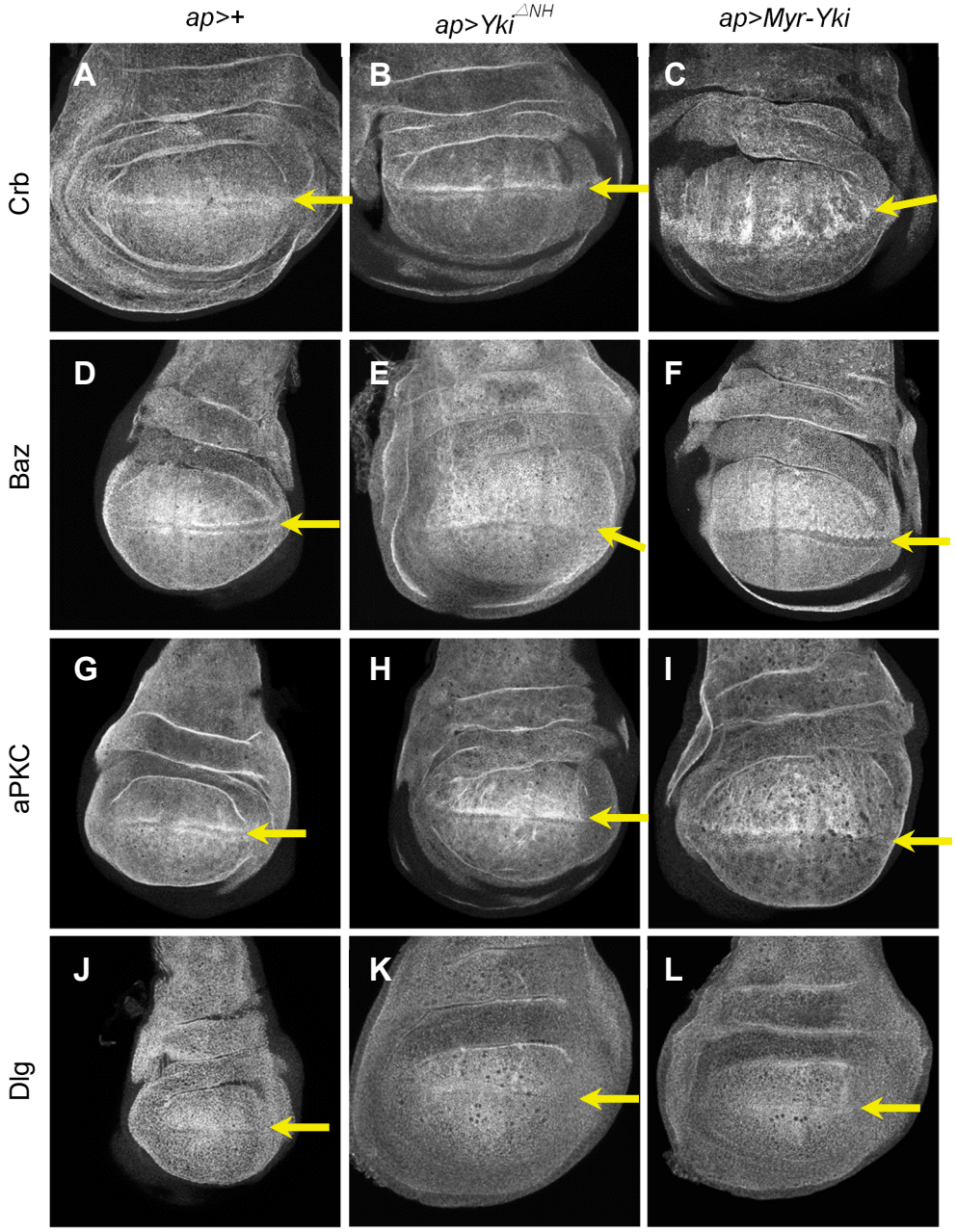

In Collaboration with P. Vanderzalm

Membrane-localized Yki is able to recruit apical polarity proteins to the AJR

Ectopic expression of Yki$^{\Delta NH}$ (**B, E, H, K**) and Myr-Yki (**C, F, I, L**) with *ap-Gal4* driver resulted in increased accumulation of apical polarity proteins Crb, Baz, and aPKC. Basolateral polarity protein Dlg was not affected.

Yellow arrows indicate expression boundary. Cells above the yellow arrows express corresponding transgenes.

Figure 3.6

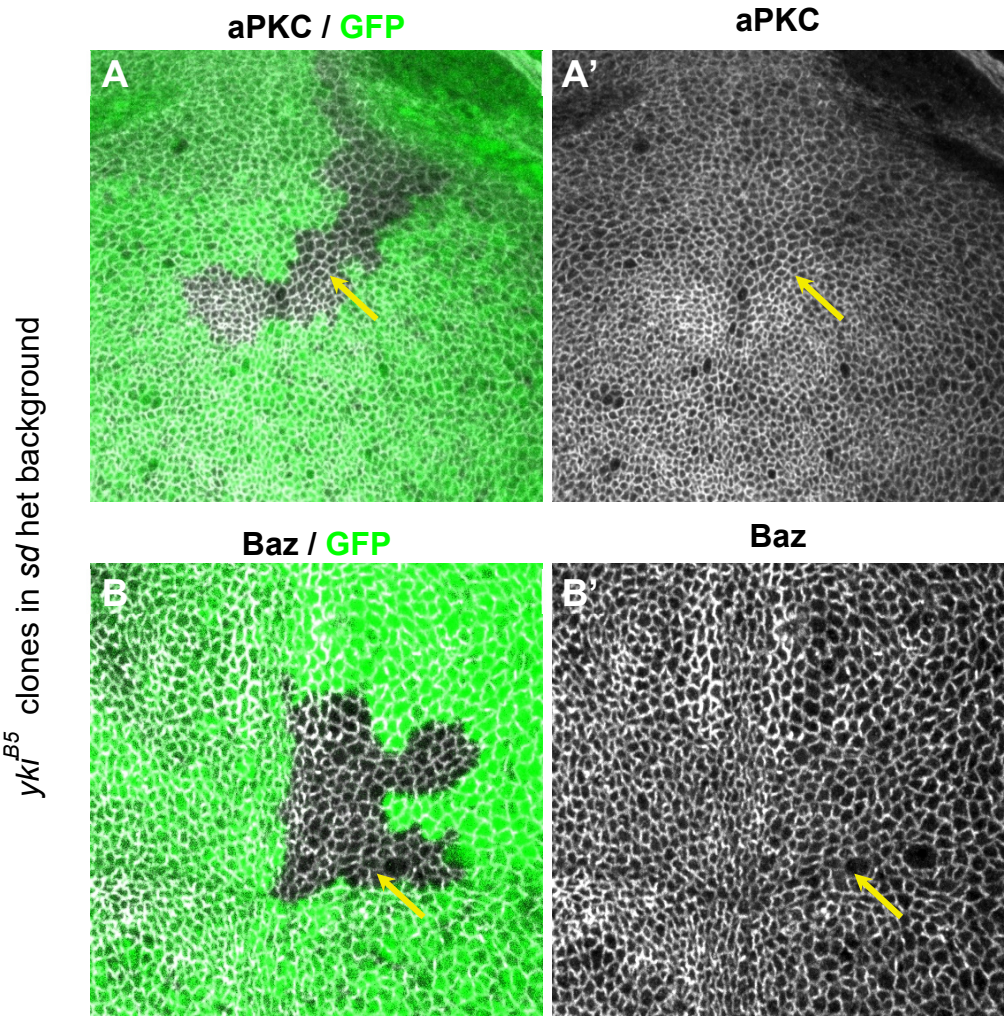

Yki is not required for localizing apical polarity protein to the AJR

yki^{B5} mitotic clones were generated in *sd*$^{+/-}$ background to enhance clone viability. Localization and abundance of apical polarity proteins aPKC (**A**) and Baz (**B**) were not affected in *yki*^{B5} clones, suggesting Yki is not required for localizing apical polarity proteins.

Yellow arrows indicate *yki*^{B5} clones.

background and found that aPKC and Baz are still properly localized at the apical cell cortex (Figure 3.6), indicating Yki is not required to maintain their cortical localization.

Genetic interactions between *yki* and apical polarity genes

To further test potential functional interactions between apical polarity proteins and Yki activity, we knocked down each apical polarity component and simultaneously expressed *yki* to test how loss of apical polarity proteins modifies the *yki* expression phenotype (Figure 3.7). Expression of *yki* alone under the *apterous-Gal4 (ap-Gal4)* driver produced a mild overgrowth phenotype. Knocking down *stardust (sdt), crb, baz,* or *aPKC* enhanced the overgrowth phenotype of *yki* overexpression, suggesting these apical polarity proteins may regulate Yki activity. Crb has been well characterized as a positive regulator of the Hippo pathway through Expanded (Ex). Sdt maintains the stability of the Crb complex in most tissues and loss of Sdt causes the same epithelial defects as does loss of Crb (Tepass 2012). In addition, *sdt RNAi* enhances *yki* overexpression overgrowth to similar degree as *crb RNAi*. These results suggest that Sdt may regulate the Hippo pathway through Crb. Therefore, I focused further efforts on Baz and aPKC, as these seemed more likely to be involved in novel mechanisms through which apical polarity proteins modulate the Hippo pathway.

Baz positively modulates the Hippo pathway

In *Drosophila*, Baz is essential in establishing AJs in embryonic and follicular epithelia (McGill et al., 2009; Morais-de-Sá et al., 2010). However, depleting Baz does not affect AJs in wing imaginal discs (Figure 3.8A-C), suggesting that it is not necessary to maintain AJ's once

Figure 3.7

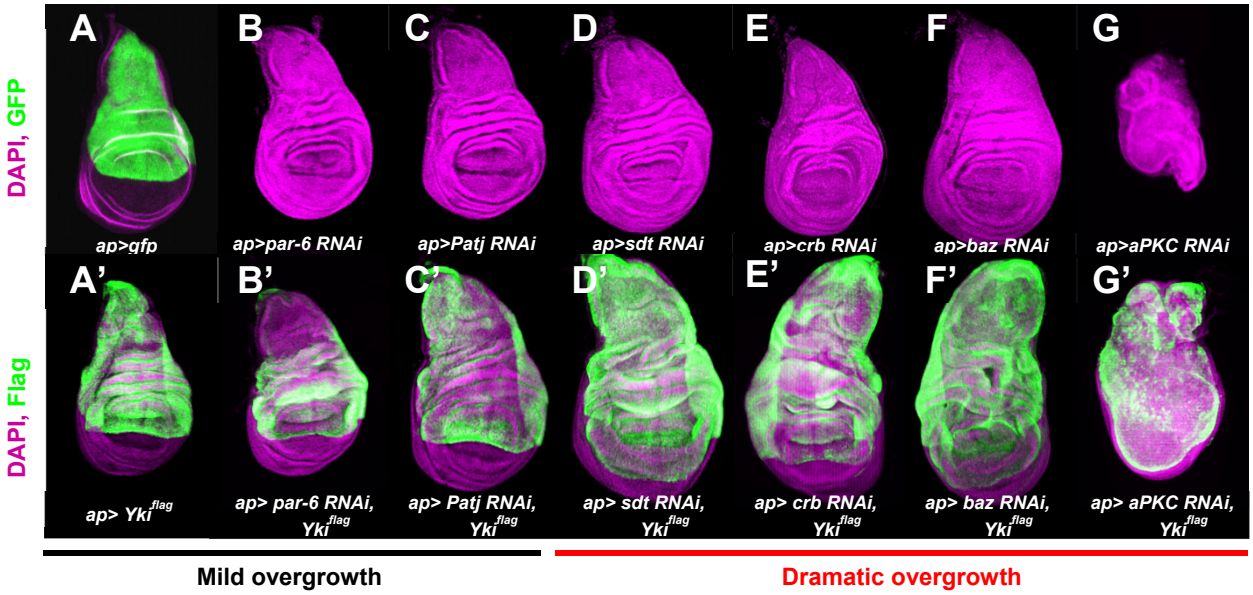

Apical polarity gene knockdown enhances the overgrowth phenotype of Yki expression
Ectopic expression of wild-type Yki with *ap-Gal4* driver resulted in mild tissue overgrowth (**A'**). Depleting apical polarity proteins Par-6 (**B**), Patj (**C**), Stardust (Sdt, **D**), Crumbs (Crb, **E**), or Bazooka (Baz, **F**) did not strongly affect tissue growth. Depleting aPKC caused strong tissue loss (**G**).
Apical polarity proteins were also depleted in Yki expressing background to assess how they interact with Yki. Depleting Par-6 (**B'**) or Patj (**C'**) did not modify overgrowth phenotype. Depleting Stardust (Sdt, **D'**), Crumbs (Crb, **E'**), Bazooka (Baz, **F'**), or (aPKC, **G'**) enhanced the overgrowth phenotype of *yki* overexpression, suggesting these proteins interact with Yki.

Figure 3.8

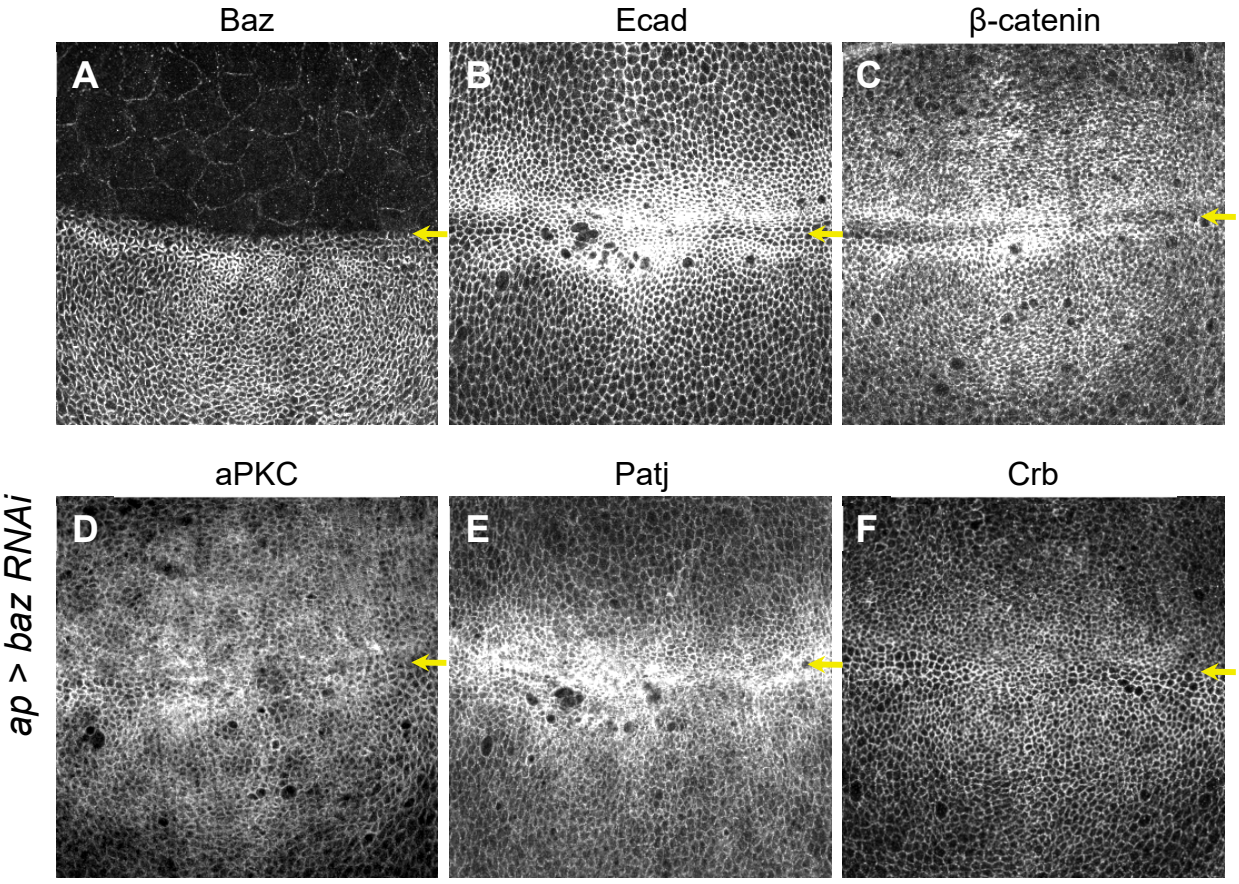

Depleting Baz does not affect Adherens Junctions or other apical polarity proteins
Baz is effectively depleted with *baz RNAi* using *ap-Gal4* driver (**A**). Localization and abundance of Adherens Junctions components Ecad (**B**) and β-catenin (**C**) were not affected by loss of Baz. Similarly, localization and abundance of apical polarity proteins aPKC (**D**), Patj (**E**), and Crb (F) were not affected by loss of Baz.
Yellow arrows indicate expression boundary. Cells above the yellow arrows express corresponding transgenes.

established. In addition, depleting Baz did not affect other apical polarity proteins (Figure 3.8D-F).

To test if Baz is involved in controlling tissue growth via the Hippo pathway, we first depleted Baz and analyzed adult wing sizes. We found that growth was not affected when Baz was depleted (Figure 3.9A-C). Interestingly, when we additionally introduced one extra copy of the *yki* gene in the form of an endogenously expressed *yki-YFP* transgene, we observed an outheld wing phenotype often associated with overgrowth (Figure 3.9F-G). The posterior compartment of the wing blade also seemed to be slightly overgrown (Figure 3.9D-E) though statistical analysis is needed to confirm this. To directly test if Baz modulates the Hippo pathway, we depleted Baz and examined the expression levels of Hippo pathway reporters *bantam-GFP, ex-lacZ,* and *Diap1-lacZ* (Figure 3.10). *baz RNAi* caused up-regulation of *bantam-GFP* (Figure 3.10A-B''). However, no change was detected for *ex-lacZ* (Figure 3.10C-D'') or *Diap1-lacZ* (Figure 3.10F-G''). *ex-lacZ* expression was not altered in baz^4 (a *baz* null allele) mutant clones either (Figure 3.10E-E''). Together these results suggest Baz positively modulates the Hippo pathway, though it does not seem to play a major role under normal conditions.

Depleting Baz results in increased JNK dependent apoptosis, concealing an overgrowth phenotype

Our hypothesis that Baz positively modulates the Hippo pathway predicts depleting Baz would lead to increased proliferation due to Yki activation. However, we did not observe such a phenotype with *baz RNAi.* One possibility is that loss of Baz also induces apoptosis, which cancels out the increased proliferation. To test this, we stained wing imaginal discs with the apoptosis

Figure 3.9

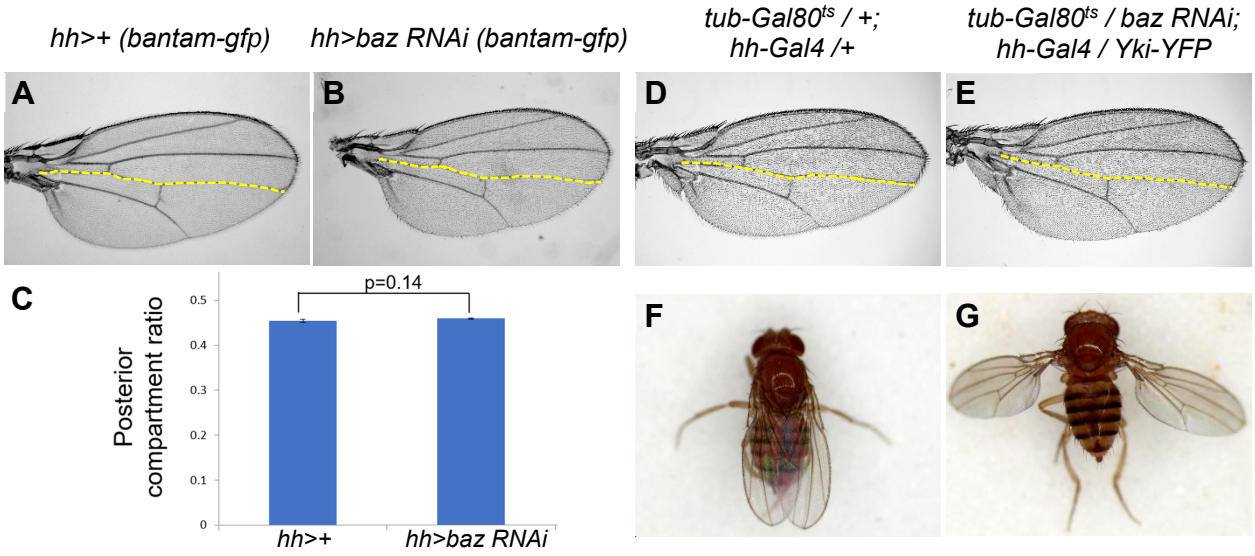

Depleting Baz causes overgrowth in the presence of one extra copy of *yki*

Depleting Baz in the posterior of the wing with *hh-Gal4* driver did not affect relative size of the posterior wing (**A-C**). Posterior compartment ratio was calculated by dividing the size of the posterior wing by the size of the entire wing. Yellow dashed lines indicate the expression boundary. p value was calculated with student's t test.

Depleting Baz caused overgrowth in the presence of one extra copy of *yki* (**D-G**).
Expression of a *baz RNAi f*or three days in the background of one copy of Yki-YFP resulted in an out-held wing phenotype often associated with overgrowth (**G**). The posterior compartment was slightly overgrown (**E**) compared with control (**D**).

Figure 3.10

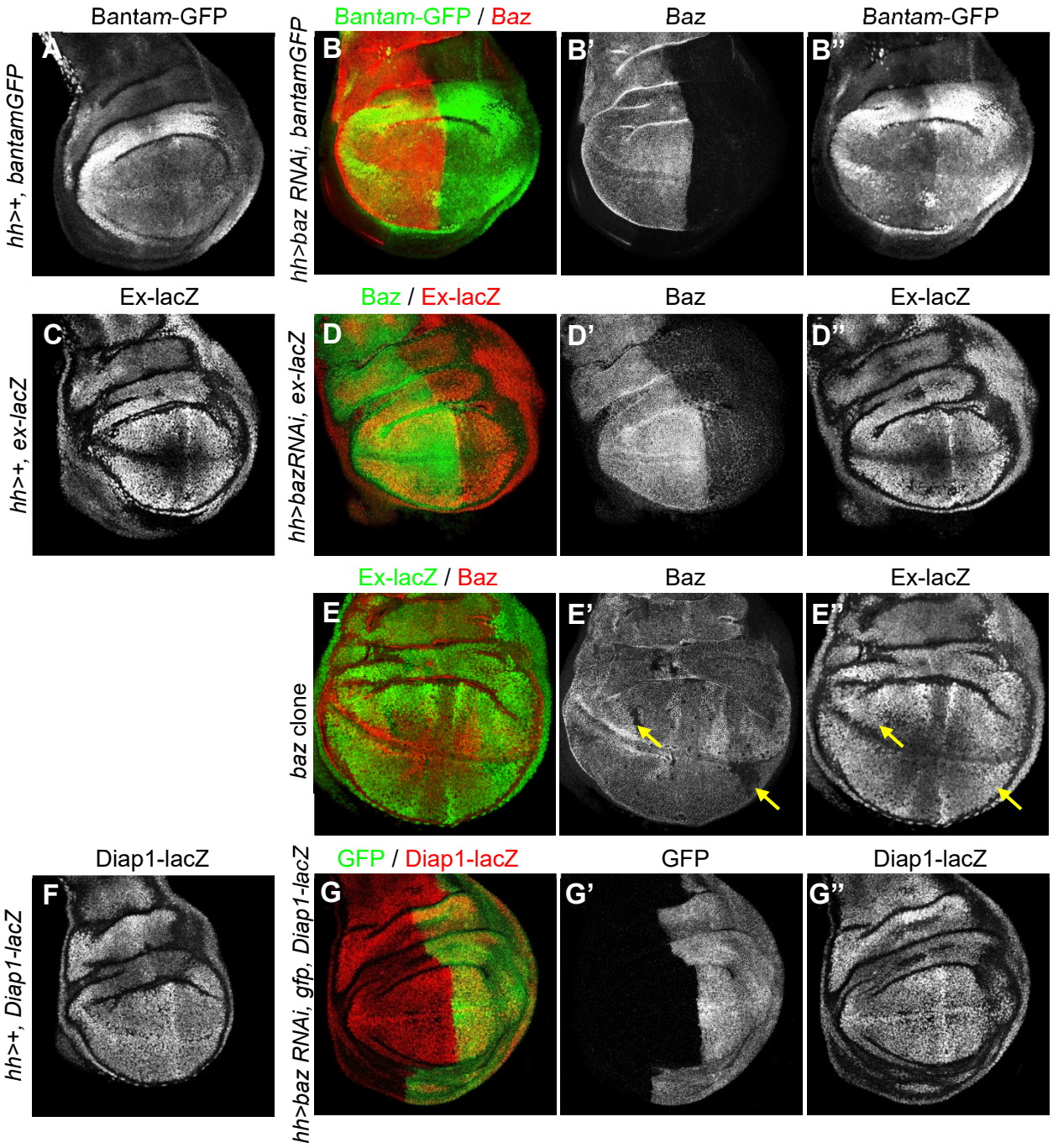

Depleting Baz causes increased expression of Hippo pathway reporter *bantam-GFP*, but not *ex-lacZ* or *Diap1-lacZ*

Depleting Baz caused increased expression of Hippo pathway reporter *bantam-GFP* (**B-B"**).
Depleting Baz did not alter expression of Hippo pathway reporter *ex-lacZ* (**D-D'**).
Completely remove Baz by generating *baz* null clones did not alter expression of *ex-lacZ* (**E-E"**). Yellow arrows indicate *baz* clones.
Depleting Baz did not alter expression of Hippo pathway reporter *exDiap1-lacZ* (**G-G'**).

Figure 3.11

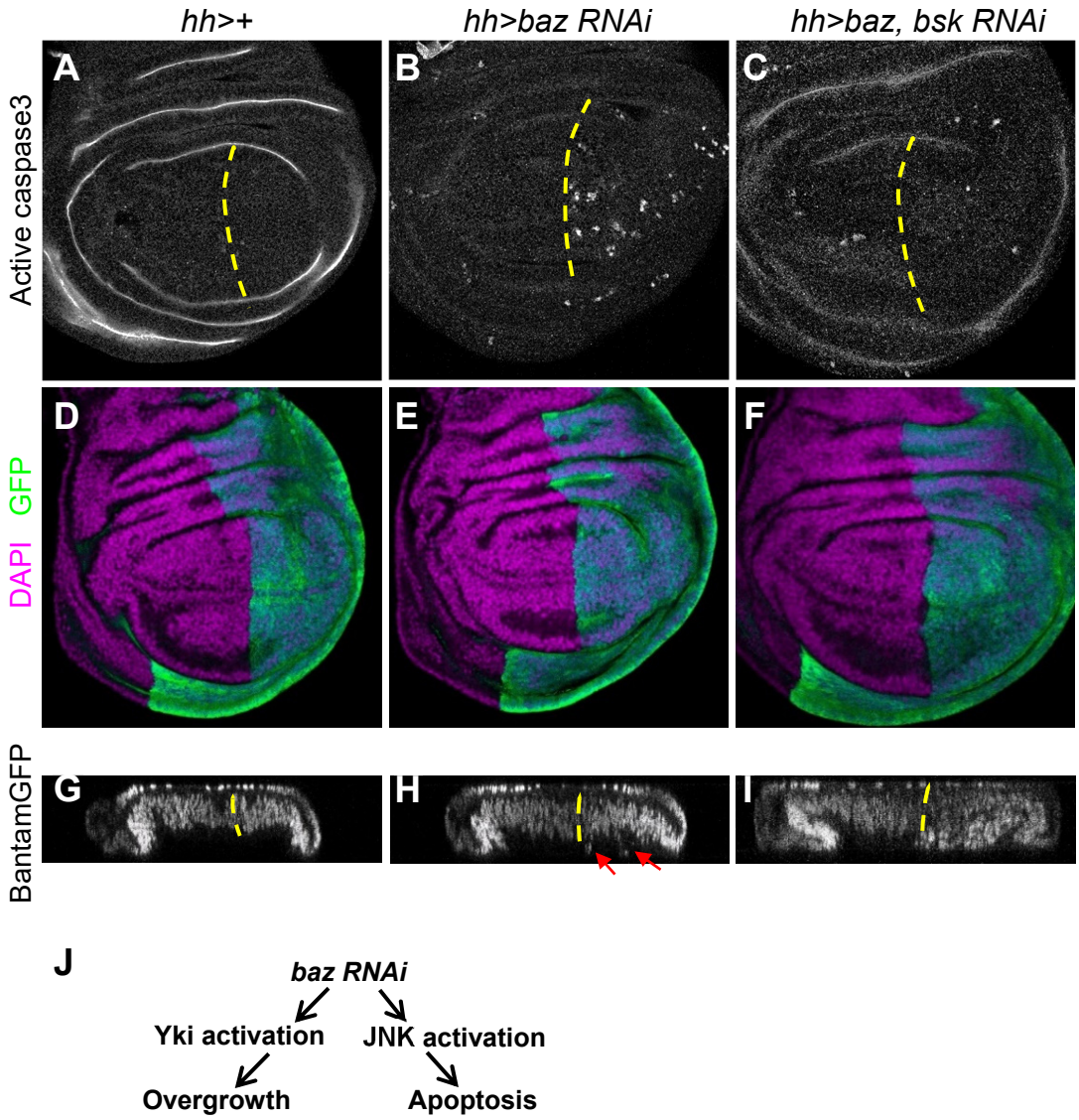

Depleting Baz results in increased JNK dependent apoptosis, concealing an overgrowth phenotype

Depleting Baz caused increased apoptosis (**B**). Apoptotic cells were excluded from the basal side, indicated by red arrows (**H**). Yellow dashed lines indicate expression boundary. BantamGFP was used to visualize nucleus. Apoptosis was suppressed when JNK signaling was blocked by depleting Bsk (**C**). Suppression of apoptosis in *baz bsk double RNAi* resulted in tissue overgrowth and multi-layering of the epithelia (**F, I**).

Depletion of Baz resulted in increased JNK dependent apoptosis that concealed the overgrowth phenotype through Yki activation (**E, H, J**).

marker active caspase 3 and found that *baz RNAi* indeed caused increased apoptosis (Figure 3.11A-B).

When we blocked the Jun N-terminal kinase (JNK) signaling pathway by depleting the *Drosophila* JNK homolog Basket, the apoptosis phenotype was fully suppressed (Figure 3.11C), resulting in overall tissue overgrowth (Figure 3.11D-I'). These results suggest loss of Baz promotes proliferation through the Hippo pathway and simultaneously causes apoptosis through the JNK pathway, presumably independent of Hippo. These two effects are antagonistic in terms of growth.

Baz does not modulate the Hippo pathway through Mer

In mammalian cells, Mer is necessary for establishing AJs by linking α-catenin to Par3, the mammalian homolog of Baz (Gladden et al. 2010). These data suggest the possibility that Baz cooperates with Mer in regulating the Hippo pathway. To study the potential interactions between *baz* and *Mer*, we used RNAi to deplete one protein and examine the expression pattern of the other. *baz* knockdown did not affect Mer localization or abundance in wing discs (Figure 3.12A); *Mer* knockdown did not affect Baz localization or abundance either (Figure 3.12B). Together these results suggest Baz does not seem to modulate the Hippo pathway through Mer localization or abundance.

aPKC positively modulates the Hippo pathway

To test if aPKC is involved in controlling tissue growth via the Hippo pathway, we depleted aPKC with RNAi and again examined the expression levels of Hippo pathway reporters *bantam-GFP, ex-lacZ,* and *Diap1-lacZ* (Figure 3.13). *aPKC RNAi* resulted in cell-autonomous and non-

Figure 3.12

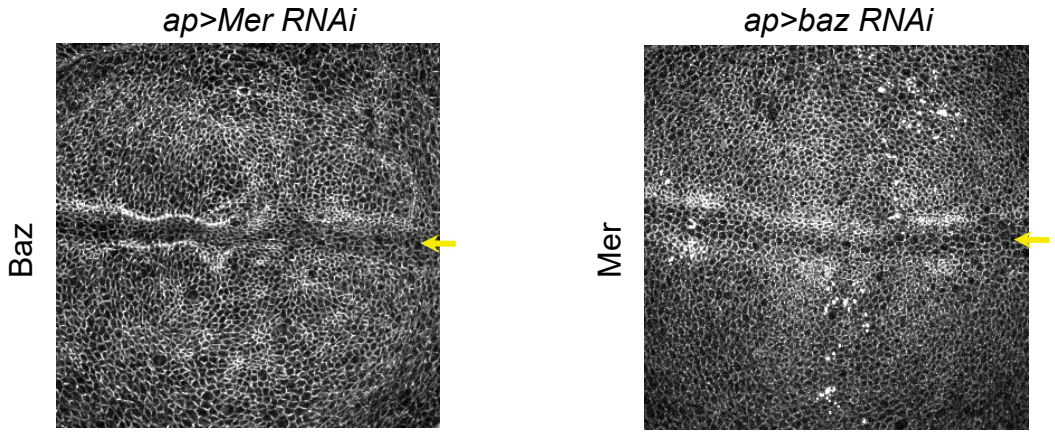

Mer and Baz does not affect localization or abundance of each other
Depleting Mer did not affect localization and abundance of Baz (**A**). Depleting Baz did not affect localization and abundance of Mer (**B**).
Yellow arrows indicate expression boundary. Cells above the yellow arrows express corresponding transgenes.

Figure 3.13

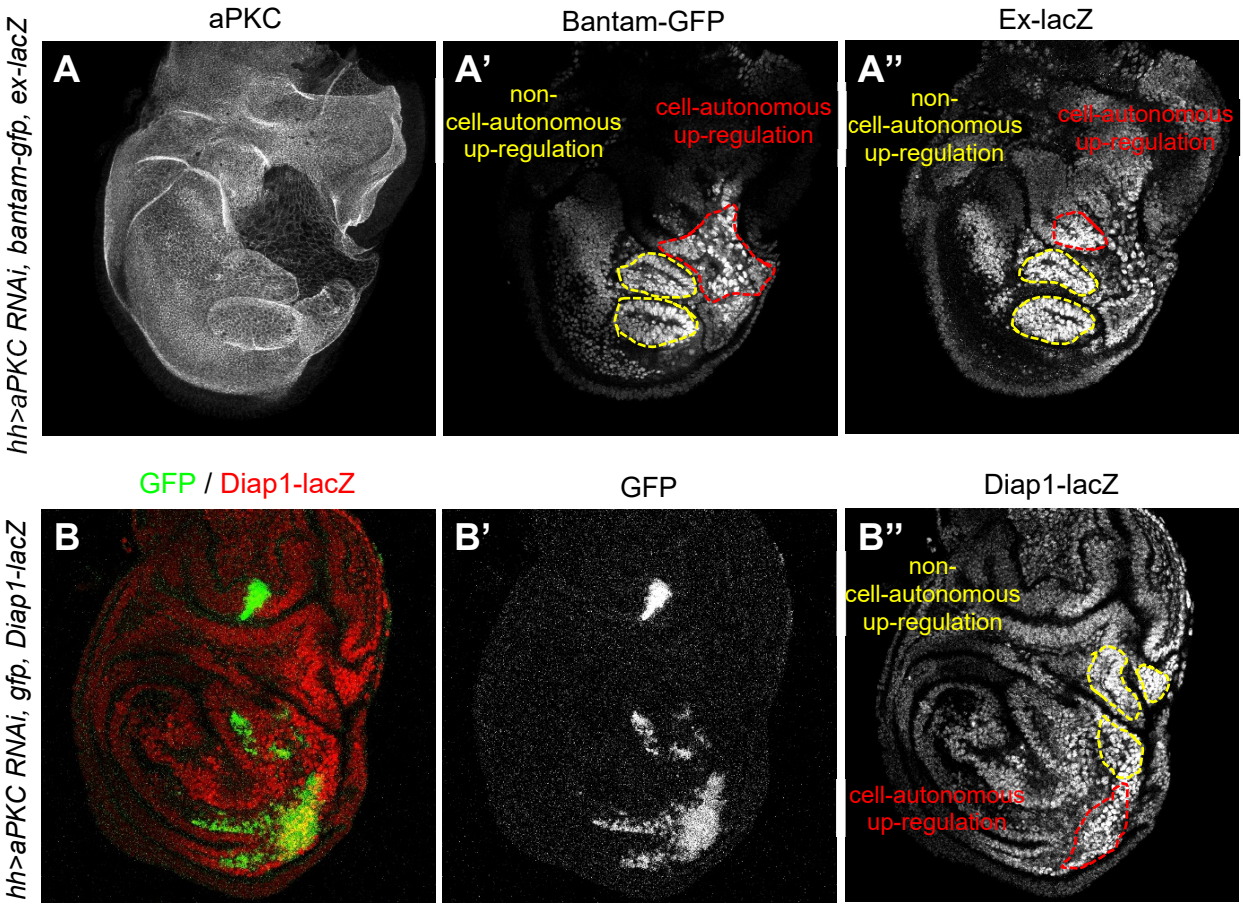

Depleting aPKC resulted in cell-autonomous and non-cell-autonomous up-regulation of Hippo pathway reporters

Depleting aPKC resulted in both cell-autonomous and non-cell-autonomous up-regulation of Hippo pathway reporters *bantam-GFP* (**A'**), *ex-lacZ* (**A"**), and *Diap1-lacZ* (**B"**).

Yellow dashed lines indicate areas with non-cell-autonomous up-regulation of reporter gene. Red dashed lines indicate areas with cell-autonomous up-regulation of reporter gene.

Figure 3.14

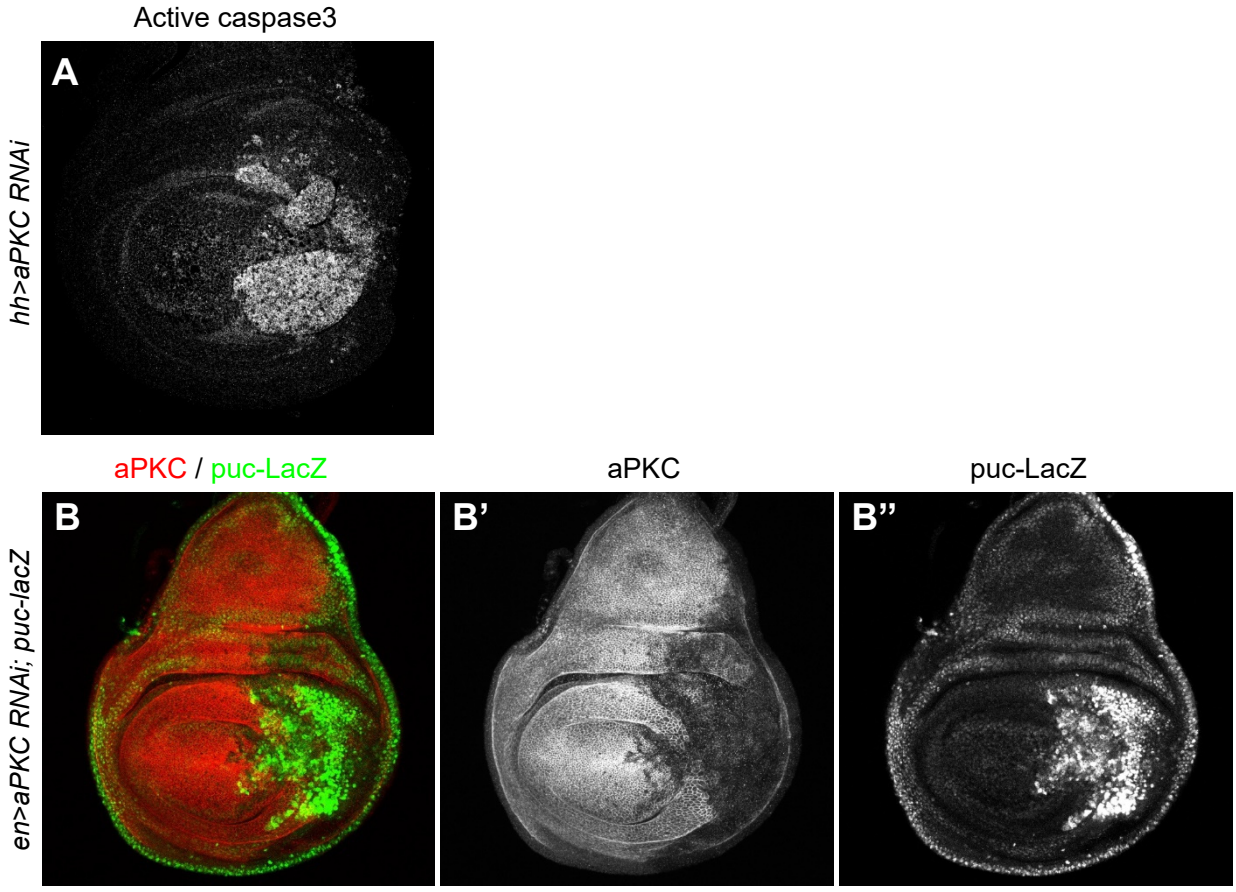

Depleting aPKC resulted in activation of JNK signaling and apoptosis
Depleting aPKC resulted in strong apoptosis indicated by strong active caspase3 staining (**A**). Depleting aPKC resulted in strong up-regulation of JNK signaling pathway reporter *puc-lacZ*, indicating strong activation of JNK signaling (**B"**).

cell-autonomous up-regulation of all three Hippo pathway reporters (Figure 3.13A', A'', B''), suggesting loss of aPKC inactivates the Hippo pathway to promote Yki transcriptional function. In terms of tissue growth, we found that *aPKC RNAi* caused severe cell-autonomous tissue loss (Figure 3.7G, 3.13A, B) as well as compensatory proliferation of neighboring tissue (Figure 3.13A). We therefore asked if tissue loss was caused by strong apoptosis using the apoptosis marker active caspase 3 and found that *aPKC RNAi* indeed caused strong apoptosis (Figure 3.14A). To test if apoptosis is mediated via the JNK signaling pathway, we examined the expression level of the JNK signaling reporter *puckered-lacZ* (*puc-lacZ*). *puc-lacZ* was strongly up-regulated in *aPKC RNAi* cells, indicating activation of JNK signaling. In addition, when we blocked the JNK signaling pathway using *bsk RNAi*, the apoptosis phenotype was fully suppressed (Figure 3.15C).

Together these results suggest loss of aPKC on one hand inhibits the Hippo pathway to promote Yki activity both cell-autonomously and non-cell-autonomously, and on the other hand causes apoptosis through the JNK pathway.

Distinct Mechanisms for cell-autonomous and non-cell-autonomous activation of Yki in *aPKC RNAi* tissue

When we blocked the JNK signaling in aPKC depleted wing imaginal discs, we observed two growth phenotypes: 1. Non-cell-autonomous growth was suppressed; 2. Cell-autonomous tissue loss was converted to overgrowth (Figure 3.15A, C). The first phenotype is consistent with a previous report that shows JNK signaling causes propagation of Yki activity into neighboring cells (Enomoto and Igaki 2012), and suggests the non-cell-autonomous activation of Yki is JNK dependent. The second phenotype plus the fact that up-regulation of the Hippo pathway reporter

Figure 3.15

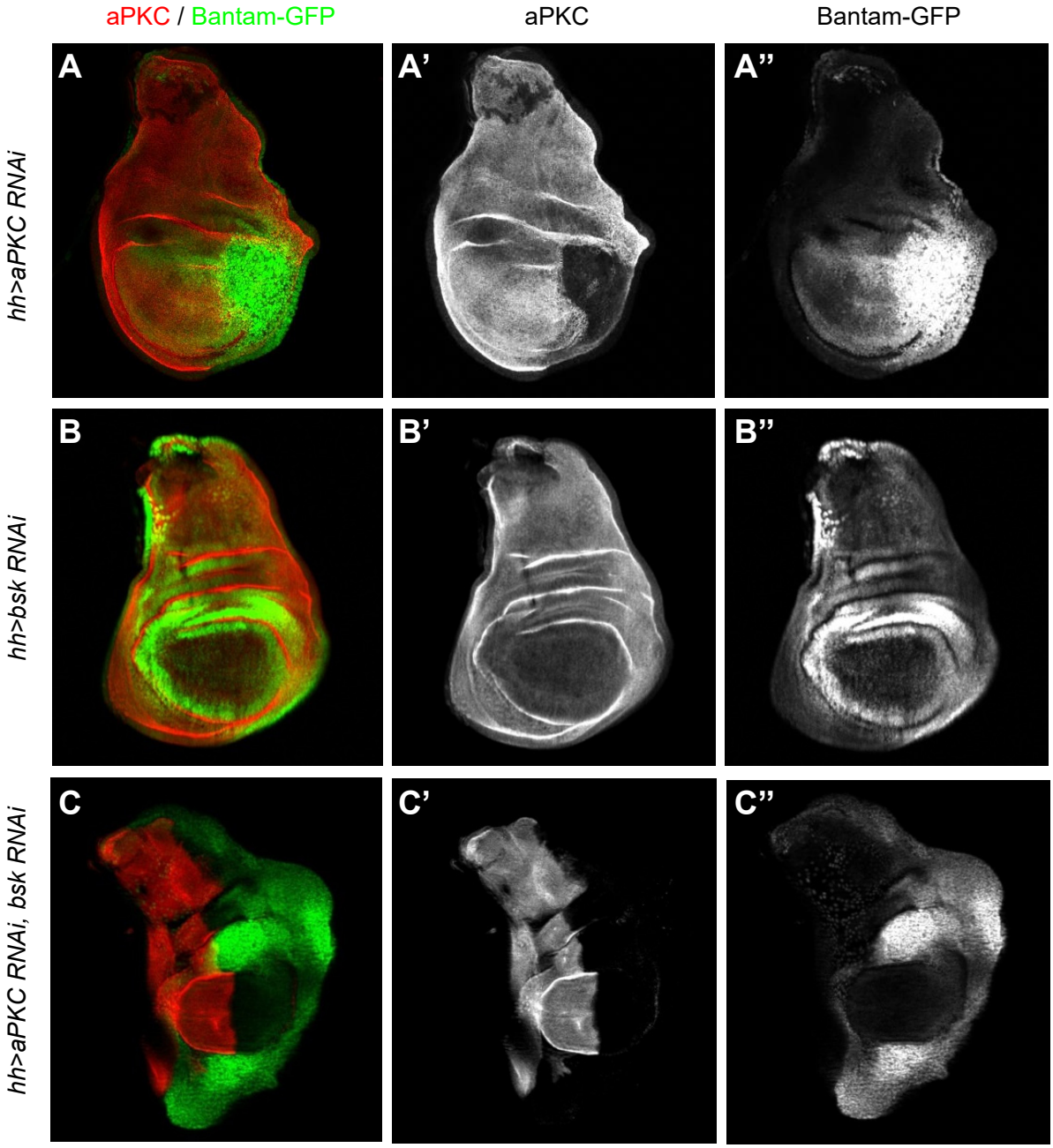

***aPKC RNAi* induced non-cell-autonomous growth depends on JNK signaling**
Depleting aPKC resulted in non-cell-autonomous tissue overgrowth (**A**). The non-cell-autonomous overgrowth was suppressed when JNK signaling was blocked by *bsk RNAi* (**C**), suggesting the overgrowth is dependent on JNK signaling. *bsk RNAi* on its own did not affect tissue growth (**B**).

Figure 3.16

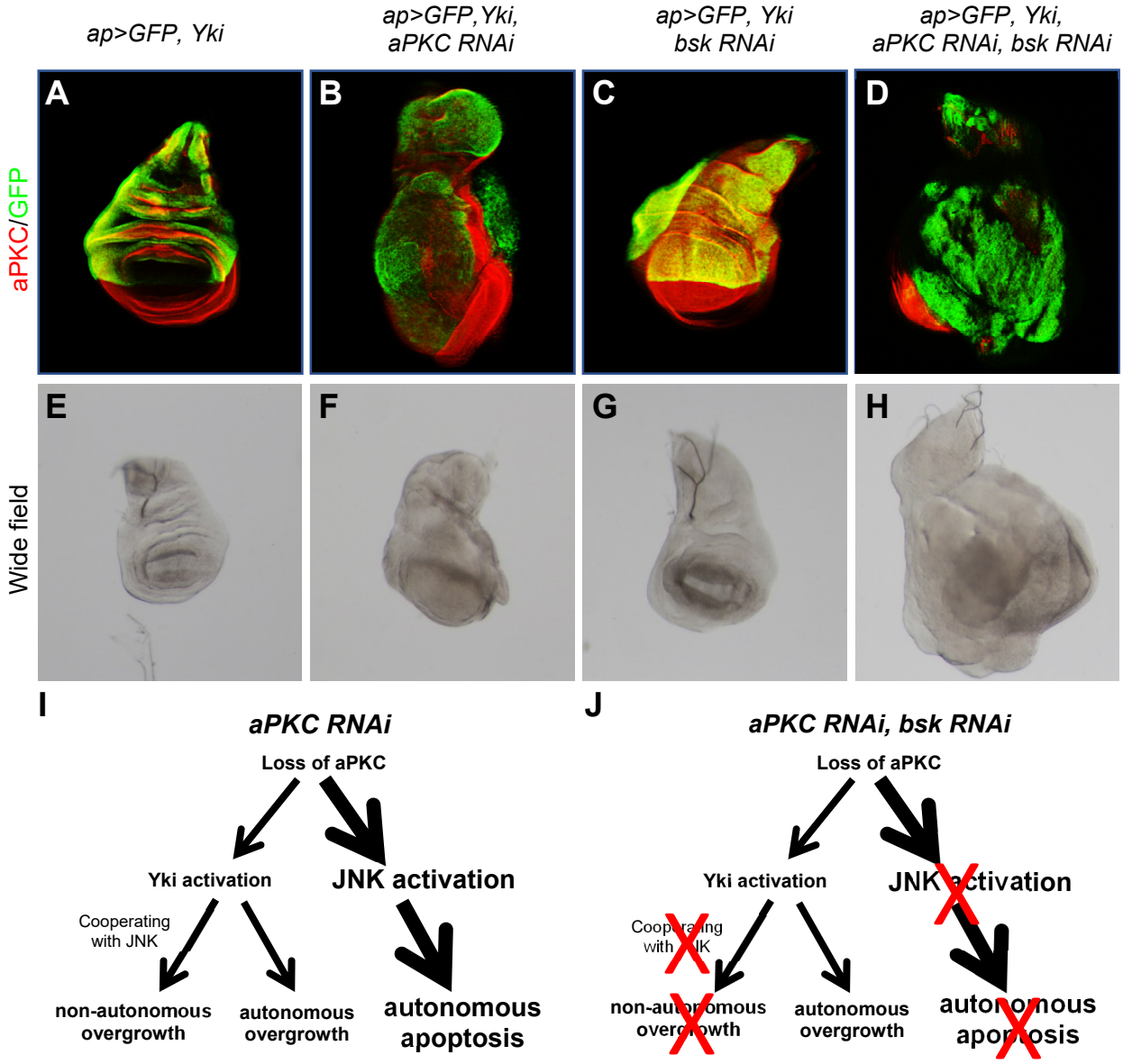

Synergism between *yki* expression and *aPKC* knockdown does not require JNK signaling
Ectopic expression of Yki resulted in mild tissue overgrowth (**A, E**). Depletion of aPKC strongly enhanced Yki mediated tissue overgrowth (**B, F**). Blocking JNK signaling by *bsk RNAi* did not suppress the enhanced overgrowth phenotype (**D, H**), suggesting the synergism in tissue growth between Yki and loss of aPKC is not dependent on JNK signaling. *bsk RNAi* on its own did not affect tissue growth (**C, G**).
In *aPKC RNAi* wing imaginal discs, JNK mediated cell-autonomous apoptosis outweighs cell-autonomous Yki activation, leading to cell-autonomous tissue loss and compensatory proliferation in the neighboring tissue (**I**) In *aPKC, bsk double RNAi* wing imaginal discs, non-cell-autonomous activation of Yki and cell-autonomous apoptosis are both blocked, leading to cell-autonomous tissue overgrowth (**J**). Bigger font size indicate stronger effect.

bantam-GFP was retained in *aPKC, bsk double RNAi* tissue (Figure 3.15C'') suggest that cell-autonomous Yki activation is JNK independent. To further explore the possibility that loss of aPKC can promote Yki activity in a JNK independent manner, we asked if blocking JNK signaling would affect the growth promoting synergism between *yki* expression and *aPKC RNAi* (Figure 3.16). We found *bsk RNAi* did not suppress the massive overgrowth caused by *yki* expression and *aPKC RNAi* (Figure 3.16D, H). On the contrary, it seems to further enhance the synergism, presumably due to reduced apoptosis. This result again suggests JNK independent regulation of Yki by aPKC.

Together our results suggest two distinct mechanisms for cell-autonomous and non-cell-autonomous activation of Yki in *aPKC RNAi* wing imaginal discs. Cell-autonomous activation of Yki is JNK independent whereas non-cell-autonomous activation is JNK dependent. In *aPKC single RNAi* wing imaginal discs, JNK mediated cell-autonomous apoptosis outweighs cell-autonomous Yki activation, leading to cell-autonomous tissue loss and compensatory proliferation in the neighboring tissue (Figure 3.16I). In *aPKC, bsk double RNAi* wing imaginal discs, non-cell-autonomous activation of Yki and cell-autonomous apoptosis are both blocked, leading to cell-autonomous tissue overgrowth (Figure 3.16J).

3.3 Discussion

Our results suggest Yki may have additional non-transcriptional functions at the cell cortex in addition to promoting myosin activation. First, Yki may facilitate the assembly of Hippo signaling complexes at the apical junctional region thereby promoting pathway activity. Second, Yki may stabilize apical polarity proteins at the cell cortex to promote apical basal polarity. These

results are preliminary and leave a lot of open questions unanswered. To start, it is unclear what Hippo pathway components can interact with Yki and how they interact. Our results show cortical Yki promotes Wts, Ex, and Mer accumulation at the cortex. Previous studies using co-immunoprecipitation have found that Yki can physically interact with Kib and Jub in addition to Ex and Wts (Genevet and Tapon 2011). Potential interactions between Yki and two other pathway components, Sav and Mats, have not been tested. It would be interesting to test if ectopic expression of cortical Yki can also promote accumulation of Kib, Jub, Sav and Mats. The next question is if there are different Hippo signaling complexes with a subset of pathway components and how Yki interacts with different complexes. Our recent finding that Kib and Mer form a complex that does not include Ex at the apical medial cortex suggests this could be the case (Su et al. 2017).

Mechanistically how Yki interacts with Hippo pathway components is not fully understood. The WW domains of Yki and PPxY motif of Ex mediate physical interaction between Yki and Ex (Badouel et al. 2009). It is unclear if WW domains of Yki also mediate interaction between Yki and other pathway components. Structure/function analysis of different Yki fragments can help us address this question.

Yki has been found to promote accumulation of apical polarity proteins through unknown mechanisms. Our results suggest Yki may stabilize apical polarity proteins at the cell cortex through direct protein-protein interactions, independent of its transcriptional function. To further strengthen this hypothesis, we can test if there are physical interactions between Yki and apical polarity proteins using co-immunoprecipitation studies in S2 cells. Our results and previous studies suggest apical polarity proteins positively regulate the Hippo pathway. Therefore, there is reciprocal regulation between them, suggesting feedback regulation. This feedback could work in

a scenario in which a minor defect in the apical basal polarity is counteracted by enhanced Yki-dependent enrichment of apical polarity proteins (Tepass 2012). This could be important during morphogenetic changes or wound-healing processes in which the apical basal polarity machinery may be temporarily compromised. Stabilization of apical polarity proteins by Yki in these situations could help maintain tissue integrity (Tepass 2012).

Our results also implicate the apical polarity proteins Baz and aPKC as potential regulators of the Hippo signaling pathway. Previous gain-of-function studies suggest aPKC negatively regulates the Hippo pathway. Ectopic expression of a membrane tethered aPKC with a CAAX prenylation motif ($aPKC^{CAAX}$) caused mis-localization of Hpo, activation of Yki, and up-regulation of Hippo pathway target genes (Grzeschik et al. 2010; G. Sun and Irvine 2011). $aPKC^{CAAX}$ also causes mislocalization of the Hpo negative regulator Ras-associated family protein (Rassf) (Grzeschik et al. 2010). Removing Rassf does not suppress the activation of Yki in aPKC expressing tissue, suggesting Rassf is not involved in aPKC mediated activation of Yki (Parsons, Grzeschik, and Richardson 2014). My results that loss of aPKC promotes Yki activation suggest aPKC may also positively regulate the Hippo pathway. Another apical polarity protein Crb has been shown to regulate the Hippo pathway in two opposing directions. On one hand, Crb recruits the Hippo pathway upstream regulator Ex to the apical cell cortex to promote pathway activity; on the other, Crb promotes Ex degradation to inhibit pathway activity(Chen et al. 2010; Ling et al. 2010; Robinson et al. 2010; Grzeschik et al. 2010; Ribeiro et al. 2014). Similarly, aPKC may also regulate the Hippo pathway in both directions. This type of dual-regulation could allow for fine tuning of Hippo pathway activity.

How Yki is activated upon depletion of Baz and aPKC is still not resolved. Depletion of both proteins resulted in simultaneous activation of JNK signaling and increased activation of Yki.

One possible scenario is that Yki activation is solely due to activation of JNK signaling since JNK signaling has been shown to positively regulate Yki activity (Grzeschik et al. 2010; G. Sun and Irvine 2011). In addition, JNK signaling has been found to positively regulate *bantam* expression (Sumabat et al. 2018 Ann. Dros. Res. Conf.). However, in aPKC depleted cells when JNK signaling was blocked by *bsk RNAi*, the increase in *bantamGFP* remained, suggesting JNK independent regulation of *bantam* by aPKC. In addition, *aPKC, bsk* double RNAi (and *baz*, *bsk* double RNAi) resulted in tissue overgrowth, suggesting Yki activation. Therefore, both Baz and aPKC seem to regulate Yki activity at least partially independently of JNK signaling. We have not examined expression levels of other Hippo pathway reporters *Diap1-lacZ* and *ex-lacZ* in *aPKC, bsk double RNAi* cells. Increased expression of *Diap1-lacZ* and *ex-lacZ* could strengthen this hypothesis. Therefore, activation of Yki upon Baz depletion also seems at least not entirely dependent on JNK signaling. To test this hypothesis more rigorously, we should examine *bantamGFP* in *baz, bsk double RNAi* tissue to see if the increase remains.

Clonal analysis of *aPKC* and *baz* null mutants could provide further evidence on how these two proteins modulate the Hippo pathway. For instance, generating *aPKC* null clones and examining the subcellular localization of Hippo pathway components could help elucidate how aPKC affects the pathway both cell-autonomously and non-cell-autonomously. One complicating factor is that loss of both proteins, and especially aPKC, leads to cell death. To overcome this problem, we can utilize the Minute mutations to promote survival of *aPKC* and *baz* mutant cells by generating *aPKC* and *baz* clones that do not carry Minute mutations in a Minute$^{+/-}$ background. Similar methods have been used to study regulation of the Hippo pathway (S.-Y. Wei et al. 2005; Y. Pan et al. 2016).

3.4 Methods

Table 3.1 Key resource used in Chapter 3

REAGENT or RESOURCE	SOURCE	IDENTIFIER
Antibodies		
Guinea pig anti-Ex	Maitra et al., 2006	N/A
Guinea pig anti-Mer	Maitra et al., 2006	N/A
Rabbit anti-HA	Santa Cruz	sc-805
Mouse anti-Myc	Cell Signaling Technology	9B11
Rabbit anti-pWts	D. Pan	N/A
Mouse anti-Flag	Sigma	F1804
Mouse anti-αtubulin	Sigma	T9026
Mouse anti-Crb	Developmental Studies Hybridoma Bank	Cq4
Rabbit anti-Baz	T. Harris	N/A
Rabbit anti-aPKC	Santa Cruz	sc-216
Mouse anti-Dlg	Developmental Studies Hybridoma Bank	4F3
Rat anti-Ecad	Developmental Studies Hybridoma Bank	DACD2
Mouse anti- β-catenin	Developmental Studies Hybridoma Bank	N27A1
Rabbit anti-Patj	Bhat et al., 1999	N/A
Rabbit anti-active caspase 3	Cell Signaling Technology	9661B
Experimental Models: Organisms/Strains		
D. melanogaster: UAS-Yki$^{\Delta NH}$	This study	N/A
D. melanogaster: UAS-Yki$^{\Delta NH}$SA	This study	N/A
D. melanogaster: UAS-Myr-Yki/TM6	Xu et al. 2018	N/A
D. melanogaster: UAS-YkiSA	This study	N/A
D. melanogaster: ap-Gal4/Cyo	Bloomington Stock Center	3041
D. melanogaster: UAS-Yki	Xu et al. 2018	N/A
D. melanogaster: UAS-Myc-Wts^{KD}/Cyo	K. Irvine	N/A
D. melanogaster: UAS-par6 RNAi	Vienna Drosophila RNAi Center	19731
D. melanogaster: UAS-patj RNAi	Vienna Drosophila RNAi Center	31620
D. melanogaster: UAS-sdt RNAi	Vienna Drosophila RNAi Center	29843
D. melanogaster: UAS-crb RNAi/Cyo	Vienna Drosophila RNAi Center	39177

Table 3.1 continued

D. melanogaster: UAS-baz RNAi	Vienna Drosophila RNAi Center	2915
D. melanogaster: UAS-aPKC RNAi	Vienna Drosophila RNAi Center	105624
D. melanogaster: hh-Gal4/TM6	Tetsuya Tabata	N/A
D. melanogaster: UAS-Mer RNAi #14	This Study	N/A
D. melanogaster: tub-Gal80^{ts}/CyodfYFP; hh-Gal4/TM6	This study	N/A
D. melanogaster: Yki-YFP	Su et al. 2017	N/A
D. melanogaster: hh-Gal4, bantamGFP/TM6	This study	N/A
D. melanogaster: Diap1-lacZ/TM6	Hay et al. 1995	N/A
D. melanogaster: ex-lacZ/Cyo	Hamaratoglu et al., 2006	N/A
D. melanogaster: UAS bsk RNAi 5680R-1	This study	N/A
D. melanogaster: pucE69(lacZ)/TM3, act-GFP	This study	N/A
Recombinant DNA		
pTFW-Myr-Yki	Xu et al. 2018	N/A
pAHW-Wts	This study	N/A
HA-Mer	This study	N/A
Hpo-pAMW	This study	N/A
pAc5.1 HA-Ex	This study	N/A
Ubi-Gal4	This study	N/A

Drosophila **husbandry**

Drosophila melanogaster was cultured using standard techniques at 25°C (unless otherwise noted). Both male and female animals were used (unless otherwise noted). All crosses were performed at 25°C unless otherwise noted. For clone induction, heat shocks were performed 60-84 hr after egg laying using the following program: 38°C for 1hr, 25°C for 1hr, 38°C for 1h, 25°C for 1hr in an EchoTherm IN35 incubator (Torrey Pines Scientific).

Drosophila Genetics

Drosophila stocks used in this study are listed in Table B.1

To generate yki^{B5} clones in *sd* heterozygous background, the following genotypes were used:

hsFLP 19AFRT/sd^{47M}*19AFRT; 42D FRT* yki^{B5}*/42D FRT Ubi-GFP*

Western blotting

8% SDS-PAGE gels were used and proteins were transferred onto nitrocellulose. General Western Blot protocol was used. Images of the blots were obtained using Odyssey CLx with ImageStudio software (LI-COR Biosciences).

Immunostaining and imaging of S2 cells

As described in Chapter 2.

Immunostaining and imaging of wing imaginal discs

As described in Chapter 2. For Crb staining, samples were treated with methanol for 10min after PFA fixation prior to staining.

Chapter 4

Discussion: conclusions and future directions

Since its discovery about two decades ago, the Hippo signaling pathway has emerged as an important regulator of growth. The core components of the Hippo pathway consist of a kinase cascade that inactivates the transcriptional co-activator Yorkie (Yki) to inhibit growth. How the Hippo pathway is regulated has been studied extensively. New regulators are being identified regularly and added into the complex regulatory network. In this dissertation, I have focused on two mechanisms of Hippo pathway regulation, namely cytoskeletal tension and apical polarity proteins.

In Chapter 2, we show that Yki can accumulate at the cell cortex to promote activation of myosin through a myosin regulatory light chain kinase, Strn-Mlck (J. Xu et al. 2018). This Yki function is not dependent on its transcriptional activity and is required for larval and adult tissues to achieve appropriate size. Based on these results, we suggest that Yorkie functions in a feed-forward 'amplifier' loop that promotes myosin activation, and thereby greater Yorkie activity, in response to tension. In Chapter 3, we show that loss of apical polarity proteins aPKC and Baz leads to simultaneous activation of the Jun Kinase (JNK) signaling and Yki. On the other hand, Yki promotes accumulation of apical polarity proteins at the apical cell cortex, suggesting reciprocal regulation of apical polarity proteins and the Hippo pathway. Together, these studies elucidate new modes of Hippo pathway regulation and hopefully will help us gain more insights into organ size regulation in development. In this chapter, I will discuss potential future directions from my dissertation research and for studying the regulation of the Hippo signaling pathway in *Drosophila*.

How is Yki recruited to the cell cortex?

A major unanswered question raised by the work presented in Chapter 2 is how Yki is recruited to the cell cortex to promote myosin activation. One possible mechanism we considered is that Yki is recruited by Expanded (Ex), which strongly localizes to the AJR and interacts directly with Yki. Indeed, transient expression of Ex caused increased cortical Yki accumulation and depleting Ex in *wts RNAi* cells suppressed the increased Yki accumulation at the AJR, suggesting Ex is able to recruit Yki to the cortex (Appendix B). However, there was still clear cortical Yki localization in *wts* clones in which Ex was depleted by RNAi. In addition, depleting Ex alone with RNAi or genetically removing Ex with a null *ex* allele did not abolish cortical Yki localization (Appendix B). Together these results suggest Ex is not the only factor that recruits Yki to the cell cortex.

Yki has been shown to interact (directly or indirectly) with several other pathway components, including Kibra, Hippo, Warts, Ajuba and 14-3-3. However, depleting Hippo pathway components with RNAi did not abolish cortical Yki localization (Appendix B). Proteins other than the Hippo pathway components could also recruit Yki to the cortex. Potential candidates include Strn-Mlck (which forms a complex with Yki as shown in Chapter 2), apical polarity proteins (which can be recruited by Yki to the cell cortex as shown in Chapter 3), and adherens junctions components (the mammalian literature indicates interactions between YAP and adherens junctions). Preliminary results suggest that depleting some components of adherens junctions (Ecad or α-catenin) disrupted cortical Yki localization. However, depleting a third AJ component, β-catenin, did not affect cortical Yki (Appendix B). One explanation might be that β-catenin does not recruit Yki to the cell cortex and depletion of β-catenin did not strongly affect localization of the other components of adherens junctions. Alternatively, β-catenin mediated Wingless signaling

may interact with Yki and depletion of β-catenin caused stronger cortical Yki through Wingless signaling to compensate for the reduced interaction with adherens junctions. A third possibility is the knockdown was too weak. We can further investigate the possibility that Ecad or α-catenin can recruit Yki by ectopically expressing these two proteins individually, verify that they could properly localize to the adherens junctions, and then test if they would cause increased Yki cortical localization. The caveat is that ectopically expressing one component might stabilize the other, endogenously expressed components. We can verify that using antibody staining of other components. If expressing Ecad or α-catenin can increase cortical Yki localization, we can test direct protein-protein interactions between Yki and these two proteins in S2 cells.

If the adherens junctions components indeed recruit Yki to the cell cortex, in could mean tension could directly affect Yki cortical localization through adherens junctions. For instance, increased tension could change the conformation of α-catenin to enhance physical interactions between α-catenin and Yki to promote cortical Yki localization.

It is possible that Yki is recruited to the cortex by parallel mechanisms, one through Ex and the other through other proteins. To test this hypothesis, we can genetically remove Ex and knockdown candidate proteins simultaneously to identify proteins that recruit Yki to the cortex using the MARCM technique. One advantage of this method is that, in *ex* null clones, cytoplasmic Yki re-localizes to the nucleus and the cortex so that cortical Yki signaling is much clearer than in wild-type tissue. Therefore, it would be easier to screen for Yki anchoring proteins in this background.

How does cortical Yki activate myosin mechanistically?

Although the work described in Chapter 2 provides insights into how cortical Yki affects myosin activity, we do not yet fully understand the underlying mechanisms. One observation from my dissertation research is that targeting endogenously expressed Yki-YFP to the cortex with GrabFP system results in weaker activation of myosin compared with ectopic expression of Myr-Yki. A possible explanation for this difference is that Yki-YFP expressed from its endogenous promoter in the GrabFP experiment accumulates at low levels compared to Myr-Yki expressed under the Gal4/UAS system. Alternatively, how Yki is recruited to the membrane and specifically the proximity of its myosin activation domain to the lipids of the membrane may be important for activating myosin. One result that supports this hypothesis is that when full length Yki is recruited to the cell cortex through a C-terminal CAAX prenylation motif (Yki-CAAX), it fails to activate myosin (Figure 4.1 A). On the other hand, adding a CAAX motif to just the first 34 amino acids of Yki (Yki$^{1-34}$-CAAX), the myosin activation domain identified in Chapter 2 (J. Xu et al. 2018), is able to activate myosin (Figure 4.1 B). The first 34 amino acids of Yki may be closer to the lipid bilayer of the membrane in Yki$^{1-34}$-CAAX than Yki-CAAX, which may account for the difference in myosin activation. Alternatively, Yki$^{1-34}$-CAAX may be more stable than Yki-CAAX. This can be tested with immunoblots. In the case of Myr-Yki and Myr-Yki$^{1-34}$, since myristoylation occurs at the N terminus, the first 34 amino acids of Yki in both proteins should be similarly close to the lipid bi-layer and therefore both cause myosin activation. To further test the hypothesis that proximity to the lipid bilayer is an important factor in myosin activation, we can compare myosin activation in Myr-Yki$^{1-34}$-GFP and Myr-GFP-Yki$^{1-34}$ in S2 cells. The only difference in these two proteins is the placement of GFP. In Myr-Yki$^{1-34}$-GFP, GFP is placed at the C terminus and the first 34 amino acids is right next to the myristoylation signal sequence and should be in close

Figure 4.1

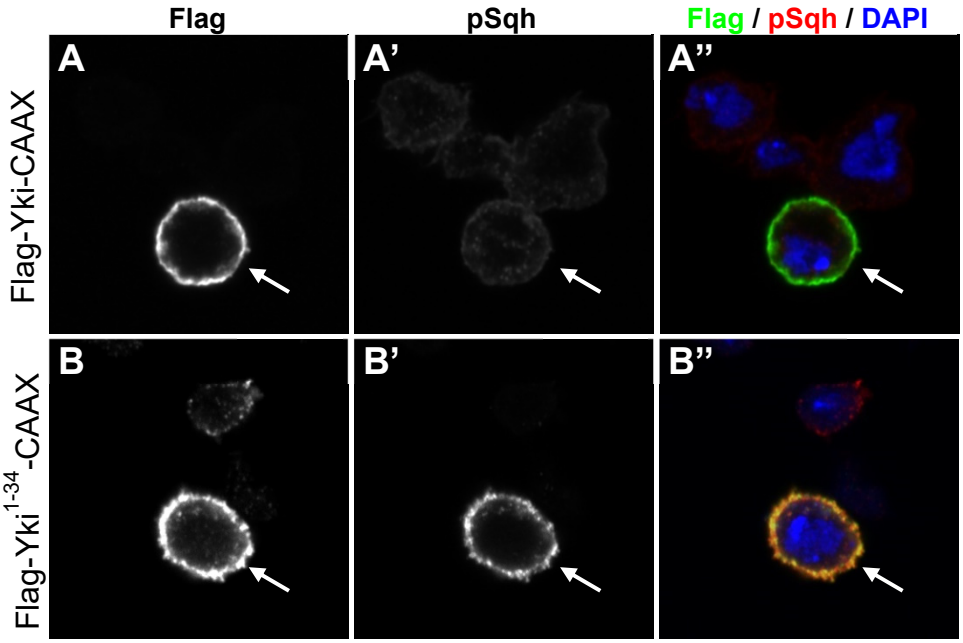

CAAX tagged Yki$^{1-34}$ but not full length Yki activates myosin
S2 cells were transfected with the indicated constructs and stained for Flag and pSqh. Myr-Yki – CAAX(A') did not cause pSqh staining whereas Myr-Yki$^{1-34}$ (B') caused strong increase in pSqh staining. White arrows indicate transfected cells.

proximity to the lipid bilayer. In Myr-GFP-Yki$^{1-34}$, GFP is placed between myristoylation signal sequence and the first 34 amino acids of Yki, therefore the first 34 amino acids may be further away from the lipid bilayer. If Myr-GFP-Yki$^{1-34}$ fails to promote myosin activation, this hypothesis would be strengthened. In addition, we can combine UAS-Yki-YFP and GrabFP system to tether Yki-YFP to the membrane and compare myosin activation with endogenously expressed Yki-YFP and GrabFP targeting, as well as USA-Myr-Yki expression alone. If similarly low activation of myosin is observed in UAS-Yki-YFP and GrabFP targeting, it would suggest a factor other than expression level accounts for the difference between GrabFP targeting and myristoylation targeting. This factor could be the proximity to the lipid bilayer. One caveat for this experiment is if the GrabFP nanobodies are already saturated when Yki-YFP is expressed at endogenous levels, it will not be able to differentiate Yki-YFP and UAS-Yki-YFP. If it is true that activation of myosin requires close proximity between Yki and the lipid bilayer, it would be interesting to explore potential interactions between Yki and specialized lipid domains and lipid modifying proteins.

What is the sub-cellular localization of endogenous Strn-Mlck?

We would like to more rigorously test the hypothesis that cortical Yki recruits Strn-Mlck to promote myosin activation. We proposed this hypothesis mainly based on the finding that Myr-Yki is able to recruit ectopically expressed Strn-Mlck to the cell cortex. We can more rigorously test our hypothesis by investigating the sub-cellular localization of endogenous Strn-Mlck and how it can be affected by cortical Yki. The *Strn-Mlck* locus encodes ten different isoforms and eight of them contain the kinase domain (Appendix C, Flybase). Among the kinase domain containing isoforms, three isoforms end about 200bps upstream of the rest (Appendix C). Due to Strn-Mlck's

complex structure, it is very difficult to tag all of the isoforms. One Strn-Mlck RNAi transgene that strongly suppresses the Myr-Yki phenotypes and causes undergrowth on its own specifically targets an exon coded exclusively by the five isoforms that extend further 3', suggesting these isoforms are important in Hippo pathway regulation. Therefore, we have used CRIPSR to tag these isoforms with GFP (Appendix C). To our surprise, we could not detect GFP fluorescence in the wing imaginal disc proper (Appendix C). Additionally, the RNAseq data set from Flybase indicates that these isoforms are not abundantly expressed in third instar larval imaginal discs (Appendix C), suggesting those isoforms might not be important for cortical Yki function. To resolve these seemingly conflicting results and find out which isoforms are expressed, we can employ the following two methods. First, we can specifically deplete the GFP tagged Strn-Mlck in Strn-Mlck-GFP homozygous animals with RNAi against GFP to see if there is any growth phenotype. If growth is affected, it is likely that our tagged isoforms are expressed and are important for Hippo pathway regulation despite being expressed at undetectable levels. Second, we can use quantitative RT-PCR with exon specific primers to more directly measure expression of different isoforms. If we find the untagged isoforms are expressed, we can then use CRIPSR to tag them with GFP and analyze their sub-cellular localization and how it is regulated by cortical Yki. If our model that cortical Yki promotes Strn-Mlck cortical localization is correct, we should see increased cortical Strn-Mlck when we ectopically express Myr-Yki. In addition, depleting Yki would result in reduced cortical Strn-Mlck.

Is there a kinase independent function of Strn-Mlck in Hippo pathway regulation?

My research implicates Strn-Mlck as a negative regulator of the Hippo pathway through myosin activation. Mechanistically, how Strn-Mlck promotes Sqh phosphorylation is not well

Figure 4.2

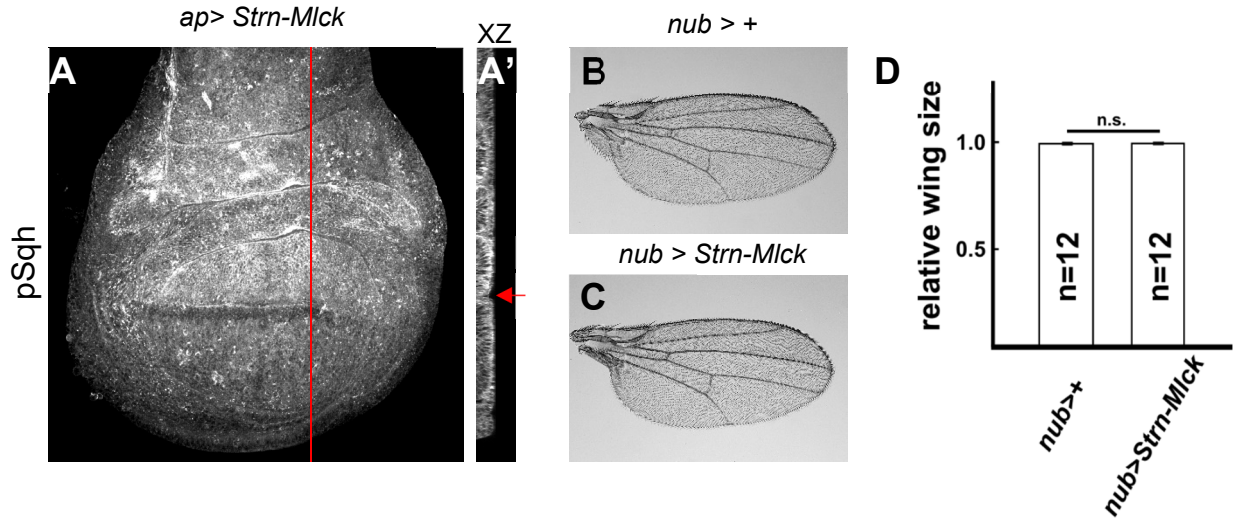

Ectopic expression of *Strn-Mlck* caused increase in myosin activation but not growth
Ectopic expression of Strn-Mlck isoform B caused increased pSqh staining (A). Red line indicates the position of the XZ plane shown in (A'). Red arrow indicates indentation of the epithelium.

Ectopic expression of Strn-Mlck isoform B did not affect adult wing sizes (B-D). Representative images of adult female wings of the indicated genotypes are shown (B, C), together with quantification of the results (D). Data are represented as mean ± SEM. Students' t test was used to calculate statistical significance.

understood. The first unanswered question is if Strn-Mlck directly phosphorylates Sqh. Two lines of evidence suggest this is the case. First, ectopic expression of Strn-Mlck isoform B causes increased Sqh phosphorylation (Figure 4.2A). In addition, Strn-Mlck purified from S2 cells can phosphorylate GST tagged Sqh purified from bacteria in an *in vitro* kinase assay (Appendix D). However, these experiments cannot rule out the possibility that Strn-Mlck has a kinase independent function to promote Sqh phosphorylation. To test if this is the case, I have engineered a kinase dead allele of *Strn-Mlck* (*Strn-Mlck^{KD}*) in which the entire kinase domain coding region is replaced by a *Pax6-DsRed* module (Figure 4.3 A, Appendix C). I then analyzed how this allele modified the increased myosin activation and overgrowth induced by Myr-Yki expression. If Strn-Mlck's kinase activity is necessary for activating myosin to inhibit the Hippo pathway, removing the kinase domain should result in full suppression of Myr-Yki phenotypes similar to Strn-Mlck RNAi (Figure 2.15). Surprisingly, the results are mixed. Strn-Mlck^{KD} mutation does not obviously suppress Myr-Yki induced myosin activation (Figure 4.3 B-C). On the other hand, Myr-Yki induced overgrowth is partially suppressed (Figure 4.3 F-H). One explanation for this apparent contradiction is that Strn-Mlck^{KD} weakly diminishes myosin activation, sufficient to suppress overgrowth but difficult to see by eye. Quantification of pSqh staining in Strn-Mlck$^{KD/KD}$ and Strn-Mlck$^{KD/+}$ should clarify this possibility.

Overall, the *Strn-Mlck^{KD}* mutation results in weaker suppression of Myr-Yki phenotypes than that caused by *Strn-Mlck* RNAi. The *Strn-Mlck^{KD}* mutation on its own causes mild undergrowth (Figure 4.3 D-E, H) but no noticeable reduced expression of Hippo pathway targets *Diap1* and *ex*. In comparison, *Strn-Mlck* RNAi caused both undergrowth and reduced expression of Hippo pathway targets *Diap1* and *ft* (Figure 2.15). Here again Strn-Mlck^{KD} resulted in weaker phenotypes than Strn-Mlck RNAi. Taken together these results suggest that the kinase activity of

Figure 4.3

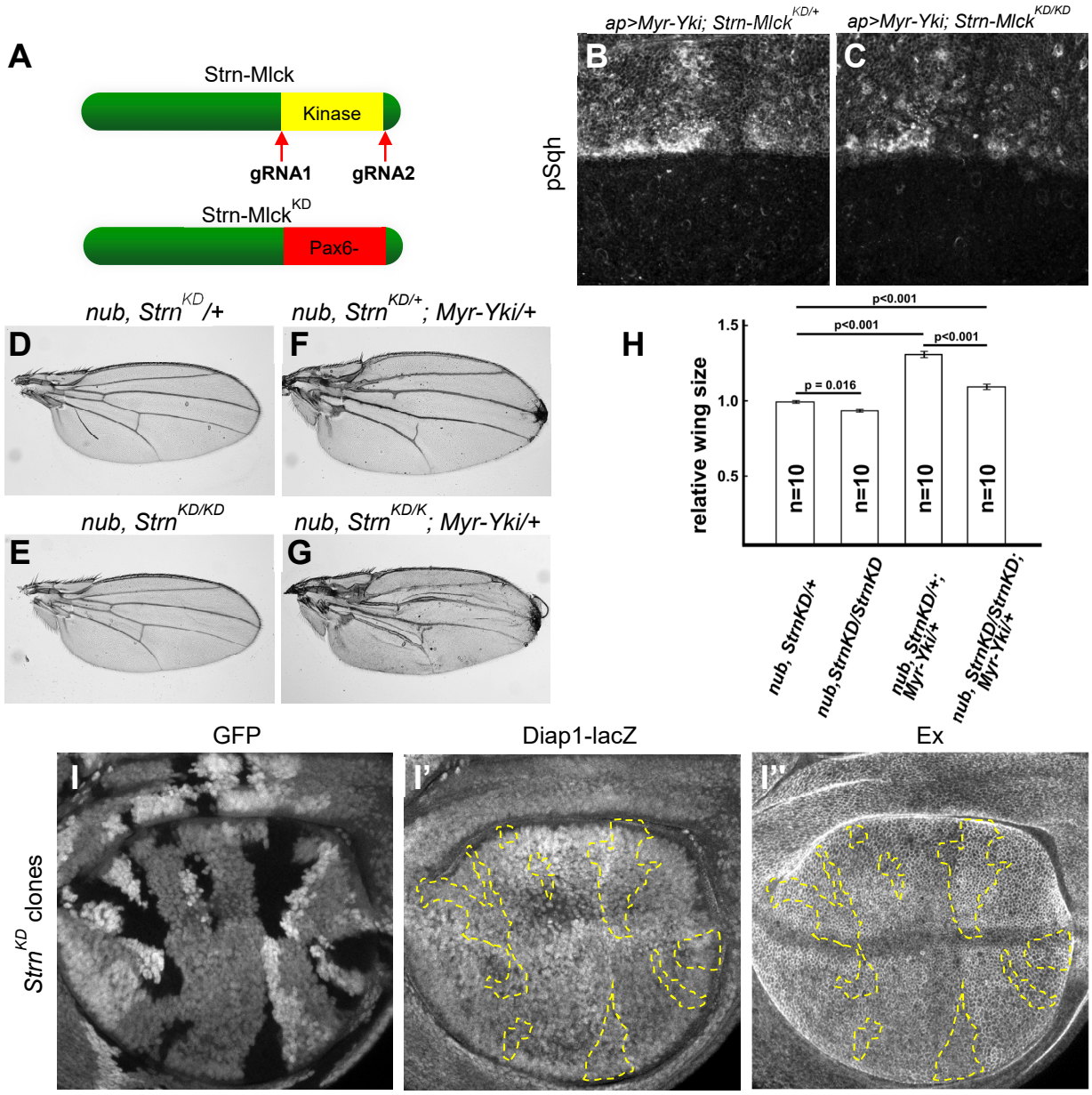

Strn-Mlck regulates growth through both kinase dependent and kinase independent mechanisms

Strn-Mlck^{KD} allele was generated by replacing the kinase domain with a *Pax6-DsRed* module (**A**). Strn-Mlck$^{KD/KD}$ did not obviously suppress the increased pSqh staining caused by Myr-Yki expression (**B-C**). Strn-Mlck$^{KD/KD}$ caused undergrowth of adult wings and suppressed the overgrowth caused by Myr-Yki (**D-G**). Representative images of adult female wings of the indicated genotypes are shown, together with quantification of the results. Data are represented as mean ± SEM. p values were calculated with one-way ANOVA and Tukey's honest significant difference (HSD) test, n = number of wings. *Strn*$^{KD/KD}$ clones did not show change in Diap-lacZ expression level(**I'**) or Ex protein staining (**I"**).

Strn-Mlck is involved in regulating growth through the Hippo pathway, but the kinase activity does not account for all the mechanisms. Therefore, there seems to be a kinase independent function of Strn-Mlck in Hippo pathway regulation.

One possibility of this kinase independent function of Strn-Mlck is to cooperate with another kinase to promote Sqh phosphorylation. To test this possibility, we can ectopically express a kinase dead version of Strn-Mlck under the UAS promoter in wing imaginal discs and S2 cells to test if myosin can be activated. The caveat is it will be difficult to express the full-length protein since the largest isoform of *Strn-Mlck* encodes a huge 926 kDa protein (Champagne et al., 2000). If we can find out which isoforms are expressed as discussed earlier, we could generate new UAS-Strn-Mlck constructs for this experiment.

How is feedback regulation of the Hippo pathway by tension coordinated?

Both positive feedback and negative feedback between tension and Hippo pathway seem to operate during development. Previous studies in both *Drosophila* and mammalian systems show tension positively regulates Yki and YAP activity. My dissertation research shows Yki promotes tension at the cell cortex independent of its transcriptional activity and studies in vertebrate systems suggest YAP promotes tension by transcriptionally up-regulating proteins that activate the myosin regulatory light chain (Lin et al., 2017; Porazinski et al., 2015; Xu et al., 2018, Chapter 2). Together these results suggest a positive feedback loop between tension and the activity of Yki/YAP. On the other hand, a recent study shows that artificially increased clonal growth reduces cytoskeletal tension within the clone due to constraint by the surrounding, slower growing cells. This decreased tension in turn reduces Yki activity (Y. Pan et al. 2016), suggesting the possibility of a negative feedback loop in situations of differential growth. In addition to the feedback

involving tension, previous work also has revealed a transcription-based negative feedback loop in which Yki promotes expression of upstream positive regulators of the Hippo pathway that in turn repress Yki activity. How these regulatory mechanisms are coordinated during development has not been investigated.

Several results suggest that tension needs to reach a certain threshold to activate positive feedback. For instance, ectopic expression of an activated form of *Drosophila* myosin light chain kinase Sqh (Sqh^{EE}) is not sufficient to cause tissue overgrowth (Rauskolb et al. 2014; Tsoumpekos, Nemetschke, and Knust 2018). Similarly, ectopic expression of Sqh kinase Strn-Mlck isoform B causes myosin activation but fails to induce overgrowth (Figure 4.2). Qualitatively, the increase in myosin activity (assayed by phosphorylation level of Sqh) in Strn-Mlck expressing cells is smaller than that of Myr-Yki expressing cells, which induces strong overgrowth (Chapter 2, Xu et al. 2018). These results suggest tension needs to reach a certain threshold to activate positive feedback. Alternatively, a small increase in Yki activity induced by the positive feedback is counterbalanced by the transcriptional negative feedback regulations of the Hippo pathway.

Time lapse analysis that simultaneously monitors tension, Yki subcellular localization, and cell division should provide valuable information on how tension regulates Yki activity during development. In recent years, laser ablation has been widely used as an indirect readout for cytoskeletal tension (Hutson et al. 2003; Rauzi et al. 2008; Mao et al. 2013; LeGoff, Rouault, and Lecuit 2013; Rauskolb et al. 2014; Y. Pan et al. 2016). However, due to its invasive nature, it is not well suited for long-term time lapse analysis. The recent development of FRET tension sensors and force inference from cell shape and connectivity provide tools for non-invasive tension measurement at the single cell level and would be better suited for simultaneously monitoring

tension and Yki localization over time (Chiou, Hufnagel, and Shraiman 2012; Ishihara and Sugimura 2012; Cai et al. 2014).

Another way to study the how tension regulates Yki activity is to directly manipulate tension in tissue and ask how that affects Yki sub-cellular localization. In our live imaging setup, wing imaginal discs are sandwiched between two coverslip fragments (Appendix A). In this manipulation, mechanical force is applied to the wing pouch and as a result presumably stretches cells at the periphery of the pouch. Under these conditions, we observe strong and reversible nuclear Yki-YFP accumulation, starting at the periphery of the pouch and propagating into its center (Appendix A). In addition, we also observe cortical accumulation of Yki-YFP in early third instar larval discs (Our live imaging method results in bright Yki-YFP punctae in the apical region of late third instar larval discs, making it difficult to analyze cortical Yki-YFP localization in this stage). Overall these results are consistent with our positive feedback model in which tension activates Yki and leads to both nuclear and cortical localization, which in turn further activate tension. To further use our live imaging method to study how tension regulates Yki, we need to validate that our live imaging method indeed generates tension in the periphery of the tissue. We can try laser ablation, FRET sensor, and force inference to measure tension. After the validation, we can use our setup to study dynamics of Yki translocation under tension. In addition, we can combine this with other genetic manipulations to study integration of mechanical cues and genetic information in Hippo pathway regulation.

Do Baz and aPKC affect proper localization of Hippo pathway components and its upstream regulators?

Our results in Chapter 3 suggest apical polarity proteins Bazooka (Baz) and atypical Protein Kinase C (aPKC) positively modulate Hippo pathway activity. Depletion of either protein caused increased Yki activation, though the mechanism by which apical polarity regulates Yki function remains unclear. One way that Baz and aPKC might modulate the Hippo pathway is by influencing the subcellular localization of its components and upstream regulators. Indeed, recent studies in our lab suggest that aPKC is required for cortical localization of Kibra, an upstream regulator of the Hippo pathway. We are currently investigating the implication of this finding in Hippo pathway regulation. We can further test the hypothesis that Baz and aPKC regulate localization of Hippo pathway components by depleting Baz and aPKC and examine the YFP tagged pathway components developed in our lab, including Tao-YFP, Hpo-YFP, Wts-YFP, and Yki-YFP (Su et al. 2017; J. Xu et al. 2018).

Activation of Yki upon aPKC depletion could be due to mis-regulation of other polarity genes that positively regulate the Hippo pathway because loss of aPKC disrupts apical basal polarity in imaginal disc epithelia (Rolls et al. 2003). One top candidate gene is *crb*, a well characterized regulator of the Hippo pathway. aPKC is required for proper localization of Crb in both embryonic and follicular epithelia (Sotillos et al. 2004; Fletcher et al. 2012). However, previous studies have not examined if depleting aPKC leads to mis-localization of Crb in imaginal discs. The first step to test if aPKC acts through Crb to modulate the Hippo pathway is to analyze Crb localization in aPKC RNAi wing imaginal discs. If aPKC RNAi indeed causes Crb mis-localization, we can then analyze genetic interactions between aPKC and Crb. For instance, we can ask if expression of Crb could suppress the activation of Yki in aPKC RNAi tissue. Since

ectopic expression of Crb alone causes Yki activation, a suppression of Yki activation in aPKC RNAi background by Crb expression would be a strong piece of evidence that aPKC can act through Crb to modulate Hippo pathway activity.

How does JNK signaling switch between Yki activation and Yki inhibition when polarity is disrupted?

Depleting the basolateral polarity protein Lethal giant larvae (Lgl) with RNAi in wing imaginal discs caused activation of JNK signaling, which in turn activates Yki (G. Sun and Irvine 2011). In contrast, clonal loss of another basolateral polarity protein Scribble (Scrib) leads to JNK mediated Yki inhibition(Chen et al. 2012). How JNK switches between those two opposing functions is unsolved. One possibility is that high level JNK activation leads to Yki inhibition whereas low level JNK activation leads to Yki activation. To test this hypothesis, we can generate *lgl* and *scrib* mutant clones and quantify activation of JNK signaling using the relative expression level of the reporter gene *puc-lacZ* normalized to wild type tissue. If *scrib* clones have higher relative *puc-lacZ* level compared with *lgl* clones, it would support our hypothesis.

Concluding statement

In my dissertation research, I identified a novel function of Yki at the cortex to promote tension as part of feedback regulation of the Hippo pathway. I also further analyzed functional interactions between apical polarity proteins and the Hippo pathway. Together, these studies provide new insights into the regulation of the Hippo pathway and point to new directions for future studies of this fascinating signaling pathway that controls tissue growth in development.

Appendix A

Live imaging of Hippo pathway components in *Drosophila* imaginal discs

1. Introduction

Examining subcellular localization of Hippo pathway components has been an important aspect of studies of this conserved tissue growth control pathway. Current models propose that the Hippo pathway regulates Yorkie (Yki, a *Drosophila* orthologue of the mammalian oncogene YAP/TAZ) activity by controlling its sub-cellular localization: when the pathway is active Yki is retained in the cytoplasm, while in the absence of pathway activity Yki accumulates in the nucleus. Therefore, the sub-cellular localization of Yki has been widely used as a readout for Hippo pathway activity (Oh and Irvine 2008; Su et al. 2017; Rauskolb et al. 2014). Upstream regulators of the Hippo pathway as well as the core kinases have been shown to localize to the Apical Junctional Region (AJR), a cortical region that extends from the lateral edge of the apical cortex through the adherens junctions, where they appear to organize into signaling complexes(Boggiano and Fehon 2012; S. Sun, Reddy, and Irvine 2015; Chung, Augustine, and Choi 2016). In addition, we recently identified the apical medial cortex as an additional subcellular domain for Hippo pathway regulators Merlin (Mer) and Kibra (Kib) (Su et al. 2017).

Further analysis of subcellular localization of Hippo pathway components under different genetic and mechanical manipulations, especially in live tissue, could provide a better mechanistic understanding of the pathway. To achieve that goal, we have generated endogenously expressed, YFP-tagged transgenes of Mer, Expanded, Hippo, Warts, and Yki, as well as GFP-tagged Kib using a combination of recombineering genomic transgenes and CRISPR/Cas-9 genome editing (Su et al. 2017). Here we describe methods for performing live imaging of *Drosophila* wing imaginal discs carrying these fluorescently-tagged Hippo pathway components.

2. Materials

1. Dissection media: Schneider's *Drosophila* Medium (for example, Sigma cat No. S9895) supplemented with 10% Fetal Bovine Serum (Thermo Fisher Scientific) (***see*** **Note 1**).
2. Incubation chamber for imaging: Glass bottom microwell dish (for example, MatTeK Corporation, Part No.: P35G-1.5-14-C) (***see*** **Note 2**).
3. Phosphate buffered saline (PBS): 155 mM NaCl, 15 mM Na_2HPO_4, 6 mM $NaH_2PO_4 \cdot H_2O$ (***see*** **Note 3**).
4. 70% EtOH. 70% EtOH in deionized water v/v.
5. Supporting beads: 45-53 μm Solid Soda Lime Glass Microspheres (for example, Cospheric SLGMS-2.5 45-53 μm) (***see*** **Note 4**).
6. Dissecting tools: Forceps (for example, FST DUMONT No.5 1125-20), a tungsten needle, a diamond-tipped pen, and micropipettes.
7. Siliconized slides for dissection (***see*** **Note 5**).
8. Zeiss LSM 880 or Zeiss LSM 800 laser scanning confocal microscope equipped with GaAsP detectors.

3. Methods

Carry out all procedures at room temperature.

3.1. Preparing an incubation chamber for imaging (Figure A.1 A)

1. Prepare top coverslip by cutting a No.1.5 thickness coverslip into ~8X8 mm fragments using a diamond-tipped pen.
2. Add 2 ml dissection media into an incubation chamber.
3. Add 5-10 µl of resuspended supporting microsphere beads near the center of the coverglass.
4. Use forceps to clear the beads from the center of the coverglass to make space for the imaginal discs. Replace cover and set aside (***see*** **Note 6**).

3.2. Dissecting wing imaginal discs from wandering third instar larvae

5. Remove wandering third instar larvae from uncrowded vials using a damp paintbrush. Place in a 50 ml beaker with ~10 ml of water.
6. Rinse several times with distilled water to remove debris.
7. Wash 1 min in 70% EtOH to clean larvae.
8. Rinse several times in dH_2O.
9. To dissect larvae, place in a drop of Dissection media on a siliconized slide.
10. Rotate the larva so that the dorsal side (tracheal tubes) is up. Identify the anterior (mouth hooks) and posterior ends. Using the less coordinated hand, grasp the larva from the posterior end at about the middle of the body.
11. Using the more coordinated hand, grasp the dorsal cuticle approximately one quarter of the way posterior from the head. Tear the dorsal cuticle toward the anterior end of the larva.

12. The wing imaginal discs should “flop out” laterally when the cuticle is torn open. They have a tear-drop shape, a translucent appearance, and lie close to the longitudinal tracheal tube.
13. Using the more coordinated hand, gently grasp the entire wing disc with the forceps (place the body of the disc between the prongs of the forceps). Pull the disc laterally to separate it from its connection to the trachea. Transfer the dissected discs to a fresh drop of Dissection media between the tips of your forceps.

3.3. Setting up an incubation chamber for imaging on an inverted microscope

14. Transfer dissected wing imaginal discs into the center of the bottom coverglass. This can be done by carrying the imaginal discs between the tips of the forceps. Alternatively, use a micropipette with a yellow tip that has been cut short to widen the opening to transfer the discs. Prewet the tip with Dissecting medium to prevent the discs from sticking to the tip.
15. Orient the wing imaginal discs with a tungsten needle so that the apical sides are facing the bottom coverglass. The pouch portion of the wing imaginal discs is bowl-shaped. The convex side of the bowl is the apical side of the wing epithelium (**Figure A.1 B**) (***see*** **Note 7**).
16. Use forceps to grasp the coverslip piece. Place on top of the dissection media at the edge of the microwell dish to wet the bottom side. Then, flip it over to wet the other side. When both sides are wet, the coverslip piece will sink to the bottom of the chamber.

17. Use forceps to grasp the coverslip piece, gently lift it from the bottom while still immersed in the dissection media and move it over the wing imaginal discs in the center of the microwell dish.
18. Gently release the top coverslip piece from the forceps so that it gently comes to rest on the basal sides of the wing imaginal discs, supported by the microsphere beads.
19. Place cover over the microwell dish and immediately transfer it to the inverted microscope.
20. For imaging imaginal discs mounted in microwell dishes we use a Zeiss LSM880 laser scanning confocal microscope equipped with GaAsP detectors mounted on a Zeiss Axio Observer Z1 inverted stand. We use 40 and 63X oil immersion objectives with Numerical Apertures of 1.3 to 1.4. The 514nm line from an argon ion laser is optimal for excitation of YFP, though the 488 nm line will work as well. Examples of YFP tagged Hippo pathway components are shown in **Figure A.2** (***see*** **Notes 8-10**).

3.4. Imaging on an upright microscope

21. For imaging on an upright microscope stand, place ~50 µl of Dissecting medium near the center of a clean standard microscope slide. Add 5-10 µl of resuspended supporting microspheres near the center of the medium.
22. Use forceps to clear the beads from the center of the drop to make space for the imaginal discs.
23. Transfer dissected wing imaginal discs into the center of the drop (see point 14 in section 3.3 above).

24. Orient the wing imaginal discs with a tungsten needle so that the apical sides are facing up. The pouch portion of the wing imaginal discs is bowl-shaped. The bottom side of the bowl is the apical side of the wing epithelium.
25. Gently place a 22X22 mm coverglass directly onto the imaginal discs in the drop of Dissecting medium (putting one edge of the coverslip down first may cause the imaginal discs to invert). Avoid moving the coverglass once it has been released onto the slide.
26. Place a small drop of melted petroleum jelly on each corner of the coverglass to secure it onto the slide.
27. These preparations can be imaged on either an inverted or an upright microscope stand. For the latter, we use a Zeiss LSM 800 laser scanning confocal microscope mounted on a Zeiss Axio Imager M2 stand, with 40 and 63X oil immersion objectives. On this system we use the 488 nm line to image both YFP and GFP labeled proteins (***see*** **Notes 8-10**).

Figure A.1

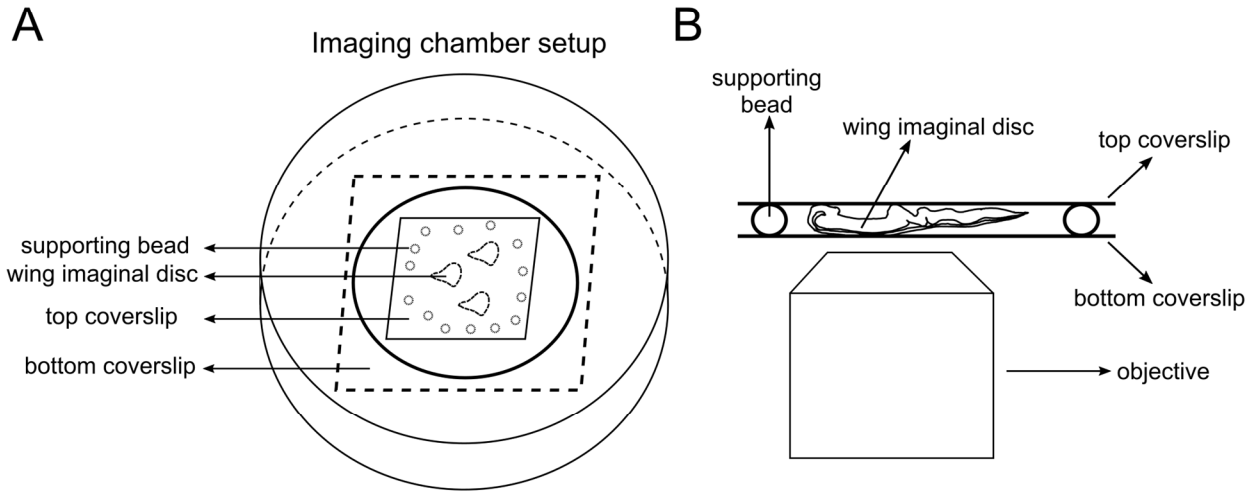

Setup for live-imaging of Hippo pathway components on an inverted microscope
(A) Imaging chamber setup. Wing imaginal discs are placed between two coverslips with the apical side facing downwards. The top coverslip is supported by glass microspheres.
(B) Illustration showing cross-sectional views of the imaginal chamber.

Figure A.2

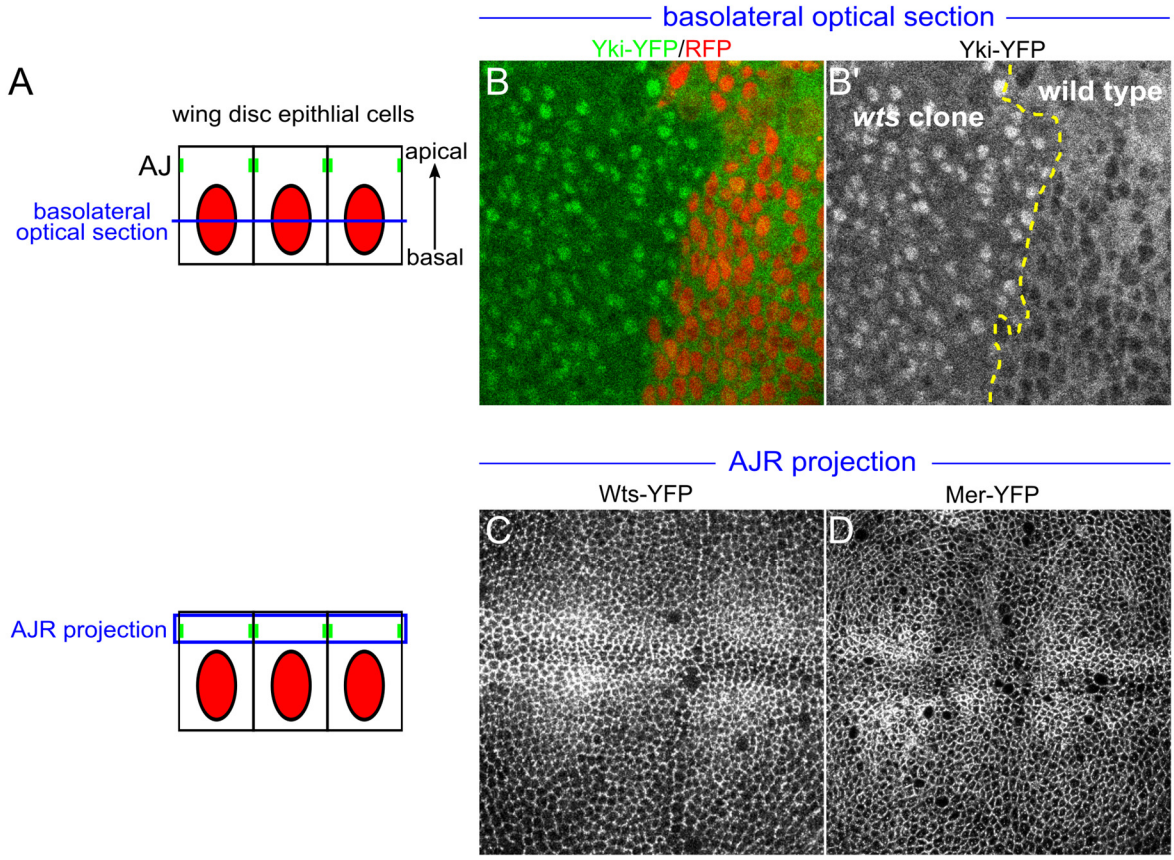

Examples of Hippo pathway components imaged in live tissues

(A) Illustrations showing cross-sectional views of the imaginal epithelium and the approximate positions of basolateral and AJR images shown in B-D. As indicated in blue, basolateral images are single sections while AJR views are maximal projections of a small number of apical sections to compensate for curvature of the epithelium.

(B) The effect of Hippo pathway inactivation on Yki subcellular localization. In basal sections of live tissues containing *wts* null mitotic clones (clone marked by the absence of RFP and a yellow dashed line), Yki-YFP is primarily cytoplasmic in normal imaginal tissue, but is strongly nuclear in *wts* mutant cells (B-B').

(C-D) Localization of endogenously expressed Wts-YFP (C) and Mer-YFP (D) under normal conditions. Both Wts-YFP and Mer-YFP are enriched at the AJR of imaginal disc cells. A portion of Mer-YFP also localizes at apical medial region.

4. Notes

1. Dissection media is prepared according to manufacturer's instructions using MilliQ deionized water and filter sterilized. Store at 4°C and warm to room temperature before using.
2. The incubation chamber is a 35mm petri dish with a No. 1.5 coverglass bottom for imaging on an inverted microscope.
3. PBS: Recipe for 1L:

NaCl	9.0 g
Na2HPO4	2.0 g
NaH2PO4•H2O	0.83 g
dH_2O to 1 liter	

4. The supporting beads prevent tissue damage by supporting the coverslip. Suspend these beads in PBS at 100mg/ml.
5. To siliconize slides, place them (within cardboard box) in an empty vacuum desiccator with 1 ml dichloromethylsilane in the bottom of a 25-50 ml glass beaker). Pull a vacuum with a pump or aspirator and leave sealed overnight. Clean slides with soap and water before using. Perform this procedure in a fume hood.
6. The chamber is typically prepared just before dissections begin and is kept at room temperature.
7. It is important to orient the wing imaginal discs so that the apical side is facing the objective to provide optimal conditions for imaging the apical region of the disc epithelium, where pathway components primarily localize and function. If the discs are

oriented the opposite way, both excitation light and emission light would need to travel through the entire tissue resulting in much weaker signal.

8. To maximize signal to noise for weakly-expressed proteins, we often increase the pinhole to 1.5-2.0 airy units rather than increasing laser excitation light, to avoid photobleaching. Re-scanning samples often causes noticeable photobleaching and should be avoided.
9. Typically, we limit imaging time to no more than 15 min after mounting the tissues. However, we have imaged tissues for up to one hour.
10. Mechanical tension has been shown to regulate the Hippo pathway (Dupont et al. 2011; Aragona et al. 2013; Rauskolb et al. 2014). Our method of mounting the wing imaginal disc between coverslips inevitably applies mechanical force to the tissue. This should be kept in mind when interpreting results. When we used this method to analyze sub-cellular localization of Yki-YFP, we found reversible accumulation of Yki-YFP to the nucleus in wondering third instar larval wing imaginal discs (**Figure A.3**). We also found accumulation of cortical Yki in early third instar larval wing imaginal discs (**Figure A.3**).

Figure A.3

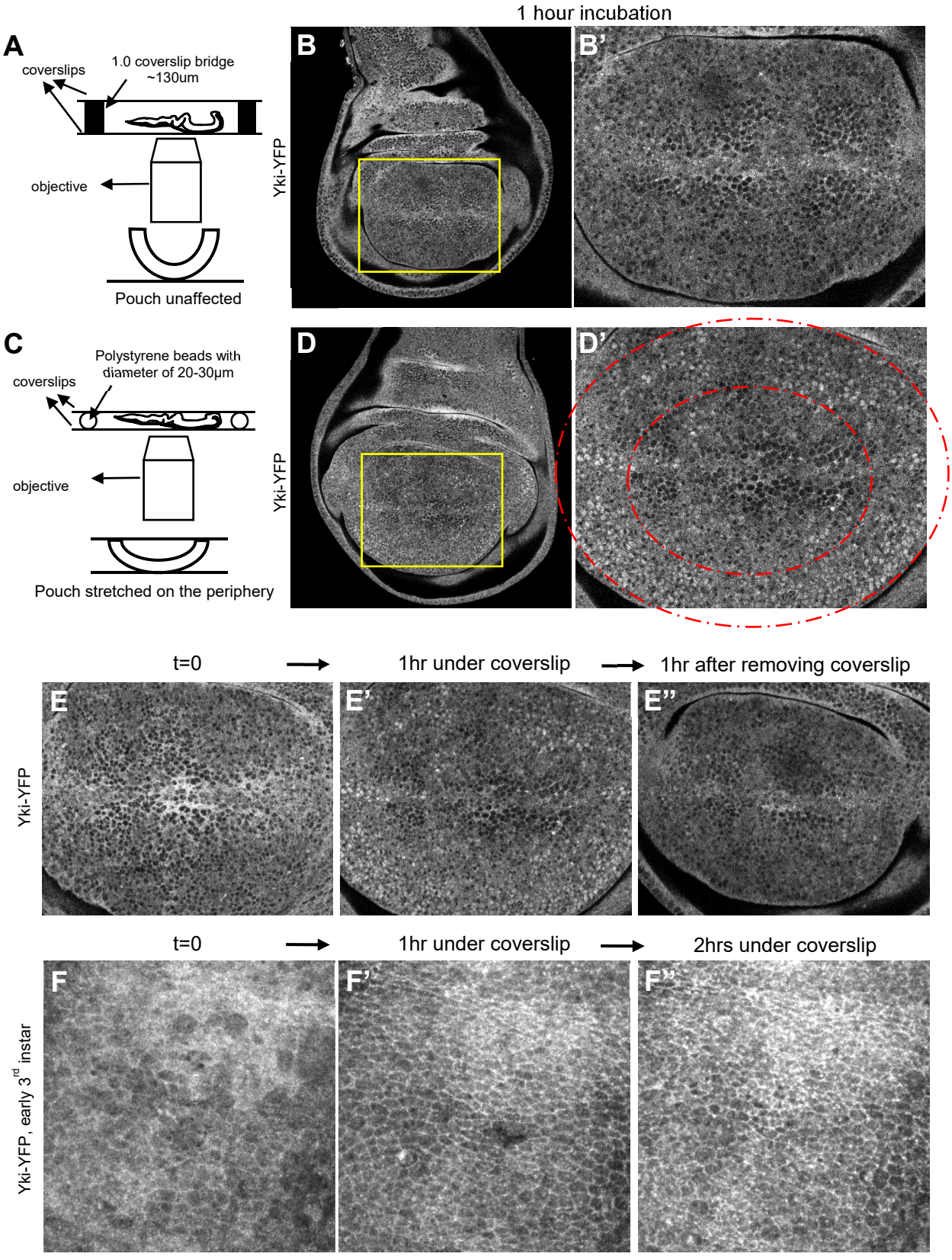
1 hour incubation
A
coverslips
1.0 coverslip bridge
~130um
objective
Pouch unaffected
B
B'
Yki-YFP
C
Polystyrene beads with
diameter of 20-30µm
coverslips
objective
Pouch stretched on the periphery
D
D'
Yki-YFP
t=0
1hr under coverslip
1hr after removing coverslip
E
E'
E''
Yki-YFP
t=0
1hr under coverslip
2hrs under coverslip
F
F'
F''
Yki-YFP, early 3rd instar

Figure A.3 continued
Mechanical force promotes nuclear and cortical Yki localization
Mechanical force promotes nuclear Yki localization (**A-D'**) Wing imaginal discs are placed between two coverslips with the apical side facing downwards. In the control setup, two coverslips were separated with 1.0 coverslip bridge ~130µm thick so that the top coverslip did not touch the wing discs (**A**). After 1 hour incubation in dissection media, Yki-YFP showed cytoplasmic localization (**B,B'**). Yellow box indicates zoomed in region in **B'**. In the experimental setup, two coverslips were separated with polystyrene beads with diameter of 20-30µm and the top coverslip pushed down on the wing discs (**C**). After 1 hour incubation in dissection media, Yki-YFP showed nuclear localization, especially at the periphery of the pouch (**D, D'**). Yellow box indicates zoomed in region in **D'**. Red dashed lines indicate the periphery of the pouch.

Nuclear localization of Yki-YFP by mechanical force is reversible (E-E''). 1 hour after removing the top coverslip, Yki-YFP re-localized to the cytoplasm.

Mechanical force promotes cortical Yki-YFP localization in early third instar wing imaginal discs(**F-F''**).

Appendix B

Investigating the mechanism of Yorkie's cortical recruitment

One possible mechanism of Yorkie's (Yki) cortical localization is that it is recruited by Expanded (Ex), which strongly localizes to the AJR and interacts directly with Yki (Badouel et al. 2009). Indeed, transiently expressing Ex caused increased cortical Yki accumulation (Figure B.1 A). In addition, depleting Ex in *wts RNAi* cells suppressed the increased Yki accumulation at the AJR (Figure B.1 B-C). Together these results suggest that Ex could be sufficient to recruit Yki to the cortex. However, there was still clear cortical Yki localization in Ex depleted *wts* clones (Figure B.1 C). Moreover, depleting Ex alone with RNAi or in particular genetically removing Ex with a null allele of *ex* did not abolish cortical Yki localization (Figure B.1 D-E'). Together these results clearly indicate Ex is not the only factor that recruit Yki to the cell cortex.

Yki has been shown to interact (directly or indirectly) with several other pathway components, including Kibra, Hippo, Warts, Ajuba and 14-3-3 (Genevet and Tapon 2011). However, depleting Hippo pathway components with RNAi did not appear to affect cortical Yki localization (Figure B.2).

Previous studies have revealed interactions between YAP and adherens junctions components (F.-X. Yu and Guan 2013). My preliminary results show that depleting either Ecad or α-catenin dramatically altered cortical Yki localization, seemingly changing it from junctional to medial in wing epithelial cells (Figure B.3 A-B). Interestingly, depleting β-catenin did not affect cortical Yki (Figure B.3 C), though the relative effectiveness of these RNAi transgenes needs to be directly evaluated.

See discussion and future directions in Chapter 4.

Figure B.1

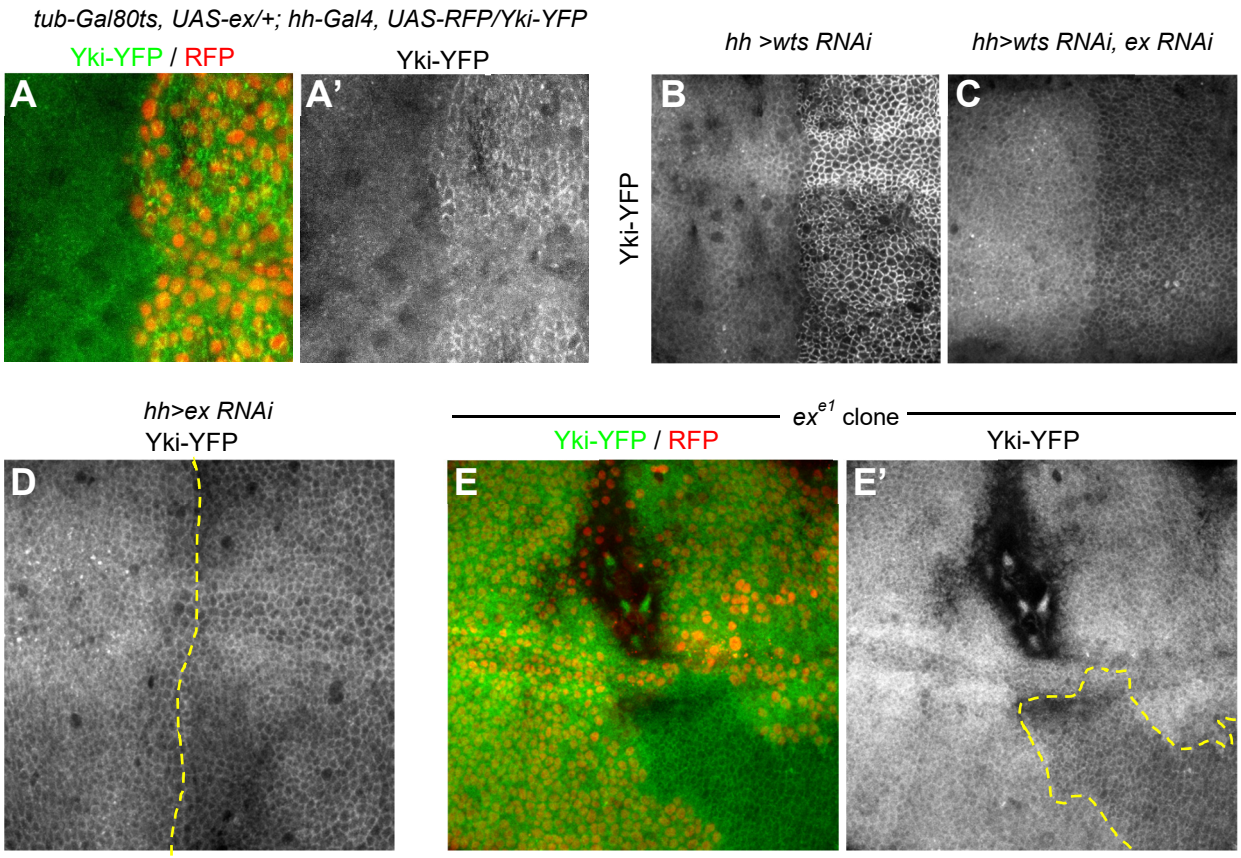

Ex is sufficient but not required for cortical localization of Yki
Transiently express Ex caused increased cortical Yki accumulation (**A-A'**).
Depleting Ex in wts null clones suppressed the increased Yki accumulation at the AJR (**B-C**).
Depleting Ex alone did not affect cortical Yki localization (**D**). Yellow dashed lines indicate expression boundary. *hh-Gal4* drives expression in the posterior (right) side.
Genetically removing Ex with a null allele of ex did not abolish cortical Yki localization (**E-E'**). Yellow dashed lines indicate *ex* clone boundary.

Figure B.2

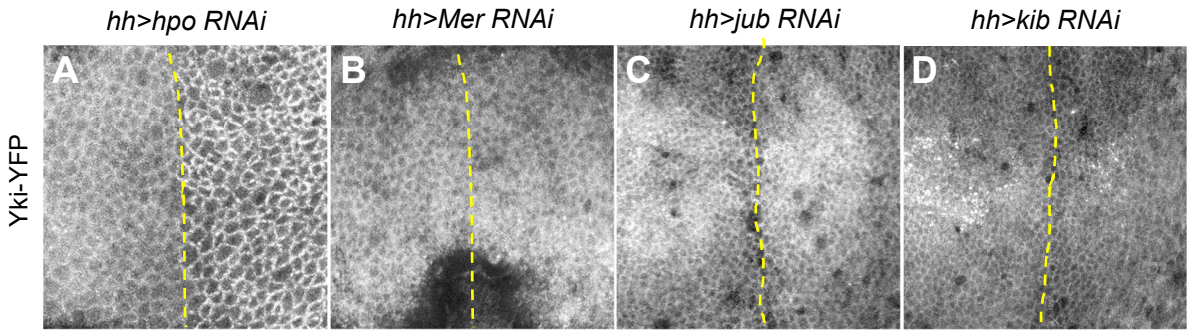

In collaboration with Yupu Wang

Hippo pathway components are not required for cortical localization of Yki
Depleting Hippo pathway component Hpo (**A**) or upstream regulators Mer (**B**), Jub (**C**), or Kib (**D**) did not abolish cortical Yki localization. Yellow dashed lines indicate expression boundary. *hh-Gal4* drives expression in the posterior (right) side.

Figure B.3

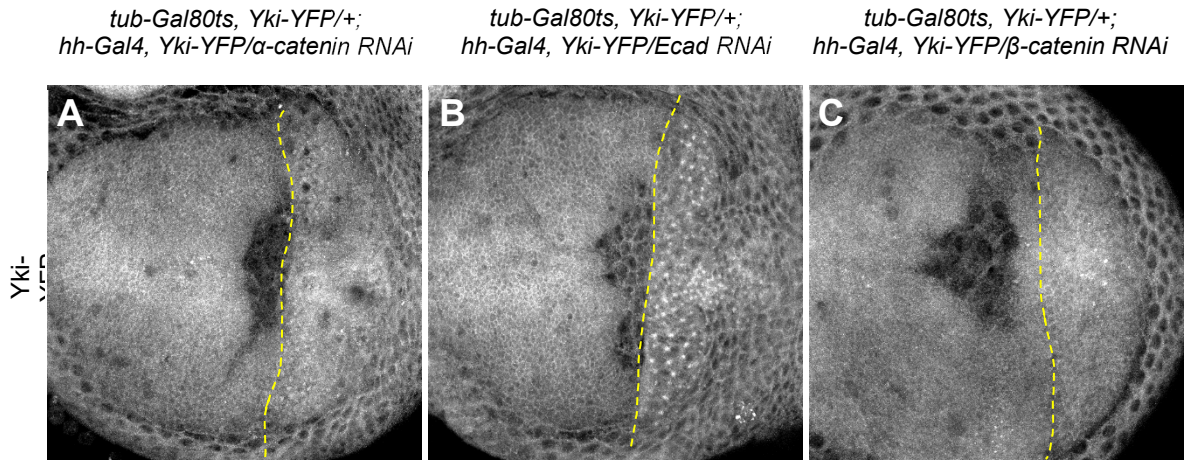

Depleting Adherens Junctions components disrupts cortical localization of Yki
Depleting adherens junctions components α-catenin(**A**) or Ecad (**B**) abolished cortical Yki localization. Depleting another adherens junctions component β-catenin did not affect cortical Yki (**C**). *α-catenin RNAi* was expressed for 38 hours. *Ecad RNAi* was expressed 33 hours. *β-catenin RNAi* was expressed 25 hours. Yellow dashed lines indicate expression boundary. *hh-Gal4* drives expression in the posterior (right) side.

Methods

Table B.1 Key resource used in Appendix B

REAGENT or RESOURCE	SOURCE	IDENTIFIER
Experimental Models: Organisms/Strains		
D. melanogaster: hh-Gal4/TM6	Tetsuya Tabata	N/A
D. melanogaster: UAS-ex, tub-Gal80^{ts}/CyodfYFP	Ting Su	N/A
D. melanogaster: hh-Gal4, UAS-RFP/TM6	Ting Su	N/A
D. melanogaster: UAS-wts RNAi/Cyo	Vienna Drosophila RNAi Center	106174
D. melanogaster: UAS-ex RNAi #9/TM6	This study	N/A
D. melanogaster: Yki-YFP	Su et al. 2017	N/A
D. melanogaster: UAS-hpo RNAi/Cyo	Vienna Drosophila RNAi Center	104169
D. melanogaster: UAS-Mer RNAi #14/TM6	This study	
D. melanogaster: UAS-jub RNAi/TM6	Bloomington Stock Center	30806
D. melanogaster: UAS-kib RNAi/TM6	Bloomington Stock Center	28683
D. melanogaster: Yki-YFP, tub-Gal80^{t}/CyodfYFP; Yki-YFP, hh-Gal4/TM6	This study	N/A
D. melanogaster: UAS- α-catenin RNAi/TM6	Bloomington Stock Center	33430
D. melanogaster: UAS- Ecad RNAi/TM6	Bloomington Stock Center	32904
D. melanogaster: UAS- β-catenin RNAi/TM6	Bloomington Stock Center	31305

Drosophila husbandry

Drosophila melanogaster was cultured using standard techniques at 25°C (unless otherwise noted). Both male and female animals were used (unless otherwise noted). All crosses were performed at 25°C unless otherwise noted. For clone induction, heat shocks were performed 60-84 hr after egg laying using the following program: 38°C for 1hr, 25°C for 1hr, 38°C for 1h, 25°C for 1hr in an EchoTherm IN35 incubator (Torrey Pines Scientific).

Drosophila Genetics

Drosophila stocks used in this study are listed in Table B.1

To generate ex null clones, the following genotypes were used:

hsFLP/+; ex^{e1} 40A FRT yki^{B5}/Ubi-RFP 40AFRT yki^{B5}; Yki-YFP/Yki-YFP

Immunostaining and live imaging of wing imaginal discs

As described in Chapter 2 and Appendix A

Appendix C

Investigating the subcellular localization of Strn-Mlck

The *Strn-Mlck* locus encodes ten different isoforms and eight of them contain the kinase domain (Figure C.1 A). Among the kinase domain containing isoforms, three isoforms end about 200bps upstream of the rest (Figure C.1 A). Due to Strn-Mlck's complex structure, it is difficult to tag all the isoforms. One Strn-Mlck RNAi that strongly suppresses the Myr-Yki phenotypes and causes undergrowth on its own specifically targets an exon coded exclusively by the five isoforms that extend further 3', suggesting these isoforms are important in Hippo pathway regulation (Figure C.1 B). Therefore, we have used CRIPSR to tag these isoforms with GFP (Figure C.1 B). GFP signal was detected in the peripodial membrane of wing imaginal discs from wandering third instar larvae (Figure C.2 A), suggesting tagging was successful. However, we did not detect GFP fluorescence in the wing imaginal disc proper (Figure C.2 B). Recently we reviewed an RNAseq data set from Flybase and found that these isoforms may be down-regulated in third instar larval imaginal discs (Figure C.1 C). See discussions and future directions for investigating Strn-Mlck sub-cellular localization in wing imaginal discs in Chapter 4.

Our GFP-tagged Strn-Mlck allele strongly fluoresces in the larval salivary glands and muscles (Figure C.2 E, F). In the salivary gland, Strn-Mlck outlines large intracellular vesicles (a few microns in diameter). These structures are presumably secretory vesicles that secrete glue proteins(Rousso, Schejter, and Shilo 2016). Previous studies show that the actomyosin network assembles around these vesicles to promote their fusion to the cell membrane and content release(Rousso, Schejter, and Shilo 2016; Segal et al. 2018). The expression pattern of Strn-Mlck is strikingly similar to that of the actomyosin network, suggesting Strn-Mlck may be also involved in the fusion of secretory vesicles to the cell membrane. We have initiated a collaboration with

Ben-Zion Shilo's lab at Weizmann Institute of Science to ask if Strn-Mlck functions in secretory vesicles. Two sets of initial experiments are currently underway. The first set is to deplete Strn-Mlck in salivary glands and examine glue protein secretion. The second set is to analyze potential co-localization of Strn-Mlck and proteins involved in glue protein secretion such as myosin and Rho kinase.

To investigate if Strn-Mlck has a kinase independent function to regulate the Hippo pathway, I have engineered a kinase dead allele of *Strn-Mlck* (*Strn-Mlck*^{KD}) in which the entire kinase domain coding region is replaced by a *Pax6-DsRed* module (Figure 4.3A). See results and discussion in Chapter 4.

Figure C.1

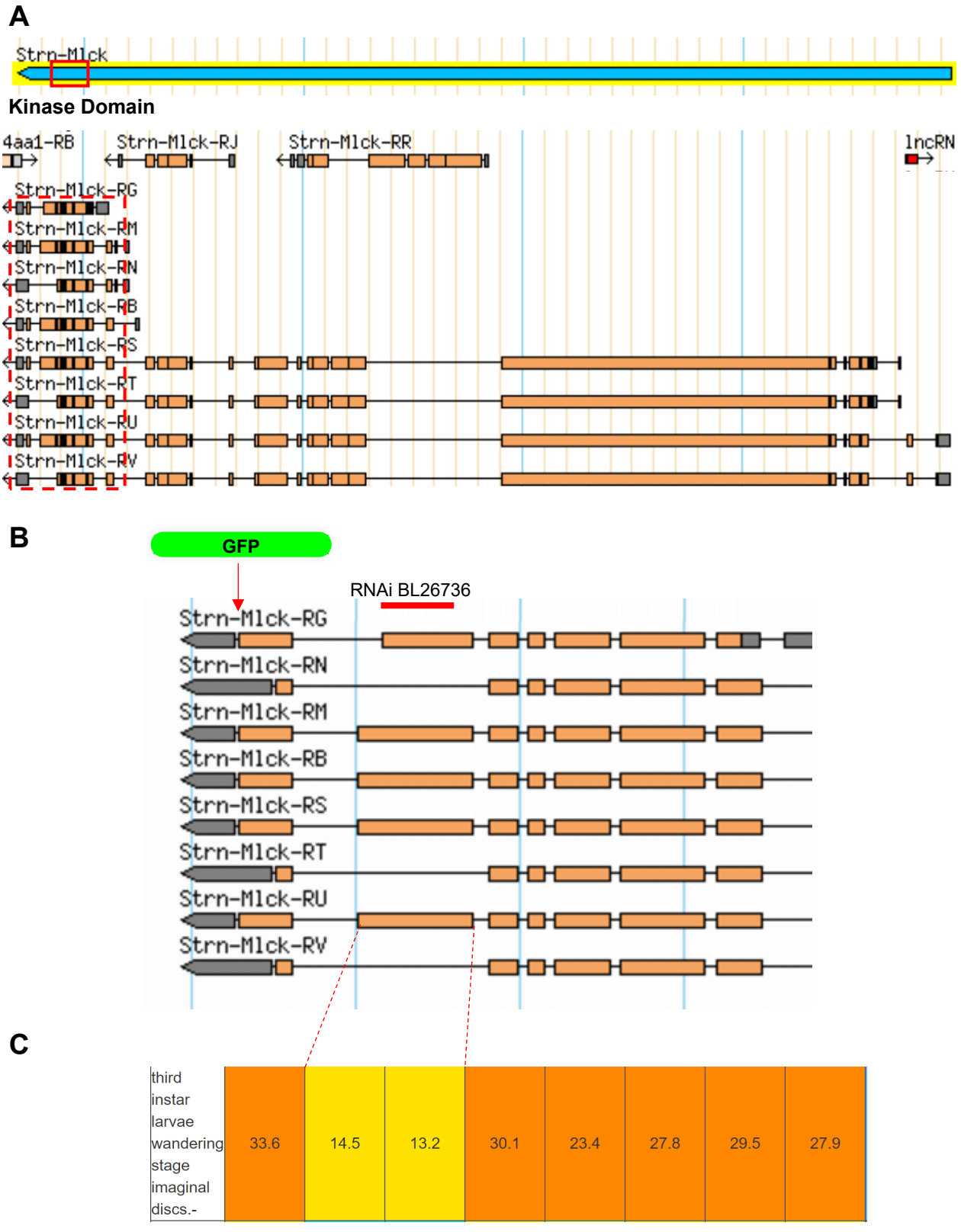
A
Strn-Mlck
Kinase Domain
4aa1-RB
Strn-Mlck-RJ
Strn-Mlck-RR
lncRN
Strn-Mlck-RG
Strn-Mlck-RM
Strn-Mlck-RN
Strn-Mlck-RB
Strn-Mlck-RS
Strn-Mlck-RT
Strn-Mlck-RU
Strn-Mlck-RV
B
GFP
RNAi BL26736
Strn-Mlck-RG
Strn-Mlck-RN
Strn-Mlck-RM
Strn-Mlck-RB
Strn-Mlck-RS
Strn-Mlck-RT
Strn-Mlck-RU
Strn-Mlck-RV
C
third instar larvae wandering stage imaginal discs.-
33.6
14.5
13.2
30.1
23.4
27.8
29.5
27.9

Figure C.1 continued
Adding GFP tag at the endogenous locus of Strn-Mlck with CRISPR
Ten isoforms are encoded by the Strn-Mlck locus (**A**). Eight of them contain the kinase domain. This diagram was obtained from Flybase. Red solid box indicate the region that encodes the kinase domain. Red dashed box indicates zoomed in region shown in **B.**

GFP tag was added to the most 3' end of the following five isoforms: RG, RM, RB, RS, and RU (**B**). Red line indicates the region targeted by the Strn-Mlck RNAi line that suppresses Myr-Yki phenotypes (BL26736).

Tagged isoforms may be down-regulated in wing imaginal discs from wandering third instar larvae (**C**). RNAseq data of the last few exons were shown. The dataset was obtained from Flybase. Deeper color indicates higher expression level. Numbers are log2 transforms of the original coverage values and are normalized for the sequence read-depth of each sample. The two light orange boxes corresponds to the exonic region indicated by red dashed lines.

Figure C.2

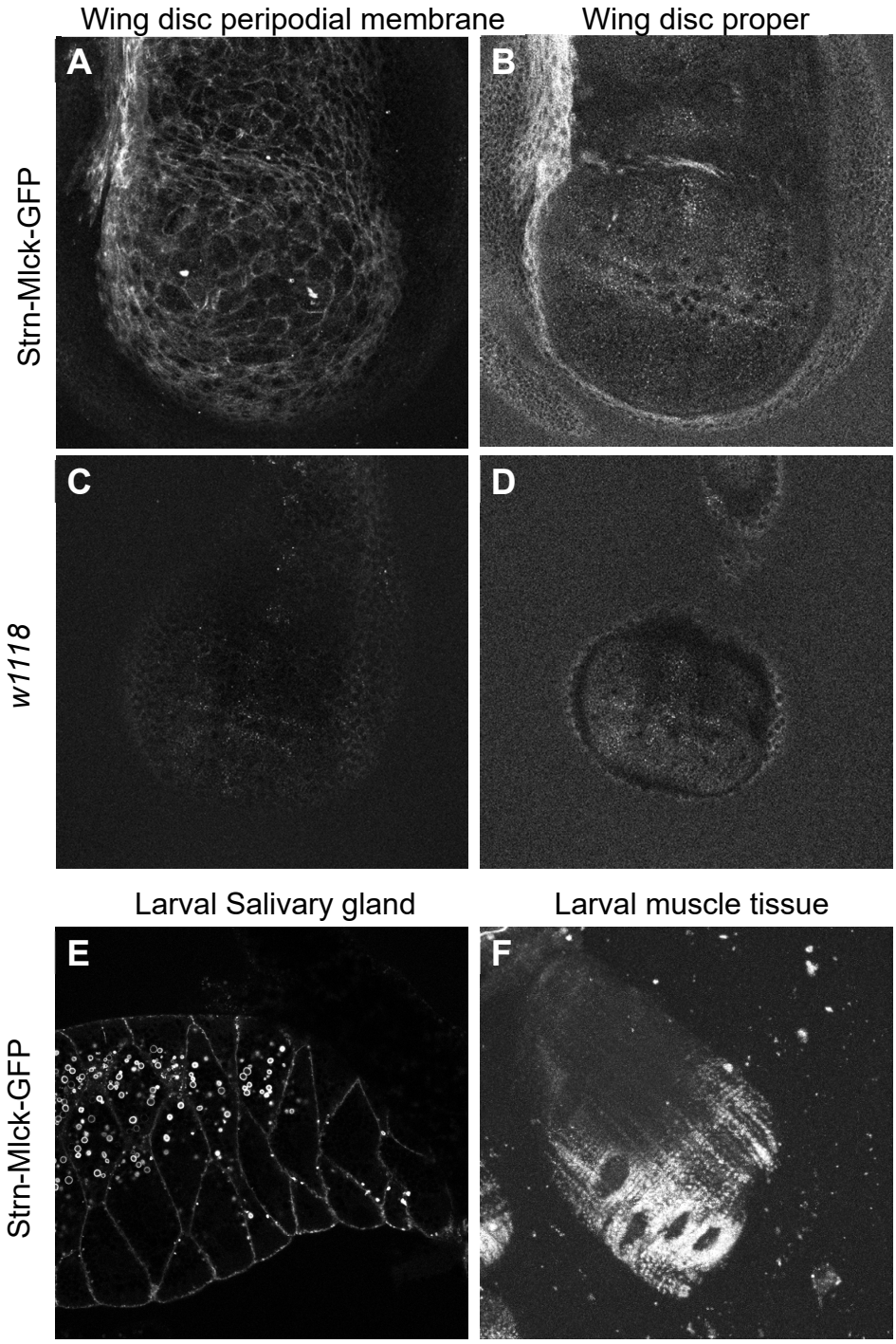

Strn-Mlck-GFP expression in larval tissue

Strn-Mlck-GFP signal was detected in the peripodial membrane of wing imaginal discs from wandering third instar larvae (**A**). However, no signal was detected in the disc proper (**B**). Wing imaginal discs from *w1118* larvae were used as control and the same configuration was used to detect GFP signal. Strn-Mlck-GFP was also robustly detected in salivary gland (**E**) and muscle tissue (**F**) from wandering third instar larvae.

Methods

Drosophila husbandry

Drosophila melanogaster was cultured using standard techniques at 25°C (unless otherwise noted). Both male and female animals were used (unless otherwise noted). All crosses were performed at 25°C unless otherwise noted.

Drosophila Genetics

Generation of Strn-Mlck-GFP allele

The Strn-Mlck-GFP allele was generated using the Scarless CRISPR/Cas9 genome engineering technique (http://flycrispr.molbio.wisc.edu/scarless). A 1.0kb left homology arm containing the sequence that ends at the last exon of *Strn-Mlck* and a 1.0kb right homology arm that starts from the end of the last exon of *Strn-Mlck* were cloned by homologous recombination (Gibson et al., 2009) into pHD-ScarlessDsRed (Drosophila Genomics Resource Center) as the donor template. This plasmid was co-injected with a pU6- Bbs1-chiRNA based plasmid expressing the guideRNA (5'- tatcacgtcctagtttaagt-3') into *vas-Cas9* embryos. G0 flies were crossed to w^{1118} and individual DsRed positive F1s were selected to establish stocks. The DsRed marker cassette was then removed through a single cross to a source of the PBac transposase (w1118; CyO, P{Tub-PBac\T}2/wgSp-1; BL8285). The GFP tagging was verified by the positive GFP signal in wandering third instar larval tissue.

Generation of *Strn-Mlck^{KD}* allele

The Strn-MlckKD allele was generated using the Scarless CRISPR/Cas9 genome engineering technique (http://flycrispr.molbio.wisc.edu/scarless). A 1.5kb left homology arm containing the sequence that ends at the start of the kinase domain and a 1.5kb right homology arm

that starts from the end of the kinase domain of Strn-Mlck were cloned by homologous recombination (Gibson et al., 2009) into pHD-ScarlessDsRed (Drosophila Genomics Resource Center) as the donor template. This plasmid was co-injected with two pU6- Bbs1-chiRNAs based plasmid expressing the guideRNA1 (5'- GTGTGGAAGTATACCGTAAA-3', 316bp upstream of the kinase domain) and guideRNA2 (5'- ttgttgctgagactatcgtc -3', 10bp downstream of the kinase domain) into vas-Cas9 embryos. G0 flies were crossed to w1118 and individual DsRed positive F1s were selected to establish stocks.

Live imaging of wing imaginal discs, salivary glands, and muscle tissue

As described in Appendix A

Appendix D

Myr-Yki and Yki do not affect Strn-Mlck kinase activity in an *in vitro* kinase assay

We developed an *in vitro* kinase assay to analyze if Strn-Mlck can directly promote Sqh phosphorylation. Strn-Mlck is predicted to be a Sqh kinase based on sequence homology (Champagne et al. 2000). However, no previous study has directly verified its Sqh kinase activity. To directly test if Strn-Mlck is able to phosphorylate Sqh, we therefore used an *in vitro* kinase assay (Figure D.1). In addition to wild-type Strn-Mlck, we engineered two kinase dead version of Strn-Mlck as our negative control by deleting domains essential for kinase activity. In Strn-Mlck-KD^1, the ATP binding region is deleted. In Strn-Mlck-KD^2, the activation loop is deleted (Figure D.1 A). We expressed and purified these Strn-Mlck proteins from S2 cells, followed by incubation with bacterially purified GST-Sqh (Figure D.1 B). Sqh phosphorylation was assayed on immunoblots using a previously characterized phospho-specific anti-Sqh antibody (Liang Zhang and Ward 2011). Wild-type Strn-Mlck was able to robustly phosphorylate GST-Sqh whereas both kinase dead versions of Strn-Mlck failed to do so (Figure D.1 C). Our results provide a strong piece of evidence that Strn-Mlck can phosphorylate Sqh.

The results in Chapter 2 suggest Yki activates myosin by recruiting Strn-Mlck to the cell cortex (Chapter 2, Xu et al. 2018). An alternative possibility, that is not mutually exclusive, is that interaction with Yki increases the kinase activity of Strn-Mlck, possibly via an allosteric mechanism. To test if interacting with Yki promotes Strn-Mlck kinase activity, we again used our *in vitro* kinase assay. We co-transfected S2 cells with Myr-Yki and Strn-Mlck or wild-type Yki and Strn-Mlck and tested if Strn-Mlck kinase activity is affected. (Figure D.2). Neither Myr-Yki nor Yki caused obvious change in phosphorylation of GST-Sqh, indicating the kinase activity of Strn-Mlck was not altered (Figure D.2 B). This could mean that cortical Yki does not promote

kinase activity of Strn-Mlck. However, there are two major concerns in our assay. First, the read out of this experiment is total Sqh phosphorylation rather than the speed of the phosphorylation. It is possible that potential increase in kinase activity only translates into faster reaction time but not total amount of phosphorylation. Second, the kinase/substrate ratio in the reaction system may be too high such that the kinase can phosphorylate all of the substrate in a very short amount of time and our assay is not sensitive enough to detect a minor change in kinase activity. To address the first concern, we performed a time course of the kinase assay by measuring Sqh phosphorylation at different time points. Co-transfection of Myr-Yki or wild-type Yki did not obviously alter Sqh phosphorylation at any timepoint, suggesting reaction speed is not altered (Figure D.2 C-D). To address the second concern, we did two sets of experiments to reduce kinase/substrate ratio. In the first set we reduced the amount of kinase to one third and one twenty-seventh of the original amount, in the second set we increased the amount of substrate to six or twelve times the original amount. In both sets of experiments, phosphorylation of Sqh was not altered by Myr-Yki or Yki co-transfection (Figure D.2 E-F). To summarize our results, co-transfection of Myr-Yki or Yki does not seem to detectably affect Strn-Mlck kinase activity.

Figure D.1

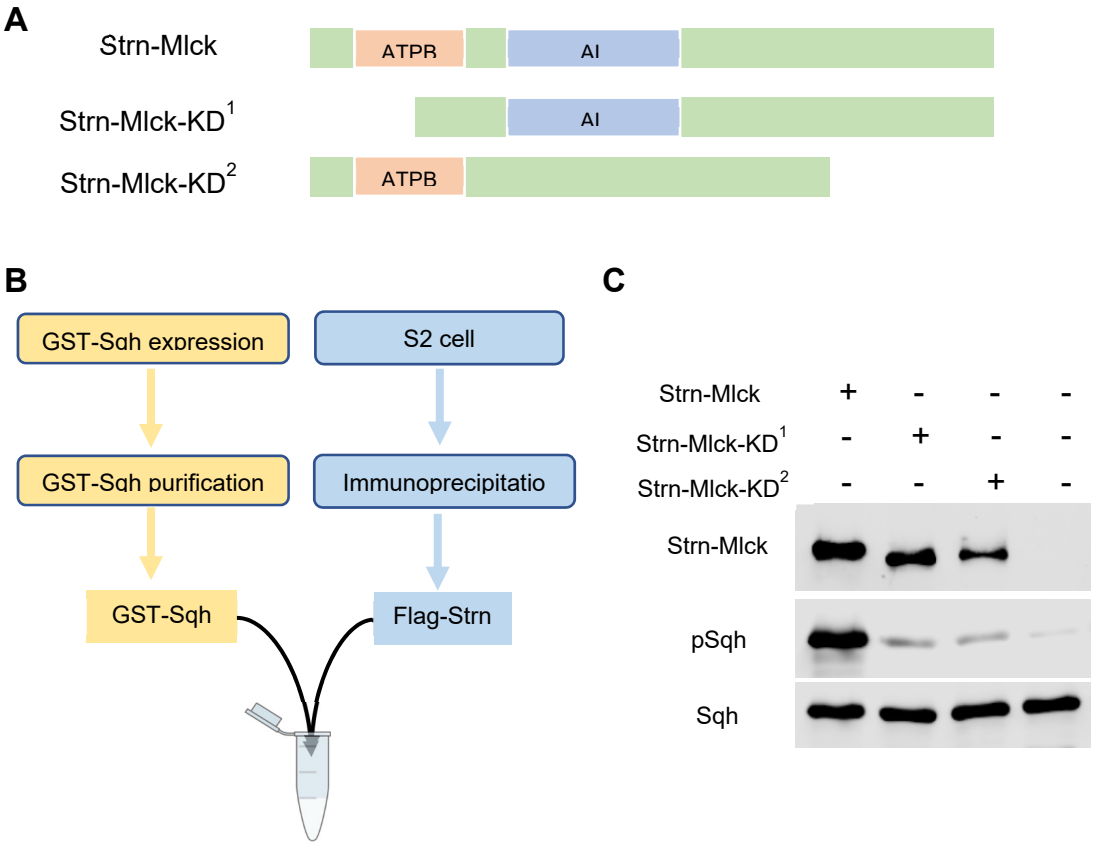

In collaboration with Yupu Wang

Strn-Mlck phosphorylates Sqh *in vitro*

Flag tagged wild-type and kinase dead versions of Strn-Mlck were used in the assa. ATP binding domain (ATPBD) was deleted in Strn-Mlck-KD[1]. Activation loop (AL) was deleted in Strn-Mlck-KD[2] (**A**). Strn-Mlck were expressed in S2 cells and purified with Flag antibody using immunoprecipitation. Substrate GST-Sqh was expressed in bacteria and batch purified using GST Sepharose 4B beads (**B**).

Wild-type Strn-Mlck was able to robustly phosphorylate GST-Sqh whereas both kinase dead versions of Strn-Mlck failed to do so (**C**). Phosphorylation of GST-Sqh was detected using an

Figure D.2

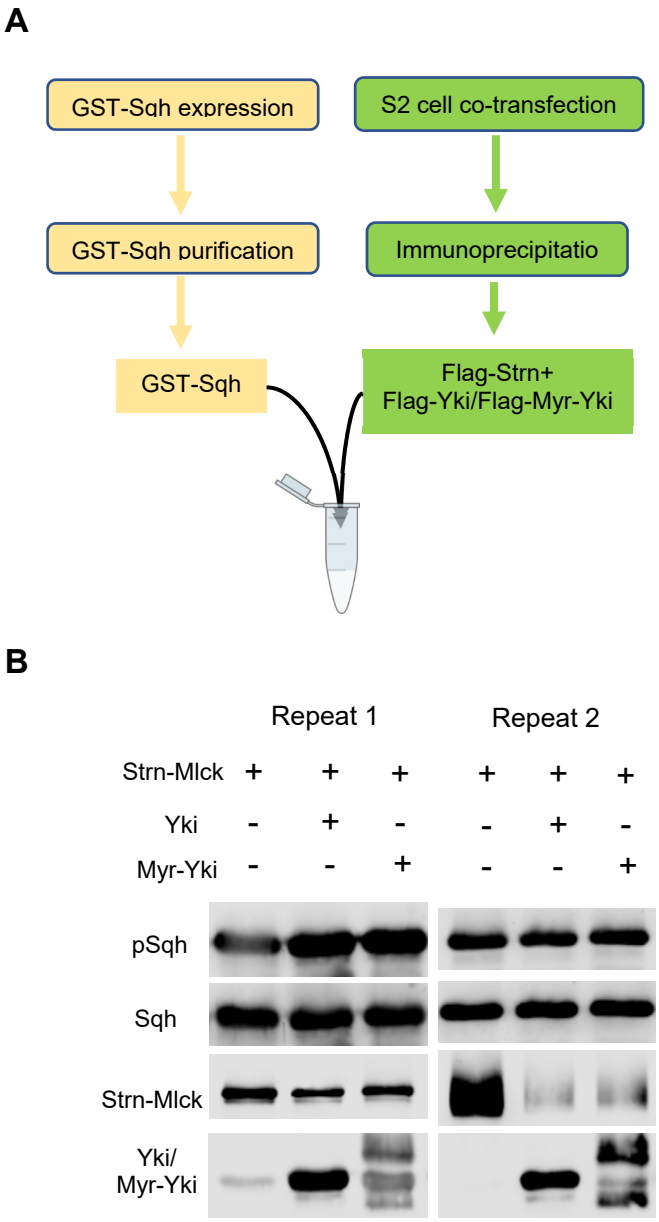

In collaboration with Yupu Wang

Co-transfection of Myr-Yki or Yki does not affect Strn-Mlck mediated Sqh phosphorylation

Flag tagged Myr-Yki or wild-type Yki was co-transfected with Flag tagged Strn-Mlck and co-purified with Flag antibody using immunoprecipitation. They were then subject the in vitro kinase assay (**A**). Neither Myr-Yki nor Yki caused obvious change in phosphorylation of GST-Sqh (**B**) Two biological replicates were shown.

Figure D.2 continued

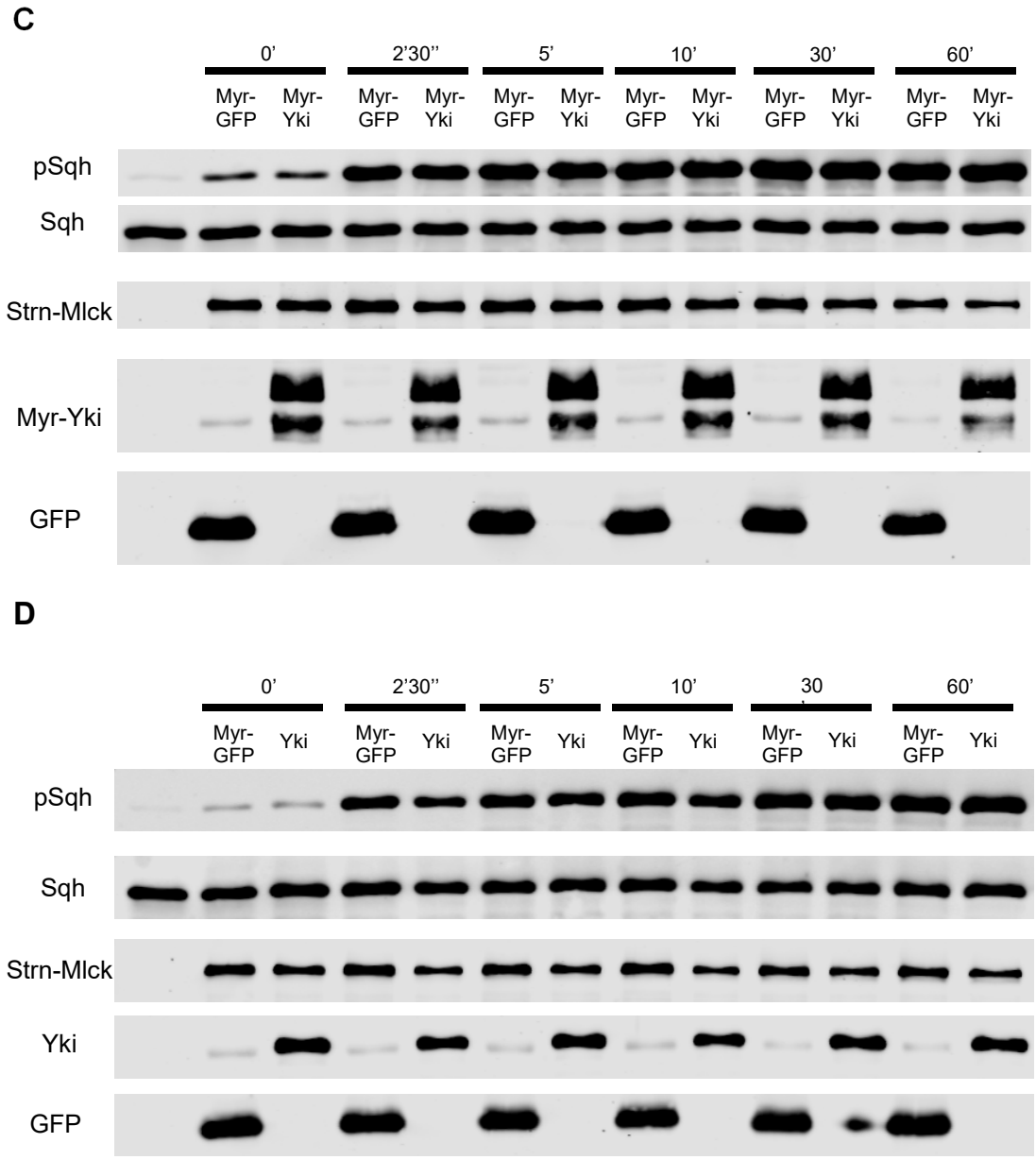

Myr-Yki did not cause obvious change in phosphorylation of GST-Sqh in any time points of the kinase assay (**C**). Myr-GFP was co-transfected with Strn-Mlck as the negative control.

Similarly Yki did not cause obvious change in phosphorylation of GST-Sqh in any time points of the kinase assay (**D**). Myr-GFP was co-transfected with Strn-Mlck as the negative control.

Figure D.2 continued

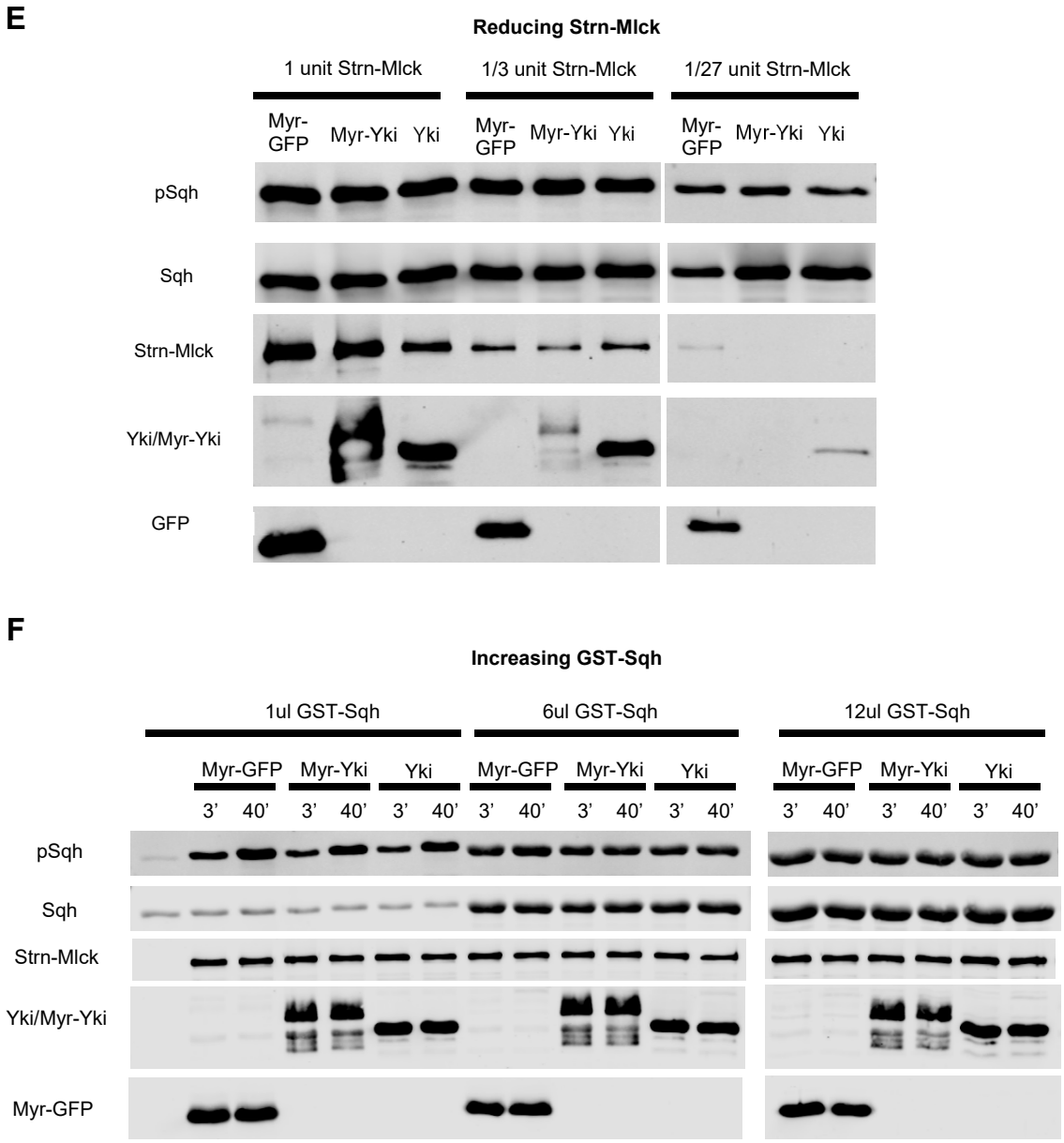

Myr-Yki or Yki did not cause obvious change in phosphorylation of GST-Sqh with reduced kinase Strn-Mlck (**E**). Myr-GFP was co-transfected with Strn-Mlck as the negative control.

Myr-Yki or Yki did not cause obvious change in phosphorylation of GST-Sqh with increased substrate GST-Sqh (**F**). Myr-GFP was co-transfected with Strn-Mlck as the negative control. Phosphorylation of GST-Sqh after 3 minutes and 40 minutes of reaction were examined.

Methods

1. Batch purification of GST-Sqh

Reagents:

Binding buffer: 140 mM NaCl, 2.7 mM KCl, 10 mM Na2HPO4, 1.8 mM KH2PO4, pH 7.3

Use 0.45 filter to filter it before use

Elution buffer: 80 mM Tris-HCl (PH=8.0) 20 mM reduced glutathione

Prepare fresh on the day of elution

Detailed Protocol:

1. Grow 100 ml overnight culture in LB-Amp from ~5 colonies from fresh (less than 1 week old) plate.

2. Dilute 40 ml of overnight into 1L of prewarmed Terrific Broth w/400mg/L Amp

3. Grow culture at 37oC until OD600 = ~1.0 (~1-1.5 hrs). Take 100µl sample for uninduced control. Spin down cells, resuspend in 100 µl 1X SDS sample buffer.

4. Induce w/1.0mM IPTG (1 ml of 1M stock).

5. Incubate at 25oC for 3-4 hr. At end of incubation take 100 µl sample, spin down, resuspend in 100 µl of 1X SDS sample buffer.

6. Cool culture on ice 15 min. Spin cells for 5 min at 4500 RPM in X-15R table top with swinging bucket rotor using 500 ml conical tube at 4oC.

7. Resuspend pellet in 500 ml ice cold binding buffer (PBS). Spin 4500 RPM and remove supernatant.

8. Cells can be stored at -80oC if needed at this step.

9. Resuspend cells in 40 ml cold binding buffer with 1X CelLytic detergent and protease inhibitors (lysozyme at 0.2mg/ml optional). Note, Sigma recommends 10-20 ml of lysis buffer per gram of cell paste – (1 gm of cells equals 250 ml of culture with OD600=2.0).

10. Resuspend pellet completely, then incubate 10-15 min at rt.

11. Centrifuge at 4750RPM for 20 min to pellet insoluble material.

12. Remove supernatant. Take 20 µl sample and add 20 µl of 2XSDS sample buffer.

13. Take 1ml GST-beads, add 5ml binding buffer and suspend the beads.

14. Centrifuge at 500g for 5min to sediment beads. Remove supernatant.

15. Add lysate to beads. Incubate at least 30min at room temperature or 2-3hrs at 4C.

16. Sediment the beads by centrifugation at 500g for 5min. Remove supernatant and collect for measuring binding efficiency.

17. Wash the beads by adding 5ml binding buffer, carefully resuspend.

18. Repeat step16 and step17 for a total of three washes.

19. Elute the bound protein by adding 0.5ml elution buffer. Incubate at room temperature for 5-10min. Using gentle agitation such as end-over-end rotation.

20. Sediment the beads by centrifugation at 500g for 5min. Collect supernatant.

21. Repeat step20 and step21 for a total three times elutions.

22. Bubble test: if bubbles formed by blowing air from a P200 in the elution fraction are retained for more than a few minutes then protein concentration is significant.

23. Run all samples and fractions on SDS-PAGE. Run size markers and BSA standards (0.2, 0.5, 2.0, 5.0 mg/ml).

24. Measure the concentration by Bradford assay.

2. *in vitro* kinase assay

Reagents:

IP buffer: 150 mM NaCl, 50mM NaF, 100mM Tris pH 8.0

Kinase buffer: 25mM HEPES pH 7.2, 25mM MgCl2, 50mM β-glycerol phosphate, 2mM dithiothreitol, 0.5mM Sodium Vanadate, 10μM ATP

Prepare as 10X stock without ATP and store at -20 °C. Thaw on ice on the day of assay and add ATP before reaction.

Detailed protocol

1. Take 10ml of buffer and add 1 tablet of protease inhibitors. Prechill all tubes that will be used. Add Tx-100 to 0.5% after tablets are fully dissolved. (1ml of 10% per 10mls buffer).
2. Collect cells and wash 1X in buffer without inhibitor. (spinning down at 1500rpm for 5min)
3. Lyse cells in 0.5ml of buffer+inhibitor+0.5%Tx by passing through a 27 gauge syringe 10X. Put on rocker in cold-room for 15min. (10 times of the cell volume)
4. Spin down cells at 14K for 10min (4℃). Transfer supernatants to prepared beads for preclearing. Put tubes for preclearing onto nutator in the cold-room for 15min.
   (Beads for preclearing: 40μl beads for each lysate, wash beads 3X in buffer without inhibitors, spin down at 2500rpm for 1min.)
5. Spin down precleared lysates at 14K for 10min. Take 10μl of the lysate to save to run on gel, put the rest of the lysate onto the prepared beads for IP. Carry out IP reaction on nutator in the cold-room for 1-2hrs.
   (Beads for IP: 20μl beads for each lysate, wash 3X in buffer without inhibitors, spinning down at 2500rpm for 1min. Add 10μl 10%TX in first wash to help beads pellet at bottom of tubes.)

6. Spin down IP reaction at 2500rpm for 1min.

   Wash in IP buffer+inhibitors+0.5%TX, spins 2500rpm for 1min.

   Wash in ½ IP buffer+inhibitors+0.5%TX + ½ IP buffer without inhibitor

   Wash in IP buffer without inhibitor

   Wash in IP ½ buffer without inhibitor + ½ Kinase buffer without ATP

   Wash in Kinase buffer without ATP

7. Resuspend the final pellet in 50µl of Kinase buffer with ATP.
8. Add 1 µl of GST-Sqh (2.8µg/µl).
9. Incubate in rotating chamber for 40min at 30℃.
10. Add 50 µl 2XSDS and boil the sample at 95℃ for 6min.
11. Run the sample on 10% SDS-PAGE gel followed by Western Blot.
12. Primary antibody concentration: guinea pig anti pSqh: 1:3000; mouse anti Sqh: 1:3000; rabbit anti Flag 1:5000.

Note1: For time course experiment, Steps 7-12 are modified as following:

7. Resuspend the final pellet in 240µl of Kinase buffer with ATP

8. Add 5 µl of GST-Sqh (2.8µg/µl)

9. Collect 20µl slurry at time 0.

10. Incubate in rotating chamber at 30℃.

11. Collect 20µl slurry at specific time points.

13. Add 20µl 2XSDS and boil the sample at 95℃ for 6min.

14. Run the sample on 10% SDS-PAGE gel followed by Western Blot.

15. Primary antibody concentration: guinea pig anti pSqh: 1:3000; mouse anti Sqh: 1:3000; rabbit

anti Flag 1:5000.

Note2: For reducing Strn-Mlck experiment, Steps 2-4 are modified as following:

2. Collect **2 wells** of cells and wash 1X in buffer without inhibitor. (spinning down at 1500rpm for 5min)
3. Lyse cells in **1ml** of buffer+inhibitor+0.5%Tx by passing through a 27 gauge syringe 10X. Put on rocker in cold-room for 15min. (10 times of the cell volume)
4. Spin down cells at 14K for 10min (4℃). Transfer supernatants to prepared beads for preclearing. Put tubes for preclearing onto nutator in the cold-room for 15min.
   (Beads for preclearing: **80µl** beads for each lysate, wash beads 3X in buffer without inhibitors, spin down at 2500rpm for 1min.)

Note2 continued. Steps 7-10 are modified as following:

7. Resuspend the final pellet in 108µl of Kinase buffer with ATP
8. Assemble the reactions of following:

Strn-Mlck unit	1	1/3	1/9	1/27
Slurry volume	54µl	18µl	6µl	2µl
Kinase buffer with ATP	0µl	36µl	48µl	52µl
GST-Sqh(2.8µg/µl)	1µl	1µl	1µl	1µl

9. Incubate in rotating chamber for 40min at 30℃.
10. Add 55µl 2XSDS and boil the sample at 95℃ for 6min.
11. Run the sample on 10% SDS-PAGE gel followed by Western Blot.

12. Primary antibody concentration: guinea pig anti pSqh: 1:3000; mouse anti Sqh: 1:3000; rabbit anti Flag 1:5000.

Note3: For increasing GST-Sqh experiment, Steps 2-4 are modified as following:

2. Collect **2 wells** of cells and wash 1X in buffer without inhibitor. (spinning down at 1500rpm for 5min)
3. Lyse cells in **1ml** of buffer+inhibitor+0.5%Tx by passing through a 27 gauge syringe 10X. Put on rocker in cold-room for 15min. (10 times of the cell volume)
4. Spin down cells at 14K for 10min (4℃). Transfer supernatants to prepared beads for preclearing. Put tubes for preclearing onto nutator in the cold-room for 15min.

   (Beads for preclearing: **80µl** beads for each lysate, wash beads 3X in buffer without inhibitors, spin down at 2500rpm for 1min.)

Note3 continued. Steps 7-10 are modified as following:

7. Resuspend the final pellet in 90µl of Kinase buffer with ATP
8. Assemble the reactions of following:

GST-Sqh(2.8µg/µl)	1µl	6µl	12µl
Slurry volume	20µl	20µl	20µl
Kinase buffer with ATP	39µl	34µl	28µl

   Note: Final ATP amount is different among different GST-Sqh reactions, but is the same within the group of the same GST-Sqh volume.

9. Incubate in rotating chamber for 40min at 30℃.
10. Collect 20µl reaction slurry at time points 3min and 40min.

11. Add 20µl 2XSDS and boil the sample at 95℃ for 6min.

12. Run the sample on 10% SDS-PAGE gel followed by Western Blot.

13. Primary antibody concentration: guinea pig anti pSqh: 1:3000; mouse anti Sqh: 1:3000; rabbit anti Flag 1:5000.

References:

Aegerter-Wilmsen, Tinri, Christof M. Aegerter, Ernst Hafen, and Konrad Basler. 2007. "Model for the Regulation of Size in the Wing Imaginal Disc of Drosophila." *Mechanisms of Development* 124 (4): 318–26. doi:10.1016/j.mod.2006.12.005.

Aegerter-Wilmsen, Tinri, Maria B Heimlicher, Alister C Smith, Pierre Barbier de Reuille, Richard S Smith, Christof M Aegerter, Konrad Basler, et al. 2012. "Integrating Force-Sensing and Signaling Pathways in a Model for the Regulation of Wing Imaginal Disc Size." *Development (Cambridge, England)* 139 (17): 3221–31. doi:10.1242/dev.082800.

Alarcón, Claudio, Alexia Ileana Zaromytidou, Qiaoran Xi, Sheng Gao, Jianzhong Yu, Sho Fujisawa, Afsar Barlas, et al. 2009. "Nuclear CDKs Drive Smad Transcriptional Activation and Turnover in BMP and TGF-β Pathways." *Cell* 139 (4): 757–69. doi:10.1016/j.cell.2009.09.035.

Antunes, Marco, Telmo Pereira, João V. Cordeiro, Luis Almeida, and Antonio Jacinto. 2013. "Coordinated Waves of Actomyosin Flow and Apical Cell Constriction Immediately after Wounding." *Journal of Cell Biology* 202 (2): 365–79. doi:10.1083/jcb.201211039.

Aragona, Mariaceleste, Tito Panciera, Andrea Manfrin, Stefano Giulitti, Federica Michielin, Nicola Elvassore, Sirio Dupont, and Stefano Piccolo. 2013. "A Mechanical Checkpoint Controls Multicellular Growth through YAP/TAZ Regulation by Actin-Processing Factors." *Cell* 154 (5). Elsevier Inc.: 1–13. doi:10.1016/j.cell.2013.07.042.

Badouel, Caroline, Laura Gardano, Nancy Amin, Ankush Garg, Robyn Rosenfeld, Thierry Le Bihan, and Helen McNeill. 2009. "The FERM-Domain Protein Expanded Regulates Hippo Pathway Activity via Direct Interactions with the Transcriptional Activator Yorkie." *Developmental Cell* 16 (3). Elsevier Ltd: 411–20. doi:10.1016/j.devcel.2009.01.010.

Banerjee, Swati, Aurea D Sousa, and Manzoor A Bhat. 2006. "Organization and Function of Septate Junctions: An Evolutionary Perspective." *Cell Biochemistry and Biophysics*. doi:10.1385/CBB:46:1:65.

Baumgartner, Roland, Ingrid Poernbacher, Nathalie Buser, Ernst Hafen, and Hugo Stocker. 2010. "The WW Domain Protein Kibra Acts Upstream of Hippo in Drosophila." *Developmental Cell* 18 (2). Elsevier: 309–16. doi:10.1016/j.devcel.2009.12.013.

Bennett, F. Christian, and Kieran F. Harvey. 2006. "Fat Cadherin Modulates Organ Size in Drosophila via the Salvador/Warts/Hippo Signaling Pathway." *Current Biology* 16 (21): 2101–10. doi:10.1016/j.cub.2006.09.045.

Bhat, Manzoor A., Shayan Izaddoost, Yue Lu, Kyung Ok Cho, Kwang Wook Choi, and Hugo J. Bellen. 1999. "Discs Lost, a Novel Multi-PDZ Domain Protein, Establishes and Maintains Epithelial Polarity." *Cell* 96 (6): 833–45. doi:10.1016/S0092-8674(00)80593-0.

Bilder, David. 2004. "Epithelial Polarity and Proliferation Control: Links from the Drosophila Neoplastic Tumor Suppressors." *Genes & Development* 18 (16): 1909–25. doi:10.1101/gad.1211604.

Bischof, J., R. K. Maeda, M. Hediger, F. Karch, and K. Basler. 2007. "An Optimized Transgenesis System for Drosophila Using Germ-Line-Specific C31 Integrases."

Proceedings of the National Academy of Sciences 104 (9): 3312–17. doi:10.1073/pnas.0611511104.

Boggiano, Julian C., and Richard G. Fehon. 2012. "Growth Control by Committee: Intercellular Junctions, Cell Polarity, and the Cytoskeleton Regulate Hippo Signaling." *Developmental Cell* 22 (4). Elsevier Inc.: 695–702. doi:10.1016/j.devcel.2012.03.013.

Boggiano, Julian C., Pamela J. Vanderzalm, and Richard G. Fehon. 2011. "Tao-1 Phosphorylates Hippo/MST Kinases to Regulate the Hippo-Salvador-Warts Tumor Suppressor Pathway Supplement." *Developmental Cell* 21 (5): Supplement. doi:10.1016/j.devcel.2011.08.028.

Bogoyevitch, Marie A., Kevin R.W. Ngoei, Teresa T. Zhao, Yvonne Y.C. Yeap, and Dominic C.H. Ng. 2010. "C-Jun N-Terminal Kinase (JNK) Signaling: Recent Advances and Challenges." *Biochimica et Biophysica Acta (BBA) - Proteins and Proteomics* 1804 (3). Elsevier B.V.: 463–75. doi:10.1016/j.bbapap.2009.11.002.

Bosch, Justin A., Taryn M. Sumabat, Yassi Hafezi, Brett J. Pellock, Kevin D. Gandhi, and Iswar K. Hariharan. 2014. "The Drosophila F-Box Protein Fbxl7 Binds to the Protocadherin Fat and Regulates Dachs Localization and Hippo Signaling." *ELife* 3 (August2014): 1–25. doi:10.7554/eLife.03383.

Bretscher, Anthony, Kevin Edwards, and Richard G. Fehon. 2002. "ERM Proteins and Merlin: Integrators at the Cell Cortex." *Nature Reviews Molecular Cell Biology* 3 (8): 586–99. doi:10.1038/nrm882.

Cai, Danfeng, Shann Ching Chen, Mohit Prasad, Li He, Xiaobo Wang, Valerie Choesmel-Cadamuro, Jessica K. Sawyer, Gaudenz Danuser, and Denise J. Montell. 2014. "Mechanical Feedback through E-Cadherin Promotes Direction Sensing during Collective Cell Migration." *Cell* 157 (5): 1146–59. doi:10.1016/j.cell.2014.03.045.

Campanale, Joseph P., Thomas Y. Sun, and Denise J. Montell. 2017. "Development and Dynamics of Cell Polarity at a Glance." *Journal of Cell Science* 130 (7): 1201–7. doi:10.1242/jcs.188599.

Champagne, M B, K a Edwards, H P Erickson, and D P Kiehart. 2000. "Drosophila Stretchin-MLCK Is a Novel Member of the Titin/Myosin Light Chain Kinase Family." *Journal of Molecular Biology* 300 (4): 759–77. doi:10.1006/jmbi.2000.3802.

Chen, C.-L., M. C. Schroeder, M. Kango-Singh, C. Tao, and G. Halder. 2012. "Tumor Suppression by Cell Competition through Regulation of the Hippo Pathway." *Proceedings of the National Academy of Sciences* 109 (2): 484–89. doi:10.1073/pnas.1113882109.

Chen, Chiao-Lin, Kathleen M Gajewski, Fisun Hamaratoglu, Wouter Bossuyt, Leticia Sansores-Garcia, Chunyao Tao, and Georg Halder. 2010. "The Apical-Basal Cell Polarity Determinant Crumbs Regulates Hippo Signaling in Drosophila." *Proceedings of the National Academy of Sciences of the United States of America* 107 (36): 15810–15. doi:10.1073/pnas.1004060107.

Chiou, Kevin K., Lars Hufnagel, and Boris I. Shraiman. 2012. "Mechanical Stress Inference for Two Dimensional Cell Arrays." *PLoS Computational Biology* 8 (5). doi:10.1371/journal.pcbi.1002512.

Cho, Eunjoo, Yongqiang Feng, Cordelia Rauskolb, and Sushmita Maitra. 2006. “Delineation of a Fat Tumor Suppressor Pathway.” *Nature Genetics* 38 (10): 1142–50. doi:10.1038/ng1887.

Choi, Sekyu, Wonho Kim, and Jongkyeong Chung. 2011. “Drosophila Salt-Inducible Kinase (SIK) Regulates Starvation Resistance through CAMP-Response Element-Binding Protein (CREB)-Regulated Transcription Coactivator (CRTC).” *Journal of Biological Chemistry* 286 (4): 2658–64. doi:10.1074/jbc.C110.119222.

Chung, Hyung-Lok Lok, George J. J. Augustine, and Kwang-Wook Wook Choi. 2016. “Drosophila Schip1 Links Expanded and Tao-1 to Regulate Hippo Signaling.” *Developmental Cell* 36 (5). Elsevier Inc.: 511–24. doi:10.1016/j.devcel.2016.02.004.

D’Avino, Pier Paolo, Matthew S. Savoian, and David M. Glover. 2004. “Mutations in Sticky Lead to Defective Organization of the Contractile Ring during Cytokinesis and Are Enhanced by Rho and Suppressed by Rac.” *Journal of Cell Biology* 166 (1): 61–71. doi:10.1083/jcb.200402157.

Degoutin, Joffrey L, Claire C Milton, Eefang Yu, Marla Tipping, Floris Bosveld, Liu Yang, Yohanns Bellaiche, Alexey Veraksa, and Kieran F Harvey. 2013. “Riquiqui and Minibrain Are Regulators of the Hippo Pathway Downstream of Dachsous.” *Nature Cell Biology* 15 (10). Nature Publishing Group: 1176–85. doi:10.1038/ncb2829.

Deng, Hua, Wei Wang, Jianzhong Yu, Yonggang Zheng, Yun Qing, and Duojia Pan. 2015. “Spectrin Regulates Hippo Signaling by Modulating Cortical Actomyosin Activity.” *ELife* 2015 (4): 1–17. doi:10.7554/eLife.06567.

Densham, R. M., E. O’Neill, J. Munro, I. Konig, K. Anderson, W. Kolch, and M. F. Olson. 2009. “MST Kinases Monitor Actin Cytoskeletal Integrity and Signal via C-Jun N-Terminal Kinase Stress-Activated Kinase To Regulate P21Waf1/Cip1 Stability.” *Molecular and Cellular Biology* 29 (24): 6380–90. doi:10.1128/MCB.00116-09.

Doerflinger, H. 2003. “The Role of PAR-1 in Regulating the Polarised Microtubule Cytoskeleton in the Drosophila Follicular Epithelium.” *Development* 130 (17): 3965–75. doi:10.1242/dev.00616.

Dong, Jing-Ming, Thomas Leung, Edward Manser, and Louis Lim. 2002. “Cdc42 Antagonizes Inductive Action of CAMP on Cell Shape, via Effects of the Myotonic Dystrophy Kinase-Related Cdc42-Binding Kinase (MRCK) on Myosin Light Chain Phosphorylation.” *European Journal of Cell Biology* 81 (4): 231–42. doi:10.1078/0171-9335-00238.

Dong, Jixin, Georg Feldmann, Jianbin Huang, Shian Wu, Nailing Zhang, A Sarah, Mariana F Gayyed, et al. 2007. “Elucidation of a Universal Size-Control Mechanism in Drosophila and Mammals.” *Cell* 130 (6): 1120–33. doi:10.1016/j.cell.2007.07.019.

Dupont, Sirio, Leonardo Morsut, Mariaceleste Aragona, Elena Enzo, Stefano Giulitti, Michelangelo Cordenonsi, Francesca Zanconato, et al. 2011. “Role of YAP/TAZ in Mechanotransduction.” *Nature* 474 (7350). Nature Publishing Group: 179–83. doi:10.1038/nature10137.

Elosegui-Artola, Alberto, Ion Andreu, Amy EM Beedle, Ainhoa Lezamiz, Marina Uroz, Anita Joanna Kosmalska, Roger Oria, et al. 2017. “Force Triggers YAP Nuclear Entry by Mechanically Regulating Transport across Nuclear Pores.” *Cell*. Elsevier Inc., (in press).

doi:10.1016/j.cell.2017.10.008.

Enomoto, Masato, and Tatsushi Igaki. 2011. “Deciphering Tumor-Suppressor Signaling in Flies: Genetic Link between Scribble/Dlg/Lgl and the Hippo Pathways.” *Journal of Genetics and Genomics = Yi Chuan Xue Bao* 38 (10). Elsevier Limited and Science Press: 461–70. doi:10.1016/j.jgg.2011.09.005.

———. 2012. “Src Controls Tumorigenesis via JNK-Dependent Regulation of the Hippo Pathway in Drosophila.” *EMBO Reports* 14 (1). Nature Publishing Group: 65–72. doi:10.1038/embor.2012.185.

Enomoto, Masato, Daisuke Kizawa, Shizue Ohsawa, and Tatsushi Igaki. 2015. “JNK Signaling Is Converted from Anti- to pro-Tumor Pathway by Ras-Mediated Switch of Warts Activity.” *Developmental Biology* 403 (2). Elsevier: 162–71. doi:10.1016/j.ydbio.2015.05.001.

Fernández, Beatriz García, Pedro Gaspar, Catarina Brás-Pereira, Barbara Jezowska, Sofia Raquel Rebelo, and Florence Janody. 2011. “Actin-Capping Protein and the Hippo Pathway Regulate F-Actin and Tissue Growth in Drosophila.” *Development (Cambridge, England)* 138 (11): 2337–46. doi:10.1242/jcs.092866.

Fernandez-Gonzalez, Rodrigo, Sérgio de Matos Simoes, Jens-Christian Christian Röper, Suzanne Eaton, and Jennifer A. Zallen. 2009. “Myosin II Dynamics Are Regulated by Tension in Intercalating Cells.” *Developmental Cell* 17 (5): 736–43. doi:10.1016/j.devcel.2009.09.003.

Fletcher, Georgina C., Eliana P. Lucas, Ruth Brain, Alexander Tournier, and Barry J. Thompson. 2012. “Positive Feedback and Mutual Antagonism Combine to Polarize Crumbs in the Drosophila Follicle Cell Epithelium.” *Current Biology : CB* 22 (12). Elsevier Ltd: 1116–22. doi:10.1016/j.cub.2012.04.020.

Fletcher, Georgina C, Ahmed Elbediwy, Ichha Khanal, Paulo S Ribeiro, Nic Tapon, Barry J Thompson, and Georgina C Fletcher. 2015. “The Spectrin Cytoskeleton Regulates the Hippo Signalling Pathway.” *Current Biology : CB* 34 (7): 940–55.

Formstecher, Etienne, Sandra Aresta, Vincent Collura, Alexandre Hamburger, Alain Meil, Alexandra Trehin, Virginie Betin, et al. 2005. “Protein Interaction Mapping：A Drosophila Case Study.” *Genome Research* 33 (February 2004): 376–84. doi:10.1101/gr.2659105.

Gaspar, Pedro, Maxine V. V. Holder, Birgit L. L. Aerne, Florence Janody, and Nicolas Tapon. 2015. “Zyxin Antagonizes the FERM Protein Expanded to Couple F-Actin and Yorkie-Dependent Organ Growth.” *Current Biology* 25 (6). Elsevier Ltd: 679–89. doi:10.1016/j.cub.2015.01.010.

Genevet, Alice, Cédric Polesello, Ken Blight, Francesca Robertson, Lucy M Collinson, Franck Pichaud, and Nicolas Tapon. 2009. “The Hippo Pathway Regulates Apical-Domain Size Independently of Its Growth-Control Function.” *Journal of Cell Science* 122 (Pt 14): 2360–70. doi:10.1242/jcs.041806.

Genevet, Alice, and Nicolas Tapon. 2011. “The Hippo Pathway and Apico-Basal Cell Polarity.” *The Biochemical Journal* 436 (2): 213–24. doi:10.1042/BJ20110217.

Genevet, Alice, Michael C. Wehr, Ruth Brain, Barry J. Thompson, and Nicolas Tapon. 2010. "Kibra Is a Regulator of the Salvador/Warts/Hippo Signaling Network." *Developmental Cell* 18 (2). Elsevier: 300–308. doi:10.1016/j.devcel.2009.12.011.

Gibson, Daniel G, Lei Young, Ray-yuan Chuang, J Craig Venter, Clyde a Hutchison, and Hamilton O Smith. 2009. "Enzymatic Assembly of DNA Molecules up to Several Hundred Kilobases." *Nature Methods* 6 (5): 343–45. doi:10.1038/nmeth.1318.

Grzeschik, Nicola A., Linda M. Parsons, Melinda L. Allott, Kieran F. Harvey, and Helena E. Richardson. 2010. "Lgl , APKC , and Crumbs Regulate the Salvador / Warts / Hippo Pathway through Two Distinct Mechanisms." *Current Biology* 20 (7). Elsevier Ltd: 573–81. doi:10.1016/j.cub.2010.01.055.

Guo, Tong, Yi Lu, Peixue Li, Meng Xin Yin, Dekang Lv, Wenjing Zhang, Huizhen Wang, et al. 2013. "A Novel Partner of Scalloped Regulates Hippo Signaling via Antagonizing Scalloped-Yorkie Activity." *Cell Research* 23 (10): 1201–14. doi:10.1038/cr.2013.120.

Guss, Kirsten a, Michael Benson, Nicholas Gubitosi, Karrie Brondell, Kendal Broadie, and James B Skeath. 2013. "Expression and Function of Scalloped during Drosophila Development." *Developmental Dynamics* 242 (7): 874–85. doi:10.1002/dvdy.23942.

Hamaratoglu, Fisun, Kathleen Gajewski, Leticia Sansores-Garcia, Clayton Morrison, Chunyao Tao, and Georg Halder. 2009. "The Hippo Tumor-Suppressor Pathway Regulates Apical-Domain Size in Parallel to Tissue Growth." *Journal of Cell Science* 122 (Pt 14): 2351–59. doi:10.1242/jcs.046482.

Hamaratoglu, Fisun, Maria Willecke, Madhuri Kango-Singh, Riitta Nolo, Eric Hyun, Chunyao Tao, Hamed Jafar-Nejad, and Georg Halder. 2006. "The Tumour-Suppressor Genes NF2/Merlin and Expanded Act through Hippo Signalling to Regulate Cell Proliferation and Apoptosis." *Nature Cell Biology* 8 (1): 27–36. doi:10.1038/ncb1339.

Hariharan, Iswar K. 2015. "Organ Size Control: Lessons from Drosophila." *Developmental Cell* 34 (3). Elsevier Inc.: 255–65. doi:10.1016/j.devcel.2015.07.012.

Harvey, Kieran F., Cathie M. Pfleger, and Iswar K. Hariharan. 2003. "The Drosophila Mst Ortholog, Hippo, Restricts Growth and Cell Proliferation and Promotes Apoptosis." *Cell* 114 (4): 457–67. doi:10.1016/S0092-8674(03)00557-9.

Hay, Bruce A., David A. Wassarman, and Gerald M. Rubin. 1995. "Drosophila Homologs of Baculovirus Inhibitor of Apoptosis Proteins Function to Block Cell Death." *Cell* 83 (7): 1253–62. doi:10.1016/0092-8674(95)90150-7.

Hirata, Hiroaki, Hitoshi Tatsumi, and Masahiro Sokabe. 2008. "Zyxin Emerges as a Key Player in the Mechanotransduction at Cell Adhesive Structures." *Communicative & Integrative Biology* 1 (2): 192–95. doi:10.4161/cib.1.2.7001.

Huang, Hong-Ling, Shimin Wang, Meng-Xin Yin, Liang Dong, Chao Wang, Wei Wu, Yi Lu, et al. 2013. "Par-1 Regulates Tissue Growth by Influencing Hippo Phosphorylation Status and Hippo-Salvador Association." *PLoS Biology* 11 (8): e1001620. doi:10.1371/journal.pbio.1001620.

Huang, Jianbin, Shian Wu, Jose Barrera, Krista Matthews, and Duojia Pan. 2005. "The Hippo

Signaling Pathway Coordinately Regulates Cell Proliferation and Apoptosis by Inactivating Yorkie, the Drosophila Homolog of YAP." *Cell* 122 (3): 421–34. doi:10.1016/j.cell.2005.06.007.

Hutson, M Shane, Yoichiro Tokutake, M.-S. Chang, J W Bloor, S Venakides, D P Kiehart, and Glenn S Edwards. 2003. "Forces for Morphogenesis Inverstigated with Laser Microsurgery and Quantitative Modeling." *Science* 300 (April): 145–49.

Ibar, Consuelo, Elmira Kirichenko, Benjamin Keepers, Edward Enners, Katelyn Fleisch, and Kenneth D. Irvine. 2018. "Tension-Dependent Regulation of Mammalian Hippo Signaling through LIMD1." *Journal of Cell Science* 131 (5): jcs214700. doi:10.1242/jcs.214700.

Irvine, Kenneth D., and Kieran F. Harvey. 2015. "Control of Organ Growth by Patterning and Hippo Signaling in Drosophila." *Cold Spring Harbor Perspectives in Biology* 7 (6): 1–16. doi:10.1101/cshperspect.a019224.

Ishihara, Shuji, and Kaoru Sugimura. 2012. "Bayesian Inference of Force Dynamics during Morphogenesis." *Journal of Theoretical Biology* 313. Elsevier: 201–11. doi:10.1016/j.jtbi.2012.08.017.

Jin, Yunyun, Jinjin Xu, Meng-Xin Yin, Yi Lu, Lianxin Hu, Peixue Li, Peng Zhang, et al. 2013. "Brahma Is Essential for *Drosophila* Intestinal Stem Cell Proliferation and Regulated by Hippo Signaling." *ELife* 2: 1–21. doi:10.7554/eLife.00999.

Jordan, P, and R Karess. 1997. "Myosin Light Chain-Activating Phosphorylation Sites Are Required for Oogenesis in Drosophila." *The Journal of Cell Biology* 139 (7): 1805–19.

Justice, R W, O Zilian, D F Woods, M Noll, and P J Bryant. 1995. "The Drosophila Tumor-Suppressor Gene Warts Encodes a Homolog of Human Myotonic-Dystrophy Kinase and Is Required for the Control of Cell-Shape and Proliferation." *Genes & Development* 9 (5): 534–46. doi:Doi 10.1101/Gad.9.5.534.

Kango-Singh, M. 2002. "Shar-Pei Mediates Cell Proliferation Arrest during Imaginal Disc Growth in Drosophila." *Development* 129 (24): 5719–30. doi:10.1242/dev.00168.

Kim, Minchul, Taekhoon Kim, Randy L. L. Johnson, and Dae-Sik Sik Lim. 2015. "Transcriptional Co-Repressor Function of the Hippo Pathway Transducers YAP and TAZ." *Cell Reports* 11 (2). The Authors: 270–82. doi:10.1016/j.celrep.2015.03.015.

Koontz, Laura M., Yi Liu-chittenden, Feng Yin, Yonggang Zheng, Jianzhong Yu, Bo Huang, Qian Chen, Shian Wu, and Duojia Pan. 2013. "The Hippo Effector Yorkie Controls Normal Tissue Growth by Antagonizing Scalloped-Mediated Default Repression." *Developmental Cell* 25 (4). Elsevier: 388–401. doi:10.1016/j.devcel.2013.04.021.

Lai, Zhi-Chun, Xiaomu Wei, Takeshi Shimizu, Edward Ramos, Margaret Rohrbaugh, Nikolas Nikolaidis, Li-Lun Ho, and Ying Li. 2005. "Control of Cell Proliferation and Apoptosis by Mob as Tumor Suppressor, Mats." *Cell* 120 (5): 675–85. doi:10.1016/j.cell.2004.12.036.

Laprise, Patrick, and Ulrich Tepass. 2011. "Novel Insights into Epithelial Polarity Proteins in Drosophila." *Trends in Cell Biology* 21 (7). Elsevier Ltd: 401–8. doi:10.1016/j.tcb.2011.03.005.

LeGoff, L., H. Rouault, and T. Lecuit. 2013. "A Global Pattern of Mechanical Stress Polarizes

Cell Divisions and Cell Shape in the Growing Drosophila Wing Disc." *Development* 140 (19): 4051–59. doi:10.1242/dev.090878.

Legoff, Loïc, Hervé Rouault, and Thomas Lecuit. 2013. "A Global Pattern of Mechanical Stress Polarizes Cell Divisions and Cell Shape in the Growing Drosophila Wing Disc." *Development (Cambridge, England)* 140 (19): 4051–59. doi:10.1242/dev.090878.

Lin, Chuwen, Erica Yao, Kuan Zhang, Xuan Jiang, Stacey Croll, Katherine Thompson-Peer, and Pao-Tien Chuang. 2017. "YAP Is Essential for Mechanical Force Production and Epithelial Cell Proliferation during Lung Branching Morphogenesis." *ELife* 6: 1–25. doi:10.7554/eLife.21130.

Ling, Chen, Yonggang Zheng, Feng Yin, Jianzhong Yu, Juan Huang, Yang Hong, Shian Wu, and Duojia Pan. 2010. "The Apical Transmembrane Protein Crumbs Functions as a Tumor Suppressor That Regulates Hippo Signaling by Binding to Expanded." *Proceedings of the National Academy of Sciences of the United States of America* 107 (23): 10532–37. doi:10.1073/pnas.1004279107.

Linke, W. A. 2000. "Stretching Molecular Springs: Elasticity of Titin Filaments in Vertebrate Striated Muscle." *Histology and Histopathology* 15 (3): 799–811.

Liu, Tao, Jennifer L Rohn, Remigio Picone, Patricia Kunda, and Buzz Baum. 2010. "Tao-1 Is a Negative Regulator of Microtubule plus-End Growth." *Journal of Cell Science* 123 (Pt 16): 2708–16. doi:10.1242/jcs.068726.

Maitra, Sushmita, Rima M. Kulikauskas, Heather Gavilan, and Richard G. Fehon. 2006. "The Tumor Suppressors Merlin and Expanded Function Cooperatively to Modulate Receptor Endocytosis and Signaling." *Current Biology : CB* 16 (7): 702–9. doi:10.1016/j.cub.2006.02.063.

Mao, Yanlan, Alexander L Tournier, Andreas Hoppe, Lennart Kester, Barry J Thompson, and Nicolas Tapon. 2013. "Differential Proliferation Rates Generate Patterns of Mechanical Tension That Orient Tissue Growth." *The EMBO Journal* 32 (21). Nature Publishing Group: 2790–2803. doi:10.1038/emboj.2013.197.

Maroto, Miguel, Javier Vinós, Roberto Marco, and Margarita Cervera. 1992. "Autophosphorylating Protein Kinase Activity in Titin-like Arthropod Projectin." *Journal of Molecular Biology* 224 (2): 287–91. doi:10.1016/0022-2836(92)90994-U.

Martin, Adam C, Matthias Kaschube, and Eric F Wieschaus. 2009. "Pulsed Contractions of an Actin-Myosin Network Drive Apical Constriction." *Nature* 457 (7228). Nature Publishing Group: 495–99. doi:10.1038/nature07522.

Matakatsu, H., and S. Blair. 2004. "Interactions between Fat and Dachsous and the Regulation of Planar Cell Polarity in the Drosophila Wing." *Development* 131 (15): 3785–94. doi:10.1242/dev.01254.

McCartney, B M, R M Kulikauskas, D R LaJeunesse, and R G Fehon. 2000. "The Neurofibromatosis-2 Homologue, Merlin, and the Tumor Suppressor Expanded Function Together in Drosophila to Regulate Cell Proliferation and Differentiation." *Development (Cambridge, England)* 127 (6): 1315–24.

McGuire, Sean E, Phuong T Le, Alexander J Osborn, Kunihiro Matsumoto, and Ronald L Davis. 2003. “Spatiotemporal Rescue of Memory Dysfunction in Drosophila.” *Science (New York, N.Y.)* 302 (5651): 1765–68. doi:10.1126/science.1089035.

Meng, Zhipeng, Toshiro Moroishi, and Kun-liang Guan. 2016. “Mechanisms of Hippo Pathway Regulation.” *Genes and Development* 30 (1): 1–17. doi:10.1101/gad.274027.115.1/2.

Mitonaka, Tomoaki, Yoshiyuki Muramatsu, Shin Sugiyama, Tomoaki Mizuno, and Yasuyoshi Nishida. 2007. “Essential Roles of Myosin Phosphatase in the Maintenance of Epithelial Cell Integrity of Drosophila Imaginal Disc Cells.” *Developmental Biology* 309 (1): 78–86. doi:10.1016/j.ydbio.2007.06.021.

Moberg, Kenneth H, Suzanne Schelble, Sharon K Burdick, and Iswar K Hariharan. 2005. “Mutations in Erupted, the Drosophila Ortholog of Mammalian Tumor Susceptibility Gene 101, Elicit Non-Cell-Autonomous Overgrowth.” *Developmental Cell* 9 (5): 699–710. doi:10.1016/j.devcel.2005.09.018.

Nance, Jeremy, and Jennifer a Zallen. 2011. “Elaborating Polarity: PAR Proteins and the Cytoskeleton.” *Development (Cambridge, England)* 138 (5): 799–809. doi:10.1242/dev.053538.

Neisch, Amanda L, Etienne Formstecher, and Richard G Fehon. 2013. “Conundrum, an ARHGAP18 Orthologue, Regulates RhoA and Proliferation through Interactions with Moesin.” *Molecular Biology of the Cell* 24 (9): 1420–33. doi:10.1091/mbc.E12-11-0800.

Neubueser, Dagmar, and DR Hipfner. 2010. “Overlapping Roles of Drosophila Drak and Rok Kinases in Epithelial Tissue Morphogenesis.” *Molecular Biology of the Cell* 21: 2869–79. doi:10.1091/mbc.E10.

Nie, Jing, Simpla Mahato, and Andrew C Zelhof. 2014. “The Actomyosin Machinery Is Required for Drosophila Retinal Lumen Formation.” *PLoS Genetics* 10 (9): e1004608. doi:10.1371/journal.pgen.1004608.

Nola, Sébastien, Reiko Daigaku, Kasia Smolarczyk, Maryke Carstens, Belen Martin-Martin, Gregory Longmore, Maryse Bailly, and Vania M M Braga. 2011. “Ajuba Is Required for Rac Activation and Maintenance of E-Cadherin Adhesion.” *Journal of Cell Biology* 195 (5): 855–71. doi:10.1083/jcb.201107162.

Nolo, Riitta, Clayton M. Morrison, Chunyao Tao, Xinwei Zhang, and Georg Halder. 2006. “The Bantam MicroRNA Is a Target of the Hippo Tumor-Suppressor Pathway.” *Current Biology* 16 (19): 1895–1904. doi:10.1016/j.cub.2006.08.057.

Oh, Hyangyee, and Kenneth D. Irvine. 2011. “Cooperative Regulation of Growth by Yorkie and Mad through Bantam.” *Developmental Cell* 20 (1). Elsevier: 109–22. doi:10.1016/j.devcel.2010.12.002.

Oh, Hyangyee, and Kenneth D Irvine. 2008. “In Vivo Regulation of Yorkie Phosphorylation and Localization.” *Development (Cambridge, England)* 135 (6): 1081–88. doi:10.1242/dev.015255.

Oh, Hyangyee, B V V G Reddy, and Kenneth D Irvine. 2009. “Phosphorylation-Independent Repression of Yorkie in Fat-Hippo Signaling.” *Developmental Biology* 335 (1). Elsevier

Inc.: 188–97. doi:10.1016/j.ydbio.2009.08.026.

Oh, Hyangyee, Matthew Slattery, Lijia Ma, Alex Crofts, Kevin P. White, Richard S. Mann, and Kenneth D. Irvine. 2013. "Genome-Wide Association of Yorkie with Chromatin and Chromatin-Remodeling Complexes." *Cell Reports* 3 (2). The Authors: 309–18. doi:10.1016/j.celrep.2013.01.008.

Pan, G., Y. Feng, A. A. Ambegaonkar, G. Sun, M. Huff, C. Rauskolb, and K. D. Irvine. 2013. "Signal Transduction by the Fat Cytoplasmic Domain." *Development* 140 (4): 831–42. doi:10.1242/dev.088534.

Pan, Yuanwang, Idse Heemskerk, Consuelo Ibar, Boris I Shraiman, and Kenneth D Irvine. 2016. "Differential Growth Triggers Mechanical Feedback That Elevates Hippo Signaling." *Proceedings of the National Academy of Sciences of the United States of America* 113 (45): E6974–83. doi:10.1073/pnas.1615012113.

Pantalacci, Sophie, Nicolas Tapon, and Pierre Léopold. 2003. "The Salvador Partner Hippo Promotes Apoptosis and Cell-Cycle Exit in Drosophila." *Nature Cell Biology* 5 (10): 921–27. doi:10.1038/ncb1051.

Parsons, Linda M., Nicola A. Grzeschik, and Helena E. Richardson. 2014. "Lgl Regulates the Hippo Pathway Independently of Fat/Dachs, Kibra/Expanded/Merlin and DRASSF/DSTRIPAK." *Cancers* 6 (2): 879–96. doi:10.3390/cancers6020879.

Patel, Sunita R, and Judith D Saide. 2005. "Stretchin-Klp, a Novel Drosophila Indirect Flight Muscle Protein, Has Both Myosin Dependent and Independent Isoforms." *Journal of Muscle Research and Cell Motility* 26 (4–5): 213–24. doi:10.1007/s10974-005-9012-y.

Peng, H Wayne, Matthew Slattery, and Richard S Mann. 2009. "Transcription Factor Choice in the Hippo Signaling Pathway: Homothorax and Yorkie Regulation of the MicroRNA Bantam in the Progenitor Domain of the Drosophila Eye Imaginal Disc." *Genes & Development* 23 (19): 2307–19. doi:10.1101/gad.1820009.

Poon, Carole L C, Jane I. Lin, Xiaomeng Zhang, and Kieran F. Harvey. 2011. "The Sterile 20-like Kinase Tao-1 Controls Tissue Growth by Regulating the Salvador-Warts-Hippo Pathway Supplemental Information." *Developmental Cell* 21 (5). Elsevier Inc.: 896–906. doi:10.1016/j.devcel.2011.09.012.

Porazinski, Sean, Huijia Wang, Yoichi Asaoka, Martin Behrndt, Tatsuo Miyamoto, Hitoshi Morita, Shoji Hata, et al. 2015. "YAP Is Essential for Tissue Tension to Ensure Vertebrate 3D Body Shape." *Nature*. Nature Publishing Group, 1–6. doi:10.1038/nature14215.

Qing, Yun, Feng Yin, Wei Wang, Yonggang Zheng, Pengfei Guo, Frederick Schozer, Hua Deng, and Duojia Pan. 2014. "The Hippo Effector Yorkie Activates Transcription by Interacting with a Histone Methyltransferase Complex through Ncoa6." *ELife* 3 (January): 1–13. doi:10.7554/eLife.02564.

Rauskolb, Cordelia, Guohui Pan, B V V G Reddy, Hyangyee Oh, and Kenneth D Irvine. 2011. "Zyxin Links Fat Signaling to the Hippo Pathway." *PLoS Biology* 9 (6): e1000624. doi:10.1371/journal.pbio.1000624.

Rauskolb, Cordelia, Shuguo Sun, Gongping Sun, Yuanwang Pan, and Kenneth D. D. Irvine.

2014. “Cytoskeletal Tension Inhibits Hippo Signaling through an Ajuba-Warts Complex.” *Cell* 158 (1). Elsevier Inc.: 143–56. doi:10.1016/j.cell.2014.05.035.

Rauzi, Matteo, Pascale Verant, Thomas Lecuit, and Pierre-François Lenne. 2008. “Nature and Anisotropy of Cortical Forces Orienting Drosophila Tissue Morphogenesis.” *Nature Cell Biology* 10 (12): 1401–10. doi:10.1038/ncb1798.

Reddy, B V V G, and Kenneth D Irvine. 2008. “The Fat and Warts Signaling Pathways: New Insights into Their Regulation, Mechanism and Conservation.” *Development (Cambridge, England)* 135 (17): 2827–38. doi:10.1242/dev.020974.

Ribeiro, Paulo, Maxine Holder, David Frith, Ambrosius P Snijders, and Nicolas Tapon. 2014. “Crumbs Promotes Expanded Recognition and Degradation by the SCFSlimb/β-TrCP Ubiquitin Ligase.” *Proceedings of the National Academy of Sciences of the United States of America*, April. doi:10.1073/pnas.1315508111.

Richardson, Helena E., and Marta Portela. 2017. “Tissue Growth and Tumorigenesis in Drosophila: Cell Polarity and the Hippo Pathway.” *Current Opinion in Cell Biology* 48. Elsevier Ltd: 1–9. doi:10.1016/j.ceb.2017.03.006.

Robinson, Brian S, Juang Huang, Yang Hong, and Kenneth H Moberg. 2010. “Crumbs Regulates Salvador/Warts/Hippo Signaling in Drosophila via the FERM-Domain Protein Expanded.” *Current Biology : CB* 20 (7). Elsevier Ltd: 582–90. doi:10.1016/j.cub.2010.03.019.

Rodrigues-Campos, M., and B. J. Thompson. 2014. “The Ubiquitin Ligase FbxL7 Regulates the Dachsous-Fat-Dachs System in Drosophila.” *Development* 141 (21): 4098–4103. doi:10.1242/dev.113498.

Rolls, Melissa M., Roger Albertson, Hsin Pei Shih, Cheng Yu Lee, and Chris Q. Doe. 2003. “Drosophila APKC Regulates Cell Polarity and Cell Proliferation in Neuroblasts and Epithelia.” *Journal of Cell Biology* 163 (5): 1089–98. doi:10.1083/jcb.200306079.

Rousso, Tal, Eyal D. Schejter, and Ben Zion Shilo. 2016. “Orchestrated Content Release from Drosophila Glue-Protein Vesicles by a Contractile Actomyosin Network.” *Nature Cell Biology* 18 (2): 181–90. doi:10.1038/ncb3288.

Sansores-Garcia, Leticia, Wouter Bossuyt, Ken-Ichi Wada, Shigenobu Yonemura, Chunyao Tao, Hiroshi Sasaki, and Georg Halder. 2011. “Modulating F-Actin Organization Induces Organ Growth by Affecting the Hippo Pathway.” *The EMBO Journal* 30 (12). Nature Publishing Group: 2325–35. doi:10.1038/emboj.2011.157.

Schlegelmilch, Karin, Morvarid Mohseni, Oktay Kirak, Jan Pruszak, J Renato Rodriguez, Dawang Zhou, Bridget T Kreger, et al. 2011. “Yap1 Acts Downstream of α-Catenin to Control Epidermal Proliferation.” *Cell* 144 (5). Elsevier Inc.: 782–95. doi:10.1016/j.cell.2011.02.031.

Schönbauer, Cornelia, Jutta Distler, Nina Jährling, Martin Radolf, Hans-Ulrich Dodt, Manfred Frasch, and Frank Schnorrer. 2011. “Spalt Mediates an Evolutionarily Conserved Switch to Fibrillar Muscle Fate in Insects.” *Nature* 479 (7373): 406–9. doi:10.1038/nature10559.

Sebe-Pedrs, Arnau, Yonggang Zheng, Iñaki Ruiz-Trillo, and Duojia Pan. 2012. “Premetazoan

Origin of the Hippo Signaling Pathway." *Cell Reports* 1 (1): 13–20. doi:10.1016/j.celrep.2011.11.004.

Segal, Dagan, Assaf Zaritsky, Eyal D Schejter, and Ben Zion Shilo. 2018. "Feedback Inhibition of Actin on Rho Mediates Content Release from Large Secretory Vesicles." *Journal of Cell Biology*, 1–12.

Shen, Shuying, Xiaocan Guo, Huan Yan, Yi Lu, Xinyan Ji, Li Li, Tingbo Liang, et al. 2015. "A MiR-130a-YAP Positive Feedback Loop Promotes Organ Size and Tumorigenesis." *Cell Research* 25 (9): 997–1012. doi:10.1038/cr.2015.98.

Silva, Elizabeth, Yonit Tsatskis, Laura Gardano, Nic Tapon, and Helen McNeill. 2006. "The Tumor-Suppressor Gene Fat Controls Tissue Growth Upstream of Expanded in the Hippo Signaling Pathway." *Current Biology* 16 (21): 2081–89. doi:10.1016/j.cub.2006.09.004.

Sotillos, Sol, María Teresa Díaz-Meco, Eva Caminero, Jorge Moscat, and Sonsoles Campuzano. 2004. "DaPKC-Dependent Phosphorylation of Crumbs Is Required for Epithelial Cell Polarity in Drosophila." *The Journal of Cell Biology* 166 (4): 549–57. doi:10.1083/jcb.200311031.

St Johnston, Daniel, and Julie Ahringer. 2010. "Cell Polarity in Eggs and Epithelia: Parallels and Diversity." *Cell* 141 (5): 757–74. doi:10.1016/j.cell.2010.05.011.

Su, Ting, Michael Z. Ludwig, Jiajie Xu, and Richard G. Fehon. 2017. "Kibra and Merlin Activate the Hippo Pathway Spatially Distinct from and Independent of Expanded." *Developmental Cell* 40 (5). Elsevier Inc.: 478–490.e3. doi:10.1016/j.devcel.2017.02.004.

Sun, Gongping, and Kenneth D. Irvine. 2013. "Ajuba Family Proteins Link JNK to Hippo Signaling." *Science Signaling* 6 (292): 1–10. doi:10.1126/scisignal.2004324.

Sun, Gongping, and Kenneth D Irvine. 2011. "Regulation of Hippo Signaling by Jun Kinase Signaling during Compensatory Cell Proliferation and Regeneration, and in Neoplastic Tumors." *Developmental Biology* 350 (1). Elsevier Inc.: 139–51. doi:10.1016/j.ydbio.2010.11.036.

Sun, Shuguo, and Kenneth D. Irvine. 2016. "Cellular Organization and Cytoskeletal Regulation of the Hippo Signaling Network." *Trends in Cell Biology* 26 (9). Elsevier Ltd: 694–704. doi:10.1016/j.tcb.2016.05.003.

Sun, Shuguo, B V V G Reddy, and Kenneth D Irvine. 2015. "Localization of Hippo Signalling Complexes and Warts Activation in Vivo." *Nature Communications* 6: 8402. doi:10.1038/ncomms9402.

Tapon, Nicolas, Kieran F Harvey, Daphne W Bell, Doke C R Wahrer, Taryn a Schiripo, Daniel a Haber, and Iswar K Hariharan. 2002. "Salvador Promotes Both Cell Cycle Exit and Apoptosis in Drosophila and Is Mutated in Human Cancer Cell Lines." *Cell* 110 (4): 467–78.

Tepass, Ulrich. 2012. "The Apical Polarity Protein Network in Drosophila Epithelial Cells: Regulation of Polarity, Junctions, Morphogenesis, Cell Growth, and Survival." *Annual Review of Cell and Developmental Biology* 28 (January): 655–85. doi:10.1146/annurev-cellbio-092910-154033.

Thakur, Meghna Das, Yunfeng Feng, Radhika Jagannathan, Midori J Seppa, James B Skeath, and Gregory D Longmore. 2010. “Ajuba LIM Proteins Are Negative Regulators of the Hippo Signaling Pathway.” *Current Biology : CB* 20 (7). Elsevier Ltd: 657–62. doi:10.1016/j.cub.2010.02.035.

Thompson, Barry J., and Stephen M. Cohen. 2006. “The Hippo Pathway Regulates the Bantam MicroRNA to Control Cell Proliferation and Apoptosis in Drosophila.” *Cell* 126 (4): 767–74. doi:10.1016/j.cell.2006.07.013.

Tsoumpekos, Giorgos, Linda Nemetschke, and Elisabeth Knust. 2018. “Drosophila Big Bang Regulates the Apical Cytocortex and Wing Growth through Junctional Tension.” *Journal of Cell Biology* 217 (3): 1033–45. doi:10.1083/jcb.201705104.

Udan, Ryan S., Madhuri Kango-Singh, Riitta Nolo, Chunyao Tao, and Georg Halder. 2003. “Hippo Promotes Proliferation Arrest and Apoptosis in the Salvador/Warts Pathway.” *Nature Cell Biology* 5 (10): 914–20. doi:10.1038/ncb1050.

Varelas, Xaralabos, Bryan W Miller, Richelle Sopko, Siyuan Song, Alex Gregorieff, Frederic a Fellouse, Rui Sakuma, et al. 2010. “The Hippo Pathway Regulates Wnt/Beta-Catenin Signaling.” *Developmental Cell* 18 (4). Elsevier Ltd: 579–91. doi:10.1016/j.devcel.2010.03.007.

Varelas, Xaralabos, Payman Samavarchi-Tehrani, Masahiro Narimatsu, Alexander Weiss, Katie Cockburn, Brett G Larsen, Janet Rossant, and Jeffrey L Wrana. 2010. “The Crumbs Complex Couples Cell Density Sensing to Hippo-Dependent Control of the TGF-β-SMAD Pathway.” *Developmental Cell* 19 (6). Elsevier Inc.: 831–44. doi:10.1016/j.devcel.2010.11.012.

Vrabioiu, Alina M. M., and Gary Struhl. 2015. “Fat/Dachsous Signaling Promotes Drosophila Wing Growth by Regulating the Conformational State of the NDR Kinase Warts.” *Developmental Cell* 35 (6). Elsevier Inc.: 737–49. doi:10.1016/j.devcel.2015.11.027.

Wei, Shu-Yi, Luis M Escudero, Fengwei Yu, Li-Hsun Chang, Li-Ying Chen, Yu-Huei Ho, Chiao-Ming Lin, et al. 2005. “Echinoid Is a Component of Adherens Junctions That Cooperates with DE-Cadherin to Mediate Cell Adhesion.” *Developmental Cell* 8 (4): 493–504. doi:10.1016/j.devcel.2005.03.015.

Wei, Xiaomu, Takeshi Shimizu, and Zhi-Chun Lai. 2007. “Mob as Tumor Suppressor Is Activated by Hippo Kinase for Growth Inhibition in Drosophila.” *The EMBO Journal* 26 (7): 1772–81. doi:10.1038/sj.emboj.7601630.

Willecke, Maria, Fisun Hamaratoglu, Madhuri Kango-Singh, Ryan Udan, Chiao lin Chen, Chunyao Tao, Xinwei Zhang, and Georg Halder. 2006. “The Fat Cadherin Acts through the Hippo Tumor-Suppressor Pathway to Regulate Tissue Size.” *Current Biology* 16 (21): 2090–2100. doi:10.1016/j.cub.2006.09.005.

Wu, Shian, Jianbin Huang, Jixin Dong, and Duojia Pan. 2003. “Hippo Encodes a Ste-20 Family Protein Kinase That Restricts Cell Proliferation and Promotes Apoptosis in Conjunction with Salvador and Warts.” *Cell* 114 (4): 445–56.

Wu, Shian, Y. Liu, Yonggang Zheng, Jixin Dong, and Duojia Pan. 2008. “The TEAD/TEF Family Protein Scalloped Mediates Transcriptional Output of the Hippo Growth-Regulatory

Pathway." *Developmental Cell* 14 (3): 388–98. doi:10.1016/j.devcel.2008.01.007.

Xu, Jiajie, Pamela J Vanderzalm, Michael Ludwig, Ting Su, Sherzod A Tokamov, and Richard G Fehon. 2018. "Yorkie Functions at the Cell Cortex to Promote Myosin Activation in a Non-Transcriptional Manner." *Developmental Cell*. Elsevier Inc., 1–14. doi:10.1016/j.devcel.2018.06.017.

Xu, T, W Wang, S Zhang, R a Stewart, and W Yu. 1995. "Identifying Tumor Suppressors in Genetic Mosaics: The Drosophila Lats Gene Encodes a Putative Protein Kinase." *Development (Cambridge, England)* 121 (4): 1053–63.

Yin, Feng, Jianzhong Yu, Yonggang Zheng, Qian Chen, Nailing Zhang, and Duojia Pan. 2013. "Spatial Organization of Hippo Signaling at the Plasma Membrane Mediated by the Tumor Suppressor Merlin/NF2." *Cell* 154 (6). Elsevier Inc.: 1–14. doi:10.1016/j.cell.2013.08.025.

Young, Paul E, Adam M Richman, Andrew S Ketchum, and Daniel P Kiehart. 1993. "Morphogenesis in Drosophila Requires Nonmuscle Myosin Heavy Chain Function." *Genes Dev* 7 (1): 29–41. doi:10.1101/gad.7.1.29.

Yu, Fa-Xing, and Kun-Liang Guan. 2013. "The Hippo Pathway: Regulators and Regulations." *Genes & Development* 27 (4): 355–71. doi:10.1101/gad.210773.112.

Yu, Fa Xing, Bin Zhao, and Kun Liang Guan. 2015. "Hippo Pathway in Organ Size Control, Tissue Homeostasis, and Cancer." *Cell* 163 (4). Elsevier Inc.: 811–28. doi:10.1016/j.cell.2015.10.044.

Yu, Jianzhong, Yonggang Zheng, Jixin Dong, Stephen Klusza, Wu-Min Min Deng, and Duojia Pan. 2010. "Kibra Functions as a Tumor Suppressor Protein That Regulates Hippo Signaling in Conjunction with Merlin and Expanded." *Developmental Cell* 18 (2). Elsevier: 288–99. doi:10.1016/j.devcel.2009.12.012.

Yue, Tao, Aiguo Tian, and Jin Jiang. 2012. "The Cell Adhesion Molecule Echinoid Functions as a Tumor Suppressor and Upstream Regulator of the Hippo Signaling Pathway." *Developmental Cell* 22 (2). Elsevier Inc.: 255–67. doi:10.1016/j.devcel.2011.12.011.

Zhang, Lei, Fangfang Ren, Qing Zhang, Yongbin Chen, Bing Wang, and Jin Jiang. 2008. "The TEAD/TEF Family of Transcription Factor Scalloped Mediates Hippo Signaling in Organ Size Control." *Developmental Cell* 14 (3): 377–87. doi:10.1016/j.devcel.2008.01.006.

Zhang, Liang, and Robert E Ward. 2011. "Distinct Tissue Distributions and Subcellular Localizations of Differently Phosphorylated Forms of the Myosin Regulatory Light Chain in Drosophila." *Gene Expression Patterns : GEP* 11 (1–2). Elsevier B.V.: 93–104. doi:10.1016/j.gep.2010.09.008.

Zhang, Xiaomeng, Claire C. Milton, Patrick O. Humbert, and Kieran F. Harvey. 2009. "Transcriptional Output of the Salvador/Warts/Hippo Pathway Is Controlled in Distinct Fashions in Drosophila Melanogaster and Mammalian Cell Lines." *Cancer Research* 69 (15): 6033–41. doi:10.1158/0008-5472.CAN-08-4592.